



**University of
Nottingham**

UK | CHINA | MALAYSIA

Probing E-cadherin Targeting Peptides Using Atomic Force Microscopy

Adam James Studd, MPhys

School of Pharmacy

University of Nottingham


A thesis submitted for the degree of

Doctor of Philosophy

2021 A.J. Studd

Declaration

I, Adam James Studd, confirm that the work presented in this thesis is my own. Where information has been derived from other sources, I can confirm that this has been indicated in the thesis.

A handwritten signature in black ink, enclosed within a black rectangular border. The signature is stylized and appears to read 'Adam James Studd'.

Signature

Acknowledgements

This research would not have been possible without the funding supplied as part of the EPSRC and MRC CDT in regenerative medicine, and the facilities provided at the University of Nottingham.

I cannot express enough thanks to my supervisors, Prof. Stephanie Allen, Prof. Phil Williams, and Prof. Cathy Merry, for their continued support and guidance throughout my work. Despite all the unforeseen difficulties, particularly in the past 18 months, they have always been a source of encouragement and support, and I am truly thankful for all their help. Also, I would like to give special thanks to Nicholas Poulson for helping me to learn the processes and procedures required for working in the labs, and for being a supportive friend throughout my work.

I would also like to thank Prof. Xinyong Chen, Paul Cooling, and Katarzyna Lis-Slimak for their support and training, alongside all my amazing friends and colleagues within the University of Nottingham. I am honoured to have been able to work with such thoughtful and incredible people, and I owe so much to their helpful nature, both academically and personally. I wish you all the best in your future work.

Throughout my PhD I have been so fortunate to have an amazingly supportive network of friends and family, and this thesis is largely thanks to their continual support. Firstly, thank you to my brothers and sisters: Ann-Marie, Christopher, Hollie, Amy, and Benjamin, who have supported me whenever I needed it, despite my ability to test their resolve with endless complaints, and test their patience with my absence from messages. I know this is nothing new as you have always been there through every challenge without expecting any thanks, but I truly would not be here without you, and I am proud to have you all by my side. Secondly, I must say a massive thank you to Brian and Deniece, who have not only given care and support throughout my PhD but have also given me a home to finish my writing, and an abundance of tea to keep me focussed. I am so lucky to be welcomed in to such a loving and supportive family. Thank you to my amazing friends, particularly Dale, Matt, and Nick, that have provided many an entertaining evening when it was needed most; I owe you more

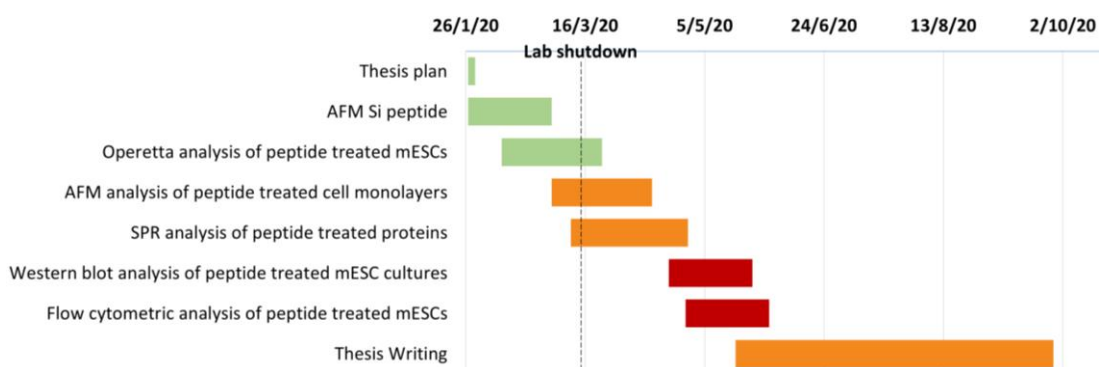
than I can say. You are all amazing people, and I appreciate every single game night, celebration, and long talk, and look forward to many more in the future!

Finally, I must give a special thanks to my parents, and of course my amazing partner Jenna. Mum and Dad, you have always given me more love and support than I thought possible, and I hope you know your daily sacrifices for those around you do not go unnoticed. You are both such thoughtful and caring people, and the most amazing parents I could wish for, and I cannot thank you both enough for everything you have done for me. I would not be where I am, nor who I am, without you. And last, but most certainly not least, I must try to find the words to express how grateful I am to have had my partner Jenna by my side through every high and every low. This thesis represents a small portion of the love and support you have given me every day that we have been together, as you have guided me through the challenges and pushed me to be the best version of myself, just as you always have done. You give me strength when I feel I have none, and remind me to focus on the good times, of which there are many. And I know there are so many more to look forward to together.

COVID-19 Impact Statement

The challenging unforeseen circumstances presented by the COVID-19 pandemic have unfortunately had a large impact on the progress of the research presented in this thesis. At the point of the initial lockdown in March 2020, I was in the process of completing biological assays based on the use of cell cultures. This meant that the sudden and drastic shutdown of research labs required me to stop my experiments and destroy my samples before I had the opportunity to complete experiments.

During this time I worked with my supervisors to try to optimise my progress, but this still resulted in a massive hindrance to my work and a large set-back in progress, as the COVID period followed on from an extended shutdown of my supervisor, Professor Cathy Merry's, research lab due to a move to a new research facility. Upon returning to the lab in August 2020 as part of an agreed short extension lasting until February 2021, I had to start my cell-based experiments from the beginning which added a lot of extra preparation time, and these issues were enhanced by the national shortage of supplies, that meant I often had to delay or change working plans on a day-to-day basis, as deliveries of consumables were late or cancelled. The outcome was that some of the originally planned experiments could not be completed, and the work that I did manage to complete in the extension period was very stressful and marred with issues such as limited working hours, lack of consumables, and absence of equipment and expertise. Further, the necessary safety protocols that were implemented for work within the university greatly limited the potential experiments that could be completed. The Gantt chart below shows the timeline originally set, with the dotted line representing the start of the shutdown due to the COVID-19 pandemic. The colour of the bars represents the progress made on each of the tasks following the re-opening of labs.



List of Contents

Declaration	<i>i</i>
Acknowledgements	<i>ii</i>
COVID-19 Impact Statement	<i>iv</i>
List of Contents	<i>v</i>
Abstract	<i>viii</i>
List of Figures	<i>x</i>
List of Tables	<i>xix</i>
Nomenclature and Abbreviations	<i>xxii</i>
Chapter 1 - Introduction	<i>1</i>
1.1 Cadherins in mESCs	<i>3</i>
1.2 Cell Adhesion and the Cadherin Superfamily	<i>7</i>
1.2.1 Biological and Mechanical Overview of the E-cadherin Protein	<i>9</i>
1.2.2 Peptide Interactions with E-cadherin	<i>13</i>
1.3 Probing Mechanical Characteristics of E-cadherin	<i>19</i>
1.3.1 Atomic Force Microscopy (AFM)	<i>22</i>
1.3.2 Single Molecule Force Spectroscopy (SMFS).....	<i>23</i>
1.4 Project Aims	<i>28</i>
Chapter 2 - Discussion of Instruments and Techniques	<i>30</i>
2.1 Atomic Force Microscopy (AFM)	<i>31</i>
2.1.1 Working Principles of AFM	<i>31</i>
2.1.2 Dynamic Force Spectroscopy (DFS)	<i>34</i>
2.1.3 The MFP-3D-SA AFM	<i>34</i>
2.2 A Brief Introduction to Optical Techniques and Principles	<i>36</i>
2.2.1 Fluorescence in Cell Biology Assays.....	<i>37</i>
2.2.1.1 Confocal Microscopy.....	<i>38</i>
2.2.1.2 High content imaging: Operetta	<i>39</i>
2.2.1.3 Flow Cytometry.....	<i>40</i>

Chapter 3 - AFM-Based Single Molecule Analysis of E-cadherin EC Domain

Interactions	42
3.1 Introduction.....	43
3.2 Materials and Methods	45
3.2.1 Structure of the Ecad-Fc Chimeric Protein	45
3.2.2 Sample Preparation.....	46
3.2.3 AFM Buffers.....	49
3.2.4 Experimental Procedure.....	49
3.2.5 Data Analysis	50
3.3 Results and Discussion	52
3.3.1 Preliminary Measurements	52
3.3.2 F-D Curve Analysis from Initial Experiments	54
3.3.3 Development of AFM Experiments	60
3.3.3.1 Investigating the Impact of Surface Protein Concentration and Tip Speed	60
3.3.3.2 Testing Sample Response to Sequential Buffer Changes.....	62
3.3.4 Discussion.....	65
3.4 Conclusions.....	69

Chapter 4 - Probing the Interaction of E-cadherin Targeting Peptides Using AFM 70

4.1 Materials and Methods	72
4.1.1 Probing the Effect of Peptide Sequences on E-cadherin Binding Via AFM	72
4.1.1.1 Peptide Solutions	72
4.1.1.2 Testing of E-cadherin Functionalised Samples.....	72
4.1.2 Proof of Concept for Cell-AFM SMFS Studies Using mESC Cultures.....	72
4.1.2.1 Preparation of Cell Cultures for AFM.....	73
4.1.2.2 AFM Buffers and Peptide Solutions for Cell-AFM Experiments	73
4.1.2.3 Experimental Process and Data Acquisition	73
4.2 Results and Discussion	75
4.2.1 Initial Testing of Peptides Using AFM.....	75
4.2.2 Detailed Epep and EpepW2R Peptide Titration Experiments	79
4.2.2.1 Binding frequency of Epep Treated Samples	80
4.2.2.2 Binding forces of Epep Treated Samples	83
4.2.2.3 Binding frequency of EpepW2R Treated Samples	86
4.2.2.4 Binding force of EpepW2R Treated Samples	89
4.2.3 Cell-AFM	92

4.2.3.1	Proof of Concept AFM Investigations of mESC-Peptide Interactions	92
4.2.4	Discussion	98
4.3	Conclusions.....	102
<i>Chapter 5 - Treatment of E14 and Ecad^{-/-} Cell Lines with Epep and EpepW2R peptides</i>		
5.1	Materials and Methods	105
5.1.1	General Cell Culture	105
5.1.1.1	Continuous culture of mESC cell lines.....	105
5.1.1.2	Freezing and Thawing Cell Stocks	106
5.1.1.3	Making peptide treated medium.....	106
5.1.2	Fluorescence and Operetta Imaging	107
5.1.2.1	Sample Preparation	107
5.1.2.2	Peptide Treatment.....	107
5.1.2.3	Immunostaining.....	107
5.1.2.4	Instrument, Data Acquisition, and Data Analysis.....	109
5.1.3	Operetta Imaging	110
5.1.3.1	Instrument Set-up and Data Acquisition.....	110
5.1.3.2	Data Analysis.....	110
5.2	Results and Discussion	112
5.2.1	Testing cell line characteristics for experimental application	112
5.2.1.1	Continuous cell growth.....	112
5.2.2	Operetta Analysis of peptide Treated mESCs.....	115
5.2.2.1	Optimising Initial Test Parameters.....	115
5.2.2.2	Unique Response of E14 Cultures to Peptide and DECMA-1 Treatment	119
5.2.2.3	Unique Response of Ecad ^{-/-} Cultures to Peptide and DECMA-1 Treatment.....	125
5.2.3	Discussion.....	131
5.3	Conclusions.....	137
<i>Chapter 6 - Conclusions and Future Work</i>		
6.1	Future Work	143
<i>References.....</i>		146

Abstract

A significant current research effort is focussed on a need to understand and regulate embryonic stem cell function *in vitro*, as their potentially limitless self-renewal and differentiative capacity could provide an effective approach for countless applications, including the development of therapeutics. As such, discovery of targeting peptides to influence stem cell behaviour, or isolate and understand cell mechanisms, is an ideal method to improve current understanding. E-cadherin is a cell surface adhesion protein commonly expressed by mESCs, and is highlighted as a potential target to probe and manipulate cell functions for a wide range of biological applications, such as preventing cell differentiation in large scale bioreactors. Due to the biological and mechanical influence of E-cadherin on cell functions, such as maintenance of pluripotency and formation of cell-cell contacts, there is ongoing research into the development of E-cadherin targeting peptide sequences to uniquely influence mESC characteristics. One recent example is the development of the Epep (SWELYPLRANL) sequence, and subsequent analogue EpepW2R (SRELYPLRANL), that were shown to uniquely affect cell expression of key transcripts while inhibiting and not inhibiting cell-cell contacts, respectively. However, the relationship between the physical and biological effects actioned by these peptides requires further research to understand the processes involved.

Atomic force microscopy (AFM) is a diverse and widely available technique often employed for the analysis of binding proteins, such as E-cadherin. Previous studies demonstrate the ability to use single molecule force spectroscopy (SMFS) to isolate individual protein adhesions, providing unique insight into the bond mechanics when compared to commonly used ensemble analysis such as surface plasmon resonance (SPR). However, the potential for AFM to be used as a complimentary technique to aid in the development and analysis of novel peptides has not yet been explored. Therefore, the work in this thesis aimed to use a multidisciplinary approach to explore the potential of a unique method for peptide screening using AFM, by probing the influence of Epep and EpepW2R targeting peptides on single molecule E-cadherin adhesions, while conducting complimentary cellular-based assays to probe the peptide mediated response of mESCs.

In this thesis we developed an SMFS AFM system capable of isolating single molecule E-cadherin adhesions between samples and AFM probes functionalised with the extracellular domain of E-cadherin. This system was subsequently used to probe the mechanical response of these samples in the presence of Epep and EpepW2R peptides, providing unique insight into their physical inhibitory effect. In contrast to previous literature, we observed that both peptide sequences were capable of a reversible inhibition of E-cadherin adhesions, with preliminary experiments on mESC monolayers highlighting the potential to develop this approach in future work. Complementary biological assays, such as high-content Operetta imaging, presented a unique response of E14 and Ecad^{-/-} mES cell lines in the expression of key targets, including surface proteins and pluripotency markers, following the addition of Epep and EpepW2R. In summary, this work explored the biophysical impact of E-cadherin targeting peptides, using AFM to observe sensitive responses not previously seen in literature, and investigating potential off-target interactions, thus highlighting the potential for this approach to be used in future peptide screening experiments.

List of Figures

Figure 1.1: **Schematic showing the physical representation of classical type I, desmosomal, and proto-cadherins.** A simplistic comparison of the extracellular and domains and intracellular complexes comprising three different members of the cadherin superfamily. The diagrams do not represent all interactions, but highlight some key differences used in cadherin classification. Figure made using BioRender.⁸

Figure 1.2: **Schematic demonstrating S-dimer and X-dimer conformations of E-cadherin proteins on adjacent cells.** The formation of X-dimers is believed to preface S-dimer formation, and is a vital step to allow smooth remodelling of E-cadherin adhesions between cells. S-dimers are believed to be the more natural and common adhesive conformation of E-cadherin bonds, and represent slip bond characteristics, as opposed to the catch bond characteristics exhibited by X-dimers. Figure made using BioRender.10

Figure 1.3: **A descriptive example F-D curve with an adhesion event.** Additional diagrams along the trace represent the relative cantilever position with regards to the sample surface, with (A) representing the approach or retraction where the cantilever is free from interactions with the sample surface, (B) showing the loading of the cantilever due to contact with the surface to a controlled force maximum resulting in bending of the cantilever, and (C) showing an adhesive force between the cantilever and the surface as the probe is retracted resulting in an eventual rupture of the adhesion which can be analysed to determine the force of the bond formed.24

Figure 2.1: **Schematic of the working principle of a typical AFM system.** The laser incident on the cantilever is used to measure bending of the cantilever which results in a shift of the position of the reflected laser beam on the position sensitive photo detector. Any fluctuations in signal recorded by the photo detector can then be converted into a force value by use of Hooke's law (see Eq. 1).33

Figure 2.2: **Annotated figure of the AFM scanning head.** Schematic of the inner workings of the AFM scanner head for an MFP-3D-SA instrument, as seen in the associated user manual¹⁴⁷.....35

Figure 2.3: **Schematic showing the process of electron transition following absorption and subsequent emission of E-M radiation.** E-M radiation of specific wavelength(s) irradiates the target sample. Electrons at rest in the sample, E_0 , are excited by specific radiation energies that allow transition to higher energy states, such as E_1 or E_2 . This is observed as absorption and is the basis measurement of techniques such as UV-Vis spectrophotometry. Over time the electron will return to the lower energy state, emitting radiation as it does so, thus giving the fluorescence wavelength observed by techniques such as fluorescence microscopy.37

Figure 2.4: **Example graphs showing common graph types obtained from FC analysis:** A) a histogram plot of fluorescence data, and B) an intensity plot showing the comparison of two fluorescence markers within a sample population.....41

Figure 3.1: **Representative schematic of a functionalised AFM system.** Schematic showing a representation of an AFM probe and Si wafer surface functionalised with the extracellular domain of a cadherin protein, in a Ca^{2+} rich environment. The blue disks represent Ca^{2+} ions, corresponding to the calcium dependency of E-cadherin adhesion, with this system shown in a calcium saturated state. This diagram represents the experimental aim of this chapter, as this work shows the development of a system that can measure specific single molecule E-cadherin interactions.44

Figure 3.2: **Schematic representing the extracellular cadherin fragment used for surface functionalisation.** Structure representing the E-cad-Fc molecule used for sample functionalisation. This comprises of the 5 EC domains of E-cadherin bound to a human IgG1 Fc domain. Amino acid sequence analysis via Uniprot highlights a greater fraction of lysine residues in the Fc region when compared to the EC domains, thus indicating adsorption to the surface will be via this region (see section 3.2.2 for further details).45

Figure 3.3: **Overview of the sample preparation process used to functionalise Si wafers and AFM cantilevers with extracellular Ecad-Fc chimeric protein fragment.** 1) Addition of MPTMS by vapour silanisation. The silane group interacts with hydroxyl groups on the sample surface. Condensation of the MPTMS could also occur between adjacent surface bound siloxanes (not shown). 2) The cross-linker AMAS binds to the thiol present in the bound MPTMS molecules. 3) The amine groups present in the

lysine residues in the Fc region of E-cad-Fc molecules binds to the NHS-ester group of the AMAS cross-linker, completing the surface functionalisation.48

Figure 3.4: **Example F-D curves demonstrating the four categories used for analysis.**

A) No events recorded, as seen by an undisturbed contact of the probe and surface, B) non-specific event occurs, as highlighted by a linear adhesion immediately at the sample surface, C) specific adhesion event, highlighted by the presence of a characteristic non-linear adhesion occurring <100 nm from the sample surface with a clear rupture force, D) multiple adhesions shown by the presence of numerous adhesion regions and rupture forces within a single F-D curve.54

Figure 3.5: **Specific adhesion event observed on an F-D curve.** Example F-D curve obtained from an MFP-3D AFM, displaying a specific adhesion event. For all graphs obtained, the approach data is displayed in red, and the retraction in blue.55

Figure 3.6: **Histograms showing the adhesion forces for specific events recorded in Ca²⁺, EGTA, and DECMA-1 buffers following the refined sample preparation process.** The distribution of forces is shown to be relatively unchanged between buffers, as expected for an E-cadherin SMFS system. A minimum of 500 F-D curves were recorded for each buffer condition.58

Figure 3.7: **Inhibition of E-cadherin binding via addition of calcium chelating EGTA buffer, and E-cadherin nAb, DECMA-1, treatment buffer.** Frequencies of each F-D curve category for samples tested in 5mM Ca²⁺ and EGTA buffers, and 50 µg·ml⁻¹ DECMA-1 buffer. This data was acquired as described in section 3.2, showing all analysis categories. A minimum of 500 F-D curves were recorded for each buffer condition.59

Figure 3.8: **Representation of the force distribution of F-D curves following the introduction of an off-target antibody buffer, and sequential buffer changes on the same sample.** Modal force analysis (captioned on figure) was more rigorously calculated using Fdist software, with this analysis available in Appendix 2. Histograms show the force distribution of specific events recorded in Ca²⁺, EGTA, DECMA-1 (E-cad Ab), and N-cad Ab buffer environments. A minimum of 500 F-D curves were

recorded for each buffer condition with forces shown only from the specific adhesions, with N=2 repeats.63

Figure 3.9: **Categorisation of F-D curves using the conditions outlined in section 3.3.2.** Frequency of F-D curves for each of the four categories outlined previously. The dominance of no events, and ideal frequency range of specific events, indicates a working SMFS system. EGTA and DECMA-1 blocking buffers reduces the frequency of specific events, whereas the addition of an N-cadherin targeting antibody does not exhibit any noticeable effect compared to the standard Ca^{2+} environment. Error bars show SD, and a minimum of 500 F-D curves were recorded for each buffer condition, with N=2 repeats.....64

Figure 4.1: **Simple presentation of the Epep and EpepW2R amino acid sequences.** Amino acid sequences shown for both the Epep (top) and EpepW2R (bottom) peptides discussed in section 1.2.2.....71

Figure 4.2: **Initial testing of 10 μM peptide treated functionalised AFM samples demonstrates the ability to sequentially change buffer environments during the experiment.** The data was acquired using a single functionalised sample and AFM tip, with washes using Ca^{2+} buffer conducted prior to the addition of a new buffer environment. The system was left for 30 minutes after changing buffer. Initial peptide testing shows both peptides at 10 μM concentration tested on the same sample. A minimum of 500 F-D curves were recorded for each buffer condition....77

Figure 4.3: **Initial testing of 100 μM peptide treated functionalised AFM samples demonstrates the ability to sequentially change buffer environments during the experiment.** The data was acquired using a single functionalised sample and AFM tip, with washes using Ca^{2+} buffer conducted prior to the addition of a new buffer environment. The system was left for 30 minutes after changing buffer. Initial peptide testing shows both peptides at 100 μM concentration tested on the same sample. A minimum of 500 F-D curves were recorded for each buffer condition....79

Figure 4.4: **Comparison of F-D curves acquired from Epep peptide treatment AFM experiments, and categorised using the method discussed in section 3.2.5.** Sample data was compared to the baseline value determined by the initial Ca^{2+} buffer to

provide a clearer representation of the influence of different buffer environments. The data in these graphs provide a clear comparison of the buffers tested for each analysis category: A) no events, B) non-specific events, C) specific events, and D) multiple events. A minimum of 500 F-D curves were recorded for each buffer condition, with N=3 repeats. All comparisons were made to the initial Ca²⁺ buffer tested with error bars showing standard deviation, and statistical analysis was performed using an average of the tested samples (N=3). Significance is shown as: * = P < 0.05, ** = P < 0.01, *** = P < 0.001, **** = P < 0.0001.....81

Figure 4.5: Comparison of the specific event frequency recorded in each concentration of Epep buffer. A minimum of 500 F-D curves were recorded for each buffer condition, with N=3 repeats. Statistical analysis of the values was performed on the baseline corrected percentages when compared to Ca²⁺ buffer, as seen in Figure 4.4, with comparisons isolated to the ascending Epep concentrations. Error bars show SD, and significance is shown as: NS = no significance, * = P < 0.05, ** = P < 0.01.....82

Figure 4.6: Representation of the distribution of rupture forces seen in specific adhesion events between all buffer conditions tested in the Epep titration experiment. Modal force analysis (captioned on figure) was more rigorously calculated using Fdist software, with this analysis available in Appendix 2. Histograms showing the binding forces observed for specific single molecule adhesions in each experimental buffer seen in the data shown in Figure 4.4. The modal force observed in each buffer environment is shown on the corresponding histogram, calculated using Fdist.85

Figure 4.7: Comparison of F-D curves acquired from EpepW2R peptide treatment AFM experiments and categorised using the method discussed in section 3.2.5. Sample data was compared to the baseline value determined by the initial Ca²⁺ buffer to provide a more clear representation of the influence of different buffer environments. The data in these graphs provide a clear comparison of the buffers tested for each analysis category: A) no events, B) non-specific events, C) specific events, and D) multiple events. All comparisons were made to the initial Ca²⁺ buffer tested, and statistical analysis was performed using an average of the tested samples

(N=2). Error bars show SD, and significance is shown as: * = P < 0.05, ** = P < 0.01, *** = P < 0.001, **** = P < 0.0001.86

Figure 4.8: **Comparison of the specific event frequency recorded in each concentration of EpepW2R buffer.** A minimum of 500 F-D curves were recorded for each buffer condition, with N=2 repeats. Statistical analysis of the values was performed on the baseline corrected percentages when compared to Ca²⁺ buffer, as seen in Figure 4.7, with comparisons isolated to the ascending Epep concentrations. Error bars represent standard deviation between samples and significance is shown as: NS = no significance, * = P < 0.05.89

Figure 4.9: **Distribution of rupture forces seen in specific adhesion events between all buffer conditions tested in the EpepW2R titration experiment.** Modal force analysis (captioned on figure) was more rigorously calculated using Fdist software, with this analysis available in Appendix 2. Histograms showing the binding forces observed for specific single molecule adhesions in each experimental buffer seen in the data shown in Figure 4.7. The modal force observed in each buffer environment is shown on the corresponding histogram, calculated using Fdist.91

Figure 4.10: **Example F-D curves acquired from probing E14 cell monolayers with an Ecad-Fc functionalised AFM probe.** These example curves demonstrate the complexity and sensitivity of testing cell samples, and indicate the increased retraction distance from the surface.94

Figure 4.11: **Initial analysis of AFM-based force experiments on E14 mESCs in Ca²⁺, DECMA-1, and Epep buffers.** Graphs showing the frequency of F-D curves recorded in Ca²⁺, Epep 100 μM, and DECMA-1 buffers. A) Frequencies of all four of the categories used when classifying F-D curves, and B) frequency of specific interactions only for more clear comparison between buffers. Due to the increased time to acquire data a minimum of 100 F-D curves were recorded for each condition.96

Figure 4.12: **Force distribution for F-D curves classified as specific E-cadherin interactions from data seen in Figure 4.11A.** Modal force analysis (captioned on figure) was more rigorously calculated using Fdist software, with this analysis available in Appendix 2. Histograms showing the force distribution of specific

adhesion events recorded in Ca^{2+} , Epep 100 μM , and DECMA-1 buffers. This data was acquired on a E14 cell monolayer with each buffer added sequentially to the same sample. A minimum of 100 F-D curves were recorded for each condition.....97

Figure 5.1: E14 cultures express E-cadherin localised at the cell surface, while Ecad^{-/-} cultures do not express E-cadherin and exhibit a less clustered morphology. A,E) Phase contrast images of E14 and Ecad^{-/-} respectively, in general culture conditions. Scale bars = 200 μm . B - D) Fluorescence microscopy imaging of E14 cultures targeting, nucleus (B, blue), E-cadherin (C, green) and actin (D, red). F - H) Fluorescence microscopy imaging of Ecad^{-/-} cultures targeting nucleus (F, blue), E-cadherin (G, green), and actin (H, red). Scale bars = 100 μm114

Figure 5.2: Confluence of E14 samples depends on seeding density, with seeding of 2,500 cells providing the most representative colony formation after 48 h compared to continuous culture images seen in Figure 5.1. Fluorescence Operetta imaging of E14 cultures maintained for 48 h and stained with DAPI. Initial cell seeding density relating to each image group is shown above the groups of 3 images taken from each sample well, with A) 500 cells, B) 1,000 cells, C) 2,500 cells, D) 5,000 cells, and E) 7,500 cell seeding densities tested. The images taken within each well were selected to represent a variety of locations. Scale bars = 100 μm118

Figure 5.3: E14 cells cultures can be maintained following the addition of Epep, EpepW2R, or DECMA-1 to the culture medium, with Epep and DECMA-1 treated E14 cultures demonstrating a less clustered morphology in comparison to control samples. Brightfield images of E14 cell monolayers in A) regular culture medium, B) culture medium supplemented with 100 μM Epep peptide, C) culture medium supplemented with 100 μM EpepW2R peptide, or D) culture medium supplemented with 100 nM DECMA-1 Ab. Each image is a single FOV taken within a sample well and gives a representative indication of the cultures. Arrows indicate example areas where a loss of tight cluster formation is lost in comparison to the control sample, A. Scale bars = 100 μm120

Figure 5.4: Cell nuclei can be isolated effectively using the Operetta analysis software, although some sensitivity is lost when analysing images with very tight clusters with 3-dimensional cell growth which is successfully accounted for by

applying parameters within the software. An example of the automated analysis conducted within the instrument software. Cell Nuclei were delineated using DAPI staining of the cultures, as shown by the coloured perimeters in the left image. Parameters were added to the analysis software to remove cells that could not be individually identified, such as those highlighted by the red area. The right image shows the cell population used for analysis, with cell clusters removed. Scale bars = 100 μm121

Figure 5.5: Peptide treated E14 cultures demonstrate a change in some of the tested cell characteristics. Bar charts showing the average values for parameters seen in Table 5.4 that displayed a significant change between treatment conditions (N=3), with the individual averages from each repeat shown by the black circles (n=2). .122

Figure 5.6: Selected cell characteristics observed for peptide treated E14 cultures do not demonstrate any change between conditions. These graphs show the remaining parameters supplementary to Figure 5.5 that are shown to have no statistically significant changes between any treatment conditions tested during analysis (N=3, n=2).123

Figure 5.7: Immunostaining and subsequent fluorescence imaging of E14 cultures using the Operetta instrument. Fluorescence imaging of E14 cultures for, A) E-cadherin (yellow), B) N-cadherin (yellow), C) Syndecan-4 (green), D) Syndecan-1 (yellow), and E) Oct-4 (green). Scale bars are 100 μm , and image fluorescence is automatically enhanced by the software for viewing. These images represent a single FOV of a sample well, and are shown to provide insight into the sample fluorescence as quantifiable analysis was performed automatically by the software.125

Figure 5.8: Successful culture and phase contrast imaging of Ecad^{-/-} cell cultures in a range of treated media conditions. Brightfield images corresponding to the fluorescence images shown in Figure 5.9, providing a visual representation of the cell cultures in each of the conditions: A) Regular culture medium, B) culture medium supplemented with 100 μM Epep peptide, C) culture medium supplemented with 100 μM EpepW2R peptide, or D) culture medium supplemented with 100 nM DECMA-1 Ab. Scale bars = 100 μm126

Figure 5.9: **DAPI staining of Ecad^{-/-} cultures via Operetta imaging indicates successful staining and imaging of the cell samples.** Operetta fluorescence images of Ecad^{-/-} cells with DAPI nuclear stain. Each sample well had several different locations imaged to provide a representative analysis of the cell sample, and each image in this figure is selected to show one of these locations for each treatment condition. The samples shown above were cultured for 48 h in, A) regular culture medium, B) culture medium supplemented with 100 μM Epep peptide, C) culture medium supplemented with 100 μM EpepW2R peptide, or D) culture medium supplemented with 100 nM DECMA-1 Ab.127

Figure 5.10: **Peptide treated Ecad^{-/-} cultures demonstrate a change in some of the tested cell characteristics.** Bar charts showing the average values for tested parameters that displayed a significant change between treatment conditions (N=3), with the individual averages from each repeat shown by the black circles (n=2) (summarised in Table 5.5).128

Figure 5.11: **Some cell characteristics observed for peptide treated Ecad^{-/-} cultures do not demonstrate any change between conditions.** Bar charts showing the average values for tested parameters that did not display a significant change between treatment conditions (N=3), with the individual averages from each repeat shown by the black circles (n=2) (summarised for simplicity in Table 5.5).129

Figure 5.12: **Immunostaining and subsequent fluorescence imaging of Ecad^{-/-} cultures using the Operetta instrument was successful in recording the fluorescent probes used, and confirms the continued absence of E-cadherin protein.** Fluorescence imaging of Ecad^{-/-} cultures for, A) E-cadherin (yellow), B) N-cadherin (yellow), C) Syndecan-4 (green), D) Syndecan-1 (Yellow), and E) Oct-4 (green). Scale bars are 100 μm, and image fluorescence is automatically enhanced by the software for viewing. These images represent a single FOV of a sample well, and are shown to provide insight into the sample fluorescence as quantifiable analysis was performed automatically by the software.131

List of Tables

Table 1.1: Ablation of E-cadherin in mESC cultures results shifts the regulation of many cell markers. Adapted from data presented by Soncin et al. (2011), showing some of the cell markers that are observed to change in Ecad ^{-/-} cultures, in comparison to wt mESCs ²⁸ . Key functions associated with the markers are shown to highlight the far-reaching influence of E-cadherin ^{15,23–28}	4
Table 1.2: Effect of selected inhibitors on cell-cell contact and pluripotency transcripts, adapted from work produced by Segal and Ward⁹³. The different inhibitors tested each resulted in a unique expression profile of the observed pluripotency transcripts.....	17
Table 1.3: Brief overview of techniques used for adhesion analysis of biological samples. Each technique follows a different working principle, and some of the key advantages and limitations considered when reviewing each force analysis technique are displayed ^{101,103,105}	21
Table 1.4: Overview of functionalisation interactions that have been seen in AFM force analysis experiments. Key characteristics and limitations are highlighted with regards to their application for AFM studies.	25
Table 3.1: Details of buffer components and their required concentrations when creating EGTA and Ca²⁺ buffers. The buffers were selected to inhibit or promote E-cadherin binding respectively due to the calcium dependence of cadherin adhesion, with concentrations relating to that of solutions commonly used during culture of E-cadherin expressing cells. All buffers were filtered using a 0.45µm syringe filter prior to use in experiments to minimise contaminants.	49
Table 3.2: Comparison of the impact of protein concentration and tip speed on categorisation of F-D curves from E-cadherin functionalised AFM experiments. Frequency (%) of events recorded when testing Si wafers and AFM cantilevers functionalised with different concentrations of E-cadherin protein. Multiple probe approach/retraction speeds were tested for each protein concentration to determine optimal experimental conditions for SMFS.	62

Table 5.1: Media components required for the culture medium of mouse embryonic stem cell lines E14 and Ecad^{-/-}. All components except β -Mercaptoethanol and LIF were added, and the solution was vacuum filtered using a 0.22 μ m filter, before the remaining components were added.....106

Table 5.2: An Overview of the antibodies used for immunostaining. The table shows the different primary and secondary antibodies used for labelling of cell samples, as seen throughout this chapter.109

Table 5.3: Seeding density of sample wells influences final cell number, and alongside Figure 5.2 indicates an ideal seeding density of 2,500 cells per well should be used when preparing experiments. Average cell counts in an individual FOV per well for each seeding condition tested for Operetta experiments. Averages were obtained from 5 separate regions within each sample well (example regions seen in Figure 5.2) and counted automatically via the analysis software discussed in section 5.1.3. Each value corresponds to the average cell number recorded in an individual image.....119

Table 5.4: A summary of the data acquired when comparing E14 cell cultures treated with Epep, EpepW2R, or DECMA-1 supplemented media with regular culture media, showing some significant changes in EpepW2R and DECMA-1 treated samples, but not in Epep treated samples. A comparative analysis of E14 cell cultures treated with peptide containing media for 48 h and imaged using the Operetta instrument. All comparisons made are in relation to regular media cultures. Statistical analysis was performed using an average of the tested samples (N=3), and significance is shown as: NS = no significance, * = P < 0.05, ** = P < 0.01, *** = P < 0.001, **** = P < 0.0001.....124

Table 5.5: Peptide treated Ecad^{-/-} cultures experience a unique response to Epep and EpepW2R peptides when compared to E14 cultures. A comparative analysis of Ecad^{-/-} cell cultures treated with peptide or nAb media for 48 h and imaged using the Operetta instrument. All comparisons made are in relation to regular media cultures. Statistical analysis was performed using an average of the tested samples (N=3), and significance is shown as: NS = no significance, * = P < 0.05.130

Table A1.0.1: Table showing data from FC analysis of E14 cell cultures treated with Epep and EPepW2R peptide media. Collated analysis of E14 cell samples showing the percentage of cells expressing the corresponding targeting fluorophore. Samples were cultured in different treatment media as outlined in the table.174

Table A1.0.2: Table showing data from FC analysis of Ecad^{-/-} cell cultures treated with Epep and EPepW2R peptide media. Collated analysis of Ecad^{-/-} samples from FC experiments, following the same fluorescent panel as seen for E14 cells previously. The values show the percentage of each cell sample that exhibit positive expression of each marker.174

Nomenclature and Abbreviations

AFM	Atomic force microscopy
AJ	Adherens junction
AMAS	N- α -maleimidoacet-oxysuccinimide
Arg (R)	Arginine
BFP	Biomembrane force probe
CPP	Cell penetrating peptide
DAPI	4',6-diamidino-2-phenylindole
DeflInvolS	Deflection inverse optical lever sensitivity
DFS	Dynamic force spectroscopy
DMEM	Dulbecco's modified eagle medium
DMSO	Dimethyl sulpho
E14	E14Tg2a mouse embryonic stem cell line
Ecad ^{-/-}	E-cadherin null mouse embryonic stem cell line
ECM	Extra-cellular matrix
EGTA	Ethylene glycol-bis(β -aminoethyl ether)-N,N,N',N'-tetraacetic acid
E-M radiation	Electro-magnetic radiation
EMT	Epithelial to mesenchymal transition
Epep	Peptide: H-SWELYYP L RANL-NH ₂
EpepW2R	Peptide: H-SRELYYP L RANL-NH ₂
FBS	Fetal bovine serum
F-D curve	Force-distance curve
FOV	Field of view
FS	Forward scatter
GCDR	Gentle cell dissociation reagent
ICC	Immunocytochemistry
iPSC	Induced pluripotent stem cells
LIF	Leukaemia inhibitory factor
LN ₂	Liquid nitrogen
Lys (K)	Lysine
MEM NEAA	Minimum essential medium non-essential amino acids
mESC	Mouse embryonic stem cell
MFP/MFP-3D-SA	Molecular force probe
MPTMS	3-mercaptopropyl trimethoxysilane

NHS	N-Hydroxysuccinimide
OT	Optical tweezers
PBS	Phosphate buffered saline
PFA	Paraformaldehyde
Phe (F)	Phenylalanine
PSD	Power spectral density
SCFS	Single cell force spectroscopy
SMFS	Single molecule force spectroscopy
SPR	Surface plasmon resonance
SS	Side scatter
STM	Scanning tunnelling microscopy
Trp (w)	Tryptophan
Tyr (Y)	Tyrosine
UV	Ultra-violet
VDW	Van der waals
Wt	Wild-type

Chapter 1 - Introduction

The potential of stem cells in therapeutic applications has received an ever-growing interest in recent years, and subsequently *in vitro* stem cell cultures are often used in the development of studies. Stem cells are unspecialised cells that are characterised by perpetual self-renewal (or proliferation) whereby identical daughter cells are produced, and the ability to differentiate into mature adult cells¹. These characteristics can vary between stem cell types, with a more detailed review discussed by Zakrzewski *et al*². Stem cells provide a key approach in many different applications, from basic research into gene expression and function, to medical applications for studying diseases and developing novel diagnostic approaches. There is also ongoing interest into the development of cell-replacement therapies, utilising the self-renewal and differentiative capacity of stem cells to treat damaged or diseased tissues. Recent advancements in stem cell research often relate to the use of pluripotent stem cells (PSCs), which are a type of stem cells characterised as being capable of differentiating into cells within all germ layers, and as such have great potential in the field of regenerative medicine for use in regeneration and repair of different tissues³.

Within PSCs there are two known types available: embryonic stem cells (ESCs) and induced pluripotent stem cells (iPSCs), within each of which multiple cell lines are available. The former, ESCs, are isolated from the inner cell mass during embryonic development, and the latter, iPSCs, are obtained by a process called cell reprogramming. The ability to reprogramme cells to achieve iPSCs is a relatively new technique, with Takahashi *et al*.⁴ identifying four key genes which when simultaneously over-expressed, induced reprogramming of mouse fibroblasts into iPSCs, known commonly as the Yamanaka factors⁴. These approaches provide a diverse selection of cell lines that can be used for studies, however, the process of reprogramming cells still exhibits relatively low conversion efficiency, as discussed in more detail elsewhere⁵. Comparatively, ESCs are commonly cultured *in vitro* and as such there are several well-established cell lines available, particularly for murine ESCs (mESCs), although strict control of culture conditions are required to maintain an undifferentiated state⁶.

Since the initial isolation of mESCs from the inner cell mass of mouse blastocyst in 1981^{7,8}, the available methods for culture of these cell lines has developed greatly. Originally, a feeder layer of mouse embryonic fibroblasts was required to maintain an undifferentiated state of the mESCs in culture, but it is now possible to control cell characteristics in the absence of a feeder layer via the manipulation of culture conditions such as culture medium with targeting molecules^{9,10}. Recently, Mohamet *et al.*¹¹ demonstrated that abrogation of the cell surface protein, E-cadherin, allows for proliferation of mESCs in shake flask bioreactors. This was in response to the limitations surrounding mESC expansion, and exploits the diverse and critical role of cadherin proteins in the maintenance of mESC pluripotency. Cadherins are proteins that are instrumental in the formation and stabilisation of cell-cell contacts, while simultaneously exhibiting influence in cell expression including maintenance of pluripotency in mESCs. It is therefore unsurprising that the use of cadherins as a target for manipulating cell function is common in literature, and as such the development of novel targeting peptides to modify cadherin behaviour, shown by Devemy and Blaschuk, provides a tailored approach for affecting cell function¹².

The close relationship of mESC fate and cadherin expression is well-observed within literature, and there is great interest in the ability to control mESC fate by targeting specific proteins. Therefore, the focus of the work in this thesis relates to the development of an analysis technique to screen the influence of novel peptide sequences on cell cultures, and probe specific mechanical and biological characteristics. In particular, E-cadherin protein expressed by mESCs will be targeted using novel peptides, with the physical analysis of single molecular interactions supplemented with biological understanding of the protein to explore these key concepts.

1.1 Cadherins in mESCs

The importance of pluripotent stem cells, such as embryonic stem cells (ESCs), is recognised throughout a wide range of research fields. The ability of these cells to differentiate to all of the three primary germ layers (pluripotency) accounts for their diverse application in research, and linked with their self-renewal capabilities it is clear why they receive such attention as they can be adapted to an *in vitro* environment for long term culture¹³. mESCs are now recognised as naïve in their pluripotency, as opposed to cells in the alternative primed state such as epiblast-derived stem cells (EpiSCs)¹⁴. This delineation is a relatively recent development in the understanding of ES cells, and corresponds to the specific stage of embryonic development that the cells were collected, with differences in morphological and phenotypic states. Transition from naïve to primed pluripotency states is often concurrent with epithelial to mesenchymal transition, and subsequently inhibition of E-cadherin expression¹⁵. Probing the underlying mechanisms governing pluripotency is thus key to the use of mESCs as disease models or as clinical therapies.

Since their establishment in 1981 by Evans and Kaufman⁸, ESCs have received great interest as the subject of regenerative medicine, tissue engineering, and biomedical research, in particular in understanding methods of controlling pluripotency of cultures *in vitro* even when attempting large scale culture¹⁶. Recent examples demonstrate directed cell behaviour in tissue engineering approaches, and manipulation and development of biomaterials, by utilising cadherin characteristics^{17,18}. To preserve the naïve state of mESCs *in vitro*, leukaemia inhibitory factor (LIF) is often added to culture medium, with E-cadherin-catenin complexes essential to enabling LIF-dependent self-renewal mechanisms and preventing spontaneous differentiation¹⁹. Consistent with this, mESCs that are mutated to knockout E-cadherin expression (*Ecad*^{-/-}) demonstrate a shift in morphology and signalling pathways such that they align more closely with primed lineages, and embryos containing *Ecad*^{-/-} cells fail to develop past the compaction stage and ultimately are not viable²⁰. Interestingly, *Ecad*^{-/-} cultures demonstrate a loss of the LIF dependent pluripotency seen in wild-type (wt) mESCS, and instead rely on Activin/Nodal signalling pathways to maintain pluripotency, similar to that

observed in human ESCs^{21,22}. This is associated with a drastic shift in the expression of key cell markers, as discussed in detail by Soncin *et al.*¹³, with Table 1.1 highlighting a small number of the markers shown to change following the ablation of E-cadherin²⁸. It is unsurprising therefore that E-cadherin persists as a key adhesion protein throughout the life cycle of mESCs, and highlights its use as a target for manipulating or stabilising ESC cultures.

Due to the vast number of cell functions shown to be mediated, at least in part, by cadherin proteins, it is unsurprising that this protein superfamily has been an important focus throughout literature. The distinctive domains observed in classical cadherins are often attributed with different roles, however ongoing research continually suggests a much more interconnected network of individual processes to

Table 1.1: Ablation of E-cadherin in mESC cultures results shifts the regulation of many cell markers. Adapted from data presented by Soncin et al. (2011), showing some of the cell markers that are observed to change in Ecad^{-/-} cultures, in comparison to wt mESCs²⁸. Key functions associated with the markers are shown to highlight the far-reaching influence of E-cadherin^{15,23-28}.

Cell Marker	Upregulated/Downregulated	Associated Functions
FGF5	Upregulated	Loss of stemness, differentiation ²³
CD44	Upregulated	Cancer stem-cell-like marker ¹⁵
Serpinb9	Upregulated	Apoptosis, differentiation ¹³
Wnt5b	Upregulated	Pluripotency ¹³
Nr0b1/Dax1	Downregulated	Self-renewal, inhibition of differentiation ²⁴
Esrrb	Downregulated	Self-renewal ²³
Tbx3	Downregulated	Wnt-signalling, differentiation ²⁵
Nr5a2	Downregulated	Cell fate ²⁶
Klf4	Downregulated	Pluripotency ²⁷

implement the resulting change in cell behaviour²⁹. One prime example of this is the study of cadherin adhesion orientations, as there is now abundant evidence that the cytoplasmic tail is an important mediator of cadherin junctions, despite the ability for the extracellular domains to bind even in the absence of the intracellular region³⁰. A reverse relationship is also observed, where the lack of mechanical interaction in the EC domains alters the protein recruitment and subsequent cellular response from the cytoplasmic region³¹. These studies have helped to extract complex cadherin mechanisms for mediating a wide range of cell properties, and have highlighted the ability for both biological and physical characteristics to manipulate properties such as cell signalling and structure^{32,33}. For example, the cadherin-catenin complexes formed by the cytoplasmic tail of classical cadherins are shown to influence the Hippo signalling pathway by modulation of Yes-associated protein (YAP), with this relationship suggested to be responsible for downstream regulation of cell proliferation³⁴. Throughout literature it is evident that there is great importance in considering both the biological and the physical characteristics of cadherin proteins, and as such there is also great interest in mechanical based analysis of protein interactions, as discussed in more detail later in this chapter.

When studying E-cadherin in mESCs it is prudent, and indeed necessary, to also consider associated molecules such as the catenin complexes already mentioned, and other related adhesion molecules such as Syndecans. The formation of cadherin-catenin complexes is a well-studied interaction due to the vast impact it can have on cell function¹⁹. Studies focussing on the regulation of pluripotency in stem cells indicate recruited proteins such as β -catenin can impact the activity of the OCT4 pluripotency pathway, and can bind to the actin cytoskeleton by the intermediate protein, α -catenin, to provide stability to adherens junctions³⁵. Furthermore, these proteins are attributed with regulating several genes via activation, or conversely lack of activation due to competing localisation, of signalling pathways such as the canonical Wnt pathway³⁶. Syndecan-1 is implicated in cell processes such as formation of cell-cell and cell-ECM adhesions and epithelial to mesenchymal transitions (EMT), and is closely associated with E-cadherin through these systems. The Syndecan family represent transmembrane proteins with extra-cellular, intra-

cellar, and transmembrane regions, and again are implicated in cell functions such as proliferation and differentiation³⁷. However, unlike E-cadherin it has been reported that Syndecan-1 knockout mice do not exhibit any obvious abnormalities except for impaired wound healing and epithelialisation, and are still considered relatively healthy. This suggests the role of Syndecan-1 is dependent on the presence of other signalling molecules, and in research it is often used as a stem cell marker due to its relationship with the proliferative and differentiation mechanisms of cells³⁸. As discussed in more detail in section 1.2.1, the influence of local proteins like Syndecans and processes such as glycosylation on cis dimer formation show vast potential for the mediation of cell mechanisms. The relationship of such molecules with cadherins may therefore explain some of the intricate functions associated with adhesion formation and present a potential in-direct target for manipulation of cell function.

The mechanisms in which E-cadherin is involved are diverse and often critical to cell survival and maintenance. As such it is unsurprising that we do not yet fully understand the adhesions formed at cell-cell junctions and at intracellular complexes, and subsequently the pathways and actions undertaken throughout E-cadherin processes. Due to the abundance of cell lineages that utilise cadherin proteins, and their diverse functions, it is important to consider individual analysis of E-cadherin environments. With regards to mESCs E-cadherin is commonly expressed, and therefore particular focus is given to this protein due to the importance of mESCs in the fields of regenerative medicine and therapy development, and within the scope of this thesis. However, it is important to view this protein within the scope of the cadherin superfamily, and as such this will be the focus of the next section.

1.2 Cell Adhesion and the Cadherin Superfamily

Cell functions and interactions rely heavily on the adhesion processes available to the cell, impacting the development, maintenance, and communication of tissues. These interactions can be adhesions between neighbouring cells, or the extra-cellular matrix (ECM) present in the cell environment, and are propagated by unique adhesion molecules. There are several groups of adhesion molecules commonly observed, such as integrins, selectins, and cadherins, each of which binds to corresponding ligands and impacts cell characteristics³⁹.

Cadherins, named due to their calcium dependent adhesion, are recognised as key cell-cell adhesion molecules and have been implicated in impacting vital cell functions throughout literature since their discovery by Yoshida and Takeichi in 1982⁴⁰. Starting with the well-known molecules E-cadherin, N-cadherin, and P-cadherin, named due to the main tissues in which they were first found (epithelial, neural, and placental, respectively), countless researchers have considered the role of cadherin molecules in an ever-extending range of processes from a critical role in embryonic development, to potential cancer suppression proteins⁴¹. As research progressed many more members of the cadherin family were discovered, and the original proteins were even found to be expressed in various tissue types, resulting in the cadherin superfamily recognised today. Although there are several classifications of cadherins within the superfamily, the most salient feature connecting each of them is the presence of a variable number of repeated domains ≈ 110 amino acids in size in the extracellular cadherin (EC) component, intercalated with calcium binding sites which act to rigidify the protein and control binding activity^{32,42}. Further structure-based comparison divides the cadherin superfamily into several categories including classical cadherins, protocadherins, and desmosomal cadherins (see Figure 1.1), with a diverse range of functions associated with each. Therefore, due to the focus of this work on mESCs, and their known cadherin expression, the focus of this work will be restricted to classical cadherins, and in particular the prototypical member of this category, E-cadherin.

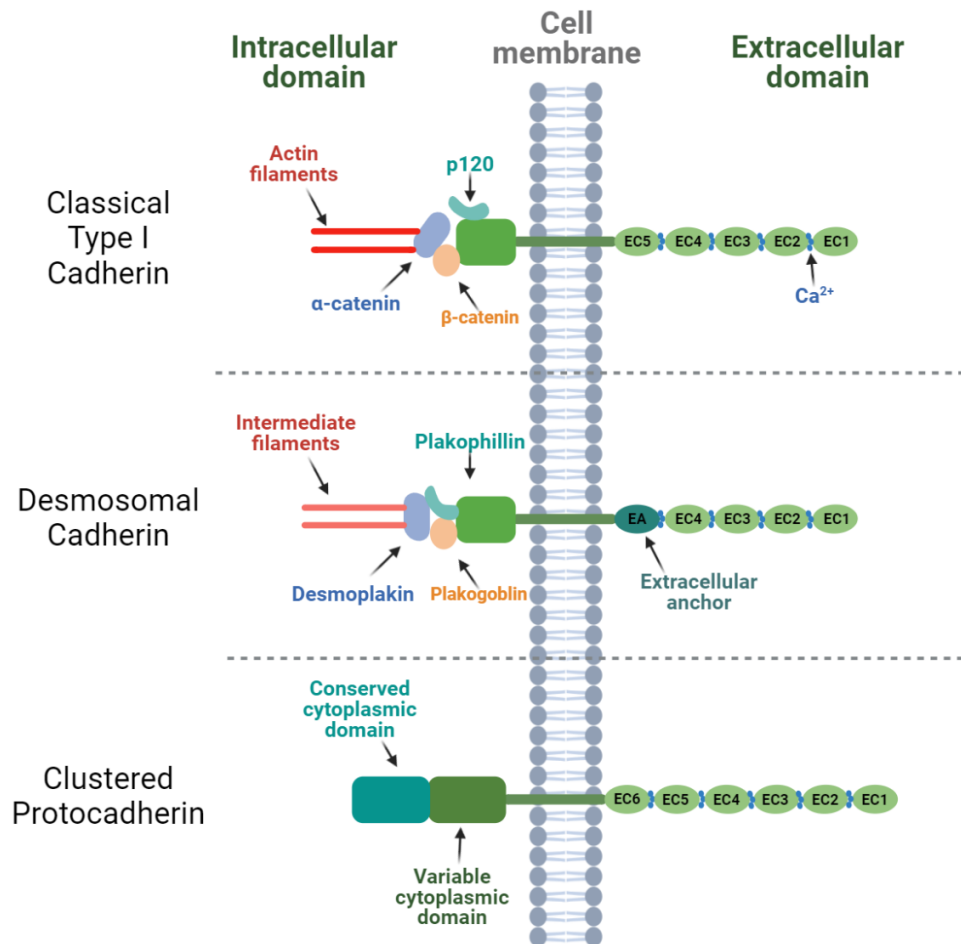


Figure 1.1: Schematic showing the physical representation of classical type I, desmosomal, and proto-cadherins. A simplistic comparison of the extracellular and domains and intracellular complexes comprising three different members of the cadherin superfamily. The diagrams do not represent all interactions, but highlight some key differences used in cadherin classification. Figure made using BioRender.

Members of the classical cadherin category are single pass transmembrane glycoproteins that contain five EC domains (EC1-5) that are highly conserved, with intracellular regions that act to strengthen mechanical adhesions and regulate cell signalling functions. Cell-cell adhesions are principally formed via interactions at cell junctions between the same cadherin type on adjacent surfaces, known as homophilic bonds, and are stabilised by interactions with the actin cytoskeleton and surrounding proteins such as β -catenin and p120-catenin^{32,33}. The diversity of tissues expressing classical cadherins rationalises the plethora of cell functions that are impacted by these proteins, such as proliferation, motility, and gene expression. The presence of cadherin-based adhesion is also essential for driving tissue morphogenesis during early development^{43,44}.

Of all proteins within the classical cadherin family, E-cadherin is perhaps the most well studied. Since its discovery in the 1980's there has been ongoing research into

understanding the structure and function of this protein, including its use as a therapeutic target. However, despite the abundance of research already conducted, the precise biophysical mechanisms underpinning key functions is still not fully understood. This is in part due to the wide range of cell processes influenced by E-cadherin, which are often underpinned by complex biological pathways. The following section therefore aims to provide an overview of our understanding of E-cadherin, highlighting the structure of the protein and key associated complexes and functions.

1.2.1 *Biological and Mechanical Overview of the E-cadherin Protein*

As mentioned, E-cadherin is a member of the classical cadherin group, meaning it is a single pass transmembrane glycoprotein with three distinct biological regions: extracellular, intracellular, and transmembrane. The extracellular region consists of five sequential domains, EC1-5, which are critical for cadherin-cadherin binding, and display a high degree of homogeneity^{31,45}. It is believed the extracellular structure of E-cadherin is approximately 20 – 25 nm in length, and adhesion occurs via interaction between highly conserved tryptophan residues in position 2 (Trp2) on the extracellular region of adjacent proteins, resulting in overlap of the individual EC domains, as seen in Figure 1.2^{46–48}. The intracellular region, known as the cytoplasmic tail, is a highly conserved complex capable of interacting with cytoplasmic proteins such as β -catenin, p120-catenin, and α -catenin, to support mechanical binding and transmit biological signalling processes. Together, these regions form adherens junctions (AJ) through their extracellular binding to adjacent cells, and intracellular binding to cytoplasmic components such as catenins, as seen in Figure 1.2.

These junctions, and the constituent interactions they consist of, allow manipulation of many cell processes including the direct reorganisation of the actin cytoskeleton, shown to be mediated by signalling from cadherin adhesions formed through the cadherin-catenin complexes⁴⁹. In epithelial tissues the formation of adherens junctions (AJs) is shown to be crucial for embryogenesis and homeostasis, as loss of these adhesions disrupts tissue architecture and influences cell signalling^{50,51}. The clustering of cadherin-catenin complexes is a key characteristic observed in

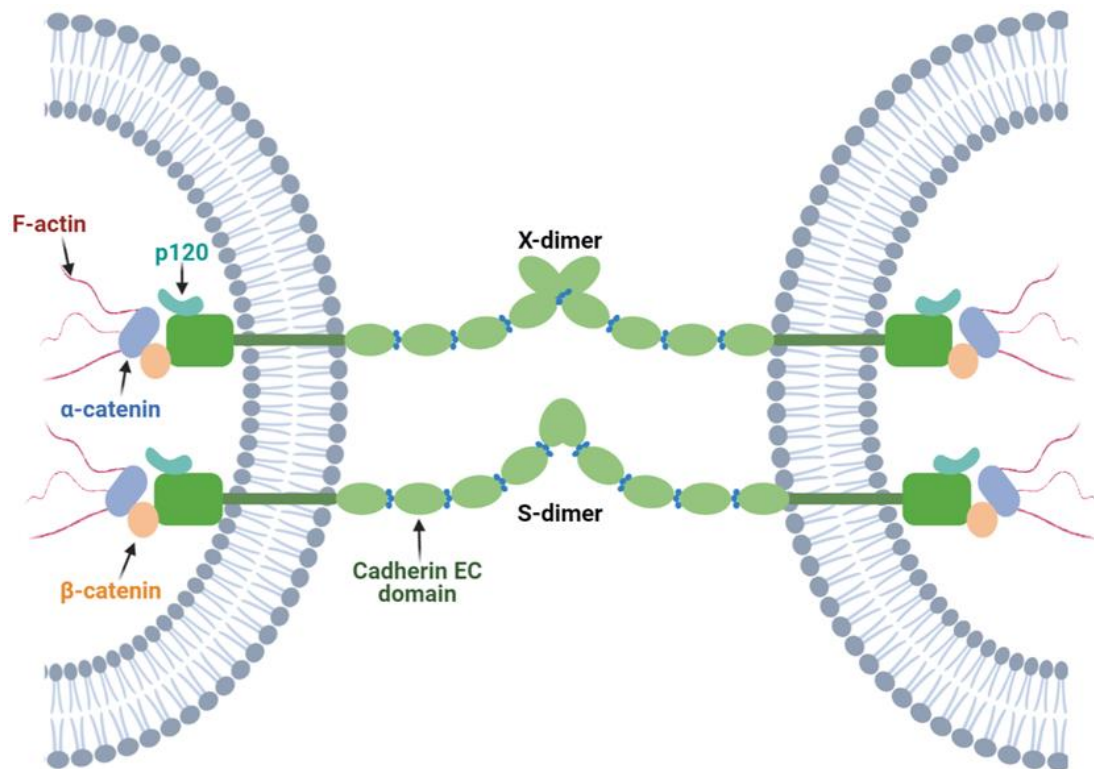


Figure 1.2: *Schematic demonstrating S-dimer and X-dimer conformations of E-cadherin proteins on adjacent cells. The formation of X-dimers is believed to preface S-dimer formation, and is a vital step to allow smooth remodelling of E-cadherin adhesions between cells. S-dimers are believed to be the more natural and common adhesive conformation of E-cadherin bonds, and represent slip bond characteristics, as opposed to the catch bond characteristics exhibited by X-dimers. Figure made using BioRender.*

monolayer cell culture, linking not only to a strengthened cell-cell adhesion, but also to the formation of cell polarisation. Epithelial cells are considered polarised due to molecularly distinct domains along different lengths of their plasma membrane, relating to the interior (basal) and exterior (apical) face of the cell⁵². As epithelial cells act as a lining for organs, the environment observed by the external face of the cell differs greatly from that within, leading to a requirement of such polarisation⁵³. Recent studies show that E-cadherin co-ordinates epidermal cell polarisation with adherens junctions to isolate formation of tight junctions to the apical cell layer. Tight junctions are connections between epithelial cells which form the continuous barrier between cells, regulating movement of substances across the epithelium, a vital function in the regulation of nutrient transfer and protection of interstitial tissues^{54,55}.

The cadherin-catenin bonds formed by E-cadherin are complex, and only with relatively recent publications have they begun to be properly understood. It has long been known that the cytoplasmic tail of E-cadherin binds with p120- and β-catenin,

the latter of which in turn binds to α -catenin^{56,57}. Due to the known ability for α -catenin to independently bind to F-actin, this complex was assumed to be the link between E-cadherin and the actin cytoskeleton. However, this was not the process observed *in vitro*, whereby it was seen that the cadherin-catenin complex exhibited a much lower affinity for F-actin than the α -catenin protein alone^{58,59}. It has since been observed that the application of a load force similar to that present in physiological conditions alters the bond mechanics of extracellular E-cadherin adhesions, such that a greater strength can be observed when under load, a biological phenomenon known as catch bonding⁶⁰. We now understand that E-cadherin can at times display catch bonds in addition to the more classical slip bonds whereby bond strength decreases under load, and, during transition between these, ideal bonds can also be observed where the interaction is insensitive to force. It has been proposed that these bonds occur as E-cadherin adhesions can form multiple different structures, each exhibiting different kinetic and mechanical properties⁶¹⁻⁶³.

The bonds formed by E-cadherin can be classified as either *trans* or *cis*, depending on if the connection is between proteins on adjacent cells or on the same cell, respectively. First considering the *trans* binding regimes, both strand-swap dimerisation and X-dimerisation have been observed. It is seen that these conformations are formed by interaction of opposing ectodomains, and exhibit distinct structural differences⁶⁴. Strand-swap dimers (S-dimer) have a higher affinity than their X-dimer counterparts, whereby the Trp2 residue present in the extracellular binding domain is accepted by a hydrophobic pocket in the EC1 domain on their adhesive partner as part of a mutual exchange, and is a crucial process for cadherin adhesion^{61,64,65}. The importance of this interaction is highlighted by previous publications working to replace the Trp2 residue with alanine, in doing so revealing a weak localisation to cell-cell junctions and near total loss of cadherin mediated adhesion due to the absence of Trp2⁶⁶. The S-dimer bond mechanism is shown to exhibit slip-bond characteristics when subjected to load, although evidence suggests a change of bond mechanism when undergoing conformational changes to X-dimer bond structure⁶⁷.

Again, shown to be related to the EC1 and EC2 domains of the extracellular region, the aforementioned X-dimers are now an accepted conformation for E-cadherin adhesion, but with lower affinity than S-dimers. Formed via intermolecular interactions at the EC1 and EC2 domain junctions, the X-dimer is now credited as an important intermediate for S-dimerisation, that reduces activation energy of the more stable S-dimer formation. Furthermore, the catch-bond characteristics exhibited by X-dimers highlights the adaptability and complex nature of E-cadherin adhesions, with some suggesting a third bond category, ideal, being shown during the conformational change between S- and X-dimers^{64,68}. However, despite observation of these adhesions, the method by which conformational changes occur, and their impact on biophysical characteristics of the protein and cell, is still not fully understood. Techniques that can vary force, and the application of force at different rates, have lent themselves to studying the importance of binding mechanisms, as the unique ability to isolate mechanical interactions allows for the calculation of bond strengths formed between molecules. This allows for the mechanical response of biological targets to be recorded in a variety of experimental environments, with the use of varied loading rates or adhesion frequency to probe the energy landscape and binding affinity of molecules with some key examples will be discussed in more detail in section 1.3.

Analysis of S- and X-dimer bonds performed using force measurements in cadherin extracellular domains has revealed an increased average rupture force for the X-dimer variant compared to the S-dimer orientation, despite the lower affinity for this conformation. Previous studies commonly suggest a rupture force for S-dimers of ≈ 30 pN, and for X-dimers ≈ 50 pN, as determined by single molecule bond rupture experiments^{69,70}. This discrepancy is now believed to be as a consequence of the change in bond-type between the interactions, with the catch bond mechanism of the X-dimer resulting in an increased rupture force in the single molecule analysis experiments, with variation seen depending on loading rate⁶⁸. It was highlighted that the translation of this finding to cell-cell junctions *in vivo* may not be trivial, as the complex adhesion processes observed may alter bond affinities and mechanisms. Instead, it was proposed that it may be prudent to consider the roles these bonds

may have in different tissues, such as static and elastic environments⁶¹. It is clear however that adhesions formed by E-cadherin molecules are diverse in nature, and research is ongoing to help understand the form and function of these biophysical bonds and their associated binding partners³⁰.

Further to the formation of cell-cell adhesions, *cis* interaction of E-cadherin proteins has also been observed. Whereas S- and X-dimers are formed by proteins on opposing cells, *cis* dimer formation instead relates to interactions between cadherins on the same cell surface. This is achieved through the EC1 and EC2 domains on neighbouring proteins, which form a relatively weak adhesion that is believed to primarily help to form cadherin clusters to stabilise intercellular junctions⁶⁰. Following *in silico* simulations it was proposed that formation of *cis* dimers is prefaced by increased rigidity due to *trans* dimer formation, allowing formation of clusters at cell junctions⁷¹, although evidence demonstrating clustering of non-adherent cadherins may question the validity of this conclusion⁷². Glycosylation of the E-cadherin ectodomain is another important factor in *cis* dimer formation^{73,74}, but unfortunately the exact mechanisms underpinning this relationship are not yet understood. Computational models of cadherin clustering were developed to account for the glycosylation of the extracellular domains, and attempted to derive a kinetic model for *cis* dimer formation that was suggested to be regulated by glycosylation⁷⁵. This represents a small branch of the potential factors for understanding and controlling cadherin function, specifically relating to bond formation and *cis* interactions. Indeed, the molecular role of *cis* dimers in cadherin function is not fully understood, but ongoing research exposes the involvement of adjacent cellular molecules such as catenins⁷⁶, integrins⁷⁷, and syndecans⁷⁸ in cadherin mechanisms, and although there is still uncertainty regarding the formation and effect of *cis* bonds it is a well-accepted conformation of protein adhesion that further expands our understanding of the biological processes^{60,74,75}.

1.2.2 Peptide Interactions with E-cadherin

One prominent example of the ongoing development and application of targeting peptides is in the field of oncology. As discussed more thoroughly by Kalmouni *et al.*, use of cell-penetrating peptides as a novel and effective transport system has been

developed to overcome the limitations currently hampering therapeutics⁷⁹. Despite ongoing recognition of the potential benefits of biomacromolecules such as proteins in drug development, there exists a number of common barriers to their application. Often the size and hydrophobicity of the molecule hinders their ability to effectively target the location of interest, particularly when required to cross the cell membrane⁸⁰. To overcome this, researchers have turned to the development of cell-penetrating peptides (CPPs). These small peptide sequences can be tailored to help direct therapeutics, potentially allowing intracellular targeting such as that proposed by Hoffman *et al.* for the development of a system capable of identifying druggable intracellular targets⁸⁰⁻⁸².

Natural and synthetic molecules are often used to understand and manipulate cell functions. This involves the use of appropriate molecules to effect a desired change in a target, or conversely to assess the resulting change in cellular behaviour after interaction with the targeting molecule. The subsequent change of cellular characteristics provides insight into the relationships underpinning the observed interactions. This principle is imperative to current biological research, with active molecules used unanimously to supplement culture medium and aid *in vitro* culture and experimentation of cell lines⁸³⁻⁸⁵. However, as research develops there also appears an increasing need to fully define the culture medium of cell lines, defining the active components within biologically complex and undefined serum, and replacing these molecules with a well-defined protein or peptide to mimic the activity or allow tuneable cell interactions⁸⁶.

Studies focussing on the role of E-cadherin in mESCs have revealed the significance of its biophysical interactions and subsequent cell adhesion complexes. As mentioned previously mechanisms such as proliferation, pluripotency, cell signalling, and tissue morphogenesis are all linked via E-cadherin, and other molecules recruited at E-cadherin adhesion sites may help to influence cell behaviour as a result²². Novel peptide molecules represent one area which many believe holds great promise for the targeting and manipulation of E-cadherin mediated processes, with ongoing development of both research-based and clinical-based sequences.

Oncology studies account for a large proportion of this research due to the prevalence of E-cadherin in cancer development and metastasis⁸⁷. The presence of adherens junctions and the associated cell polarity provide clear barriers to tumour progression, and as such events such as ablation of cell-cell adhesions and induction of EMT processes often occur throughout tumour development, progression, and metastasis^{88,89}. These are functions in which E-cadherin has a primary role, and therefore is an obvious potential target for delivery of therapies. One such approach presented by Figueiredo *et al.*⁹⁰ targets the E-cadherin encoding gene (CDH1) as a method of probing the underlying mechanisms involved in hereditary gastric cancer⁹⁰. Similarly, Battistini *et al.*⁹¹ present a potential approach to regulate cadherin function in cancers expressing E-cadherin, via use of an intermembrane protease to promote shedding of the extracellular domain of E-cadherin⁹¹. Song *et al.*⁹² have provided a review of E-cadherin targeting with small molecules for cancer treatment, that can be viewed for further information⁹².

Due to the therapeutic potential and subsequent prevalence of mESCs in research, it is unsurprising that similar approaches have been studied to aid in the culture and maintenance of cell cultures *in vitro*. As mentioned in section 1.1, there is particular interest in the ability to scale up the culture of mESCs while maintaining pluripotency, and the introduction of E-cadherin targeting sequences is one method considered to help achieve this¹⁶. Studies have shown that it is possible to culture mESCs in large scale bioreactors when treated with the E-cadherin targeting antibody, DECMA-1. This antibody is shown to bind specifically to the extracellular binding domain of E-cadherin, thus inhibiting the binding function of the protein. Mohamet *et al.*¹¹ report that abrogation of E-cadherin contacts in mESC cultures via the addition of neutralising DECMA-1 antibody, or via E-cadherin gene knockout, results in a near single cell suspension of ES cells without the need for addition media supplements³⁶. However the viability of this for routine culture is questionable due to the large cost implications and vast alterations in biological signalling¹¹. As manipulation of antibodies is complex and unreliable due to the off-target influences it may incur, the introduction of defined peptide sequences may therefore provide a more practical alternative. Leading to the ongoing development of novel peptides for targeting of

E-cadherin, with the aim of probing the function and processes of E-cadherin mechanisms to better understand and therefore influence fundamental cell behaviour.

One prominent recent example is the determination of a dual E-/N-cadherin antagonist sequence by Devemy and Blaschuk (2009)¹², whereby phage display was used to identify potential therapeutics to influence biological processes. This resulted in a phage clone capable of interacting with the extracellular domain of the cadherin protein, similar to the well-known DECMA-1 antibody. Interestingly, all isolated sequences were also shown to bind the EC domain of human N-cadherin protein, likely due to the high conservation of EC1-2 domains between proteins, attributed as the prominent binding region for classical cadherins⁹³. From this, one sequence that was displayed throughout several isolated phage clones was synthesised and labelled 'Epep', with the amino acid sequence H-SWELYPLRANL-NH₂. This peptide sequence was shown to bind to human E- and N-cadherin EC domains, and disrupted cadherin expressing cell monolayers of cell lines MCF-7 and MDA-MB435. Subsequent work by Segal and Ward adapted the original Epep sequence via single amino acid substitutions, and probed their effect on mouse ES cell lines. This work demonstrated that the basic Epep sequence, and many of the modified analogues, interact with mESCs as well as the previously tested human cell lines.

Upon studying the effect of the modified Epep sequences on mESCs alongside the E-cadherin targeting DECMA-1 antibody, Segal and Ward noted that the inhibitory effect observed with Epep was lost following some of the single amino acid changes. Particularly when changing the Trp2 residue of the original sequence, they recorded no observed loss of cell-cell contact in cell monolayers⁹³. This analysis process was adopted throughout their work with significant differences noted between treatments, particularly when comparing the effects of the peptides to those of the DECMA-1 antibody. An indication of the diverse range of responses available to mESCs following inhibition of E-cadherin is seen in previous studies of Ecad^{-/-} cell cultures, whereby the abrogation of E-cadherin expression results in maintenance of cell pluripotency via the Activin/Nodal pathway. These studies, alongside the recent use of Epep variations, led to the conclusion that the type of E-cadherin inhibitor

Table 1.2: Effect of selected inhibitors on cell-cell contact and pluripotency transcripts, adapted from work produced by Segal and Ward⁹³. The different inhibitors tested each resulted in a unique expression profile of the observed pluripotency transcripts.

Inhibitor	Abrogation of cell contacts	Loss of pStat3	Loss of Nanog	Loss of Klf4	Loss of Esrrb	Loss of Tbx3	Loss of Nr0b1	Loss of Nr5a2
DECMA-1	Yes	Yes	No	Yes	No	No	Yes	Yes
Epep	Yes	Yes	Yes	Yes	Yes	Yes	Yes	Yes
EpepW2R	No	No	Yes	No	No	Yes	Yes	Yes

applied to mESC cultures affects the cellular phenotype and signalling profile observed as summarised in Table 1.2⁹³, and highlights the ability to influence these processes via short bespoke peptide chains as an exciting prospect for future work.

Segal and Ward discussed several characteristics of interest that can be potentially tailored by modifying the Epep sequence, such as the ability to abrogate cell-cell contact, their influence on cell signalling, and physical characteristics, such as solubility and binding affinity⁹³. The peptide sequences developed by Segal and Ward were chosen such that they preserved, to some degree, their aqueous solubility. This is a crucial characteristic when considering potential applications of the peptide sequences, as an insoluble sequence would introduce potentially insurmountable challenges in the use of the product. Within this criteria several key variations were highlighted, with one particular analogue being the EpepW2R peptide discussed previously, due to the importance of the Trp2 residue in the formation of homotypic E-cadherin bonds^{65,93}. Subsequently, it is perhaps unsurprising that following the exchange of the Trp residue, the EpepW2R sequence was not found to abrogate cell-cell contact when assessed via phase contrast imaging of cell monolayers. However, analysis of the mESC cultures following a 24 h treatment with EpepW2R indicates a unique transcript expression profile compared to that seen in Epep or DECMA-1 treated samples (see Table 1.2).

It is well accepted that formation of strand swap dimers during adhesion of type I classical cadherins is a critical initial stage during bond formation, relying on the adhesion mediated by the Trp2 residue and corresponding hydrophobic pocket that is exchanged between interacting molecules^{67,94,95}. It is this characteristic residue that is the proposed target of the Epep sequence, with the presence of the Trp2 residue in the peptide allowing population of the hydrophobic pocket, and subsequently preventing interaction between adjacent cadherin molecules.

However, if this hypothesis is correct, the mechanism by which the EpepW2R sequence induces changes in the expression of cell markers is not fully understood, and could indicate off-target binding or a weaker affinity for the binding residue of the cadherin molecule.

This work represents the initial stages of testing, and more thorough and quantifiable assessments would be required to better understand the influence of the novel sequences. However, the implications of determining a peptide sequence capable of binding E-cadherin and subsequently influencing cell behaviour are boundless, not least due to the potential to modify the sequence to selectively manipulate processes for the maintenance and study of mESC cultures.

1.3 Probing Mechanical Characteristics of E-cadherin

The plethora of functions mediated by E-cadherin, and the complex response observed when testing targeting molecules, shows the importance of reviewing both biological and physical characteristics. This relies on use of complimentary techniques to probe the resulting response to selected culture conditions, and over time many approaches have been taken to attempt to fully understand the individual processes attributed to E-cadherin. Molecular biology-based techniques, such as that seen in section 1.1 whereby expression of the binding partners to the cytoplasmic tail of E-cadherin were systematically perturbed, demonstrate the powerful manipulation possible with methods such as the development of knockout cell lines and inhibition of cellular signalling. These methods are crucial to our understanding of E-cadherin processes and continue to provide an effective basis for teasing apart specific pathways such as the cadherin-catenin complexes^{96,97}.

There is ever-growing evidence of the biomechanical influence of cell adhesion proteins, which are continually recognised for their ability to influence cell behaviour in response to both biological and mechanical cues^{98,99}. Many previous studies use averaged ensemble measurements to probe protein mechanics, which can fail to elucidate the diverse interactions that may be associated with biological proteins¹⁰⁰. This explains the need for sensitive force measurement techniques that are capable of probing individual interactions between molecules, helping to more accurately represent the complex underlying relationships that may be lost in ensemble measurements.

There are now many exciting techniques available for force analysis experiments, with ongoing developments to adapt and improve these techniques for application with a wide range of biological targets. The procedure selected often depends on the force regime being observed, and the experimental factors considered when planning the work, such as time scale or sample environment¹⁰¹. Table 1.3 provides a brief comparison of several key characteristics of some common force analysis techniques, AFM, optical tweezers (OT), and bioforce probe (BFP), with particular focus on single molecule or single cell interaction analysis, such that they could be used to assess cadherin interactions. AFM has been widely applied for cadherin

interaction analysis, and is perhaps one of the most versatile techniques available, allowing testing of functionalised instrument cantilevers and sample surfaces as well as biological samples. This technique also boasts a relatively high maximum force around 10^4 pN, although it is not as capable at measuring smaller sub-pN forces and requires physical contact with the sample surface; however, a high spatial and force resolution allows for in-depth analysis of forces over a sensitive sample surface¹⁰². In contrast, OT allow for a more sensitive force measurement, down to around 0.1 pN, however this is traded with a lower maximum force value of around 100 pN¹⁰³. A key difference for this technique when compared to AFM is that samples are required to be in suspension for force analysis, as OT rely on a highly focussed laser to 'trap' a particle of interest. This is ideal to supplement samples that the contact-based AFM technique would struggle to test, and demonstrates the need to carefully consider experimental conditions to select an appropriate method. The final technique mentioned, BFP, relies on micropipette manipulation of a single cell, and features the largest theoretical force range of the three instruments, with around 0.1 – 1000 pN¹⁰⁴. The system also allows for an adjustable loading rate on the sample to refine interaction conditions, and as such is an excellent technique employed for investigations of biological interfaces. However, many of these systems are hindered by an inferior spatial resolution when compared to AFM, are not commercially available, and at times report that the system is sensitive to error over longer experiments¹⁰⁵.

This brief comparison highlights the potential differences observed between the available techniques and demonstrates the need for careful consideration of experimental conditions to optimise the selected method. As the focus of this work is directed at the study of E-cadherin interactions and the effect of targeting peptide sequences on mESC cultures, value must be given to factors such as expected adhesion strength and sample preparation. As discussed in section 1.2.1, cadherin interactions demonstrate multiple discrete orientations that result in the observation of different adhesion forces, which are often reported in literature to be approximately 30 – 60 pN, with some experiments recording interactions reaching values around 150 pN¹⁰⁶ which could potentially exceed the limit of force sensitivity

Table 1.3: Brief overview of techniques used for adhesion analysis of biological samples. Each technique follows a different working principle, and some of the key advantages and limitations considered when reviewing each force analysis technique are displayed^{101,103,105}.

Technique	Approximate Force Range (pN)	Main Applications and Features	Advantages	Limitations	References
Atomic Force Microscopy (AFM)	10 - 10 ⁴	<ul style="list-style-type: none"> • Functionalised samples • Contact based technique • High force pulling 	<ul style="list-style-type: none"> • High resolution (spatial and force) • Adjustable loading rate 	<ul style="list-style-type: none"> • Higher minimal force • Contact based method can alter cell properties 	(Leckband and Israelachvili 2021)
Optical Tweezers (OT)	0.1 – 10 ²	<ul style="list-style-type: none"> • Single cell • 3D manipulation (suspension) • Non-contact technique 	<ul style="list-style-type: none"> • High spatial resolution • High force sensitivity 	<ul style="list-style-type: none"> • Possible photodamage • Low maximum force 	(Ungai-Salánki et al 2019)
Biomembrane Force Probe (BFP)	0.1 - 10 ³	<ul style="list-style-type: none"> • More physiologically representative • Single cell 	<ul style="list-style-type: none"> • High force sensitivity • Adjustable loading rate 	<ul style="list-style-type: none"> • Lower spatial resolution • Unstable experimental conditions 	(Šmit et al 2017)

in OT (see Table 1.3). Further, the use of OT requires a sensitive set-up that is more susceptible to changes in experimental environments in comparison to techniques such as AFM, and although successful use of this technique has been seen in literature^{107,108}, the capabilities are not as well suited to the focus of this work when compared to AFM.

The AFM technique is one that has seen widespread use for the application of probing the mechanical properties of cadherin proteins, as the instrument has an impressive measurable force range, systems can be modified relatively easily to optimise the experimental environment, and the high spatial and force resolution allows for determination of discrete adhesion orientations and bond rupture lengths^{61,68,109}. The BFP technique has also seen successful application for the study of cadherin characteristics, with the sensitive and yet wide force range providing a unique benefit for the analysis of biophysical properties. However, the complexity and limited commercial availability of this system could introduce an unnecessary complication for use with our work, and as such the AFM system provides a more suitable method for our work^{110,111}. The following will therefore focus on the AFM system for probing E-cadherin mechanisms, specifically bond formation and rupture, although it is evident from this brief overview that these systems provide complimentary analysis to provide a more comprehensive understanding of interactions.

AFM is one common technique implemented for the analysis of cadherin function, particularly relating to adhesive processes of the protein. Functionalisation of AFM samples with Ecad-Fc molecules has been used to obtain sensitive analysis of interaction events, and has allowed determination and understanding of discrete dimer formations of the extracellular domains. That work has been subsequently developed into the use of cell culture samples, providing information that could help deduce the method of cadherin interactions and subsequent functions that occur throughout the cell^{31,112}. One clear example of this is the determination of slip, catch, and ideal bond mechanisms through various cadherin bond conformations, which was developed from initial discrepancy between theoretical and experimental understanding of interactions⁶⁸. Once resolved, it became clear that the application of force to native cadherins alters the biophysical response of the protein, and can improve the stability of adhesion junctions via adaptation of bond type⁴⁹.

1.3.1 Atomic Force Microscopy (AFM)

In 1986, Binnig *et al.*¹¹³ published their development of the atomic force microscope, a machine capable of investigating insulating surfaces on an atomic scale by use of a cantilever probe¹¹³. Some of the first experiments measuring the force of interaction between biomolecules using AFM assessed the interaction forces of complementary DNA strands, and the receptor-ligand binding of biotin and streptavidin¹¹⁴⁻¹¹⁶. For the latter, results suggested a range of binding forces were possible, which future work would prove using multiple techniques including AFM and bioforce probe (BFP) relates to the various binding conformations of the system^{117,118}. Cadherin based experiments were quickly adopted due to their importance in biological processes, although some difficulties were faced due to the tendency of cadherin molecules to aggregate on cell surfaces, making it difficult to analyse in a natural environment. However, in 2000 Baumgartner *et al.*¹¹⁹ successfully observed the interactions of VE-cadherin-Fc molecules via AFM in a liquid environment by adsorbing them to a mica surface and recording the unbinding force¹¹⁹.

Subsequent publications have tested many different cadherin proteins with AFM, often testing the binding of extracellular domains via adsorption to a hard surface, providing invaluable insight into the adhesion orientation and processes

underpinning cadherin function. This method provides a tuneable sample surface that can be simplified to isolate protein characteristics or interactions. However, it has not been until more recently that more physiologically relevant *in vivo* models have begun to develop, and the use of living cells has been more widely incorporated^{111,120}. Such developments now allow for single-molecule force spectroscopy (SMFS) and single-cell force spectroscopy (SCFS) analysis, which provide naturally complimentary force analysis methods that focus on the adhesion profile of the isolated molecule of interest and the cell-wide mechanical response, respectively. Regarding cadherins specifically, this allows for the complex binding mechanisms exhibited by the extracellular domains to be analysed in-depth, while then considering the influence that the intracellular cytoplasmic tail may have on the resulting cell behaviour. The relationship observed between these conditions can then reveal regions that may be responsible for any changes observed, or contrastingly regions that appear not to influence the process in question^{109,121}.

1.3.2 Single Molecule Force Spectroscopy (SMFS)

The application of SMFS has seen great success throughout previous literature, particularly when studying mechanically mediated biological systems. As alluded to in section 2.1 and discussed further by Yang *et al.*, there are many publications highlighting unique analysis using SMFS¹²². Some of the first experiments measuring the force of interaction between biomolecules using AFM assessed the interaction forces of complementary DNA strands¹¹⁵, and the single molecule receptor-ligand binding of biotin and streptavidin^{116,123,124}. Since then, studies have advanced SMFS techniques to optimise data acquisition and analysis of force spectroscopy, such as for extracellular proteins and cell adhesion molecules¹²². This of course includes cadherin proteins, as discussed in more detail in section 1.3.1.

Based on the concept of force measurements, SMFS isolates interactions between a functionalised AFM probe and corresponding surface. This is achieved by contacting the sample surface normally with a functionalised probe at a set force, and measuring the cantilever deflection during a vertical contact/retraction cycle, thus producing force-distance (F-D) curves. This process is repeated multiple times on set x,y co-ordinates, such that the cantilever movement is isolated solely to the z-plane

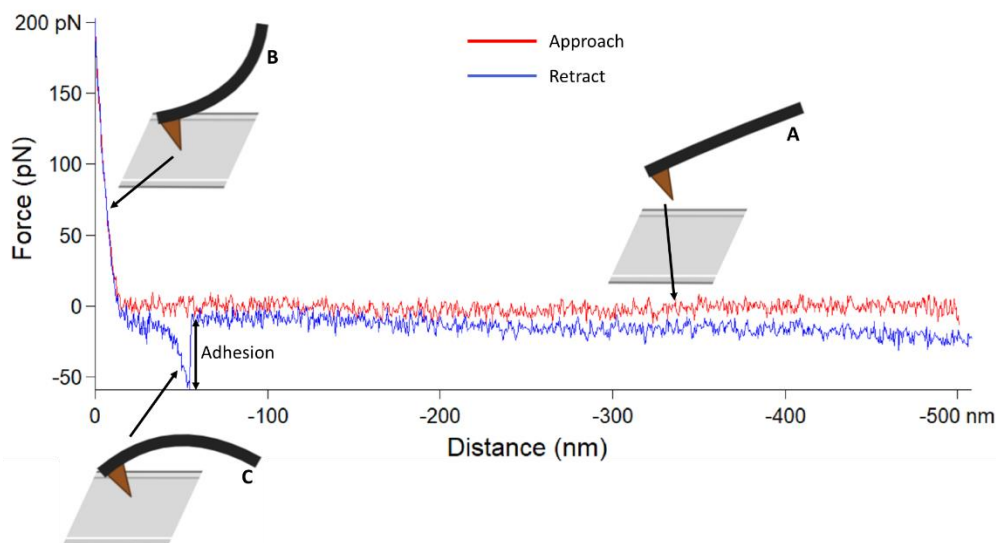


Figure 1.3: A descriptive example F-D curve with an adhesion event. Additional diagrams along the trace represent the relative cantilever position with regards to the sample surface, with (A) representing the approach or retraction where the cantilever is free from interactions with the sample surface, (B) showing the loading of the cantilever due to contact with the surface to a controlled force maximum resulting in bending of the cantilever, and (C) showing an adhesive force between the cantilever and the surface as the probe is retracted resulting in an eventual rupture of the adhesion which can be analysed to determine the force of the bond formed.

for many contact measurements. The F-D curves are critical to the analysis of single molecule adhesions, as they record interaction forces between the functionalised probe and sample as a function of separation distance¹²⁵. An example F-D curve showing adhesion can be seen in Figure 1.3.

Analysis of biological materials via SMFS relies on a suitably functionalised sample and probe surface. There have been many approaches developed, tailored with relation to the biological molecule of interest and proposed characteristic to be assessed, with one key consideration being the substrate used¹²⁶. Throughout literature it is evident that mica, silicon, and glass are amongst the substrate materials successfully used for SMFS experiments. Mica, perhaps the most common, is easily cleavable by use of adhesive tape, providing an easily accessible atomically flat surface layer. Similarly, silicon wafers can provide a smooth surface following a series of cleaning steps to remove contaminants from the sample surface, while boasting improved industry relevant material properties when compared to mica.

The presence of an anatomically flat surface is crucial to allow attachment of small biological molecules for SMFS, as large surface artefacts could interfere with any measurement performed on the target of interest. Despite the greater roughness of

glass surfaces, this material allows imaging of the sample via additional techniques using visible light, such as fluorescence microscopy. This is particularly beneficial when assessing cell samples, whereby the greater surface roughness is negligible compared to the cell target of interest^{127,128}. However, greater limitations can be observed when testing individual molecular interaction with shorter adhesive mechanisms for functionalising the sample surface, and as such glass is less common in high resolution AFM systems¹²⁹.

To allow testing of biomolecules via SMFS the AFM probe, and at times the sample surface, must be functionalised appropriately. This process is critical to enable single molecules to bind between the probe and sample during contact. Many methods have been applied for probe and surface functionalisation, relying on attachment via covalent, non-covalent, or non-specific interactions, depending on the use of chemisorption or physisorption; a brief overview can be seen in Table 1.4. Each

Table 1.4: Overview of functionalisation interactions that have been seen in AFM force analysis experiments. Key characteristics and limitations are highlighted with regards to their application for AFM studies.

Immobilisation Technique	Key Characteristics	Consideration/Limitations
Non-specific adsorption ^{122,130,131}	<ul style="list-style-type: none"> • Often uses gold or mica surfaces • Allows for a variety of functionalised surfaces • Established in literature 	<ul style="list-style-type: none"> • Potential for underestimation of unbinding forces which can skew the energy landscape)
Non-covalent interactions ^{116,122,123}	<ul style="list-style-type: none"> • Receptor-ligand binding • Biotin-Streptavidin (key in development of AFM SMFS) • Can be modified using His-tags or Ni-NTA to modify/optimize binding 	<ul style="list-style-type: none"> • Relatively low pulling forces possible • Limited suitable biomolecules due to bond strength
Covalent bonding ^{122,132,133}	<ul style="list-style-type: none"> • Relatively high bond rupture (allows testing of stronger biomolecular bonds) • Can incorporate NHS coupling to bind lysine residues 	<ul style="list-style-type: none"> • Specificity of protein localisation to the surface can be hindered by native multiplicity of cysteine or lysine

method of adsorption presents unique advantages and disadvantages, although to achieve the strongest functionalisation covalent bonding is commonly applied, sometimes with non-covalent based ligand tags to further optimise the system^{122,134}. It is paramount when preparing samples that the functionalisation method adopted provides adsorption that exhibits a greater integrity than the molecule adhesions being tested, as otherwise the system will record adsorbed molecules cleaving from the surface. The full diversity of adsorption techniques and methods are too numerous to be covered in this work, although the importance of selecting a suitable surface preparation method specific to the target of interest cannot be understated, especially when isolating a sensitive mechanical bond such as with membrane adhesion molecules.

When conducting SMFS experiments it is vital to confirm the preparation and experimental processes result in samples that when contacted produce adhesions that are indeed due to single molecule interactions. Due to the delicate and dynamic nature of molecular bonds it is possible for a system to present misleading data if not properly validated, for example if multiple adhesions are reported within a single F-D curve. The most common approach to ensure analysis of single bonds is to refer to the adhesion probability as outlined by Poisson based statistical analysis¹³⁵.

Poisson based approximations of the expected frequency of adhesion events help to determine the accuracy and reliability of a system, focussing on the probability that a probe-surface contact will result in an adhesion event, and subsequently if that is a single or multiple event^{106,136,137}. According to this approach specific single molecule adhesion events should be rare and ideally occur with between 10-20% frequency, resulting in an accuracy of $\geq 90\%$ ¹³⁸. It is therefore common, and indeed often necessary, to obtain a multitude of F-D curves for each sample such that a representative frequency of events can be determined. Alternative approaches can also be seen in literature to compliment the use of statistical approximations, such as the filtering out of multiple bonds during analysis or the consideration of known mechanical characteristics such as ligand length and rupture forces of bound molecules to eliminate irrelevant or misleading data¹³⁹.

The use of SMFS is often accompanied by dynamic force spectroscopy (DFS) (see section 2.1.2) to further test the mechanical profile of the measured interactions. Although the inclusion of DFS is not necessary for the work in this thesis (as outlined in chapter 3), the following section provides a brief introduction to DFS to outline the importance of this approach.

1.4 Project Aims

The ability to understand and manipulate mESC cell function is of great interest due to the impressive potential in areas including but not limited to disease modelling, therapeutic development, and continuous cell culture. As discussed throughout this chapter, the prevalence of E-cadherin in both physical and biological mESC functions cannot be understated, and as such the targeting of E-cadherin to influence cell behaviour has already shown promise, as seen in the ability to culture mESCs in bioreactors by abrogating E-cadherin adhesions. However, in this context the mechanisms underpinning E-cadherin function, and the interaction and influence of novel targeting peptides requires further understanding. The work in this thesis aimed to develop an AFM based approach capable of detecting and investigating the interaction of cadherin targeting peptides. By specifically investigating the effects of the Epep and EpepW2R peptides, it was hoped that this approach would provide new insight into the mechanical response of E-cadherin proteins, and subsequently our ability to screen peptide sequences using this approach.

Following an introduction to the key experimental approaches in Chapter 2, Chapter 3 outlines the key initial step of this project, namely the development of an AFM system tailored to isolate E-cadherin adhesions; a system that is capable of measuring the frequency of binding events and the unbinding forces of single molecule interactions. The chapter details the validation and optimisation of the system using sample surfaces functionalised with the extracellular domains of E-cadherin, similar to that seen in previously developed SMFS systems from literature, and key E-cadherin molecular characteristics, to determine the efficacy of the AFM system presented. Here, the objective is to demonstrate the ability to isolate single molecule E-cadherin adhesions using functionalised Si surfaces, providing the basis for continued work in the subsequent chapters.

Chapter 4 details the subsequent development of this system as a format to allow the investigation of E-cadherin targeting peptides. Specifically, the peptides Epep and EpepW2R are applied to the functionalised samples, and the impact on the frequency and force of the observed E-cadherin adhesions assessed. The ability of the system to allow the sequential addition of different buffers, including peptide treatment, is

also explored, as it was hoped that this could provide a simple and diverse approach for peptide screening in the future. This chapter also outlines the key step of demonstrating the feasibility of using mESC cultures within the AFM setup, to achieve a more biologically relevant assay, in comparison to using functionalised samples. This chapter probes the hypothesis that the SMFS AFM system developed in chapter 3 can be used to probe different peptides added sequentially to a functionalised sample via measurement of E-cadherin inhibition, with the overarching possibility to modify this system to allow for use on a wide range of biological targets.

Finally, in Chapter 5, the use of biological assays to further enhance our understanding of the influence of Epep and EpepW2R peptides on mESC cultures are explored, using advanced analytical techniques to monitor key cell characteristics such as cell proliferation and protein expression. This work develops from that of Segal and Ward (2017) by probing the response of ESC proteins associated with E-cadherin function, such as syndecans, with the potential to elucidate peptide functions and the processes mediating their interaction with mES cell cultures. This chapter provides a complimentary biological analysis to the mechanical focus of chapter 3 and chapter 4, and is crucial when considering the capacity for these peptides to be used to influence cell behaviour in future research.

In summation, the work in this thesis aimed to develop a unique approach for the investigation of E-cadherin targeting peptides using AFM, testing the hypothesis that a functionalised SMFS AFM can be used for peptide screening that is relatively fast (owing to the ability to test sequential buffers on the same sample) and low volume (due to the minimal contact area of the AFM), while providing high sensitivity and resolution force data of biomolecular interactions. It was hoped that by using the Epep and EpepW2R targeting peptides the approach could also further our understanding of E-cadherin mediated mechanisms and responses in mESCs. This represents the combination of several interesting research areas currently seen in literature, whereby the biological and physical response of cellular proteins (E-cadherin in this case) is studied with consideration to novel targeting peptides that may be exploitable in fields such as the development of therapeutics or advancing standard culture approaches.

Chapter 2 - Discussion of Instruments and Techniques

This chapter provides a general overview of some of the key methods adopted for the work in this thesis. Specific materials and methods used in this work will be discussed in the relevant experimental chapter, and instead here the basic principles and knowledge underpinning the use of these techniques will be presented. Specific focus will be given to AFM, and in particular single molecule force analysis, and also optical based imaging techniques, as these provide the basis for the experiments presented in later chapters.

2.1 Atomic Force Microscopy (AFM)

Since its conception by Binnig *et al.* in 1986¹¹³, AFM has been rapidly adopted as a critical technique for high resolution single molecule analysis. Originally adapted from scanning tunnelling microscopy (STM) to aid in the visualisation of ultrasmall forces down to the atomic scale and to overcome the limitation of STM to image non-conductive surfaces, the AFM technique soon saw widespread use in the study of many materials, including biological samples, as can be seen in reviews^{102,140,141}. Therefore, it is no surprise that the application of AFM has provided many significant contributions to a multitude of research fields.

Despite the numerous additional techniques capable of providing insight into single molecule interactions, such as optical tweezers, magnetic tweezers, or biomembrane force probe, AFM benefits from its ability to test samples that can be functionalised with an ever-increasing range of biological targets with high spatial x,y resolution. Furthermore, AFM allows sample assessment in both liquid and gas environments with minimal instrument changes required, with an ideal force range for assessing biological adhesions due to the sensitivity of the instrument^{140,142,143}.

The importance of probing adhesion proteins at a single molecule level has been highlighted by ongoing research. For example, Marshall *et al.*¹⁴⁴ report on the identification of both catch and slip bond behaviour in P-selectin adhesion, a characteristic that otherwise would not have been accessed by averaged measurements obtained from ensemble binding analysis. Following this, Rakshit *et al.*⁶⁸ demonstrated the presence of catch bonds in the intercellular adhesion proteins, cadherins. As recently summarised by Leckband¹⁰⁰, the ability to probe single molecule events has not only provided novel insight into many proteins and their associated biological function, but subsequently transformed the way in biomedical research and technology can be developed.

2.1.1 Working Principles of AFM

The basic principle of AFM relies on the use of an extremely sharp nanometre-scale silicon or silicon nitride probe attached to a cantilever (radius ca. 1 nm). In most imaging modes the probe is used to contact the surface, measuring

distance-dependent interaction forces as the probe and sample interact. To record fluctuations in the probe-sample interaction a laser, incident on the back of the cantilever surface, translates physical movement of the cantilever as the probe moves over a surface into electrical signals via positional photodetectors. Calibration is required to determine the position sensitivity of the photodetector when measuring laser displacement, known often as the deflection inverse optical lever sensitivity (DeflInvOLS). This value allows for the change in voltage recorded by the photodetector to be converted into a distance moved by the cantilever. To calibrate this parameter, the probe is typically impacted on a hard surface such as a glass slide and the relative forces during the contact are recorded and displaying on a force-distance (F-D) curve. Due to the contact with a hard surface, the F-D curve produced often presents a linear contact region, with the DeflInvOLS value calculated from this. A schematic representing a typical AFM system is shown in Figure 2.1.

The data provided in the F-D curves can be used to determine an accurate force measurement by application of Hooke's law, which allows the cantilever movement distance to be related to the force causing that movement. Represented in Figure 2.1, the system presents such that the cantilever acts as a Hookean spring with spring constant, k , and the single z-axis displacement defines the displacement value, x , with this relationship shown in Eq. 1. The spring constant value is often found via an in-built thermal fluctuation method whereby a thermal power spectral density (PSD) is recorded to determine the resonant frequency of the cantilever in a liquid environment in a state of equilibrium; i.e. fluctuating in response to thermal noise¹⁴⁵⁻¹⁴⁷. Eq. 1 can then be applied to provide the recorded force, F , throughout the contact shown by the F-D curve, including that of any adhesion that occurs. A detailed example of the analysis performed in this work is discussed later in chapter 3.

$$F = -k \times x \quad \text{Eq. 1}$$

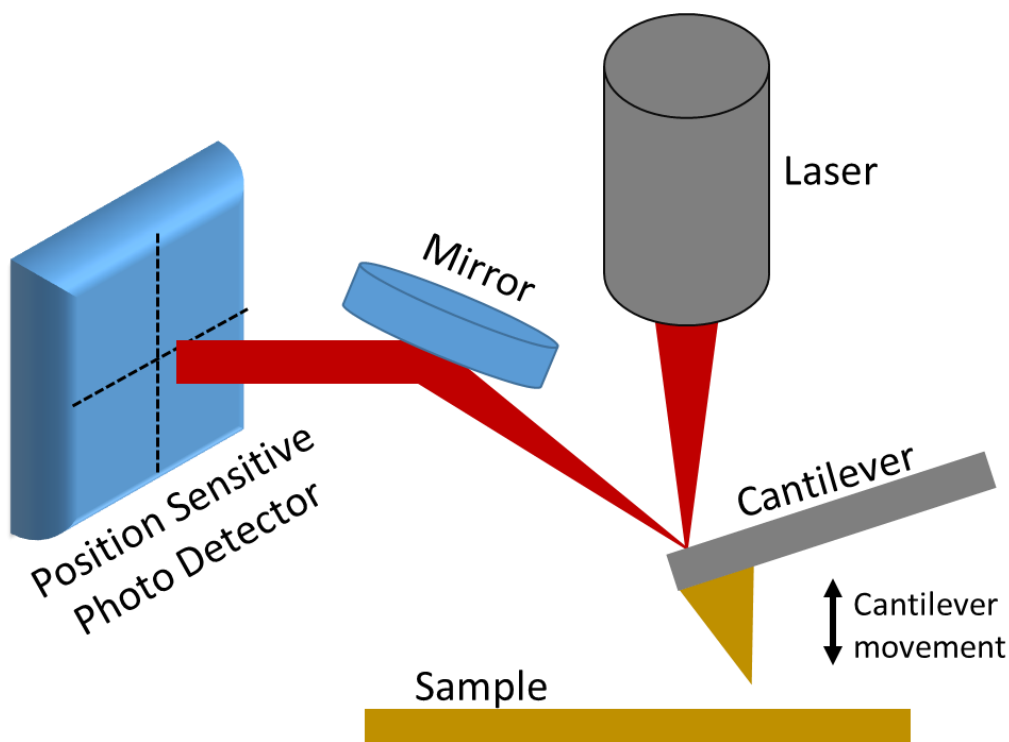


Figure 2.1: **Schematic of the working principle of a typical AFM system.** The laser incident on the cantilever is used to measure bending of the cantilever which results in a shift of the position of the reflected laser beam on the position sensitive photo detector. Any fluctuations in signal recorded by the photo detector can then be converted into a force value by use of Hooke's law (see Eq. 1).

The spring constant of the cantilever is represented by the value, k (unit: $\text{N}\cdot\text{m}^{-1}$), and its displacement by the value, x (unit: m). F (unit: N) therefore represents the force required to displace the cantilever of spring constant k by a value of x .

Many AFM imaging modes have been developed, making minor but crucial changes to the basic working principle. Perhaps the most common, contact mode, functions with the probe making constant contact with the sample as it measures in the x,y plane across its surface, providing a continuous feedback relating to the surface topography. However, this mode is often unsuitable for biological samples due to the potential damage caused by lateral 'dragging' forces imparted by the probe during imaging¹⁴⁸. Furthermore, the lateral component of this mode prevents effective use for assessment of single molecule adhesions, as the presence of these forces can not only damage the sample, but also alter the binding mechanics of the adhesive targets¹⁴⁹. This is characteristic of imaging experiments using contact mode methods, with approaches such as tapping mode and peak force imaging used to help overcome these issues. However, our work does not use AFM imaging and instead focuses on probing single molecule adhesions. Therefore, to effectively achieve this

objective, alternative modes have been developed. Of most relevance to this work is the development of the single molecule force spectroscopy (SMFS) method, which is a prime example of an analysis method used for extracting the behaviour of single molecule interactions.

2.1.2 *Dynamic Force Spectroscopy (DFS)*

When considering SMFS, the introduction of DFS is often considered in parallel, and indeed follows a very similar experimental method to probe molecular adhesion. Due to the stochastic nature of protein folding/unfolding there are many influencing factors that may be considered when studying adhesion forces, and subsequently the initial concept of DFS was born from development of Kramers' work relating to the consideration of Brownian motion and kinetic characteristics of molecular bonds^{150,151}.

DFS is a method of studying the unbinding energy landscape of receptor-ligand adhesion processes by testing multiple loading rates on the sample¹¹⁴. The loading rate corresponds to the force applied to the bond by the system, and relatively soon after the introduction of SMFS it was recognised that the strength of mechanical bonds existed as a spectrum that was dependent on this loading rate, and that this characteristic could be probed by AFM experiments^{118,152}. This leads to the simplified concept that the SMFS principle provides a fixed representation of the bond mechanics with information on the frequency of specific interactions, with DFS providing a more complete understanding of how the energy landscape of the adhesion/rupture, and perhaps even the folded structure of the complex, may shift under load. It is therefore clear why these approaches are often seen as complimentary when studying receptor-ligand interactions, and many publications use these methods to elucidate the mechanics of interactions such as streptavidin-biotin^{118,124}, RNA dissociation^{153,154}, and cadherin bonds^{119,133}, with more comprehensive reviews available elsewhere^{126,155,156}.

2.1.3 *The MFP-3D-SA AFM*

The 3D molecular force probe (MFP) stand alone (MFP-3D-SA) was the instrument used throughout the AFM work conducted in this thesis, with a schematic of the scanning head shown in Figure 2.2. This instrument was developed to allow

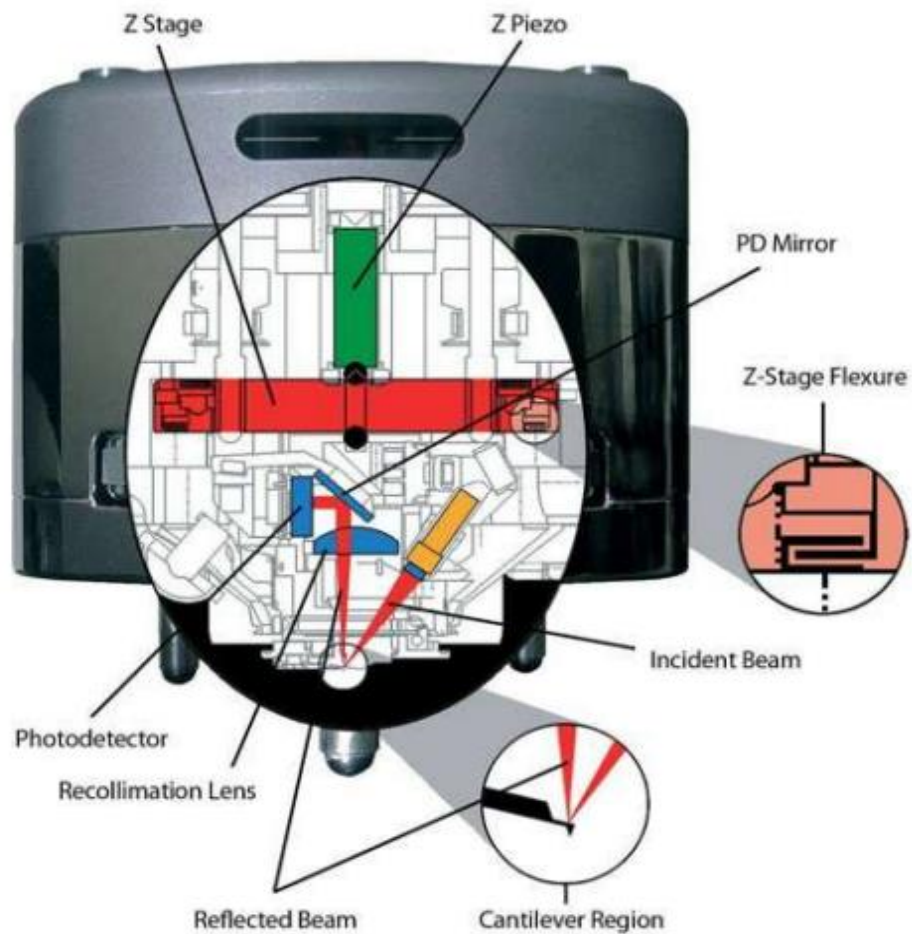


Figure 2.2: **Annotated figure of the AFM scanning head.** Schematic of the inner workings of the AFM scanner head for an MFP-3D-SA instrument, as seen in the associated user manual¹⁴⁷.

multi-purpose analysis, even for opaque samples (such as silicon wafers), and has a reduced sensitivity to vibrational noise when compared to some alternate systems such as the MFP-3D-Bio, potentially allowing for more sensitive force measurements¹⁴⁷. The instrument is capable of testing in both air and liquid environments, with the latter a key characteristic to allow for a suitable environment for biological molecules and cell monolayers. Alongside the instrument there is the analysis software (Igor Pro, Wavemetrics) capable of displaying and assessing F-D curves. The ability to use a range of functionalised samples in a liquid environment with suitable force sensitive F-D curve acquisition was ideal for working with cadherin molecules, both functionalised to sample surfaces and natively expressed in cell monolayers, and was therefore suited to the work presented throughout this thesis.

2.2 A Brief Introduction to Optical Techniques and Principles

The use of optical techniques in research has been a crucial implement throughout several decades, and ongoing development has resulted in a diverse range of approaches. The basis of these techniques relies on the use of electro-magnetic (E-M) radiation irradiating and interacting with electrons within a sample. For example, certain molecules will absorb specific wavelengths relating to the environment of their electrons, transitioning from a ground state to an excited state (as shown in Figure 2.3). Due to the specific energy gaps required for electron excitation, a characteristic absorption spectrum is produced by the sample, providing information on specific characteristics such as the molecular structure of the sample. As the absorption of incident radiation is dependent on the energy required to excite electrons to higher energy states, the subsequent emission wavelength is also dependent on this energy value. Excited electrons (at level E_1 or E_2 in Figure 2.3) eventually fall back to their ground state energy level, E_0 . As this occurs, the appropriate portion of the absorbed energy is emitted as fluorescence of a defined wavelength. Similar to the absorption profile measured during excitation, the release of E-M radiation during de-excitation results in a measurable emission profile. It is this principle of absorption and emission that underpins many optical techniques.

For routine measurements of peptide sequences, many turn to spectroscopic techniques such as ultraviolet (UV) absorbance and fluorescence emission spectroscopy. These techniques can be employed to extract information on peptide structure when taking advantage of well-developed peptide characteristics, such as common absorbance/emission wavelengths^{157,158}. When reviewing an amino acid sequence in this manner, it is well understood that the observed UV absorption is primarily due to three sources: 1) the peptide backbone/peptide bond, 2) aromatic amino acids, 3) prosthetic groups and metal ion binding^{157,159}. Of these sources, absorption recorded from peptide bonds is often the strongest, and appears in the far-UV wavelength range of 180 – 220 nm, with a maximum around 190 nm. Absorption by the aromatic amino acids tryptophan (W), tyrosine (Y), and phenylalanine (F), is present around wavelengths of 230 – 300 nm, with a possible weak contribution from disulphide bonds^{159–161}. This absorption and subsequent

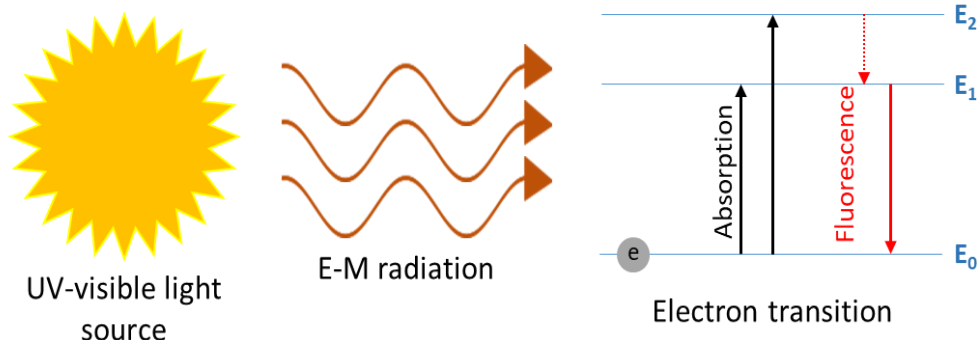


Figure 2.3: **Schematic showing the process of electron transition following absorption and subsequent emission of E-M radiation.** E-M radiation of specific wavelength(s) irradiates the target sample. Electrons at rest in the sample, E_0 , are excited by specific radiation energies that allow transition to higher energy states, such as E_1 or E_2 . This is observed as absorption and is the basis measurement of techniques such as UV-Vis spectrophotometry. Over time the electron will return to the lower energy state, emitting radiation as it does so, thus giving the fluorescence wavelength observed by techniques such as fluorescence microscopy.

emission of EM-radiation only occurs in certain functional groups, and as such helps researchers to isolate optical responses such as changes to the absorption spectrum of a peptide sample, and attribute these to a change to peptide structure or function¹⁶². These approaches are well established in research, and a detailed review of these and other similar techniques is presented by Da Silva *et al.*¹⁶³. However, the following will focus primarily on the techniques and analysis relevant to the more advanced optical approaches used in later chapters, with more biologically aligned applications such as cellular imaging.

2.2.1 Fluorescence in Cell Biology Assays

Many techniques are available for imaging of features and processes of interest in cellular biology. Of these, optical imaging methods are especially responsible for revolutionising research, with ongoing developments continuously overcoming previous barriers, allowing us to acquire more information than ever before, see Cox (2012) for more detail¹⁶⁴. Fluorescence microscopy has a wide variety of applications, and is the basis of many imaging techniques including confocal fluorescence microscopy, super-resolution fluorescence microscopy, and light sheet microscopy, among many others¹⁶⁵. Previous research has shown effective application of fluorescence microscopy to measure cell movement¹⁶⁶, biomarker location¹⁶⁷, and cell interactions^{165,168}.

Fluorescent labelling of targeting molecules provides the basis on which optical imaging builds its success. Often, antibodies are tagged with a fluorescent probe that

can be excited with distinct laser irradiation, providing a unique emission profile. Similar to the process shown in Figure 2.3, the fluorophores can be excited by a suitable radiation wavelength, and sensors can then selectively record the emission fluorescence of the target. However, unlike with basic fluorometry, the location of the signal from the sample is also recorded alongside the signal intensity, to allow for a spatial analysis of the emission. This is the basic process by which a fluorescence sample image is produced.

Gao *et al.* provide an informative review of biological imaging and computational processing methods for cellular applications¹⁶⁹, with this chapter focussing on techniques related to the work presented within this thesis. Therefore, a brief overview of confocal microscopy, flow cytometry, and operetta high-content imaging will be discussed.

2.2.1.1 Confocal Microscopy

The basis of a confocal microscope relies on the ability to focus laser light illuminated on a sample into a small focal plane, reducing the signal received from out of focus sample layers, and maximising the signal received from the imaged layer. This is achieved by use of a small pinhole type aperture to focus the beam. The system then allows for movement to re-focus the beam onto a new sample layer, thus imaging multiple 'slices' of the sample that can be collated to produce a more high quality 3D image¹⁷⁰. As stated in section 2.2, the use of fluorophores allows excitation of specific targets within the sample, highlighting not only the presence of a target but its position in the x, y, and z-plane¹⁷¹.

The ability to remove out of focus signal when imaging the sample is a key benefit of this technique, and allows for a more quantitative analysis of the images produced due to drastically reduced interference¹⁷². Most samples are prepared with multiple fluorescent targets to image different biological markers. This requires fluorophores of differing excitation and emission wavelengths, alongside excitation lasers of specific wavelengths to prevent spectral overlap between the targets. Furthermore, there is a biological requirement that the antibody or molecule used to target the proteins of interest are sourced from different host species to prevent cross-reactivity^{171,173}. These aspects of confocal microscopy can incur a high initial

cost, as developing a panel of fluorescent antibodies that can be used simultaneously also requires suitable excitation lasers and emission detectors. Careful preparation of samples is also required to minimise non-specific off-target binding of the antibody, or background staining of the sample. However, as evidenced by the technique's popularity, these factors are not enough to deter users from the undeniable benefits of confocal microscopy.

2.2.1.2 High content imaging: Operetta

High-content imaging is a method that is commonly applied in drug discovery research, and is a technique that uses automated fluorescence microscopy to allow plate based imaging and assessment of cell samples¹⁷⁴. As with many optical techniques, these methods rely on the principle of fluorescence microscopy, incorporating optimised equipment and software to overcome some of the initial limitations outlined previously.

One such example is the PerkinElmer® Operetta® high-content imaging system. This instrument automates image acquisition, and provides in-built analysis to allow for quantifiable, and therefore statistical, assessment of the images. The ability to automate sample analysis allows for a reduction in both the user input time, and potential bias that may occur if manually selecting imaging regions. Furthermore, the operating software for the instrument allows for many imaging fields to be selected within the sample, and a number of imaging plates to be used¹⁷⁵. Therefore, with the ability to image 96-well, 384-well, or even 1536-well plates, this system far exceeds the data output possible with manual fluorescence microscopy¹⁷⁶. The operetta instrument allows for analysis of many cell features such as morphology, roundness, and proliferation (by recording average cell number). The supplied Harmony software contains many analysis tools, including the ability to initiate machine learning of cell populations based on numerous cell parameters, and highlight prominent factors of variation between multiple samples. The combination of refined imaging equipment and advanced operating software demonstrates the capability for fluorescence microscopy to be tailored to suit specific research needs; and the operetta instrument is an impressive example of high-content imaging. Use

of this technique is seen in Chapter 5 of this thesis, whereby fluorescently labelled cell samples were assessed using qualitative and quantitative analysis.

2.2.1.3 *Flow Cytometry*

Flow cytometry instruments use advanced techniques to investigate biochemical, biophysical, and marker expression characteristics of cell samples. As with all techniques discussed in section 2.2, fluorescence microscopy is a key function of these instruments. However, flow cytometers combine fluorescence analysis with the measurement of light scattering from the sample, also providing forward scatter (FS) and side scatter (SS) components. FS records the scattering of visible light in the forward direction and can provide indication of the relative size of the analyte. SS is recorded at 90° to the incident light and relates to the internal complexity (or granularity) of the cell, effected by components such as granules or nuclei^{177,178}.

The system flows a single cell suspension through the path of laser light of suitable wavelength to excite the sample, and records the emission alongside FS and SS to investigate the cell sample. As discussed previously, the recorded emission depends upon the fluorescent targets used, with multiple wavelengths available for co-staining of cell markers. Due to the increase in available reagents for such analysis the potential targets and parameters that can be assessed has improved dramatically, highlighting the capability and popularity of this technique for detailed analysis of cell samples¹⁷⁸. Typically, use of this approach provides insight into the positive or negative expression of markers of interest for individual cells, which are collated to give a global sample response. Subsequently, graphs showing the distribution of cell expression can be plotted, even showing comparative expression of two different fluorophores, similar to those shown in Figure 2.4A and Figure 2.4B. These graphs show a histogram representation of fluorescence intensity for a selected marker against a negative control sample, and a density plot showing comparative expression of two markers within a sample population, respectively.

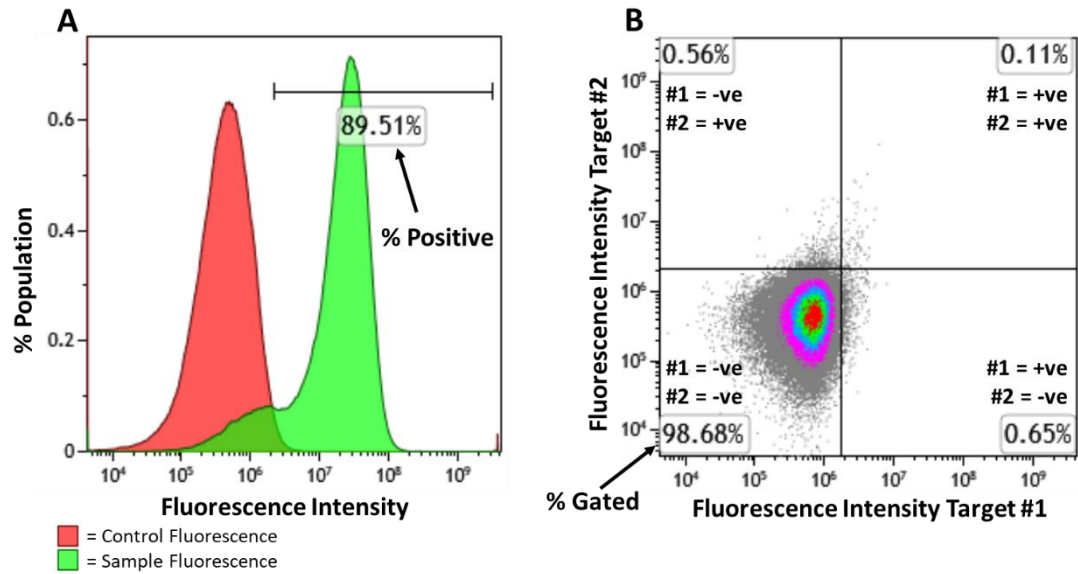


Figure 2.4: **Example graphs showing common graph types obtained from FC analysis:** A) a histogram plot of fluorescence data, and B) an intensity plot showing the comparison of two fluorescence markers within a sample population.

Of course, as with any technique there are some considerations that can hinder the application of flow cytometry, not least of which are the associated costs. The initial cost of acquiring a suitable flow cytometer can be very substantial, especially when considering the expertise often required to operate and maintain the instrument, and the fluorescent probes that must be obtained for each experiment¹⁷⁹. However, the precision analysis offered by this technique explains the ongoing interest and prevalence in current research, and preliminary analysis using this technique is shown in Appendix 1.

Chapter 3 - AFM-Based Single Molecule Analysis of E-cadherin EC Domain Interactions

As discussed in chapter 1, the ability to probe single molecule interactions of biological proteins is one key area of research to which AFM is applied, commonly referred to as single molecule force spectroscopy (SMFS). This approach was developed from the initial concept of AFM¹¹³, and has notable success in observing and understanding individual protein adhesion mechanics¹⁸⁰. This chapter outlines the key initial stage of this project, namely the establishment of an AFM based approach capable of measuring specific molecular interactions between E-cadherin molecules.

3.1 Introduction

AFM has been used extensively to successfully probe a number of biological binding events, allowing for sensitive analysis at the single molecule binding level on a range of functionalised surfaces and biological samples^{110,181–183}. Therefore, it was evident from previous research that this technique can be applied effectively to probe binding of cadherin molecules, with many members of the cadherin superfamily already investigated^{119,184}. E-cadherin is perhaps the most studied member of the cadherin superfamily. However, despite the plethora of research, key mechanics and characteristics are still the subject of many ongoing investigations, highlighting the need for further research into E-cadherin^{185,186}. Furthermore, the ability to use AFM to screen potential cadherin interacting peptides has not yet been realised in literature. Often techniques such as surface plasmon resonance (SPR) are used to assess molecular binding and affinity. However, this approach focusses on ensemble analysis of interactions over the sample surface, meaning the use of AFM can provide an adaptable single molecule-based alternative. The use of AFM therefore allows for experiments that more closely correspond to native biological and mechanical environments on a single molecule level, providing crucial information on sample interactions under controlled force; and the commercial availability of this approach means application and development is much simpler in comparison to techniques such as BFP.

The aim of this chapter was therefore to develop and test a robust single molecule E-cadherin binding system using AFM such as that shown in Figure 3.1, isolating specific E-cadherin adhesions and comparing the obtained measurements to known mechanical characteristics observed in literature to measure interactions. Figure 3.1 provides a simplified representation of the experimental aim of this chapter, namely the presence of a functional E-cadherin binding system capable of isolating single molecular interaction in different buffer environments. Although the figure shows extracellular E-cadherin domains directly connected to the Si wafer and vertically presented from the sample surface, it is important to note that this does not accurately recreate the known molecular conformation of E-cadherin. Therefore, this representation should be viewed with consideration to the information provided in

chapter 1 detailing the biological conformation of cadherin proteins, and the subsequent binding interactions that have been observed in literature.

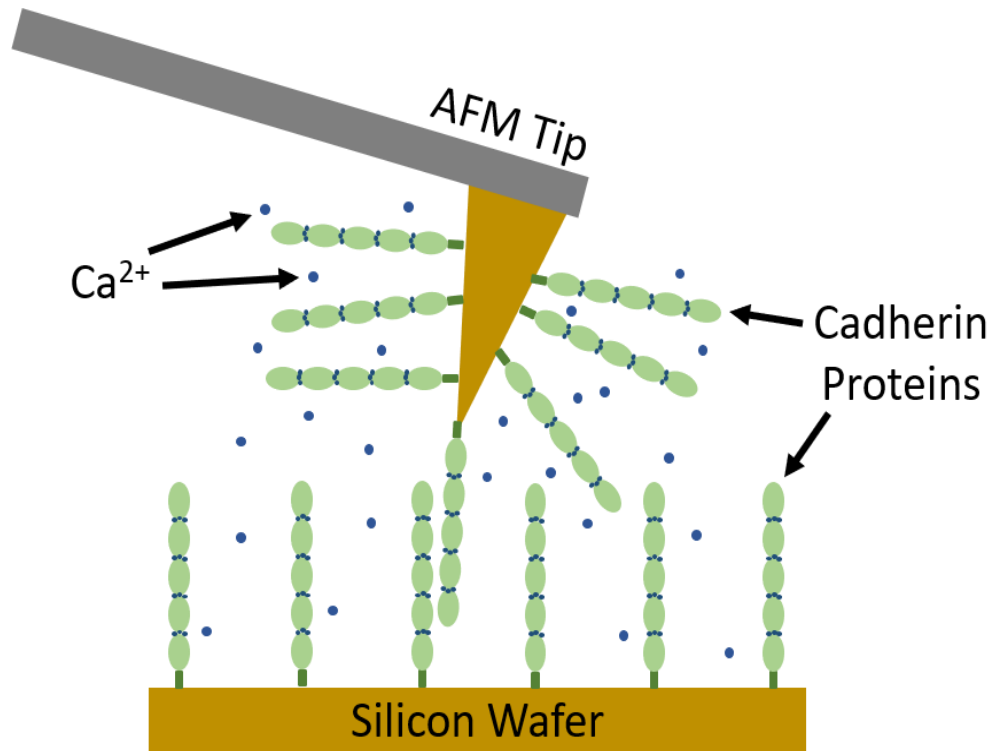


Figure 3.1: Representative schematic of a functionalised AFM system. Schematic showing a representation of an AFM probe and Si wafer surface functionalised with the extracellular domain of a cadherin protein, in a Ca^{2+} rich environment. The blue disks represent Ca^{2+} ions, corresponding to the calcium dependency of E-cadherin adhesion, with this system shown in a calcium saturated state. This diagram represents the experimental aim of this chapter, as this work shows the development of a system that can measure specific single molecule E-cadherin interactions.

This chapter details the development of the sample preparation process and provides an explanation of the experimental and analytical techniques underpinning our AFM-based experiments. This system provided the initial basis for future peptide investigation experiments presented later in this thesis.

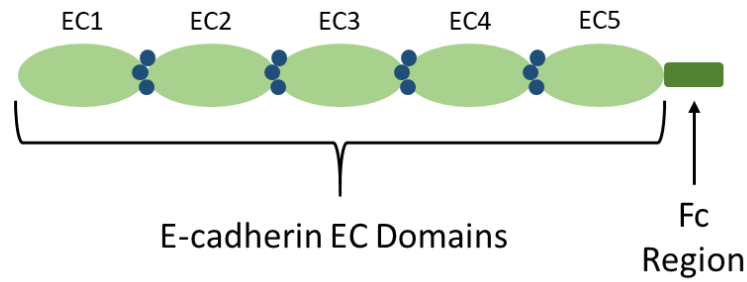


Figure 3.2: Schematic representing the extracellular cadherin fragment used for surface functionalisation. Structure representing the E-cad-Fc molecule used for sample functionalisation. This comprises of the 5 EC domains of E-cadherin bound to a human IgG1 Fc domain. Amino acid sequence analysis via Uniprot highlights a greater fraction of lysine residues in the Fc region when compared to the EC domains, thus indicating adsorption to the surface will be via this region (see section 3.2.2 for further details).

3.2 Materials and Methods

3.2.1 Structure of the Ecad-Fc Chimeric Protein

The preparation of our samples for SMFS AFM required a suitable protein construct to be functionalised to the surface of the cantilever probe and wafer. To achieve this we used an E-cadherin/Fc chimeric recombinant protein (represented by Figure 3.2) expressed in mouse myeloma NS0 cells, labelled from here as Ecad-Fc (E2153, Sigma-Aldrich, USA). This product is formed from the extracellular domain of mouse E-cadherin (amino acids 1- 709) fused via a polypeptide linker to a human IgG1 Fc region, that in turn is 6x histidine tagged at the C-terminus¹⁸⁷.

The Ecad-Fc sequence can be immobilised to the sample surface using N-Hydroxysuccinimide (NHS) ester chemistry. This process is mediated primarily by lysine (K) amino acid residues present within the protein, and as such the Ecad-Fc-amino acid sequence was assessed via the Uniprot database for the presence and local density of lysine. From this it can be seen that the human IgG Fc region contains a greater lysine density than the EC E-cadherin domains, with 28 of the 330 residues being lysine in the IgG1 domain ($\approx 8.5\%$), and 30 out of the 709 in the E-cadherin EC domains ($\approx 4.2\%$). This indicates the orientation of Ecad-Fc molecules on the functionalised surface is suited to allow cadherin-cadherin interaction, as the Fc region is likely to adhere to the surface allowing the E-cadherin EC domains to be free for binding. This was further validated throughout the work in this thesis by use of a targeting functional inhibitory antibody to the E-cadherin EC domain, used with both the Ecad-Fc protein and natively expressed E-cadherin on the surface of mESCs.

The use of protein fragments for surface functionalisation is common in binding analysis, as discussed previously in this thesis (see chapter 1). Therefore, although the Ecad-Fc molecule does not possess the transmembrane region or cytoplasmic tail of the E-cadherin protein, it has been shown in literature that the EC domains are still capable of forming cadherin-cadherin adhesions¹⁸⁸.

3.2.2 Sample Preparation

The process selected to prepare our samples follows common functionalisation procedure for similar materials^{189,190}, and develops primarily from previous work conducted in our group¹³³.

To help remove any debris or organic matter present on the sample, this process was initiated by cleaning silicon (Si) wafers (University Wafer, USA) and AFM cantilevers (MLCT, Bruker, USA) via a series of washes in acetone and ethanol, with the samples dried using nitrogen gas between each wash. Following this, the wafers and probes were irradiated with UV light (Bioforce Nanosciences, USA) for 2 h to further clean the sample, and condition the surfaces with hydroxyl groups, as required for the functionalisation process¹⁹¹. As can be seen in Figure 3.3, the processes involved in surface functionalisation can be viewed in several key steps. Step 1: immediately following UV cleaning, which subsequently populates the surface with hydroxyl (OH) groups, the samples and probes were placed into an argon filled desiccator for 48 h alongside containers of 15 μL of triethylamine and 40 μL of 3-mercaptopropyl trimethoxysilane (MPTMS) (Sigma-Aldrich, USA). MPTMS reacts with the hydroxyl groups present on the sample surface, resulting in the addition of thiol group functionality. The drying agent, Drierite (Fisher Scientific, USA), was also placed in the desiccator to remove water molecules from the air environment which may interfere with the reaction. This process is known as vapour silanisation¹⁹⁰. Step 2: Again, the samples were washed sequentially in acetone and ethanol, before being placed in N- α -maleimidoacet-oxy succinimide ester (AMAS) (ThermoFisher Scientific, USA) dissolved in dimethyl sulphoxide (DMSO) (VWR International, USA) at a concentration of 1.25 $\text{mg}\cdot\text{ml}^{-1}$ for 3 h at room temperature. AMAS is an amine-to-sulphydryl (or amine-to-thiol) cross-linking agent containing NHS-ester and maleimide reactive groups, attached via a short spacer arm. This results in the

thiol reactive fraction of AMAS binding to the sample surface, leaving the amine reactive NHS group free to complete the functionalisation. Step 4: The samples were placed in a $10 \mu\text{g}\cdot\text{ml}^{-1}$ solution of Ecad-Fc in phosphate buffered saline (PBS) at 4°C for a minimum of 12 h. During this step the amine groups present in the lysine residues of the Fc region bind to the NHS-ester species from the AMAS cross-linker on the sample surface, completing the functionalisation process.

The above method produced AFM cantilevers and Si wafers functionalised with the extracellular domain of the cadherin protein of interest, with a schematic representing the experimental set-up with the functionalised surfaces shown in Figure 3.1. This process was repeated prior to each AFM experiment, minimising any inconsistencies that may arise due the impact of possible time-related factors, such as sample degradation.

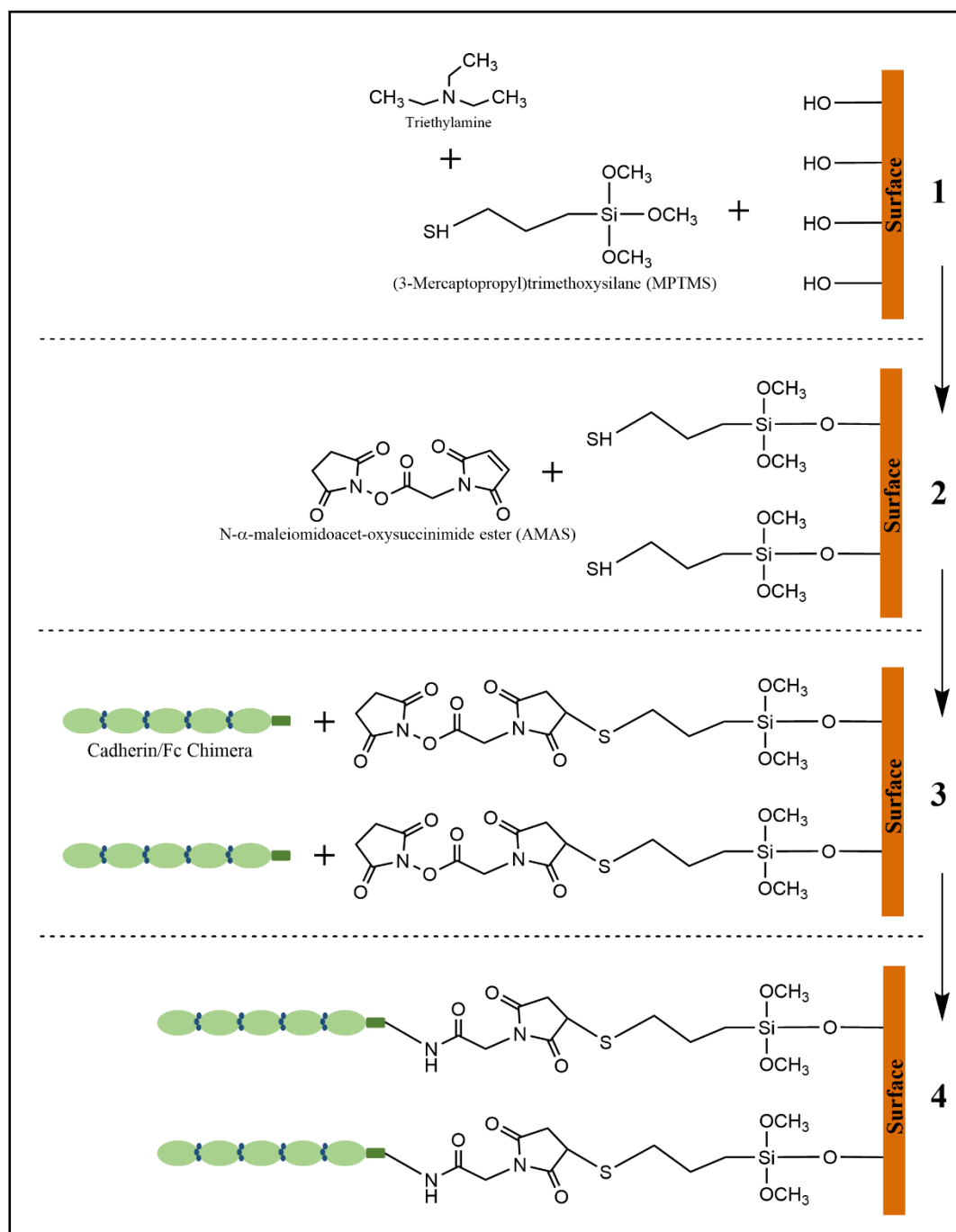


Figure 3.3: Overview of the sample preparation process used to functionalise Si wafers and AFM cantilevers with extracellular Ecad-Fc chimeric protein fragment. 1) Addition of MPTMS by vapour silanisation. The silane group interacts with hydroxyl groups on the sample surface. Condensation of the MPTMS could also occur between adjacent surface bound siloxanes (not shown). 2) The cross-linker AMAS binds to the thiol present in the bound MPTMS molecules. 3) The amine groups present in the lysine residues in the Fc region of E-cad-Fc molecules binds to the NHS-ester group of the AMAS cross-linker, completing the surface functionalisation.

3.2.3 AFM Buffers

To ensure the set-up used for testing cadherin binding demonstrated signature biological characteristics, such as a calcium dependent adhesion, a range of buffers were prepared. A calcium or ethylene glycol-bis(β -aminoethyl ether)-N,N,N',N'-tetraacetic acid (EGTA) containing buffer was prepared by adding either calcium chloride (CaCl_2) (Sigma-Aldrich, USA) or EGTA (Sigma-Aldrich, USA) at a concentration of 5 mM to a HEPES based buffer containing 150 mM sodium chloride (NaCl) (Sigma-Aldrich, USA) (see Table 3.1). All buffers were prepared using ultrapure water (resistivity 18.2 $\text{M}\Omega\cdot\text{cm}$) and were sterile filtered using a 0.45 μm syringe filter. Sodium hydroxide (NaOH) and hydrochloric acid (HCl) were used to achieve pH 7.4 for each buffer, in line with the most common pH of cell culture environments¹⁹². Cadherin binding is a calcium dependent process, and as such the calcium containing buffer promotes cadherin binding, whereas the addition of a chelating agent such as the EGTA buffer inhibits adhesion of the system^{193,194}.

Table 3.1: Details of buffer components and their required concentrations when creating EGTA and Ca^{2+} buffers. The buffers were selected to inhibit or promote E-cadherin binding respectively due to the calcium dependence of cadherin adhesion, with concentrations relating to that of solutions commonly used during culture of E-cadherin expressing cells. All buffers were filtered using a 0.45 μm syringe filter prior to use in experiments to minimise contaminants.

EGTA Buffer (5mM)	Ca^{2+} Buffer (5mM)
dH ₂ O	dH ₂ O
150mM NaCl <i>Same concentration as saline solution</i>	150mM NaCl <i>Same concentration as saline solution</i>
25mM HEPES <i>Same concentration as DMEM media</i>	25mM HEPES <i>Same concentration as DMEM media</i>
5mM EGTA	5mM CaCl

3.2.4 Experimental Procedure

An Asylum Research 3D molecular force probe instrument (MFP-3D-SA) was used for all AFM-based experiments. The instrument was situated on an electronic self-levelling table to help reduce noise during experiments. For all data collection and analysis MFP-3D software version 6.3.7.2 was used (Asylum Research).

Before acquiring data, prepared Si wafers and AFM cantilevers (discussed in section 3.2.1) were secured for use on the AFM instrument. This consisted of carefully placing

the cantilevers in the holder provided for the AFM head, and securing Si wafers onto a glass slide placed beneath the AFM head. As all experiments were conducted in liquid environment, 100 μL of the required buffer was added to the centre of the wafer and the probe was lowered such that it was submerged in the liquid. Initial calibration of the AFM instrument was performed by manually aligning the AFM laser on the functionalised cantilever, ensuring that the recorded voltage output on the photodetector was maximised.

Once the samples were in place several washes were performed using 5mM Ca^{2+} and 5mM EGTA buffers to remove any unbound protein from the sample surface. Prior to performing research in each buffer, the sample was washed using the same buffer to help remove any remnants of previous environments. Once the relevant testing buffer was added to the sample, the system was left for 30 minutes to allow the temperature to equilibrate before obtaining data to minimise drift during testing¹⁹⁵.

As this work focuses on the research of probe-sample adhesion in the presence of multiple buffer environments, force distance (F-D) data was acquired using the MFP-3D AFM for single molecule force spectroscopy, whereby the deflection of the cantilever is monitored as it is brought into and out of contact with the sample surface, and the corresponding force calculated. This method allows us to observe any adhesion events between the functionalised probe and sample. To ensure sufficient data for analysis of single molecule binding events, a minimum of 500 F-D curves were recorded for each buffer condition. A single probe approach/retraction speed ($1\mu\text{m}\cdot\text{s}^{-1}$) was employed to allow for comparison between all data sets.

Due to the potential damage caused to the probe when calibrating the system, this process was completed once the experiment was finished. Calibration was performed by finding the deflection inverse optical lever sensitivity (DeflInvOLS) of the system and spring constant of the cantilever to allow for the measured displacement of the cantilever to be calculated as a force, as detailed in section 2.1.1.

3.2.5 Data Analysis

The data obtained from the MFP-3D were analysed using Asylum Research software version 6.3.7.2. F-D curves were selected to display the deflection of the cantilever

as a force, calculated via the DeflInvOLS and spring constant calibration values determined as described previously. Each curve represents a single contact and retraction from the sample surface, and individual analysis was performed to assess any adhesion forces observed during the contact.

Figures were developed using SPSS software, with in-built statistical analysis performed where necessary, for evaluation of F-D curve categorisation frequency. Rupture force values obtained from F-D curves were assessed using the in-house developed FDist software, created by Prof. Philip M. Williams (University of Nottingham). The modal rupture force for each experimental condition was determined using the FDist software, which creates the cumulative (all data) and cropped (removing values exceeding 1.5x modal value) probability distribution for the force data with consideration to the experimental noise (for all experiments within this thesis the noise value was set to 10 pN). This software applies a Bootstrap statistical method to allow calculation of the standard error of the modal force, with resampling repeated 100 times.

3.3 Results and Discussion

3.3.1 Preliminary Measurements

To begin the process of validating and developing a method for measuring single molecule E-cadherin interactions, F-D curves were acquired between silicon wafers and AFM tips functionalised with Ecad-Fc. These provide a representation of the force observed between the probe and surface during an approach and retraction cycle, and are used to extract information about the adhesion system. From this, we used our knowledge of E-cadherin from previously published data to validate the specificity of the interactions recorded by the system.

As discussed in section 1.3.2, an accurate SMFS system demonstrates a relatively low binding frequency. Therefore, it is important to be able to reliably isolate specific adhesions, and correctly categorise the F-D curves obtained in an experiment. It is common in literature to observe classification of F-D curves into multiple distinct groups, using known parameters to isolate specific adhesions. An example of common F-D categories is shown in Figure 3.4: A) no adhesion event, B) non-specific adhesion event, C) specific adhesion event, and D) multiple adhesion event. These classifications are defined by using factors such as the distance of the adhesion from the surface, and the linearity of the force recorded when the bond is under tension, with specific information relating to the biological target used.

To allow for the low adhesion frequency of an accurate SMFS system many F-D curves are acquired in each sample location. From this, a well-established system should show most probe-surface interactions do not have any distinct change in force, producing a “no event” curve similar to that seen in Figure 3.4A. However, non-specific interactions may occur due to forces not related to E-cadherin binding, such as van der Waals (VDW) interactions. These are often short-range forces, and as such occur immediately at the sample surface and show a non-linear tensile region prior to rupture, such as that seen in Figure 3.4B. It is important to identify and categorise the non-specific and no event interactions to provide insight into the binding system, alongside clarification of specific binding events. Unlike non-specific interactions, the distance at which specific adhesions occur depends on the length of the biological target functionalised to the surface, and as such often occurs further

from the surface than non-specific events. Furthermore, tension in a biological bond presents as non-linear as greater force is applied as seen in Figure 3.4C, producing another difference to help delineate between specific and non-specific interactions. Finally, it is evident from literature that the presence of multiple binding events within a single F-D curve can affect the characteristics of the recorded bonds, leading to misrepresentation of the single bond mechanics aimed to be tested with this system. Thus, data showing multiple interactions between the probe and surface, such as that shown in Figure 3.4D, can be categorised due to the presence of multiple distinct tensile regions. It is important to note that when isolating single adhesions, there is the potential for error in the F-D curve classification, particularly for the single and multiple interaction events. For example, a multiple interaction could simultaneously unbind under load, resulting in a F-D curve with a single rupture profile, similar to a single adhesion event. Therefore, it is important to apply consistent analysis parameters when categorising data, and to take into consideration the accuracy of the system, as discussed in more detail in section 3.3.2.

The F-D curves shown in Figure 3.4 were selected to display examples of the categories used when testing a single molecule binding system, and highlight some of the standard parameters used to categorise data. However, to accurately determine the specificity of this system we must determine the cause of the specific events recorded. In this chapter we focus solely on E-cadherin functionalised surfaces, which limits the potential targets for adhesions. We can therefore assess the specific events with regards to previously published data assessing E-cadherin binding to confirm the nature of the interactions, as shown in the following section.

Following the preparation and experimental processes for AFM SMFS, discussed in section 3.2, the F-D curves acquired from experiments required individual manual analysis. This was performed to identify and quantify specific adhesion events between cadherin molecules on the sample and probe. F-D curves were manually categorised into the four groups outlined in Figure 3.4 to determine event frequency, and results were omitted if ambiguity arose in the classification of the F-D curve recorded. This helped to remove issues such as high background noise, minimising any spurious representation of the data that may interfere with our analysis.

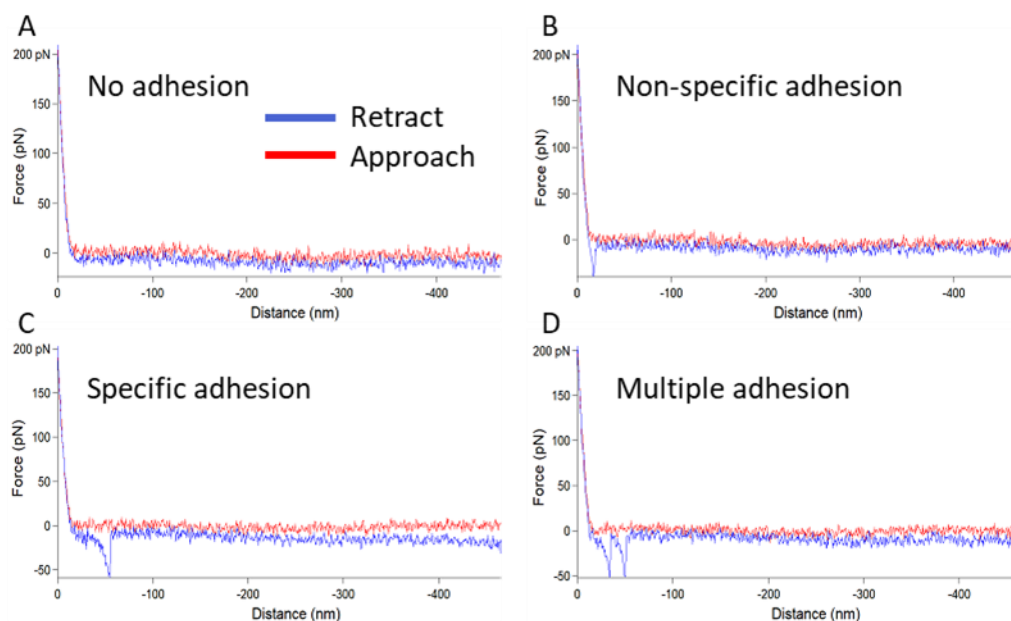


Figure 3.4: **Example F-D curves demonstrating the four categories used for analysis.** A) No events recorded, as seen by an undisturbed contact of the probe and surface, B) non-specific event occurs, as highlighted by a linear adhesion immediately at the sample surface, C) specific adhesion event, highlighted by the presence of a characteristic non-linear adhesion occurring <100 nm from the sample surface with a clear rupture force, D) multiple adhesions shown by the presence of numerous adhesion regions and rupture forces within a single F-D curve.

3.3.2 F-D Curve Analysis from Initial Experiments

To ensure the specific adhesions recorded were due to cadherin interactions between the functionalised surfaces, key characteristics were assessed during analysis. Previous research indicates extracellular domains of classical cadherins have been found to be of length ≤ 25 nm^{31,48,196}, and the chemical modification of the sample surfaces outlined in section 3.2.1 is shown to add near-negligible length between the protein and surface (< 1 nm) as inferred from analysis of similar chemical structures^{197–199}. Therefore, all forces recorded more than 100 nm from the sample surface were omitted from analysis as it is believed this exceeds the physical length for a specific cadherin-cadherin interaction. The distance was measured from the point of contact between the probe and surface (where the initial contact region begins), as shown in Figure 3.5. For all F-D curves the profile of the adhesion event prior to bond rupture was assessed to ensure a non-linear tensile region, indicating stretching of the cadherin domains under load from retraction of the probe from the surface, and a clear rupture force at the point the adhesion ends.

An example F-D curve annotated to show the characteristics of an E-cadherin specific adhesion event is shown in Figure 3.5. As seen, the red line indicates the approach of

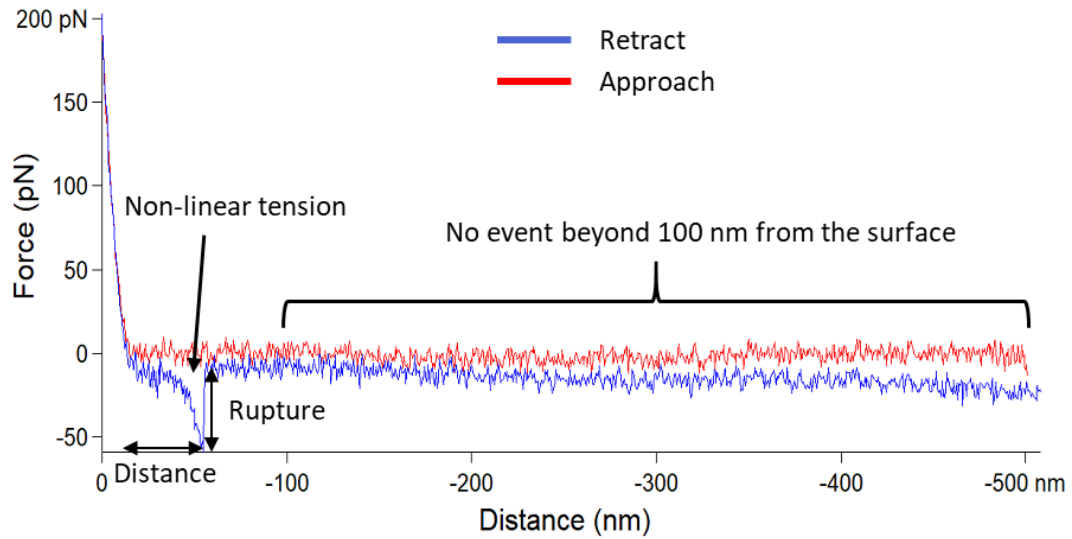


Figure 3.5: *Specific adhesion event observed on an F-D curve.* Example F-D curve obtained from an MFP-3D AFM, displaying a specific adhesion event. For all graphs obtained, the approach data is displayed in red, and the retraction in blue.

the cantilever to the surface, and the blue line represents the retraction. As this F-D curve displays a specific adhesion event, it can be seen that the rupture is confirmed to occur <100 nm from the sample surface, with a non-linear adhesion region and clear rupture force. We can therefore assume that this event is due to a specific cadherin-cadherin interaction as no other biological targets are present, and the adhesion characteristics are synonymous with that of E-cadherin when viewed in literature. Specific adhesion events were further analysed to quantify the bond strength and distance from the sample surface. Graphs displaying a specific adhesion event were analysed using the information tool available in the Asylum Research software. Rupture force was measured as the linear release recorded immediately following the adhesion event, with the bond distance determined from the sample surface to the point of release. Although not the primary focus of this work, understanding the forces produced for each experimental condition allows for greater insight into any underlying physical changes that may occur. This can help to confirm a reliable SMFS system, as the adhesion forces recorded throughout our work should remain consistent, with only the frequency at which they occur being subject to change.

To probe the efficacy of our initial SMFS experiments, the adhesion force for each specific 'single' interaction was reviewed as part of a histogram, seen in Figure 3.6.

This was performed for data obtained in a range of buffers, which included an EGTA and DECMA-1 antibody blocking buffer to introduce a chemical and biological inhibition, respectively. From our understanding of E-cadherin adhesion mechanisms, well studied in previous literature, both blocking buffers should result in a loss of E-cadherin adhesion events^{32,200,201}. The histogram of forces obtained in each buffer was viewed individually to determine any changes in the force distribution of recorded interactions.

A key characteristic of cadherin adhesion is the calcium dependency, which can be exploited to assess the ability of our system to record specific E-cadherin adhesions. This characteristic is the basis for the use of EGTA buffer as an inhibitor, as EGTA is well established as a chelating agent, with greater selectivity for Ca^{2+} ions in comparison to the similar EDTA molecule. Therefore, the addition of EGTA results in a reduction in the free Ca^{2+} ions that are critical to allowing the binding conformation of E-cadherin, subsequently resulting in a loss of adhesion frequency¹⁹³. Contrastingly, the inhibition of E-cadherin interactions by addition of DECMA-1 antibody relies on the affinity of DECMA-1 to bind to the adhesive EC1-2 region of E-cadherin, thus affecting the activity of the Trp2 binding region in extracellular E-cadherin domains^{93,202}. These inhibitors provide complimentary methods to investigate the specificity of recorded E-cadherin interactions.

Therefore, due to the calcium dependence of cadherin adhesion, each experiment was started by using a Ca^{2+} buffer to maximise the specific adhesion frequency observed. The frequency recorded in the Ca^{2+} buffer was then used as a baseline to compare all other buffers tested, highlighting any changes induced by the buffer environment. Where required, following testing in each different experimental condition, data was again acquired in fresh Ca^{2+} buffer to ensure the functionalised probe and sample did not experience any degradation throughout testing. For visualising the analysed data GraphPad Prism 8.4.2 was used to create the required graphs, and perform statistical assessments as required. This process was repeated for each experiment and each buffer tested, with multiple locations or samples used to allow for an average adhesion frequency to be determined. As the preliminary experiments seen in this section were performed solely to provide initial insight into

the viability of the functionalised SMFS AFM system, the data is shown without error bars, as it represents the sum of the multiple tested locations with a single probe and sample. However, it was still maintained that a minimum of 500 F-D curves were acquired in each experimental condition.

For our SMFS AFM system, the addition of blocking buffers should act to reduce the frequency of specific adhesion events, with the force distribution remaining largely unchanged. This is because the binding orientation of the E-cadherin molecules should be consistent between all conditions, as the EGTA and DECMA-1 inhibition does not interfere with the type of bond formed, but simply reduces the chance that the bond will form during tip-sample contact. From Figure 3.6 it can be seen that the force distribution is similar between all buffer conditions, with a modal force of $\approx 30\text{pN}$, and a secondary peak $\approx 60\text{pN}$. These values correlate with the forces reported in the literature for the breakage of E-cadherin S-dimers and X-dimers, respectively⁷⁰. This therefore supported the conclusion that the initial development of our AFM system successfully enabled the specific measurement of E-cadherin interactions to the single molecule level, demonstrating the obtained forces, and ability to specifically block these, align with well accepted characteristics within the literature.

This analysis approach was adopted for all F-D curves acquired in subsequent experiments. F-D curves were always individually scrutinised to minimise the potential for incorrect classification, and more than 250 F-D curves were produced for each experimental condition to ensure sufficient data for reliable analysis.

Continuing from the assessment of the F-D curves with rupture forces, shown in Figure 3.6, testing of the accuracy of the adhesion functionalisation and analysis process was performed using an EGTA and DECMA-1 blocking buffer as before. The frequency of F-D curves showing specific adhesion events was recorded in each of the buffers, and then compared to a Ca^{2+} buffer to highlight any changes in the system due to the blocking buffers. This not only provides a baseline for adhesion frequency, which can be used to assess the accuracy of the system as detailed previously, but also offers another characteristic that can be used to confirm the

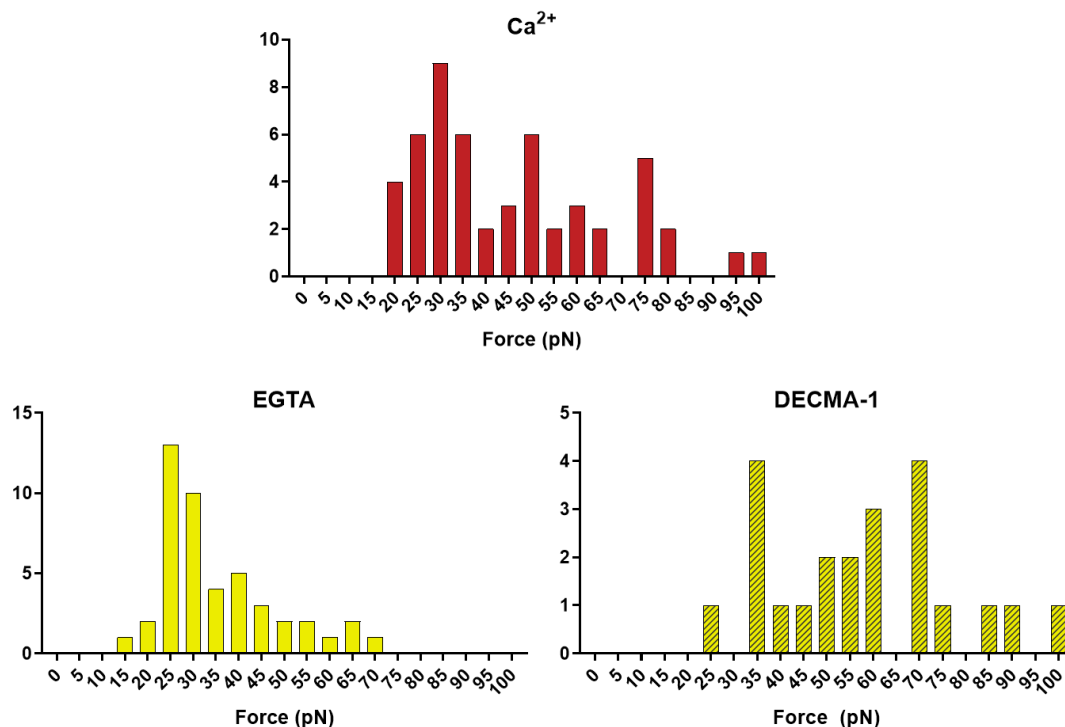


Figure 3.6: Histograms showing the adhesion forces for specific events recorded in Ca^{2+} , EGTA, and DECMA-1 buffers following the refined sample preparation process. The distribution of forces is shown to be relatively unchanged between buffers, as expected for an E-cadherin SMFS system. A minimum of 500 F-D curves were recorded for each buffer condition.

presence of E-cadherin binding specifically. The frequency of specific events recorded in each buffer environment is compared in Figure 3.7.

As discussed in section 1.3.2, adhesion frequency is an important indication of single molecule binding. Poisson based approximations of the recorded adhesion profile are commonly applied to help ensure measured interactions are due to single molecule events, with the frequency of events reviewed to determine accuracy and reliability of the system^{106,136,137}. From this it is suggested that a maximum adhesion frequency between 10 – 20% results in a SMFS system with $\geq 90\%$ accuracy¹³⁸. The frequency of specific events was subsequently calculated as the fraction of F-D curves categorised as specific adhesions in comparison to the total data set observed (all categories). This is a common and necessary process for developing a single molecule binding system using AFM, and provides crucial preliminary evidence of specific E-cadherin adhesion.

Initial review of the data in Figure 3.7 demonstrates that a vast majority of F-D curves displayed no interactions between the probe and sample, as would be expected for a refined SMFS system. The frequency of specific events shows that in the presence

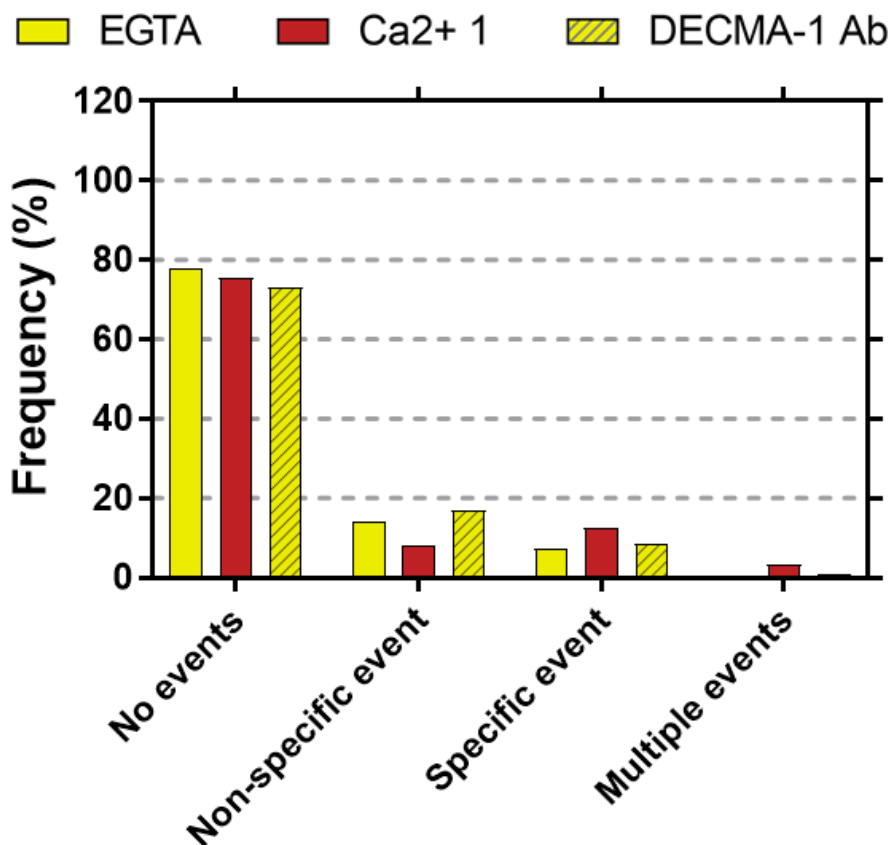


Figure 3.7: Inhibition of E-cadherin binding via addition of calcium chelating EGTA buffer, and E-cadherin nAb, DECMA-1, treatment buffer. Frequencies of each F-D curve category for samples tested in 5mM Ca²⁺ and EGTA buffers, and 50 $\mu\text{g}\cdot\text{ml}^{-1}$ DECMA-1 buffer. This data was acquired as described in section 3.2, showing all analysis categories. A minimum of 500 F-D curves were recorded for each buffer condition.

of Ca²⁺ buffer $\approx 13\%$ of F-D curves exhibit properties that suggest the presence of a single adhesion event. This value is ideally situated within the theoretical range proposed to allow for the accuracy of recorded adhesion to be $>90\%$, as recommended for SMFS. Furthermore, the introduction of EGTA or DECMA-1 to the sample results in a noticeable reduction in the number of specific events. This trend is indicative of cadherin binding, as the chelation of calcium by EGTA, and the specific biological targeting of DECMA-1, hinders the ability for E-cadherin to form homotypic bonds.

To improve the accuracy of our SMFS system ongoing refinement of the sample preparation process was conducted as experience was gained. Reaction times were adapted to allow for improved functionalisation with E-cadherin molecules. This included extending the initial cleaning of the samples using UV and chemical washes, and prolonging the vapour silanisation to improve the prepared surface¹⁹⁹. This

resulted in the methods discussed in section 3.2, with the samples again tested to determine the calcium dependence of the specific adhesions.

The F-D curve analysis and categorisation outlined above provides an intuitive method of interpreting the data obtained from our AFM-SMFS system. The consideration and comparison of each F-D curve category offers confidence in our ability to ensure a representative E-cadherin binding system, as any fluctuations between samples or buffers can easily be viewed. This is largely due to the efforts taken to ensure consistent analysis, using key characteristics such as non-linear adhesion and distance from the sample surface to identify cadherin-cadherin adhesions. Histograms of the rupture forces observed for single molecules interactions provides further insight into the stability of the samples in various buffers, showing that the inhibition of E-cadherin adhesion via EGTA or DECMA-1 does not alter the force distribution of the specific events recorded.

3.3.3 Development of AFM Experiments

As can be seen throughout literature, there are many methods that can be utilised for the functionalisation of silicon wafer samples, with specific processes chosen on an individual basis^{190,199,203,204}. However, previous work conducted within our research group helped refine a functionalisation method to provide the required experimental set-up, with this process providing the basis for initial experiments¹³³. The underlying reaction principles of this process is shown in Figure 3.3, however the specific protocol applied for our work had to be refined to achieve optimal sample preparation, resulting in the method detailed in section 3.2.1.

3.3.3.1 Investigating the Impact of Surface Protein Concentration and Tip Speed

Section 3.3.2 demonstrates the capability of our system to assess specific E-cadherin adhesions via AFM SMFS following an optimised functionalisation process. However, when performing SMFS for binding proteins, such as E-cadherin, it is crucial to review the frequency of specific adhesions recorded to a representative analysis for the system^{68,106,137}.

As seen in Figure 3.3, the addition of extracellular E-cadherin/Fc chimera completes the functionalisation of the sample surfaces. The concentration of protein used for

surface functionalisation is therefore one method of controlling the frequency of specific interaction, with the aim of achieving a specific single molecule adhesion frequency $\approx 10 - 15\%$, thus indicating an accuracy $>95\%$ ¹³⁸. A complimentary factor that can be adapted to aid in the refinement of single molecule adhesion events is to optimise the contact time of the probe on the sample surface, via control of the probe approach and retraction speed. Previous work within our group suggested that the different probe-sample contact times, induced as a product of a change in tip velocity, resulted in a shift of the cadherin adhesion force but not the adhesion frequency¹³³. This could be related to the ability of the cadherin ectodomains to interact in the contact time set by the tip velocity, and could therefore act as a method to minimise the formation of multiple contact F-D curves, while maintaining a sufficient frequency of single molecule events. As discussed in section 3.2.4, a single probe velocity will be selected for continued experiments, however initial assessment of multiple probe velocities provides a more comprehensive platform to validate our experimental process, alongside control of protein concentration.

Therefore, AFM probe velocities of $100 \text{ nm}\cdot\text{s}^{-1}$, $250 \text{ nm}\cdot\text{s}^{-1}$, and $1000 \text{ nm}\cdot\text{s}^{-1}$ were tested in parallel with protein concentrations of $1 \mu\text{g}\cdot\text{ml}^{-1}$ and $10 \mu\text{g}\cdot\text{ml}^{-1}$ for sample functionalisation. F-D curve analysis was performed as detailed above, with the frequency seen for each condition shown in Table 3.2. At lower probe speeds and protein concentration, a noticeable increase in the frequency of non-specific events is recorded, with comparatively little benefit with regards to the specific events. This is indicative of insufficient molecule density on the surfaces, with the slower speeds likely acting to increase the ability for short-range non-specific adhesions to form, such as VDW interactions, which in similar systems have been shown to present as attractive forces^{195,205}.

Table 3.2: Comparison of the impact of protein concentration and tip speed on categorisation of F-D curves from E-cadherin functionalised AFM experiments. Frequency (%) of events recorded when testing Si wafers and AFM cantilevers functionalised with different concentrations of E-cadherin protein. Multiple probe approach/retraction speeds were tested for each protein concentration to determine optimal experimental conditions for SMFS.

	No Events				Non-specific Events			
	1 $\mu\text{g}\cdot\text{ml}^{-1}$		10 $\mu\text{g}\cdot\text{ml}^{-1}$		1 $\mu\text{g}\cdot\text{ml}^{-1}$		10 $\mu\text{g}\cdot\text{ml}^{-1}$	
	Ca2+	EGTA	Ca2+	EGTA	Ca2+	EGTA	Ca2+	EGTA
100nm/s	38.46	28.21	29.92	52.38	23.08	61.54	7.09	8.84
250nm/s	52.17	23.81	50.98	60.29	28.99	66.67	13.73	9.57
1000nm/s	59.72	56.45	71.43	77.05	33.22	38.71	10.20	6.82
	Specific Events				Multiple Events			
	1 $\mu\text{g}\cdot\text{ml}^{-1}$		10 $\mu\text{g}\cdot\text{ml}^{-1}$		1 $\mu\text{g}\cdot\text{ml}^{-1}$		10 $\mu\text{g}\cdot\text{ml}^{-1}$	
	Ca2+	EGTA	Ca2+	EGTA	Ca2+	EGTA	Ca2+	EGTA
100nm/s	19.23	2.56	32.28	20.41	19.23	7.69	30.71	18.37
250nm/s	8.70	2.38	22.06	15.31	10.14	7.14	13.24	14.83
1000nm/s	5.30	4.03	14.44	12.87	1.77	0.81	3.92	3.26

Further review of the data in Table 3.2 highlights the condition using 1000 $\text{nm}\cdot\text{s}^{-1}$ with 10 $\mu\text{g}\cdot\text{ml}^{-1}$ protein concentration as the most promising for analysis of single molecule events, when considering the theoretical ideals discussed previously. As shown, this condition provides specific adhesion frequency around 10-20%, with the least non-specific and multiple events proportionately, thus suggesting a more robust and reliable testing condition.

3.3.3.2 Testing Sample Response to Sequential Buffer Changes

To ensure the adhesion events recorded during testing were due to the biological target selected (E-cadherin), protein specific functional blocking antibodies were tested to selectively inhibit adhesions between the molecules of interest. Therefore, alongside the E-cadherin DECMA-1 clone targeting antibody previously introduced to the functionalised AFM system, an N-cadherin GC-4 clone targeting antibody was also tested to determine any off-target inhibitory effects that may be introduced. Fluctuations in adhesion frequency, or rupture force, following the addition of the N-cadherin antibody, could indicate that the AFM system was not reliably isolating single E-cadherin adhesions, as the antibody should be biologically inactive in the prepared system. Simultaneously, this approach investigated the ability to use multiple different buffers sequentially on the same sample, with data acquired in a

standard Ca^{2+} buffer in between each different environment to monitor degradation of the probe or sample, as this is a key process to allow development into peptide testing as seen in chapter 4. Adhesion frequency was again calculated via analysis of F-D curves as discussed in previous sections, providing insight into the specificity of the E-cadherin adhesions.

Histograms showing the force distribution of specific events recorded in each buffer is shown in Figure 3.8. In each environment there is a modal force of $\approx 35\text{pN}$, which corresponds to the most characteristic homotypic E-cadherin bond, S-dimers. There is also a secondary cluster of forces at $\approx 60\text{pN}$, likely relating to the intermediate X-dimer conformation of cadherin bonds. The profiles observed are consistent even through a change of buffer, and at times a loss of adhesion frequency. This again highlights the stability of the SMFS analysis throughout a range of buffer environments, and suggests the sample is not subject to degradation in response despite the extra washes and buffers used.

This observation is supported by the frequency data shown in Figure 3.9, whereby the distribution of the categorised F-D curves shows that most of the interactions

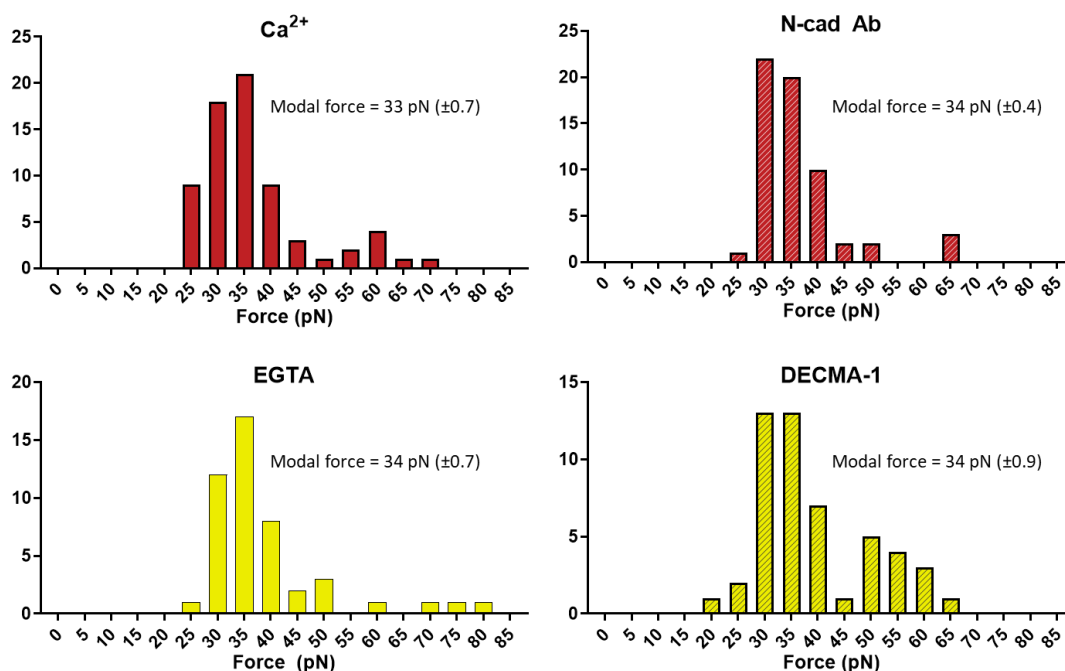


Figure 3.8: Representation of the force distribution of F-D curves following the introduction of an off-target antibody buffer, and sequential buffer changes on the same sample. Modal force analysis (captioned on figure) was more rigorously calculated using Fdist software, with this analysis available in Appendix 2. Histograms show the force distribution of specific events recorded in Ca^{2+} , EGTA, DECMA-1 (E-cad Ab), and N-cad Ab buffer environments. A minimum of 500 F-D curves were recorded for each buffer condition with forces shown only from the specific adhesions, with $N=2$ repeats.

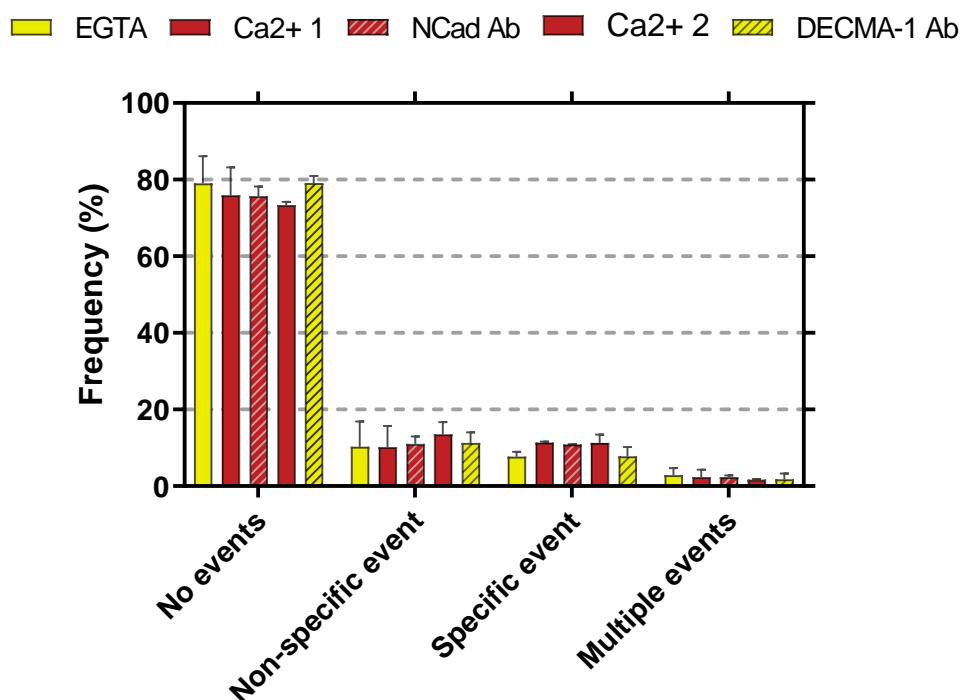


Figure 3.9: **Categorisation of F-D curves using the conditions outlined in section 3.3.2.** Frequency of F-D curves for each of the four categories outlined previously. The dominance of no events, and ideal frequency range of specific events, indicates a working SMFS system. EGTA and DECMA-1 blocking buffers reduces the frequency of specific events, whereas the addition of an N-cadherin targeting antibody does not exhibit any noticeable effect compared to the standard Ca²⁺ environment. Error bars show SD, and a minimum of 500 F-D curves were recorded for each buffer condition, with N=2 repeats.

resulted in no event. Similarly, there is relatively low non-specific interactions, and specific adhesions show a frequency between 10 – 20%. This profile is maintained throughout all buffer conditions, showing that sequential buffer changes on the same sample can be performed with minimal interference. This is an important realisation as it prevents error due to variation in the sample, as the same sample can be used for each experiment, also allowing a higher throughput analysis.

The results shown in Figure 3.9 suggest an inhibitory effect of specific adhesion following the addition of both EGTA and DECMA-1 Ab buffers. A much smaller and seemingly negligible loss of adhesions is presented in the GC-4 Ab buffer, with the discrepancy possibly due to random variation in adhesion frequency, or perhaps a slight steric blocking effect. However, when comparing all conditions it can be reasonably deduced that the chemical and biological blocking buffers, EGTA and DECMA-1 respectively, show the greatest reduction in specific adhesions when compared to a calcium buffer environment. This evidence supports the specificity of

our system, indicating the specific adhesions recorded are due to binding of E-cadherin molecules.

3.3.4 Discussion

Analysis of binding proteins via SMFS has achieved great success when applied in previous literature, including when tested by members within our research group¹³³. Therefore here, application of SMFS via AFM was coupled with previous development and experience within our group, with the aim of further refining and certifying the ability to test specific E-cadherin adhesions using our system. Although DFS is at times seen as a complimentary additional approach to SMFS, and successful application has been seen consistently throughout literature^{114,155}, the emphasis of the work in this thesis was on the ability of AFM based measurements to successfully screen targeting peptide interactions with cadherin molecules. As the considered effect relates to the inhibition of physical adhesion, there is little benefit in attempting to replicate the DFS analysis of cadherins already seen previously. This is supported by the suggestion, from previous work within our group, that the frequency at which specific E-cadherin adhesions occurred did not show any significant change in response to a change in probe velocity¹³³. Conversely, it was suggested that the rupture force observed may be susceptible to a change in the probe velocity, potentially affecting the accuracy of the SMFS AFM system due to increased frequency of multiple adhesion events.

Several substrates are commonly utilised for biological AFM experiments, with most groups opting to use mica, glass, or silicon wafers. Mica provides an atomically planar surface (surface roughness ≈ 0.1 nm) via a simple cleaving process requiring only adhesive tape, and can be modified using silane-based surface chemistry to allow binding of biomolecules^{127,206}. Similarly, silicon wafers can undergo chemical washes to remove surface contaminants and yield a more planar surface, which again can be modified to bind target biomolecules. Glass provides some unique advantages when compared to mica and Si wafer substrates, such as the ability to view samples using microscope equipment due to the transparency of the material. However, the notable increase in surface roughness is not ideal for single molecule experiments, particularly for developing systems such as that presented in this thesis. The work in

this thesis therefore utilises Si wafers functionalised with Ecad-Fc target molecules, to allow for the isolation of E-cadherin interactions.

To test the validity of the developed system, SMFS experiments were performed to obtain F-D curves showing interactions between the functionalised probe and surface. This then allowed for categorisation of the curves into the distinct groups outlined in section 3.3, identifying specific E-cadherin interactions using known parameters from literature, such as bond strength and protein length. The distribution of rupture forces calculated for specific adhesions is shown in Figure 3.6, and show adhesion strength similar to that seen in E-cadherin binding experiments from published reports. Subsequent analysis of binding frequency, which was determined by calculating the percentage of specific adhesions from the entire population of F-D curves, is shown in Figure 3.7. As suggested by the calcium dependent nature shown in this figure, the specific forces observed indicate successful E-cadherin binding, as the addition of a Ca^{2+} chelating agent (EGTA) or functional blocking antibody (DECMA-1) reduces the binding frequency without any noticeable change in force distribution.

Following the clarification that the system developed in this work results in specific E-cadherin binding, focus was then directed on optimising the experimental system. This involved testing multiple protein concentrations and AFM probe speeds. Therefore, protein concentrations of $1 \mu\text{g}\cdot\text{ml}^{-1}$ and $10 \mu\text{g}\cdot\text{ml}^{-1}$ were selected to test the latter value used in previous work by Graumuller, 2019, and the lower concentration to assess if this could improve the single molecule analysis of the AFM system. From Table 3.2 it can be seen that the $1 \mu\text{g}\cdot\text{ml}^{-1}$ concentration consistently resulted in a higher frequency of non-specific events when compared to the $10 \mu\text{g}\cdot\text{ml}^{-1}$ condition, and also presented a very low fraction of specific single molecule interactions ($< 10\%$). This instantly suggests the higher $10 \mu\text{g}\cdot\text{ml}^{-1}$ concentration produces a more suitable experimental environment. These considerations can be further applied to the tested AFM probe speeds, whereby the lower speeds demonstrate a higher proportion of multiple adhesion events. Furthermore, as previously discussed in section 3.3.2, specific adhesion events should ideally occur between 10-20% frequency, as determined by Poisson based statistical analysis and

previous SMFS publications^{136–138}. From Table 3.2 it can be seen that the lower speeds indicate a higher frequency of specific events when compared to the 1000 nm·s⁻¹ probe speed, with only the fastest probe speed producing a frequency within the 10-20% frequency range. Thus, 10 µg·ml⁻¹ protein concentration was selected for sample functionalisation, with an AFM probe speed of 1000 nm·s⁻¹.

Finally, to ensure a biologically specific E-cadherin binding regime, an N-cadherin targeting antibody was assessed for any inhibitory properties. Due to the Ecadherin/Fc chimeric protein fragment used to functionalise the probe and sample, the N-cadherin targeting antibody introduced should demonstrate little to no effect on the adhesion frequency recorded. Conversely, the E-cadherin targeting DECMA-1 epitope antibody has been shown to inhibit E-cadherin binding, as stated in previous literature and by the manufacturer^{202,207,208}. From Figure 3.9 it can be seen that the introduction of the N-cadherin antibody imposes little-no inhibition of E-cadherin binding, particularly when compared to the inhibition recorded upon addition of the E-cadherin antibody. This inhibitory effect is also noted following the addition of an EGTA buffer. This data highlights the effectiveness of our biological AFM system and provides a platform for development of future experiments.

Further, this test demonstrates the ability to rapidly change buffer environment using the same sample, with washes using Ca²⁺ buffer conducted to neutralise the sample, a feature that is exploited in chapter 4. The buffers seen in Figure 3.9 were added sequentially, and still the characteristic mechanical responses were observed when probing the sample in the presence of adhesion promoting and inhibiting environments. This finding emphasises the ability to easily manipulate the liquid environment of the system, which is ideal for application with novel peptide sequences, as multiple sequences and concentrations can be tested on the same sample. The ability to rapidly modify the experimental environment is an invaluable attribute for the continuation of our studies. This is due to the need to sequentially assess multiple different buffers, to firstly confirm the presence of a calcium dependent adhesion mechanism (relating to cadherin-cadherin adhesion), and secondly to probe the effect of E-cadherin targeting peptides. Therefore, the system

presented in this chapter provides an ideal platform to develop our work to include the testing of peptide sequences, as discussed in chapter 4.

3.4 Conclusions

Throughout this chapter the development of a robust AFM system for assessing E-cadherin adhesion has been discussed, resulting in an improved sample preparation process. SMFS analysis demonstrates single molecule binding of E-cadherin proteins as determined by careful consideration of key E-cadherin characteristics derived from literature. Further, this work demonstrates the ability to introduce a chemical and biological inhibitor to the system, confirming the specificity of the system. Experimental conditions were also optimised in line with statistical analysis performed throughout previous literature, testing several protein concentrations and AFM probe speeds to ensure the ideal parameters. This technique, alongside the optimisation and quality assurance demonstrated throughout this chapter, can therefore be confidently applied to further experiments, incorporating more complicated factors such as the addition of custom targeting peptides, or analysis of cell monolayers. It was also shown in this work that multiple different buffers can be tested sequentially on the same sample, simply using Ca^{2+} buffer to neutralise between conditions, thus highlighting the ability to progress to the testing of peptide sequences seen later in this thesis.

Chapter 4 - Probing the Interaction of E-cadherin Targeting Peptides Using AFM

Therefore, considering the ongoing development of targeting peptides in biological applications, and the prevalence of cadherin proteins in cellular processes, a clear development of our AFM system was the introduction of cadherin targeting peptides. The most prominent of these is perhaps the dual E/N cadherin binding peptide, referred to as 'Epep'¹². Epep (amino acid sequence: SWELYPLRANL) is a novel peptide sequence originally derived by Devemy and Blashcuk via phage display technology, that targets the extracellular domain of E-/N-cadherin proteins. It has been shown that addition of this peptide to several cell lines expressing either E- or N-cadherin induces a loss of cell-cell contact, and prevents cell aggregation during culture^{12,93}.

This work was further developed by Segal and Ward⁹³, where it was demonstrated that a single amino acid change in the Epep peptide sequence could alter both biological and physical effects when acting on mouse embryonic stem cells. One sequence of interest highlighted by this work is the EpepW2R (amino acid sequence: SRELYPLRANL) peptide, as when compared to the Epep sequence the samples exhibited a unique expression of key pluripotency markers, and unlike the Epep peptide the addition of EpepW2R to mES cell cultures did not result in a loss of cell-cell contact. This work therefore demonstrated the ability of these novel peptide sequences to elicit a unique response in the biological and physical characteristics of E-cadherin, with the two sequences mentioned selected to allow for comparison of peptide effect.

For the work in this thesis we selected two of the peptide sequences tested by Segal and Ward, namely Epep (SWELYYPLRANL) and EpepW2R (SRELYYPLRANL), to further analyse any inhibitory effect imparted by the peptide sequences when interacting with E-cadherin (see Figure 4.1). Throughout this chapter the two peptides, Epep and EpepW2R, were utilised alongside AFM to assess its ability to reveal new information related to their interaction with E-cadherin and explore its potential as a method for peptide screening. Building upon the work discussed in chapter 3, this work aims to isolate the changes observed in homotypic E-cadherin binding due to the presence of multiple peptide concentrations, assessing the ability to monitor peptide influence and attempt to further our understanding of the interaction with E-cadherin. This approach probes the hypothesis outlined in section 1.4, namely, that SMFS AFM can be used to sequentially screen peptide buffers on a single functionalised sample with small peptide volumes; therefore, highlighting the potential to develop this approach for use with other biological molecules.

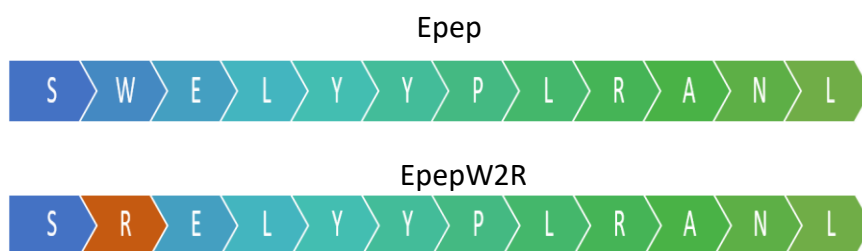


Figure 4.1: **Simple presentation of the Epep and EpepW2R amino acid sequences.** Amino acid sequences shown for both the Epep (top) and EpepW2R (bottom) peptides discussed in section 1.2.2.

4.1 Materials and Methods

Though much of the methods applied throughout this chapter follow directly from those discussed in chapter 3, there were some changes required to successfully incorporate the novel peptide sequences into the AFM experiment, and to allow testing on cell monolayers. As such the following sections will therefore solely focus on the new considerations introduced from this work, with the materials and methods consistent with those used in chapter 3 unless otherwise stated.

4.1.1 *Probing the Effect of Peptide Sequences on E-cadherin Binding Via AFM*

4.1.1.1 *Peptide Solutions*

The custom peptides Epep and EpepW2R were synthesised by Pepceuticals Ltd (UK), and once obtained were reconstituted to make 10 mM stock solutions using ddH₂O. These solutions were stored at -20°C and were used to make experimental concentrations as required, immediately prior to experiments. For use in the AFM experiment, the peptide solutions were diluted to the desired concentrations using 5mM Ca²⁺ buffer as described in section 3.2.3, to ensure any change in adhesion was solely due to the presence of the peptide.

4.1.1.2 *Testing of E-cadherin Functionalised Samples*

When testing Ecad-Fc functionalised samples with multiple concentrations of Epep or EpepW2R solutions, the solutions were always added in order of ascending concentration. Between each test condition washes were performed with Ca²⁺ buffer, and F-D data acquired in Ca²⁺ buffer environment before and after applying each peptide type. This ensured no interference between sample conditions.

4.1.2 *Proof of Concept for Cell-AFM SMFS Studies Using mESC Cultures*

Two mouse embryonic stem cell lines, E14 and Ecad^{-/-}, were selected (as detailed in chapter 5) to allow us to provide a more biologically representative model of E-cadherin binding in the AFM experiment. This required culture of selected cell lines prior to AFM testing, and adaptation in the AFM experimental method to incorporate these samples.

The process required for testing cell monolayers using AFM was similar in principle to that used for functionalised samples, as discussed in section 3.2 and 4.1.1.

Therefore, this section will focus primarily on the aspects that are different when compared to previous methods, with any information not discussed assumed to be the same as that described previously.

4.1.2.1 Preparation of Cell Cultures for AFM

Continuous culture of mouse embryonic stem cell lines, E14 and Ecad^{-/-}, is discussed in detail in chapter 5. However, to prepare the cell monolayers for use with the AFM instrument an alternative culture surface was required to ensure samples were of suitable dimensions. Cell cultures were seeded into 6cm Nunclon™ delta coated culture dishes (ThermoFisher Scientific, USA) 48 h prior to AFM testing. Cultures were maintained using standard culture medium, and were checked regularly for cell attachment and proliferation to ensure viability of the samples, with samples tested when the culture dish reached ≈70% confluency.

4.1.2.2 AFM Buffers and Peptide Solutions for Cell-AFM Experiments

Due to the use of cell monolayers, EGTA buffer could not be used to inhibit cadherin interactions, as the presence of this buffer would result in the detachment of the cells from the culture surface^{194,209}. Furthermore, Ca²⁺ buffer was not required, as instead cell culture medium was used that contains calcium ions and provides a more suitable environment for cell cultures.

The addition of Epep and EpepW2R peptides to the AFM system was achieved via dilution of stock peptide in cell culture medium, to provide the desired experimental concentration. Peptide treated culture medium was created immediately prior to testing, and was maintained in the same environment as regular medium. Peptide solutions were left on the sample for 30 minutes prior to data acquisition to allow the system to thermalise.

4.1.2.3 Experimental Process and Data Acquisition

E-cadherin functionalised cantilevers were first secured on the AFM instrument, and initial calibration was performed via manual alignment of the AFM laser. Following this, the cell medium used for the prepared cell cultures was renewed to remove any debris that may have developed during culture. The instrument settings were also adapted to minimise the contact force of the cantilever on the cell monolayers, as a

high force could damage the cells and provide incorrect data due to a change in the sample or probe surface. Also, the retraction distance of the AFM cantilever from the sample surface was increased to ensure any cell-probe bonds formed during contact were broken prior to the acquisition of subsequent force-distance (F-D) curves.

Force curves were recorded as detailed in section 3.2.4. Due to the greater retraction distance when compared to experiments detailed in chapter 3, fewer F-D curves were obtained due to time constraints, resulting in ≈ 250 –500 curves for each environment.

Furthermore, due to the inability to apply EGTA buffer to the system, the application of specific cadherin targeting antibodies was used to ensure recorded adhesions were due to binding of cadherin proteins. Upon completion of data acquisition calibration of the system was conducted as discussed in section 3.2.2.

Acquired force curves were analysed to determine the rupture force and adhesion frequency following the same process as discussed previously in chapter 3. However, the criterion for classifying a specific adhesion event was adapted to account for the complexity of the biological samples and increased ambiguity in determining the position of the sample surface. As such, the maximum distance permitted for a specific adhesion event was increased beyond the previous 100 nm limit, to account for the potential for cadherin binding events to occur at greater sample-probe separation distances. The remaining analysis parameters discussed in chapter 3 were still employed to ensure exclusion of irrelevant data.

4.2 Results and Discussion

To assess the viability of using the AFM system to observe the effect of the Epep and EpepW2R peptide sequences on E-cadherin binding, we had to first adapt the AFM setup developed in chapter 3 to evaluate detection of the addition of peptides. Therefore, working concentrations of peptide solutions were prepared by performing serial dilutions of the stock peptides in 5 mM Ca²⁺ buffer, and added to the functionalised AFM system.

4.2.1 Initial Testing of Peptides Using AFM

To ensure an effective system for testing peptide effects on cadherin binding, a single peptide concentration was initially selected to assess our ability to monitor changes in specific adhesion frequency following the addition of peptide. A peptide concentration of 10 µM was chosen initially to mimic the concentration used by Segal and Ward when determining transcription profiles of peptide treated mESC cultures⁹³. This concentration is above the equilibrium value determined for the Epep peptide, and therefore provides a peptide condition that would be expected to impact E-cadherin adhesion, similar to the ensemble-based adhesion analysis seen in literature. As the preliminary experiments seen in this section were performed to provide initial insight into the viability of probing peptide treated samples in the developed SMFS AFM system, the data is shown without error bars, as it represents the sum of the multiple tested locations with a single probe and sample. However, it was still maintained that a minimum of 500 F-D curves were acquired in each experimental condition.

In addition to monitoring the effects of the peptide addition on adhesion frequency, it was crucial in these initial experiments to understand if application of the peptide also resulted in an irreversible change of the binding system. Therefore, experiments were designed such that the system was tested with Ca²⁺ buffer before and after performing measurements in the presence of each peptide, ensuring any changes in adhesion frequency could be easily monitored. Furthermore, an E-cadherin specific functional antibody (DECMA-1) was applied following completion of each experiment as a positive biological inhibitor control that selectively blocked E-cadherin binding. This simultaneously tested whether interaction with the E-cadherin domains was still

possible following peptide treatment, indicating the reversibility of peptide interactions.

F-D curves were obtained following the approach outlined in chapter 3. The data was then analysed and grouped into one of four categories as described in that chapter, namely: no events, non-specific event, specific event, and multiple events. Variations in the frequency of specific events between different environments was monitored to assess the presence of any inhibitory effects, as seen in chapter 3 when testing in the presence of DECMA-1, with this process naturally developed to incorporate treatment with Epep and EpepW2R peptides.

To initially test the ability to monitor peptide mediated effects, the frequency of specific adhesion events between a functionalised sample and probe was recorded in multiple environments. Data from preliminary experiments testing 10 μM Epep and EpepW2R peptide concentrations is shown in Figure 4.2, with the frequency of specific adhesion events displayed alongside the baseline adhesion frequency observed in the Ca^{2+} environment.

As in chapter 3, it was crucial in the experiments to first assess the influence of the presence of EGTA and DECMA-1 antibody, as this provided an indication that the measured interactions were due to homotypic E-cadherin bonds. From the data in Figure 4.2 it can be seen that the chemical and biological blocking solutions, EGTA and DECMA-1 respectively, resulted in a reduction in the frequency of E-cadherin adhesions when compared to the Ca^{2+} environment; these initial observations reinforcing the ability to selectively record specific E-cadherin binding using the developed AFM system.

As discussed in section 1.2.2, the Epep peptide has been attributed with disruption of E-cadherin contacts in cell cultures, and as such would be expected to inhibit the formation of E-cadherin adhesions between the sample and probe in this AFM system. This inhibitory impact is suggested when reviewing Figure 4.2, with the adhesion promoting environment, Ca^{2+} buffer, consistently showing the highest frequency of adhesion events, and a reduction seen following the addition of the Epep peptide. Further review of Figure 4.2 shows an inhibitory effect of both the

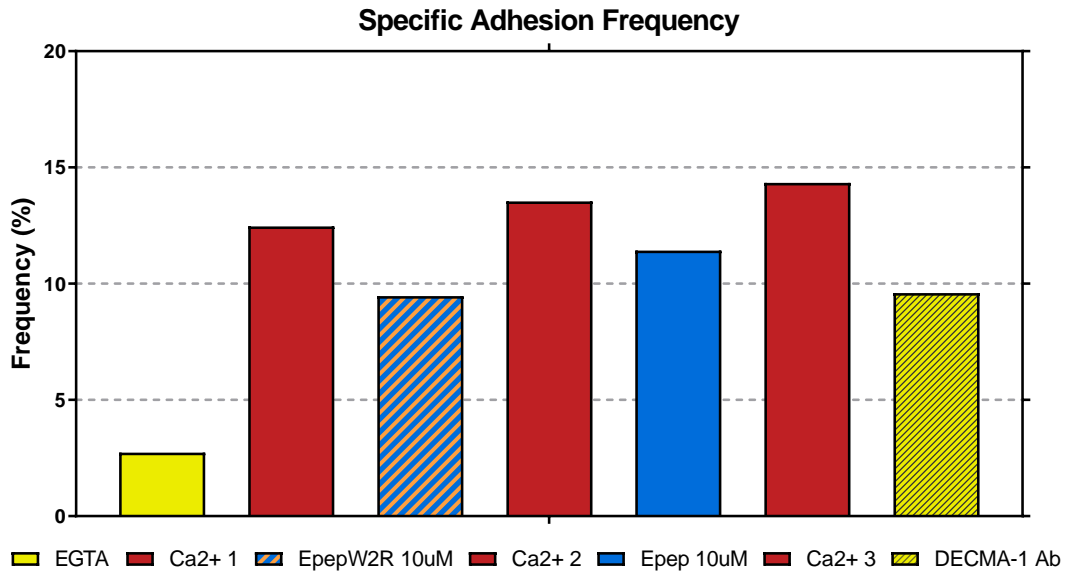


Figure 4.2: Initial testing of 10 μ M peptide treated functionalised AFM samples demonstrates the ability to sequentially change buffer environments during the experiment. The data was acquired using a single functionalised sample and AFM tip, with washes using Ca^{2+} buffer conducted prior to the addition of a new buffer environment. The system was left for 30 minutes after changing buffer. Initial peptide testing shows both peptides at 10 μ M concentration tested on the same sample. A minimum of 500 F-D curves were recorded for each buffer condition.

Epep and EpepW2R sequences at a 10 μ M concentration, despite previous publication suggesting the latter does not induce loss of cell-cell contact in treated mES cell cultures⁹³. Also, as the equilibrium concentration for EpepW2R was estimated by Segal and Ward to be 55 μ M, the inhibitory effect observed may become more prominent at a higher peptide concentration, thus prompting investigations of additional concentrations in our experiments. Although further studies would be required to fully understand the mechanism, the data shown by this initial AFM study may indicate the presence of off-target binding on cell cultures which is not possible in the simplified AFM system, or due to the superior binding analysis achieved with the AFM instrument.

Interestingly, the replacement of Ca^{2+} buffer to the sample following peptide treatment can be seen to result in a return of the adhesion frequency, indicating that the inhibitory characteristics demonstrated by the addition of peptide solutions were reversible. This reversibility is a key quality when trying to understand peptide interaction and when considering potential future applications, perhaps most notably as a supplement to improve large scale culture of cell lines. As the focus for this application is primarily to maintain undifferentiated ES cells for large scale

culture, the use of peptides must be reversible to allow subsequent application of cell cultures without complications arising due to the initial culture conditions¹¹.

Following the initial assessment of 10 μM peptide concentrations, a second preliminary experiment was performed with both peptides at a higher concentration (100 μM), such that the estimated equilibrium concentrations were exceeded. This would hopefully provide a saturated system whereby any effects on E-cadherin binding would be maximised, as evident via analysis of the adhesion frequency recorded.

As can be seen in Figure 4.3, the addition of both peptide solutions again resulted in a loss of E-cadherin binding, with this inhibition shown to be reversible following the addition of a Ca^{2+} buffer. Consideration of the EGTA and DECMA-1 conditions suggests a similar inhibitory effect of both the Epep and EpepW2R peptides, further supporting the observations seen in Figure 4.2.

Preliminary experiments incorporating peptide solutions into our AFM system therefore demonstrated successful analysis of their effect on E-cadherin binding, by reviewing the event frequency recorded during testing. Both tests demonstrated that the sequential addition of inhibitory experimental solutions (including Epep and EpepW2R buffers) results in a reversible inhibitory effect. Furthermore, the data suggested that development of these experiments to further test the effect of protein concentration could prove beneficial, such as those seen later in this chapter, as any peptide mediated influences could be monitored in relation to progressive concentration changes. The addition of EGTA or DECMA-1 appeared to inhibit E-cadherin binding when compared to Ca^{2+} buffer, providing an ideal basis for further testing of peptide concentrations to isolate any peptide mediated inhibition of E-cadherin adhesions.

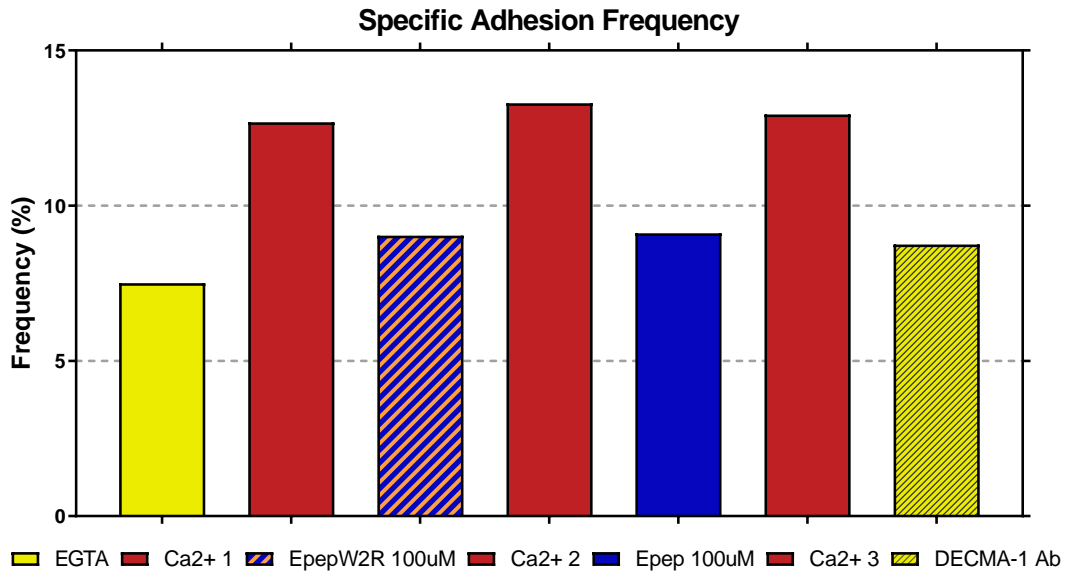


Figure 4.3: Initial testing of 100 μM peptide treated functionalised AFM samples demonstrates the ability to sequentially change buffer environments during the experiment. The data was acquired using a single functionalised sample and AFM tip, with washes using Ca^{2+} buffer conducted prior to the addition of a new buffer environment. The system was left for 30 minutes after changing buffer. Initial peptide testing shows both peptides at 100 μM concentration tested on the same sample. A minimum of 500 F-D curves were recorded for each buffer condition.

4.2.2 Detailed Epep and EpepW2R Peptide Titration Experiments

To develop from the initial testing shown in section 4.2.1, multiple peptide concentrations were subsequently tested in the AFM based titration experiments, to investigate the progressive characteristics imparted by gradual increase of concentration. First we focussed on the Epep peptide sequence, as the characteristics recorded for this peptide supported previous data published by Segal and Ward, in that the addition of this peptide sequence inhibits E-cadherin binding⁹³. Following as a natural progression from this, we also tested the EpepW2R peptide to allow for comparison of peptide effects. Peptide concentrations were again selected based on the concentrations used in previous publications, and to ensure applied peptide solutions were both above and below the estimated equilibrium concentrations for Epep and EpepW2R as determined by Segal and Ward (3.4 μM and $\approx 55 \mu\text{M}$ respectively)⁹³. Therefore, the selected peptide concentrations for this analysis were: 1 μM , 10 μM , and 100 μM . These values also correspond to those used in the preliminary experiments conducted in section 4.2.1.

AFM experiments were performed as discussed in section 4.1, obtaining ≈ 1000 F-D curves for each condition, and using EGTA and DECMA-1 containing solutions to allow comparison to known E-cadherin inhibitors, and Ca^{2+} buffer to represent an adhesion

promoting environment. Subsequent categorisation was performed during data analysis, with four categories selected: no event, non-specific event, specific event, and multiple events. All AFM samples were assessed to determine the average frequency of each event category observed as discussed in detail in chapter 3, with at least three different functionalised samples and AFM tips tested to provide biological repeats (N=3), and multiple different locations tested on each of the sample surfaces during the experiments to act as technical repeats (n=2). Subsequent statistical analysis was performed by using one-way ANOVAs with post-hoc analysis to compare event frequency of inhibitory buffers with the baseline seen in the Ca²⁺ environment. The rupture forces isolated from specific adhesion events were also compared between experimental conditions, as a system that reliably isolates single molecule interactions would be expected to demonstrate a consistent modal force, as the inhibitory buffers solely reduce the adhesion frequency²¹⁰.

4.2.2.1 *Binding frequency of Epep Treated Samples*

As discussed in chapter 3, maintaining an adhesion frequency below 20% suggests an accuracy >90% when performing single molecule adhesion experiments^{139,211}. Therefore, the distribution of categorised F-D curves shown in Figure 4.4 indicates a reliable single molecule binding analysis, as the frequency of specific events (single molecule binding) does not exceed 20% frequency, even in the presence of the Ca²⁺ buffer. This is compounded by the very low frequency of multiple events in all tested buffers, again showing the system provides a robust method of single molecule analysis, even in the presence of novel targeting solutions. Furthermore, the use of peptide solutions does not interfere with the sample surface stability, as shown by the relative absence of non-specific events throughout testing, and consistent dominance of F-D curves categorised as non-events.

Figure 4.4 allows for detailed understanding of the changes observed when testing the different environments, and is supplemented by statistical analysis of the comparison of specific events between each inhibitory condition with the initial Ca²⁺ environment. Reviewing Figure 4.4C, it is shown that only the specific event category displays significant change for different experimental environments when compared to Ca²⁺, with a consistent loss of adhesion frequency in all peptide concentrations

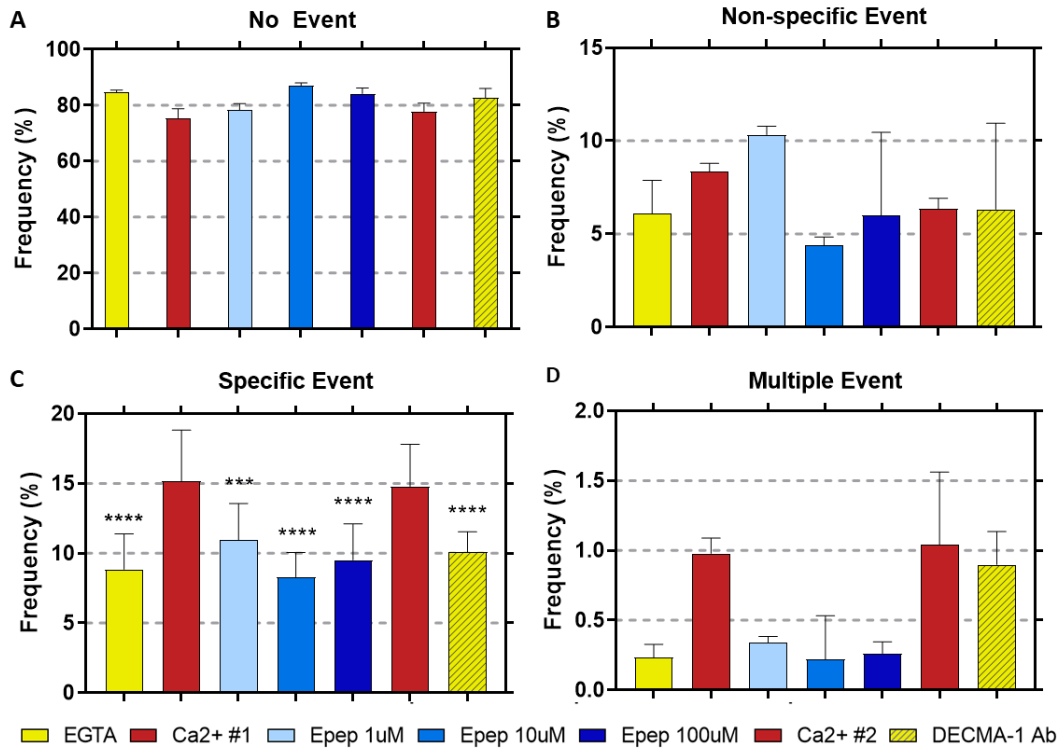


Figure 4.4: Comparison of F-D curves acquired from Epep peptide treatment AFM experiments, and categorised using the method discussed in section 3.2.5. Sample data was compared to the baseline value determined by the initial Ca²⁺ buffer to provide a clearer representation of the influence of different buffer environments. The data in these graphs provide a clear comparison of the buffers tested for each analysis category: A) no events, B) non-specific events, C) specific events, and D) multiple events. A minimum of 500 F-D curves were recorded for each buffer condition, with N=3 repeats. All comparisons were made to the initial Ca²⁺ buffer tested with error bars showing standard deviation, and statistical analysis was performed using an average of the tested samples (N=3). Significance is shown as: * = P < 0.05, ** = P < 0.01, *** = P < 0.001, **** = P < 0.0001.

tested, alongside EGTA and DECMA-1 solutions. This loss is relative to the Ca²⁺ buffer environment, with the EGTA and peptide inhibition shown to be reversible by replacement of the inhibitory buffer with a non-restrictive buffer (Ca²⁺). This highlights the calcium dependent nature of the specific events recorded, as expected for a cadherin system, and supports the initial experiments discussed in chapter 4.2.1 that originally suggested the reversible inhibitory effect of the Epep sequence.

Considering the significant loss of single specific adhesions shown in Figure 4.4C, this feature further supports that the loss of adhesion events is due to inhibition of E-cadherin interactions. The system also suggests a resistance to permanent manipulation of the sample surface, as demonstrated by the consistency of both no events and non-specific events categories throughout all buffers tested, and the ability to recover adhesion frequency by addition of Ca²⁺ buffer.

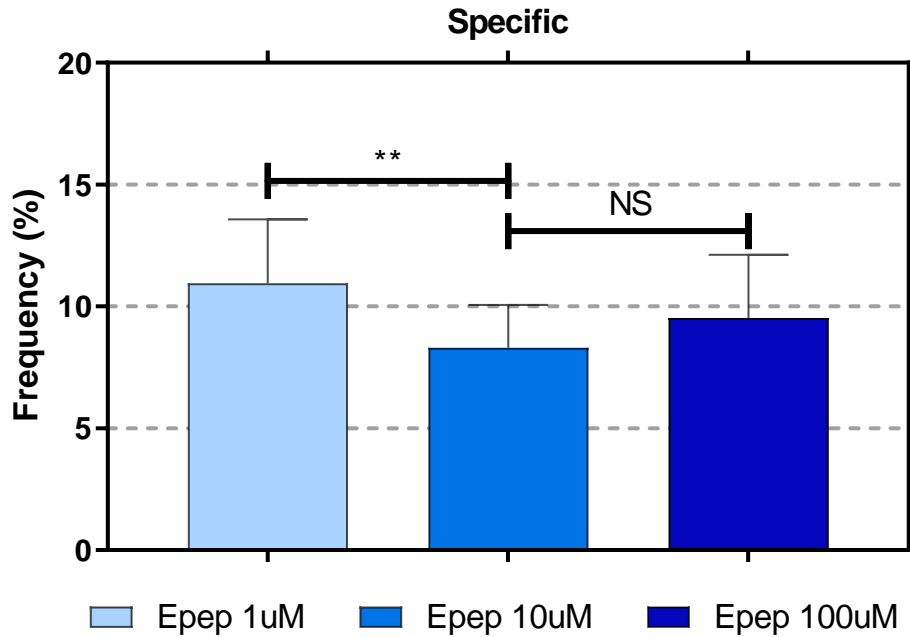


Figure 4.5: **Comparison of the specific event frequency recorded in each concentration of Epep buffer.** A minimum of 500 F-D curves were recorded for each buffer condition, with $N=3$ repeats. Statistical analysis of the values was performed on the baseline corrected percentages when compared to Ca^{2+} buffer, as seen in Figure 4.4, with comparisons isolated to the ascending Epep concentrations. Error bars show SD, and significance is shown as: NS = no significance, * = $P < 0.05$, ** = $P < 0.01$.

The inhibition of E-cadherin binding shown by the Epep peptide in these AFM experiments supports previous publications, with this analysis providing a different E-cadherin binding system that is based on the mechanical response of the protein. Previous work by Segal and Ward shows the addition of the peptide induces a loss of cell-cell contact, similar to the effect observed upon addition of the E-cadherin targeting antibody DECMA-1⁹³. Considering that work alongside the AFM-based experiments conducted in this chapter, it is reasonable to deduce that the peptide targets the extracellular domain of E-cadherin to induce inhibition of the physical binding of the cadherin protein.

Figure 4.5 isolates the frequency of specific events recorded in the presence of Epep, showing the multiple concentrations used for the experiment. As seen, there is a significant reduction of E-cadherin adhesion events when comparing the 1 μ M and 10 μ M treated samples, with no further significant change observed in the 100 μ M samples. This response of the Epep treated system indicates a progressive inhibition related to the peptide concentration. Further, recalling the estimated saturation concentration of 3.4 μ M for the Epep peptide, determined by Segal and Ward, the inhibition observed in this AFM system suggests the inhibitory effect plateaus after

surpassing this value. Considering the data shown in Figure 4.4, it is seen that the final inhibitory capability of the peptide closely resembles that of the DECMA-1 antibody, with the 1 μ M peptide condition providing an intermediate inhibition.

4.2.2.2 *Binding forces of Epep Treated Samples*

Following from the information shown in section 4.2.2.1, the adhesion forces recorded for single molecule interactions (specific events) were also reviewed to further understand the interactions involved. Due to the comprehensive analysis of cadherin proteins, including E-cadherin, already conducted throughout previous literature, we can compare the force distribution profiles obtained from our work with that of untreated E-cadherin samples^{68,106,109,133,212}. Although it is important to note that measurement of cadherin force distribution profiles is sensitive to instrument settings, such as probe velocity, it is also prevalent to recall that our work focusses on a single probe velocity to assess adhesion frequency.

As reported in numerous publications and discussed throughout this thesis, homotypic E-cadherin adhesions can produce several force regimes due to the multiple binding orientations available for this protein^{68,183,213}. Therefore, the force measured for the binding events could help identify the adhesion mechanism.

As seen in Figure 4.6, the modal force recorded for all experimental conditions is stated to be between 25-45 pN. This consistency in the rupture force of isolated E-cadherin bonds is synonymous with a successful SMFS system, as the inhibition of adhesion frequency is shown not to impact the bond mechanics of the protein. Furthermore, it is well founded that when assessing E-cadherin adhesion force using AFM, a distinctive rupture force around 30 pN is observed⁶¹. This is a characteristic rupture force suggesting strand dimer formation, which is commonly accepted as the critical initial binding orientation for trans homotypic E-cadherin adhesion. Also, it is shown in previous publications that a lower retraction velocity often produces a slightly lower modal force, which must be considered when reviewing this data. Therefore, considering this characteristic when assessing cadherin E-cadherin adhesion force, the 30-40 pN range recorded in this experiment again agrees with previous data for both E- and N-cadherin^{133,186,214}.

The consistent force distribution profiles observed in all tested buffer conditions supports our belief that this system produces stable representation of E-cadherin binding. This stability can further our understanding of the inhibitory nature of the Epep peptide, as it is again shown that the addition of the peptide to E-cadherin molecules implements a reversible change in the mechanical binding characteristics. Due to the absence of change in the force distribution profiles displayed in Figure 4.6, it can be assumed that although the frequency of events is reduced by addition of the peptide sequence, the binding mechanism is unchanged and single molecule measurements maintained.

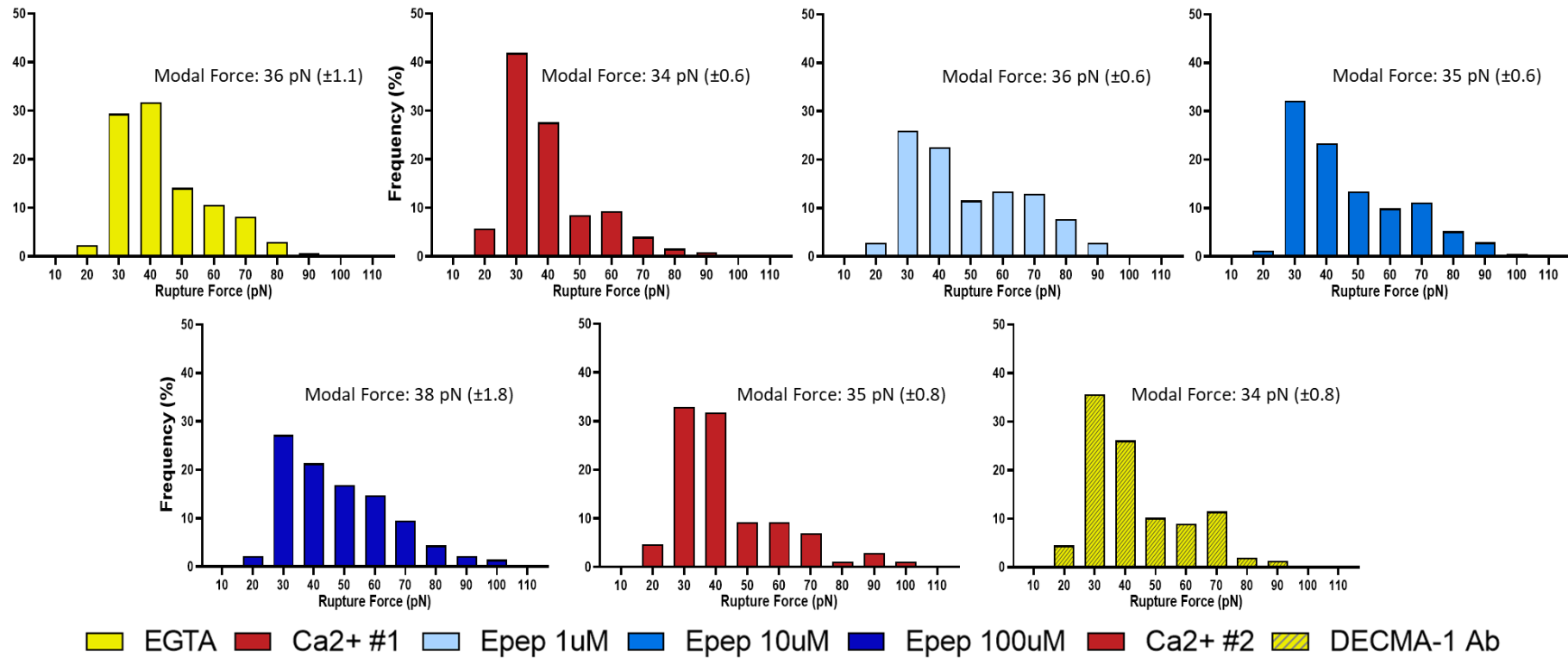


Figure 4.6: Representation of the distribution of rupture forces seen in specific adhesion events between all buffer conditions tested in the Epep titration experiment. Modal force analysis (captioned on figure) was more rigorously calculated using Fdist software, with this analysis available in Appendix 2. Histograms showing the binding forces observed for specific single molecule adhesions in each experimental buffer seen in the data shown in Figure 4.4. The modal force observed in each buffer environment is shown on the corresponding histogram, calculated using

4.2.2.3 Binding frequency of EpepW2R Treated Samples

As discussed in section 4.2.2.1, categorisation of F-D curves obtained from AFM testing was performed following the well-defined guidelines mentioned previously. As shown in Figure 4.7, the frequency of specific events is below 20% in all buffers tested, with the highest adhesion frequency recorded in the Ca^{2+} buffers as expected. This again indicates that the F-D curves categorised as specific events represent single molecule adhesions with an accuracy greater than 90%. Furthermore, the prominent F-D curve category recorded in all tested conditions represents an absence of any events during the probe-sample contact. This again indicates the stability of the system due to the low occurrence of non-specific or multiple adhesions in comparison. It can be seen from Figure 4.7 that the addition of EpepW2R peptide does not disrupt the stability of the system, as the relationship between the analysis categories remains consistent in all buffers.

As this work aimed to assess the effect of the EpepW2R peptide on specific adhesion frequency, each buffer condition was compared to the Ca^{2+} buffer tested in each

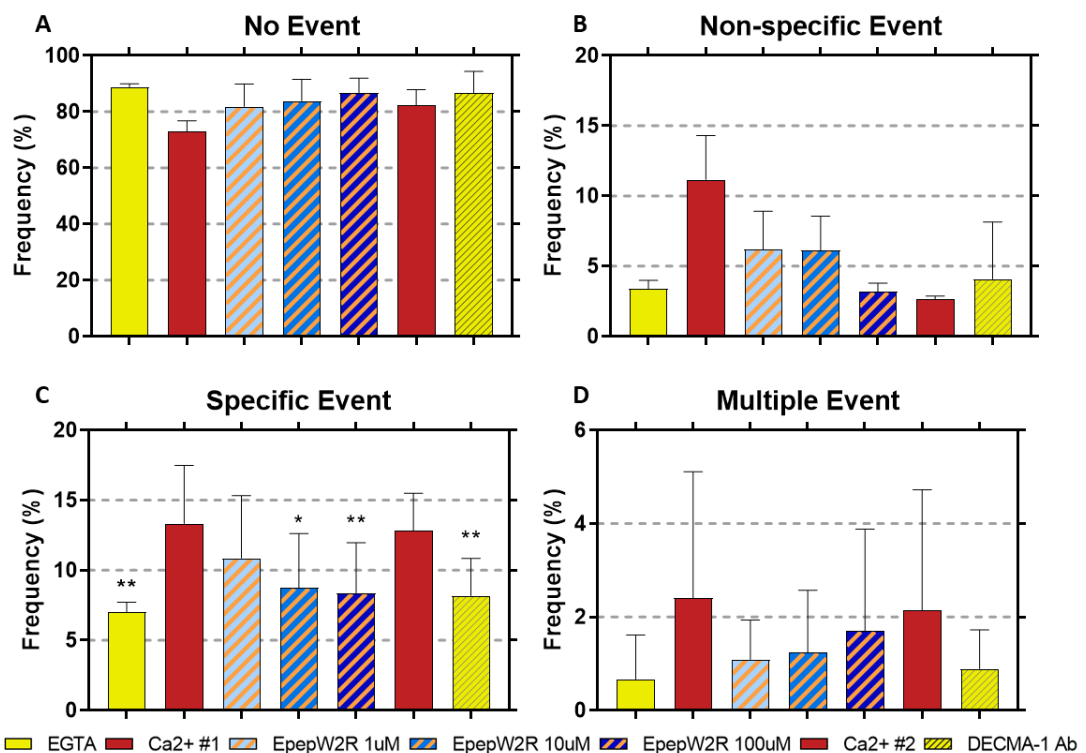


Figure 4.7: Comparison of F-D curves acquired from EpepW2R peptide treatment AFM experiments and categorised using the method discussed in section 3.2.5. Sample data was compared to the baseline value determined by the initial Ca^{2+} buffer to provide a more clear representation of the influence of different buffer environments. The data in these graphs provide a clear comparison of the buffers tested for each analysis category: A) no events, B) non-specific events, C) specific events, and D) multiple events. All comparisons were made to the initial Ca^{2+} buffer tested, and statistical analysis was performed using an average of the tested samples ($N=2$). Error bars show SD, and significance is shown as: * = $P < 0.05$, ** = $P < 0.01$, *** = $P < 0.001$, **** = $P < 0.0001$.

experiment. Although data in Figure 4.7A suggests a change in the recorded frequency of F-D curves with no events, the variation between buffers is still relatively small, and is only shown to increase when compared to the Ca^{2+} buffer. This change correlates with a reduction in other event categories, such as that seen in specific events of differing buffers (Figure 4.7D), accounting for the small differences between frequencies. It can also be seen in Figure 4.7B that the change of buffer, including the addition of EpepW2R peptide solution, only proves to reduce the frequency of non-specific interactions relative to testing in Ca^{2+} environment. Furthermore, despite the absence of significance in a number of buffer conditions, Figure 4.7D suggests a reduction in the frequency of multiple events.

When reviewing the frequency of specific events recorded in each buffer, as shown in Figure 4.7C, a significant loss of adhesion events is demonstrated following the addition of EpepW2R peptide solution. This inhibitory characteristic is uniquely found via our AFM experiments, as previous analysis of the EpepW2R peptide on cell cultures did not demonstrate an inhibition of cell-cell contact⁹³. The inhibition is shown to increase with higher concentrations, in line with the estimated equilibrium concentration of 55 μM , and at the highest peptide concentration of 100 μM shows an equivalent loss of adhesion events to testing in EGTA and DECMA-1 buffers. This data suggests addition of EpepW2R does not cause any permanent changes to the E-cadherin protein, as the introduction of DECMA-1 antibody still effectively inhibits E-cadherin adhesion as expected. It is also shown that any inhibition induced by the addition of EpepW2R can be removed by replacing the peptide solution with a Ca^{2+} buffer, with the adhesion frequency returning to the same level as initially recorded in the first Ca^{2+} buffer.

Furthermore, numerous studies assessing the E-cadherin adhesion process have isolated the tryptophan residue in the EC1-2 extracellular domains of E-cadherin proteins as a critical amino acid in the process of E-cadherin homodimer formation^{32,65,67,193,196}. It is the presence of this Trp2 residue that Devemy and Blaschuk refer to when reviewing the ability for the original Epep peptide sequence to bind to the E-cadherin protein. They also show that changing the Trp2 amino acid for Arginine (Arg) removes the binding of peptide to E-cadherin, as tested in cell

cultures¹². This finding was further developed by Segal and Ward as they again assessed the effect of the EpepW2R peptide sequence (therefore exchanging the Trp2 residue in Epep for Arg as before) on cell cultures, and determined that there was no loss of cell-cell contact following treatment.

It is therefore not clear how the EpepW2R peptide is inhibiting E-cadherin adhesion in our AFM system, as it does not demonstrate this ability in cell cultures. One possibility could be that the peptide demonstrates preferential off-target binding in cell cultures, thus it is not targeting E-cadherin binding domains in that environment, but still demonstrates inhibition in our simpler AFM experimental format. In addition, due to the importance of the Trp2 residue in E-cadherin homodimer formation, the lack of Trp residue in the EpepW2R sequence could explain a weak binding to E-cadherin, or perhaps suggest that any inhibition recorded in the AFM experiment, is steric in nature.

The unique approach implemented by use of the AFM system allowed for E-cadherin interactions to be observed while under load, and as such provided an analysis of E-cadherin interactions in response to peptide treatment that has not yet been seen. As discussed in chapter 1, the application of force to adhesion proteins can act to stabilise or manipulate bonds, and may be an important factor in the observation and understanding of peptide influence. For example, the results obtained following EpepW2R treatment may suggest the detection of an inhibitory mode that is related the mechanical nature of E-cadherin; while this requires further investigation, this work highlights the potential of the AFM approach over ensemble measurements, that probe interactions without the application of force.

As seen in Figure 4.8, the inhibitory impact of the EpepW2R peptide does not show any significant change through the progressive peptide concentrations tested. Whereas the Epep treated samples seen in Figure 4.5 demonstrate an increased inhibition between the 1 μM and 10 μM conditions, the addition of EpepW2R immediately induces inhibition at 1 μM to a similar extent to that seen in the 100 μM concentration. As the estimated equilibrium concentration for EpepW2R was estimated by Segal and Ward to be $\approx 55 \mu\text{M}$, it can be seen that this value does not appear to reflect a noticeable change in the peptide function. This intriguing realisation highlights the need to further understand the function of these peptides, as our AFM system not only suggests an inhibitory capability of the EpepW2R peptide not previously seen, but also that the potency of this interaction is perhaps greater than previously believed.

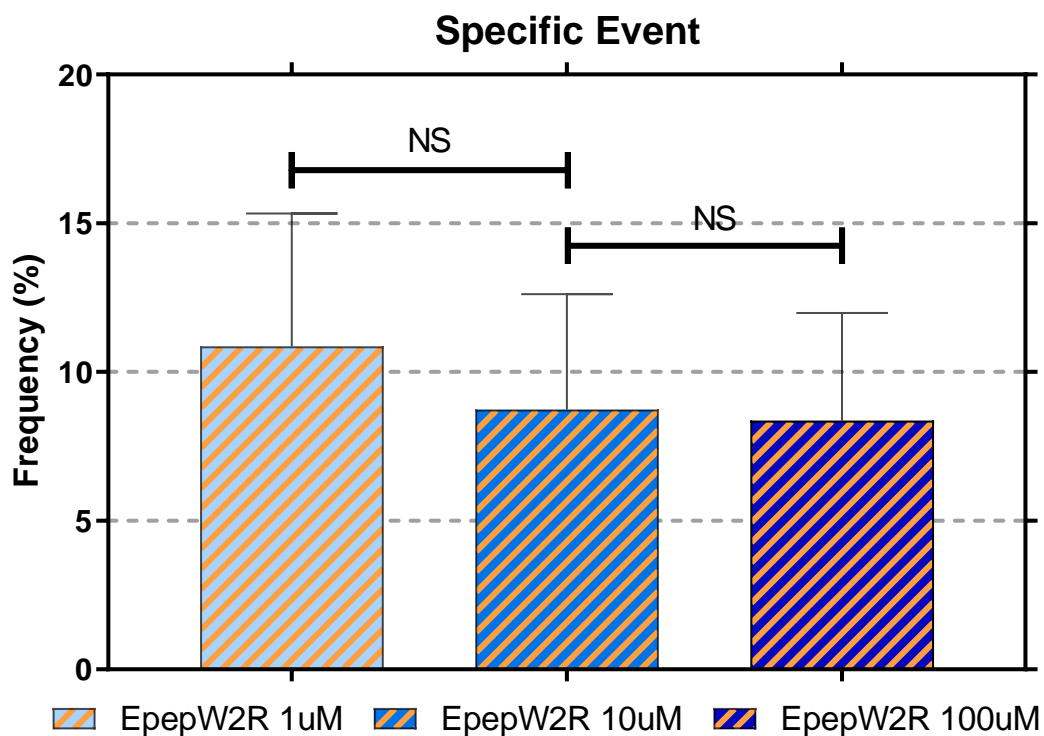


Figure 4.8: Comparison of the specific event frequency recorded in each concentration of EpepW2R buffer. A minimum of 500 F-D curves were recorded for each buffer condition, with N=2 repeats. Statistical analysis of the values was performed on the baseline corrected percentages when compared to Ca^{2+} buffer, as seen in Figure 4.7, with comparisons isolated to the ascending Epep concentrations. Error bars represent standard deviation between samples and significance is shown as: NS = no significance, * = $P < 0.05$.

4.2.2.4 Binding force of EpepW2R Treated Samples

As seen in chapter 4.2.2.2, the forces recorded from specific event F-D curves were plotted as a histogram. The force data for all conditions tested during EpepW2R experiments is shown in Figure 4.9. This data demonstrates a modal binding force in

the range of 30 – 35 pN for all buffers tested, which again correlates with previous publications assessing E-cadherin adhesion, and suggest the presence of strand dimer interactions between E-cadherin proteins^{61,133,183}. This modal force is also seen throughout our Epep AFM experiments (4.2.2.2), indicating a consistent adhesion profile of our system in all buffer conditions, including both peptide sequences selected.

Work by Shi *et al.* assessed the binding capability of a W2A variant of E-cadherin proteins, and concluded that although a tryptophan residue is essential for cadherin function, interaction of W2A/W2A variants (where the tryptophan residue in EC1 is replaced with alanine) do maintain a weak binding regime. Furthermore, interactions are shown between W2A variants and EC3-5 cadherin domains, again demonstrating binding is possible. Therefore, the EpepW2R peptide may still be capable of adhesion to the extracellular domains of E-cadherin following similar processes, as supported by the presence of an inhibitory effect of the peptide. Furthermore, the force analysis seen for 100 μ M EpepW2R peptide solution in Figure 4.9 suggests a more prominent secondary binding force around 60 – 70 pN when compared to other peptide conditions. This peak is distinct from the initial low force adhesion seen throughout all buffers. The presence of these higher force adhesion events may be due to the formation of X-dimer bonds, as discussed by Rakshit *et al.* and further considered by Leckband and Rooij^{61,68}. It can be seen that formation of X-dimer bonds are possible in W2A variants of E-cadherin proteins, indicating a secondary binding site may be present that may be the site of interaction for the EpepW2R peptide.

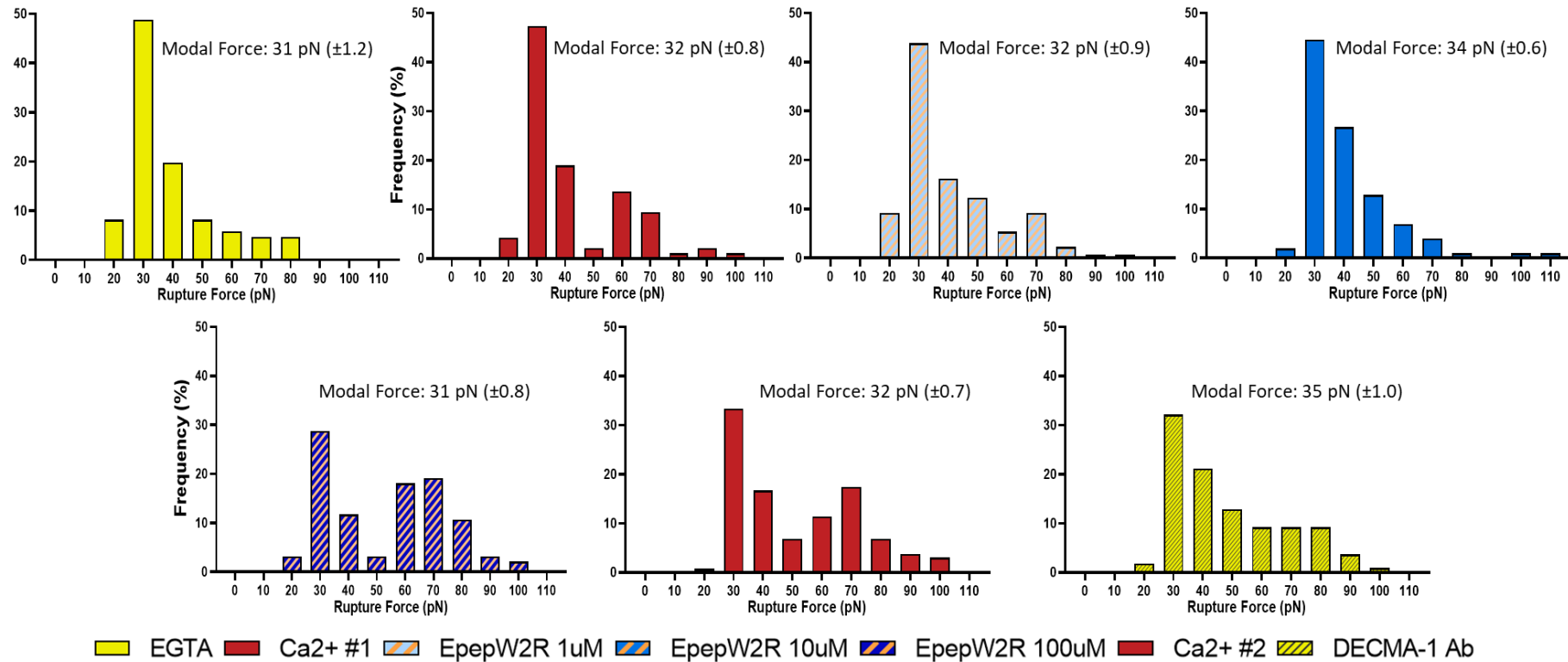


Figure 4.9: *Distribution of rupture forces seen in specific adhesion events between all buffer conditions tested in the EpepW2R titration experiment. Modal force analysis (captioned on figure) was more rigorously calculated using Fdist software, with this analysis available in Appendix 2. Histograms showing the binding forces observed for specific single molecule adhesions in each experimental buffer seen in the data shown in Figure 4.7. The modal force observed in each buffer environment is shown on the corresponding histogram, calculated using Fdist.*

4.2.3 Cell-AFM

Previous sections present clear evidence of successful AFM-SMFS analysis of E-cadherin functionalised samples in the presence of novel peptide sequences. This was a key achievement within this project, as it highlights the potential for similar systems to be used in the future for the detailed study of the peptides, and potentially for their screening, with a wide range of potential targets available due to the adaptability of AFM systems. Therefore, a natural progression for this work was to also assess the efficacy of more biological relevant sample surfaces, namely cell monolayers.

As discussed in chapter 1, the use of mESCs is paramount throughout research and therapeutics. E14 cells represent one of the most commonly adopted mESC cell lines, and are known to express surface bound E-cadherin protein that is prominent in cell-cell adhesion²¹⁵. As such this is the ideal initial cell line to be used for development hard sample surfaces, allowing the AFM system developed thus far to be used with more clinically relevant samples. The application of AFM for cell analysis is receiving ever greater interest, and indeed cell-AFM studies are now quite common in literature, due to the precise control and analysis available with AFM instruments. This includes the ability to test samples in a liquid environment, which is paramount for the survival of many cell cultures, and helps to maintain a more stable sample throughout testing. However, there is very limited insight into the ability to probe peptide interaction with cell monolayers and the observed cell response using AFM.

This section therefore uses E14 cell cultures in place of functionalised hard sample surfaces, to test the ability to screen the inhibitory effects of the Epep peptide sequence. This experiment aims to highlight the potential development of this technique by testing several buffers sequentially on the cell surface, while reviewing the specific adhesion forces observed, as in previous sections.

4.2.3.1 Proof of Concept AFM Investigations of mESC-Peptide Interactions

Testing of E14 cell monolayers required a slightly altered approach when compared to that of functionalised hard surfaces seen previously. This is due to the sensitive and more complex nature of biological systems, and considerations for maintaining sample stability for experiments. Therefore, as detailed above these experiments

were performed using cell culture treated petri dishes that allowed for the AFM probe to contact the cells unimpeded, and buffers were tested sequentially to limit the possible variation between culture samples. However, the F-D curve analysis and categorisation remains consistent with previous experiments, providing a robust method of determining specific E-cadherin adhesions that form between the functionalised AFM probe and cell layer. Due to the preliminary nature of this work, the data represents analysis conducted with a single functionalised AFM probe and single cell monolayer, with a minimum of 250 F-D curves acquired in each condition. Example F-D curves obtained from probing E14 cell monolayers can be seen in Figure 4.10. When compared to F-D curves obtained from functionalised surfaces, seen in section 3.3.2, those obtained from cell monolayers display consistently higher noise. Furthermore, it can be seen from the example data that the force recorded when the tip is not under load can shift following contact with the surface. These characteristics show some of influences that must be considered due to the sensitive and complex nature of these experiments.

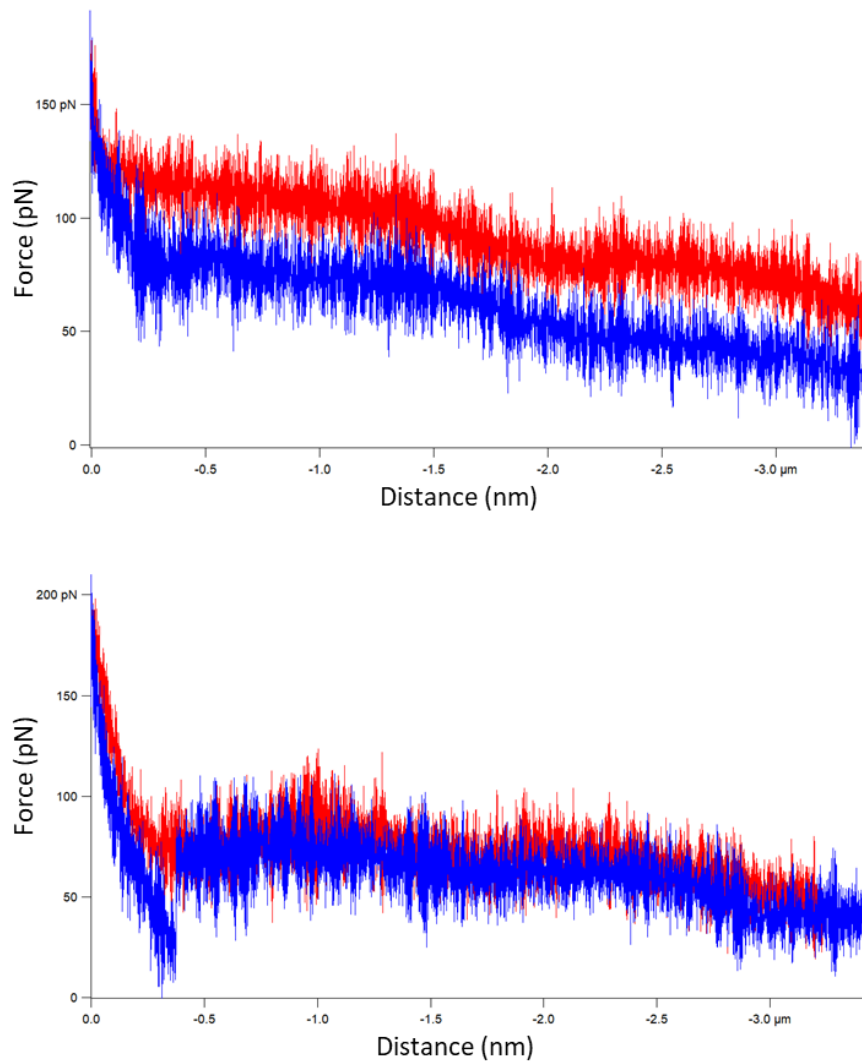


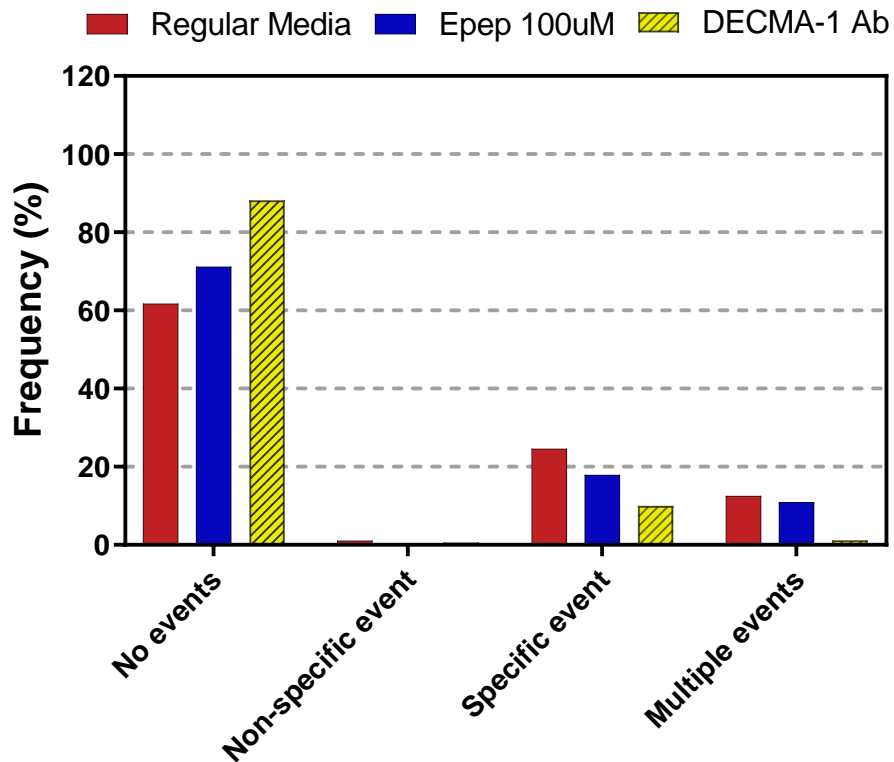
Figure 4.10: Example F-D curves acquired from probing E14 cell monolayers with an Ecad-Fc functionalised AFM probe. These example curves demonstrate the complexity and sensitivity of testing cell samples, and indicate the increased retraction distance from the surface.

As seen in Figure 4.11, the categorisation of F-D curves still shows success when applied to cell-AFM studies. The predominance of no events being recorded in all buffers and the lack of non-specific events indicates that the system is successfully isolating specific E-cadherin adhesions. Compared to the data seen in previous sections the frequency of multiple adhesion events seen in Figure 4.11A, particularly in the Ca^{2+} buffer environment, is shown to be higher. When testing in Ca^{2+} buffer there is a multiple adhesion frequency of $\approx 12\%$, with a similar value seen in the $100 \mu\text{M}$ Epep buffer. This correlates with a specific adhesion frequency of $\approx 24\%$ and 17% respectively. These values are slightly above the suggested optimal frequencies obtained from Poisson based statistical analysis ($10\% - 20\%$ specific adhesion) for the measurement of single molecule events, suggesting the specific experimental

conditions could be further refined for future work. However, the discrepancies are relatively small, and the values still correspond to an accuracy greater than 90%¹³⁸.

Following confirmation of a working SMFS system, as discussed above, the data was reviewed to assess the ability to test novel peptide sequences, In this case Epep. As seen in Figure 4.11A, and more closely in Figure 4.11B, the frequency of specific adhesion events does change between the tested buffers. Moreover, it shows an obvious loss of E-cadherin binding in the presence of the inhibitory DECMA-1 antibody, indicating a biologically relevant adhesion analysis. It can also be seen that the addition of the Epep sequence to the cell sample inhibits E-cadherin interaction, although to a lesser extent than the blocking antibody. This relationship is synonymous with that observed in literature, particularly the work of Segal and Ward⁹³, whereby Epep was shown to inhibit cell-cell contact of mESCs.

A



B

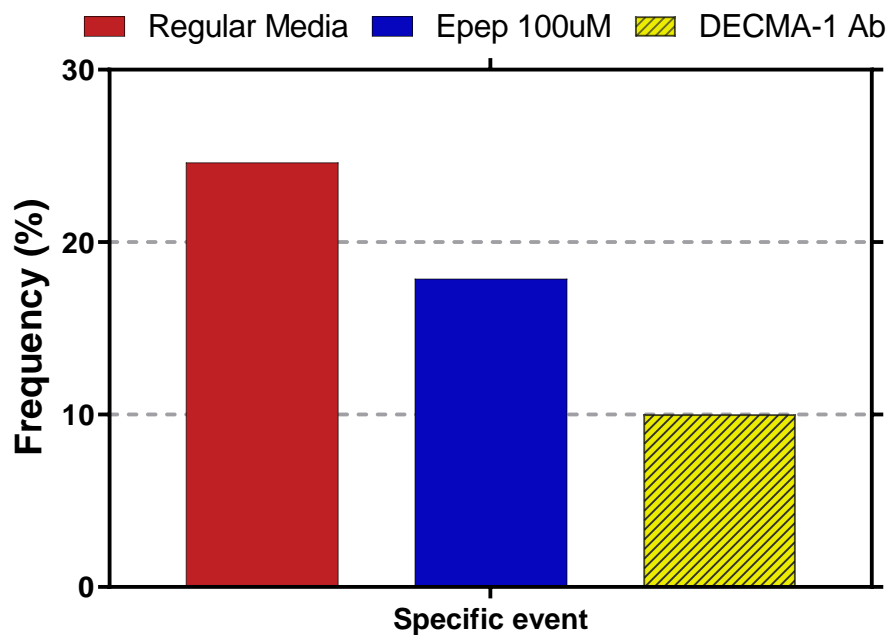


Figure 4.11: Initial analysis of AFM-based force experiments on E14 mESCs in Ca^{2+} , DECMA-1, and Epep buffers. Graphs showing the frequency of F-D curves recorded in Ca^{2+} , Epep 100 μ M, and DECMA-1 buffers. A) Frequencies of all four of the categories used when classifying F-D curves, and B) frequency of specific interactions only for more clear comparison between buffers. Due to the increased time to acquire data a minimum of 100 F-D curves were recorded for each condition.

Therefore, the AFM-SMFS analysis of E-cadherin proteins binding between a cell sample and functionalised AFM cantilever shows success in isolating specific

E-cadherin adhesion, as determined by the inhibitory influence of the targeting antibody DECMA-1. Furthermore, the introduction of the novel Epep peptide sequence is also shown to inhibit specific E-cadherin adhesions in our system. This further reinforces our ability to use this approach with targeting peptide sequences, as the loss of E-cadherin mediated cell-cell contact in literature is mimicked by the data shown in Figure 4.11.

Analysis of the forces recorded for each specific event between the E14 cell monolayer and E-cadherin functionalised AFM probe is shown in Figure 4.12. As with previous analysis, these histograms provide an insight into the distribution of forces recorded, which can be considered against the rupture forces predicted from literature. Again, a modal force near to 30 pN is prominent in each buffer environment, which correlates with our understanding of S-dimer formation between adjacent EC domains of E-cadherin proteins⁷⁰. The force distribution remains similar between each buffer, despite the loss of adhesion frequency, indicating a stable and specific SMFS system that can isolate E-cadherin bonds in a multitude of environments, including the presence of novel peptides.

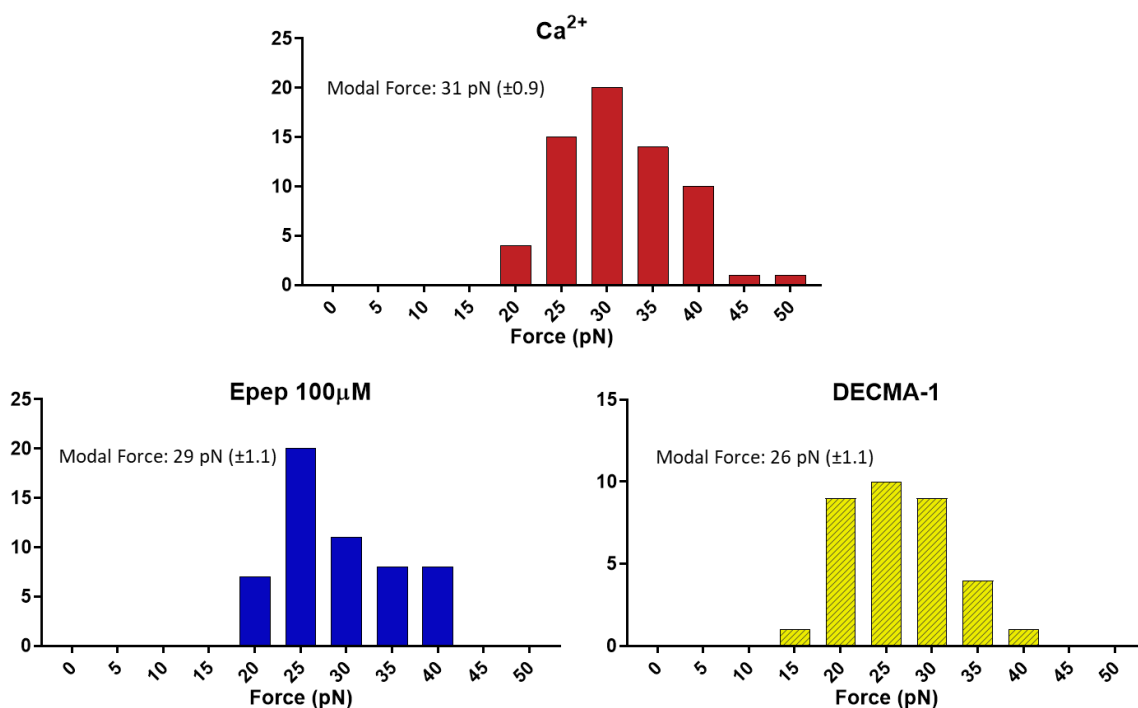


Figure 4.12: Force distribution for F-D curves classified as specific E-cadherin interactions from data seen in Figure 4.11A. Modal force analysis (captioned on figure) was more rigorously calculated using Fdist software, with this analysis available in Appendix 2. Histograms showing the force distribution of specific adhesion events recorded in Ca²⁺, Epep 100 µM, and DECMA-1 buffers. This data was acquired on a E14 cell monolayer with each buffer added sequentially to the same sample. A minimum of 100 F-D curves were recorded for each condition.

4.2.4 Discussion

Throughout this chapter we have seen that multiple peptide concentrations can be tested using our AFM set-up. The system reported a maximum specific adhesion frequency below 20% in all experiments, indicating single molecule analysis with an accuracy >90%^{139,211}. This allowed for analysis of single molecule adhesions in the presence of various concentrations of both Epep and EpepW2R peptides.

From the data shown throughout section 4.2.2, it can be seen that Epep acted to inhibit E-cadherin adhesion, as shown by a reduction in the frequency of single molecule binding events. This agrees with previous publications stating the inhibitory characteristics of the Epep sequence when interacting with E-cadherin proteins^{12,93}. It can be seen that the inhibition recorded is exaggerated in increasing peptide concentrations, with a plateau seemingly reached above the 3.4 μM equilibrium concentration for the peptide. The inhibition of E-cadherin adhesion events by Epep is also shown to be similar to the addition of an E-cadherin functional targeting antibody, DECMA-1. Furthermore, the binding forces measured in single molecule adhesions demonstrate a consistent modal peak between 30 – 40 pN between all buffer conditions. This value is consistent with the formation of strand-swap dimers, which are commonly accepted as high affinity initial interactions between E-cadherin molecules and are characterised by exchange of tryptophan residues between binding molecules^{61,64}. These findings further support previous publications regarding interaction properties of Epep with E-cadherin molecules and provides a new method of assessing the novel peptide characteristics.

As highlighted in section 4.2.2, the introduction of an AFM based approach for the analysis of EpepW2R on E-cadherin adhesion suggested a novel peptide effect not yet seen in literature. Despite previous publications suggesting a lack of inhibition of physical E-cadherin adhesion, our data demonstrates that the addition of EpepW2R solutions did inhibit the interaction in the AFM experiment, resulting in a reduced frequency of binding events. As discussed, the absence of a Trp2 residue in the peptide sequence may greatly reduce the affinity for functional blocking of E-cadherin proteins in cell cultures, with off-target or competitive binding preventing the inhibitory effect in some tested cell lines⁹³. However, in our isolated system the

EpepW2R peptide is shown to successfully inhibit binding, with a similar loss to that measured when testing the functional blocking DECMA-1 antibody. This effect is observed at all peptide concentrations, with increased concentration not demonstrating a significant increase in the loss of specific adhesions. It can also be seen in Figure 4.9 that the modal binding force for specific E-cadherin adhesions is in the range of 30 – 35 pN. This is consistent for all tested conditions, and demonstrates stability in the ability for the system to isolate specific E-cadherin adhesions, even in the presence of peptide solutions. The observed loss of adhesion frequency while maintaining consistent force distribution profiles indicates a novel peptide characteristic, suggesting EpepW2R can interact specifically with E-cadherin ectodomains, despite previous cellular assays demonstrating no loss of cell-cell contact. The blocking properties of EpepW2R observed uniquely with AFM may therefore be suggestive of competitive binding in cell cultures, or preferential off-target binding of the peptide in more complex systems. Although further assessment is required to fully understand EpepW2R characteristics, this analysis provides a detailed understanding of E-cadherin binding, with a greater understanding achieved from the unique outcomes detailed above.

Development of this system to allow use of mESC cell monolayers in place of functionalised hard surfaces was successfully demonstrated, as seen in section 4.2.3. The ability to carefully modify the sample preparation and experimental conditions allowed for a relatively simple transition between sample types, and the use of a liquid environment provides ideal conditions for maintaining stable cell cultures even during testing. This is observed as the categorisation of F-D curves for an E14 cell monolayer in multiple different buffers, seen in Figure 4.11, produced a similar frequency profile to that seen with hard surfaces in section 4.2.2. Thus, the predominance of no event F-D plots and relatively low frequency of specific events indicates a high system accuracy, as determined by Poisson based analysis¹³⁸. From Figure 4.12 it can be seen that the force distribution for specific events correlates with the results expected from literature.

A recent publication by Hammond *et al.*¹⁴⁸ expands upon the potential for AFM to be used as a method of monitoring cell membrane disruption in response to the addition

of peptides; however, this work simultaneously highlights the lack of current research developed in this area. One key barrier suggested for this is the difficulty in maintaining live cell cultures during AFM experiments, and ensuring contact forces remain non-destructive to the cell^{148,216,217}. The developments shown in this chapter naturally align with these considerations, and although currently limited in diversity, show potential for widespread application. This could help to bridge the gap in literature between AFM-based experiments and live cellular response to targeting peptides.

As discussed previously, the natural orientation for homotypic E-cadherin bonds is the S-dimer, which is often represented by a force of ≈ 30 pN. This corresponds to the modal force observed when testing E14 cultures in all buffer conditions used. This result not only indicates a stable SMFS system, as the inhibitory nature of the buffers acts to prevent bond formation as opposed to altering the bond structure, but also highlights the possibility of using this system for peptide screening in more biologically relevant systems. Techniques such as surface plasmon resonance (SPR) are common when testing peptide binding to targets, and indeed initial studies by Segal and Ward testing the Epep sequence and close analogues, used SPR to assess the peptide binding⁹³. This approach provides ensemble analysis of protein interaction and is therefore more limited in the ability to isolate single protein interactions when compared to AFM, and requires a greater amount of sample. The influence of mechanical forces has been of particular interest in recent years, due to the finding that bond formation and stabilisation can be heavily influenced by the application of force. This is evident in E-cadherin, as highlighted in chapter 1, as the formation of slip, catch, and ideal bonds have been observed^{61,63,68}. Our work therefore demonstrates the capability of AFM-SMFS analysis as a novel approach to assess peptide interactions, allowing the introduction of mechanical force to provide a more comprehensive and accurate model of interaction.

Our results show that the use of AFM allows for a more in depth assessment of physical binding characteristics, and has already shown to be able to highlight information that could not be obtained using regular cellular assays, such as the inhibitory effect of EpepW2R peptide⁹³. Similar techniques have been employed

previously to assess biological proteins such as E-cadherin, demonstrating the efficacy of this analytical system. However, the introduction of these novel peptides provides us with a unique platform to further develop our knowledge of novel peptide sequences, and help provide a greater understanding of the underlying processes and characteristics.

4.3 Conclusions

Overall, this chapter has demonstrated novel assessment of the Epep and EpepW2R peptide sequences. Analysis of binding frequency and force shows that both the Epep and EpepW2R peptides exhibited inhibitory effects on E-cadherin binding in the AFM experiment, despite previous publications suggesting a lack of inhibitory capability for EpepW2R. It can also be seen that the force distribution profiles observed show the same modal force of 30pN between all conditions for both peptides, and that the inhibitory effect observed is reversible by the replacement of peptide solution with calcium buffer. This work shows successful use of the Epep peptide sequence with mESC monolayers, with sequential application of buffers tested on the same sample, while producing SMFS data showing a correlative trend compared to that seen with functionalised sample surfaces.

Chapter 5 - Treatment of E14 and Ecad^{-/-} Cell Lines with Epep and EpepW2R peptides

The importance of developing and understanding targeting peptides for biological impact has been communicated in part within chapters 1 and 4. As this chapter details cell-based assays to monitor response to Epep and EpepW2R, the focus will similarly shift to encompass more cell related applications.

The use of embryonic stem cells in research is widespread, constituting an important avenue for the potential development and testing of therapeutics. Therefore, the need to understand and influence cell behaviour is crucial. As discussed in chapter 4, novel peptides targeting mESCs have been developed with the aim of influencing cell behaviour, with the introduction of phage display providing a novel approach to the search for ESC markers and targets, alongside ongoing research to fully define culture conditions^{12,218}. Similarly, antibodies have been applied due to their natural interaction with specific cellular targets, although these can be more expensive to synthesise and possess a more limited ability to be modified to control any undesirable properties²¹⁹. Following the focus of this work on cadherin proteins, specifically E-cadherin due to its expression by mESC cell lines, it is pertinent to consider the work of Mohamet *et al.*, Segal and Ward, and Devemy and Blaschuk^{11,12,93}. The first of these publications demonstrates successful use of E-cadherin targeting antibody DECMA-1 as a method for maintaining pluripotent mESC cultures in stir tank bioreactors. Due to the abrogation of cell-cell contact by the antibody the authors recorded an improved cell proliferation with limited spontaneous differentiation, highlighting the potential of targeting molecules to selectively influence cell behaviour. However, as stated the use of antibodies is not a cost-effective method for long-term scale-up culture^{11,220}. This issue is partially addressed by the identification of E-cadherin targeting peptide sequences first determined via phage display by Devemy and Blaschuk, and further developed by Segal and Ward, providing the Epep and EpepW2R peptides seen in previous chapters^{12,93}. The original peptide sequence, and single amino acid variants, were shown to produce unique responses in the expression of key pluripotency markers

in mES cell cultures, and provided initial insight into the specific regions in the sequence responsible for cell interactions.

To continue from our work in chapter 4, this section used Epep and EpepW2R peptides alongside E14 and Ecad^{-/-} mESC cell lines to assess the biological impact during culture. This work naturally developed from that of Segal and Ward, providing insight into factors such as cell morphology, proliferation, and expression of common mESC pluripotency markers, complimentary to that seen previously.

5.1 Materials and Methods

5.1.1 General Cell Culture

5.1.1.1 Continuous culture of mESC cell lines

Two immortalised (passage unknown) mESC lines E14TG2a²²¹ (a gift from Prof. Austin Smith, University of Cambridge, UK) and Ecad^{-/-222} (Prof. Cathy Merry, University of Nottingham) were cultured using knockout Dulbecco's modified eagle medium (DMEM) (Thermo Fisher Scientific, USA), supplemented with 10% (v/v) Hyclone FBS (Perbio, UK), 1% (v/v) L-Glutamine (Gibco, UK), 1% (v/v) minimum essential medium non-essential amino acids (MEM NEAA) (Gibco, UK), 0.1% (v/v) β -mercaptoethanol (Gibco, UK), with the addition 0.1% (v/v) leukemia inhibitory factor (LIF) (Millipore, USA) to aid in the maintenance of pluripotency of the cultures^{223,224}. Prior to the addition of LIF and β -mercaptoethanol the media was filtered using a 0.22 μ m vacuum filter (Thermo Fisher Scientific, USA). See Table 5.1 below for media components. Routine culture was performed using treated T25 or T75 culture flasks (Thermo Fisher Scientific, USA) that had been coated with 0.1% (v/v) gelatin (Sigma Aldrich, USA) prior to cell seeding. Following standard culture protocols, cell cultures were incubated at 37°C with a humidified 5% CO₂ environment, with a media change or passage performed every 48-72 h as required by flask confluency. When passaging, cultures were first washed with phosphate buffered saline (PBS) (Gibco, USA), before adding trypsin-EDTA (Gibco, USA) to detach cells from the culture flasks by adding a minimum volume to the culture surface (0.5 ml or 1.5 ml for T25 or T75 flasks respectively) and then removing immediately. The cultures were then left to incubate at 37°C for 1-3 minutes before neutralising the trypsin with culture medium. The subsequent cell suspension was then diluted further as required, before reseeding into culture flasks, plates, or dishes depending on desired application. Upon thawing, cell cultures were denoted as passage 1 (P1), and no cultures beyond P35 were used experimentally.

Table 5.1: *Media components required for the culture medium of mouse embryonic stem cell lines E14 and Ecad^{-/-}. All components except β -Mercaptoethanol and LIF were added, and the solution was vacuum filtered using a 0.22 μ m filter, before the remaining components were added.*

<u>Product</u>	<u>Manufacturer</u>	<u>Composition</u>
Knockout DMEM	Gibco (10829-018)	-
Hyclone FBS	Perbio (CH30160.03)	10%
L-Glutamine (200 mM)	Gibco (25030-024)	1%
MEM-NEAA (10 mM)	Gibco (11140-035)	1%
2-Mercaptoethanol (50mM)	Gibco (31350-010)	0.1%
LIF (1×10^6 U/mL)	Millipore (ESG1107)	0.1%

5.1.1.2 Freezing and Thawing Cell Stocks

Original cell stocks were received as cryovials containing 0.5 ml volumes comprising 10% (v/v) DMSO in culture medium. These vials were stored in liquid nitrogen (LN₂) until required. Freezing of cell stocks was performed using 10% (v/v) DMSO in culture medium, with cell solutions initially frozen to -80°C using a cell freezing container (Corning, USA) to ensure controlled temperature change of 1°C·min⁻¹. Following this, the frozen cryovials were transferred to LN₂ for long term storage.

To thaw stock solutions and revive cell cultures, culture medium (detailed in section 5.1.1.1) was prepared and warmed to 37°C before adding 5 ml to a T25 flask unless otherwise directed. The cryovial containing the cells was then quickly thawed using a water bath set to 37°C, and 0.5 ml of pre-warmed culture medium was added to the vial. The vial contents were gently mixed using a pipette, before being transferred to the culture flask containing medium. The flask containing the cells was then incubated at 37°C for 6 – 24 h to allow cell attachment before a media change was performed to remove any remnants of DMSO from the culture.

5.1.1.3 Making peptide treated medium

Where peptide treatment was required, 10mM stock solutions of Epep and EpepW2R peptides (Pepceuticals, UK) were diluted in cell culture medium before being added

to the cultures. To ensure sterility of the culture medium, the peptide solutions were added prior to β -mercaptoethanol and LIF, as to allow filtration using a 0.22 μ m filter (Millipore, USA) as discussed in section 5.1.1.1. Treated culture medium was then added to cell cultures immediately following seeding.

5.1.2 Fluorescence and Operetta Imaging

5.1.2.1 Sample Preparation

To prepare samples for fluorescence labelling, and subsequent imaging, E14 and Ecad^{-/-} cell lines were seeded into gelatin coated 6 well or 96 well plates as required. The samples were incubated dependent on experimental requirements up to a maximum of 72 h.

To provide a more quantifiable analysis of biomarker expression, Operetta imaging of cell samples was conducted using a PerkinElmer Operetta[®] High Content Imaging System (PerkinElmer, USA). This technique allows for fluorescent imaging of treated samples alongside mathematical quantification of multiple cell parameters, providing a more robust analysis of cell cultures treated with varying peptide concentrations.

For testing with the PerkinElmer Operetta system, samples were prepared in gelatin coated CellCarrier 96 well plates (PerkinElmer, USA). Samples were cultured until confluent unless otherwise stated up to a maximum of 72 h, with appropriate treatment conditions maintained throughout culture.

5.1.2.2 Peptide Treatment

Where peptide treatment was required, peptide culture medium was added immediately following cell passage. Samples were then incubated until confluent, often for a period of 48 h unless otherwise stated.

5.1.2.3 Immunostaining

To image cell expressed markers of interest, immunostaining of cell cultures was performed. This process first required samples to be fixed using formaldehyde-based cross-linking. For this we formed a 4% (v/v) paraformaldehyde (PFA) solution by diluting 16% (v/v) PFA (Polysciences, USA) with phosphate buffered saline (PBS). Cell samples were then washed using PBS, and the PFA solution was added for a period

of 15 minutes at room temperature. Once complete the PFA was removed, and the samples were immediately stained or washed and then stored in PBS at 4°C for later use. Once the samples were fixed, immunocytochemistry (ICC) methods were implemented to label targets of interest. For intracellular markers, samples had to first be permeabilised using 0.1% (v/v) Triton-X (Sigma-Aldrich, USA), which disrupts the cellular membrane to allow targeting antibodies to bind effectively. All samples were then blocked for non-specific binding using 10% (v/v) Goat serum before specific primary antibodies were added.

For fluorescence imaging multiple targets of interest were selected, with the antibodies used for each as follows: E-cadherin (Cell signalling technology, 3195, monoclonal, 1:200, USA), N-cadherin (Abcam, ab76057, polyclonal, 1:100, UK), Oct4 (Cell signalling technology, 83932, monoclonal, 1:500, USA). Samples were incubated with primary antibody solutions overnight at 4°C, before being washed using PBS. Subsequently, a fluorescently tagged secondary antibody was incubated on the sample in the dark for 1 h at room temperature. The secondary antibody used was a goat anti-rabbit type, with an AlexaFluor(AF) 488 tag (Invitrogen, a11008, AF488, USA). All samples were also stained with 4',6-diamidino-2-phenylindole (DAPI) and rhodamine phalloidin (ThermoFisher scientific, R415, 1:1000, USA) to target DNA and F-actin respectively.

Table 5.2: **An Overview of the antibodies used for immunostaining.** The table shows the different primary and secondary antibodies used for labelling of cell samples, as seen throughout this chapter.

Antibody/Fluorophore	Manufacturer	Product Code	Isotype	Dilution
Primary				
E-cadherin	Cell Signalling Technologies	3195S	Rabbit, IgG	1:200
N-cadherin	Abcam	Ab76057	Rabbit, IgG	1:100
Oct4	Cell Signalling Technologies	83932	Rabbit, IgG	1:500
E-cadherin	ThermoFisher	16-3249-82	Rat, IgG1	1:200
N-cadherin	ThermoFisher	13-2100	Rat, IgG2a	1:500
Oct4	Abcam	ab19857	Rabbit, IgG	1:200
Syndecan-1	BD Biosciences	553712	Rat, IgG2a	1:25
Syndecan-4	Abcam	ab24511	Rabbit, IgG	1:100
Secondary				
Goat anti-rabbit AF488 (Ex/Em: 494 nm/517 nm)	Invitrogen	a11008	IgG (H+L)	1:500
Goat anti-rat AF546 (Ex/Em: 556 nm/573 nm)	Invitrogen	a11081	IgG (H+L)	1:400

For Operetta imaging the following primary antibodies were used as required: E-cadherin (ThermoFisher, 16-3249-82, monoclonal, 1:200, USA), N-cadherin (ThermoFisher, 13-2100, monoclonal, 1:500, USA), Oct4 (Abcam, ab19857, polyclonal, 1:200, UK), syndecan-1 (BD Biosciences, 553712, monoclonal, 1:25, USA), Syndecan-4 (Abcam, ab24511, polyclonal, 1:100, UK). Primary antibodies were left on the sample overnight at 4°C to incubate, followed by washes with blocking buffer to remove unbound antibodies. The following secondary antibodies were then applied as required: goat anti-rabbit AF488 (Invitrogen, a11008, 1:500, USA), goat anti-rat AF546 (Invitrogen, a11081, 1:400, USA). Secondaries were left on the samples for 1 h at room temperature, before performing PBS washes to remove unbound antibody. Samples were also stained with DAPI and Phalloidin for nuclear and F-actin targeting, respectively. A Table showing the information of all antibodies used in this chapter is seen in Table 5.2. All ICC based experiments included control samples which were treated with each individual secondary antibody only, all secondary antibodies together, or no antibodies.

5.1.2.4 Instrument, Data Acquisition, and Data Analysis

Fluorescence imaging was performed using a Leica TCS SPE confocal microscope (Leica, Germany) to obtain images taken as 1024x1024 z-stack files, with filters for AF488 (494/517), DAPI (345/455), and TRITC (544/570). Images were processed using

Fiji software v1.51w. All parameters were adjusted in parallel for imaging channels to provide a clearer image of the fluorescence recorded.

Images acquired using a PerkinElmer Operetta® High Content Imaging System (PerkinElmer, USA) were processed via the associated Harmony software provided by PerkinElmer. Filters were applied to monitor AF488, AF594, TRITC, and DAPI. Each plate was imaged such that multiple areas of interest were selected in each individual well, and multiple wells were tested for each condition. Control samples were also imaged to ensure the specificity of antibody binding, including individual and grouped secondary antibody controls. Instrument settings were optimised prior to data acquisition and were maintained throughout the experiment. The software allows for initial user set-up which included selecting imaging planes to optimise focus and adjusting laser power and acquisition time to produce accurate images. This set-up was then automatically applied by the system for the remaining sample wells.

5.1.3 Operetta Imaging

5.1.3.1 Instrument Set-up and Data Acquisition

Images were acquired using a PerkinElmer Operetta® High Content Imaging System (PerkinElmer, USA) with the associated Harmony software provided by PerkinElmer. Filters were applied to monitor AF488, AF594, TRITC, and DAPI. Each plate was imaged such that multiple areas of interest were selected in each individual well, and multiple wells were tested for each condition. Control samples were also imaged to ensure the specificity of antibody binding, including individual and grouped secondary antibody controls. Instrument settings were optimised prior to data acquisition and were maintained throughout the experiment. The software allows for initial user set-up which included selecting imaging planes to optimise focus and adjusting laser power and acquisition time to produce accurate images. This set-up was then automatically applied by the system for the remaining sample wells.

5.1.3.2 Data Analysis

Data acquired from the Operetta system was exported using the Columbus Transfer function. Subsequent analysis was then performed using Columbus or Harmony

software. Image processing involved the application of an in-built cell segmentation and analysis function, whereby cell properties were calculated by delineation of DAPI and phalloidin localisation on the cell images. This process allowed for determination of a 'true' sample image, whereby inclusion of artefacts is minimised by characteristics such as marker expression or nuclear size. This initial cell analysis was then followed by further in-built analysis functions as required. When completed, the analysis script was applied to each experiment to ensure consistency in data analysis.

5.2 Results and Discussion

5.2.1 Testing cell line characteristics for experimental application

Experimental cell lines first required assessment for viability with our work. Two mESC cell lines, E14 and Ecad^{-/-}, were cultured following standard protocols outlined in section 5.1.1 and monitored via phase contrast microscopy and fluorescence microscopy. This section aimed to monitor the cells lines in regular culture conditions to ensure successful culture, before then introducing targeting peptides.

5.2.1.1 Continuous cell growth

As discussed in chapter 1, many mESC cell lines are used in biological research. Of these, E14 is perhaps one of the most common, and provided a well-established reference cell line for use throughout²²¹. The Ecad^{-/-} cell lines were also used to allow for a comparative mESC culture with the absence of E-cadherin²²². Cultures were maintained using well established protocols, detailed previously, and continuously monitored to determine viable cell growth. Phase contrast imaging was used to view the cultures, with proliferation evident from the increased cell confluency, and well-established culture morphology used to assess for widespread differentiation.

As seen in Figure 5.1, the phase contrast imaging of E14 cells shows a rounded colony formation in general culture conditions, with clear E-cadherin expression when using fluorescence microscopy with E-cadherin targeting antibodies. Throughout culture it was ensured that the flask confluency was increasing at a similar rate alongside the rounded colony formation, denoting cell proliferation and subsequently pluripotency. From Figure 5.1C, it can be seen that E-cadherin is localised to the membrane of cells, particularly at regions of cell-cell contact. As a well-known adhesion protein this is the expected expression profile as seen in previous publications, again indicating that the standard culture procedures proved sufficient to maintain the E14 cell line²²⁵.

Ecad^{-/-} cultures demonstrated a more individual growth morphology, in-keeping with previously published data using this cell line³⁶. Fluorescence targeting of E-cadherin also highlighted the absence of this protein as expected for the knockout cell line, with no observable fluorescence in Figure 5.1G. The more isolated growth

morphology observed in phase contrast imaging of Ecad^{-/-} cultures is again seen with fluorescence microscopy. Expression of actin within the cells shows a visibly lower expression profile, with minimal interaction between cells. This is a stark contrast to the characteristics of E14 cells, whereby cytoskeletal staining shows a more expansive and interactive network, in agreement with the E-cadherin expression observed.

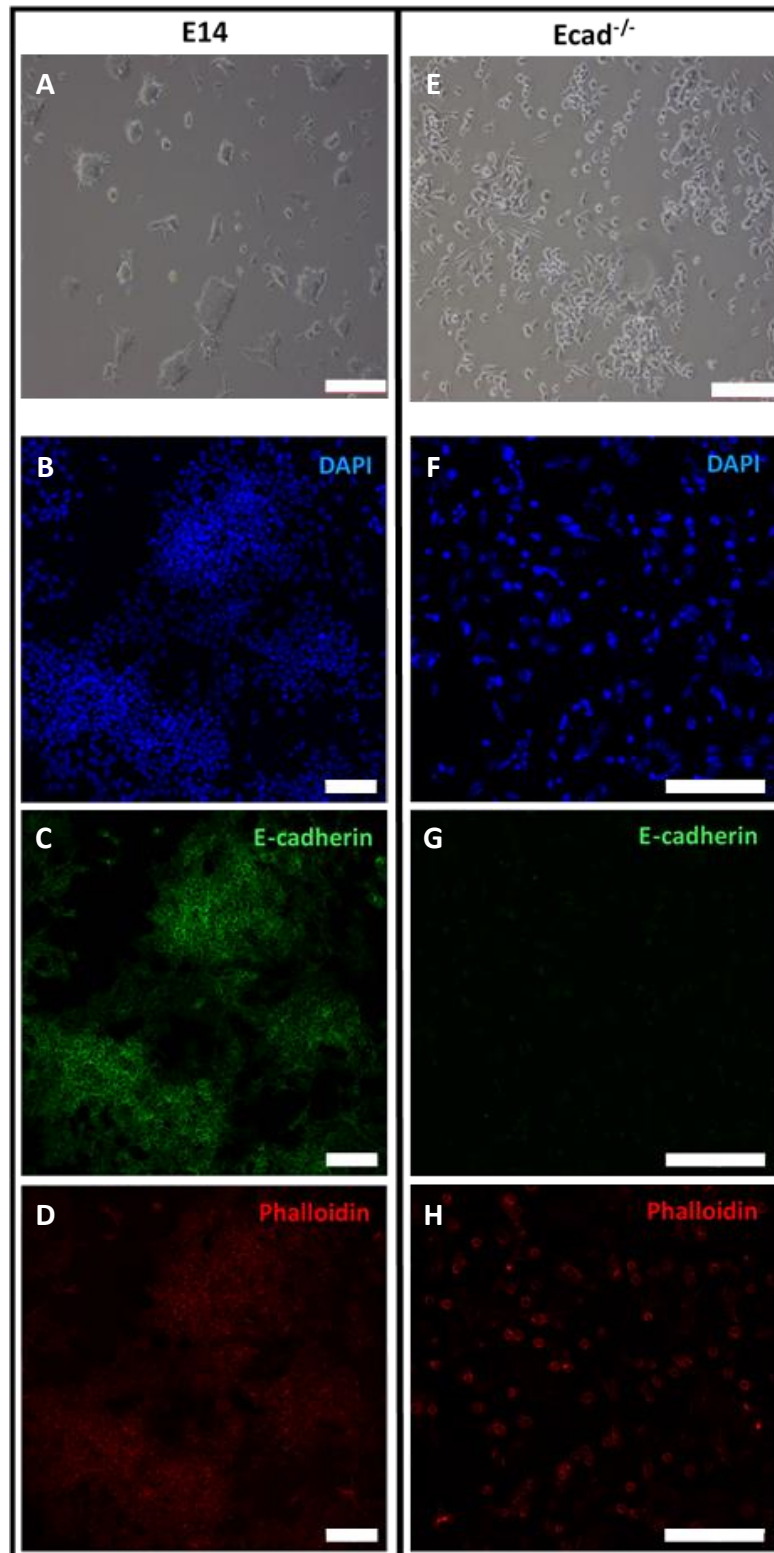


Figure 5.1: E14 cultures express E-cadherin localised at the cell surface, while Ecad^{-/-} cultures do not express E-cadherin and exhibit a less clustered morphology. A, E) Phase contrast images of E14 and Ecad^{-/-} respectively, in general culture conditions. Scale bars = 200 μ m. B - D) Fluorescence microscopy imaging of E14 cultures targeting, nucleus (B, blue), E-cadherin (C, green) and actin (D, red). F - H) Fluorescence microscopy imaging of Ecad^{-/-} cultures targeting nucleus (F, blue), E-cadherin (G, green), and actin (H, red). Scale bars = 100 μ m.

5.2.2 Operetta Analysis of peptide Treated mESCs

In the previous section it was shown that E14 and Ecad^{-/-} cell cultures could be maintained *in vitro*, with successful fluorescence labelling of key biomarkers. Further, the cultures exhibited familiar characteristics based on previous work, such as localisation of E-cadherin to regions of cell-cell contact on the cell membrane in E14 cells, and a complete absence of E-cadherin expression in Ecad^{-/-36,225}. However, this analysis is not quantifiable and provides limited information on the global cell population, thus limiting the confidence in conclusions drawn from this data beyond basic observation.

The importance of understanding peptide effects on biological characteristics of cells is well recognised and discussed in detail in previous chapters of this thesis. This work introduces the E-cadherin targeting Epep and EpepW2R peptide sequences to cultures of E14 and Ecad^{-/-} cell lines, with the aim of studying any effects via Operetta imaging and analysis. Although some studies have been conducted by other research groups using these peptide sequences on mESC cell lines, this technique represents a unique approach to observe and understand peptide effects via quantifiable analysis, something that has not yet been achieved with these peptides. As discussed in section 2.2.1.2, this instrument was developed with advanced analysis software to allow acquisition of unbiased fluorescence images across a greater proportion of the experimental cultures. In this section we analysed E14 and Ecad^{-/-} cultures using the Operetta system, focussing on assessing the impact of Epep or EpepW2R peptide treatment.

5.2.2.1 Optimising Initial Test Parameters

To determine ideal cell seeding conditions for Operetta experiments, a range of seeding densities were initially tested to assess their viability with the Operetta system. Due to the imaging and analysis processes used, this system is best suited to single cell layers, and is particularly sensitive to layered cell growth. This is an important factor to consider, especially relating to the E14 cell line, due to the tendency to grow in tight cell clusters. Therefore, cell densities above and below common seeding conditions for passaging were selected, with sample wells seeded in a 96 well plate with either: 500, 1000, 2500, 5000, or 7500 cells initially. These

samples were then left for a period of 48 h, selected to correspond to the common culture time possible before becoming overconfluent or beginning spontaneous differentiation.

Several locations within each sample well were imaged, providing a representative view of the sample, and allowing analysis of the cultures observed. From Figure 5.2 it is clearly noticeable that the lowest cell densities were unsuitable for testing, as the confluency was too low such that many of the selected imaging planes would contain insufficient cells for analysis. The 500 and 1000 cell seeding conditions could therefore be disregarded. Conversely, although the highest cell seeding conditions had much greater surface coverage and thus provided an abundance of cell data, the cell cultures demonstrated a loss of tight colony morphology alongside an increased layered growth of the cells, perhaps due to overcrowding of the plate. This is therefore not ideal for use with the Operetta system, as not only would the abnormal cell growth interfere with the analysis process as mentioned previously, but the samples may not be representative of the healthy culture conditions they are required to replicate. These observations are supported by quantified analysis of cell number via in-built functions, shown in Table 5.3. It is important to note that the quantification presented in Table 5.3 is the average cell number recorded in a single field of view for samples seeded at the stated cell density. This corresponds to the imaging and analysis processes performed by the Operetta software, and therefore allows for experimental set-up to be optimised for the technique used. The cell number analysis shows very few numbers of cell nuclei in the lower seeding densities, supporting the visual absence of cells in Figure 5.2. The cell number recorded in the higher seeded samples again reflects initial observation of the fluorescence images, but viewed alongside the corresponding cell nuclei delineation image there is obvious difficulty when attempting to individually analyse the cells.

Therefore, perhaps unsurprisingly, of the conditions tested the 2500 cell seeding condition presents the optimal sample for Operetta analysis. This is supported by the clear presence of cells in each imaging panel, with adequate cell numbers to allow for quantifiable analysis using the in-built functions, while demonstrating the most similar growth profile for the cells when compared to general cell culture seen in

Figure 5.1. This will also allow any effect on cell proliferation due to experimental treatments to be observed, as the Operetta instrument can analyse samples of higher or lower cell populations. Therefore, experiments were conducted using a seeding density of approximately 2500 cells for each sample well in a 96 well plate.

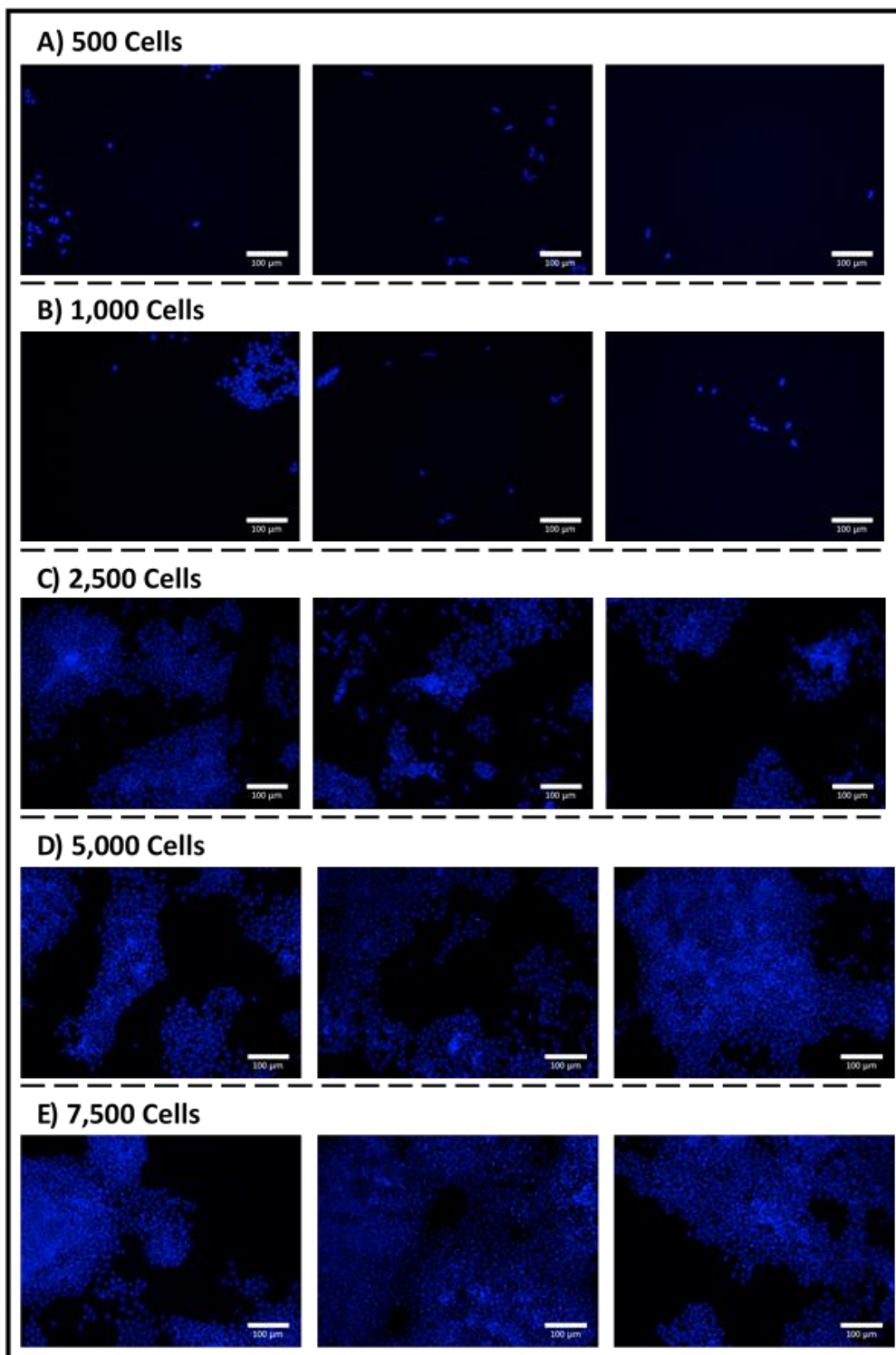


Figure 5.2: Confluence of E14 samples depends on seeding density, with seeding of 2,500 cells providing the most representative colony formation after 48 h compared to continuous culture images seen in Figure 5.1. Fluorescence Operetta imaging of E14 cultures maintained for 48 h and stained with DAPI. Initial cell seeding density relating to each image group is shown above the groups of 3 images taken from each sample well, with A) 500 cells, B) 1,000 cells, C) 2,500 cells, D) 5,000 cells, and E) 7,500 cell seeding densities tested. The images taken within each well were selected to represent a variety of locations. Scale bars = 100 μm.

Table 5.3: Seeding density of sample wells influences final cell number, and alongside Figure 5.2 indicates an ideal seeding density of 2,500 cells per well should be used when preparing experiments. Average cell counts in an individual FOV per well for each seeding condition tested for Operetta experiments. Averages were obtained from 5 separate regions within each sample well (example regions seen in Figure 5.2) and counted automatically via the analysis software discussed in section 5.1.3. Each value corresponds to the average cell number recorded in an individual image.

Cell Seeding Number	Average Cell Count (48 h)
500	17
1,000	24
2,500	429
5,000	569
7,500	722

5.2.2.2 Unique Response of E14 Cultures to Peptide and DECMA-1 Treatment

To assess the influence of Epep and EpepW2R peptides via Operetta analysis, E14 cells were cultured for 48 h in gelatin coated 96 well plates in a range of media conditions. The conditions tested were: regular media (no change to general culture medium), Epep treated (regular media with the addition of Epep peptide at concentrations of 1, 10, or 100 μM), EpepW2R treated (regular media with the addition of EpepW2R peptide at concentrations of 1, 10, or 100 μM), or DECMA-1 treated (regular media with the addition of the E-cadherin neutralising DECMA-1 Ab at a concentration of 100 nm). Imaging and analysis was then performed using the high content PekinElmer Operetta instrument, allowing quantifiable insight into cell characteristics, and therefore a robust novel analysis of mESCs treated with Epep and EpepW2R peptides.

To ensure the samples were suitable for analysis, and that cultures were successfully adhered to the plate surface, brightfield images were taken alongside fluorescence images. Figure 5.3 shows representative images of cells in the different treatment conditions, with the highest (100 μM) peptide concentrations selected for this comparison. It is important to note that the images shown are a single field of view

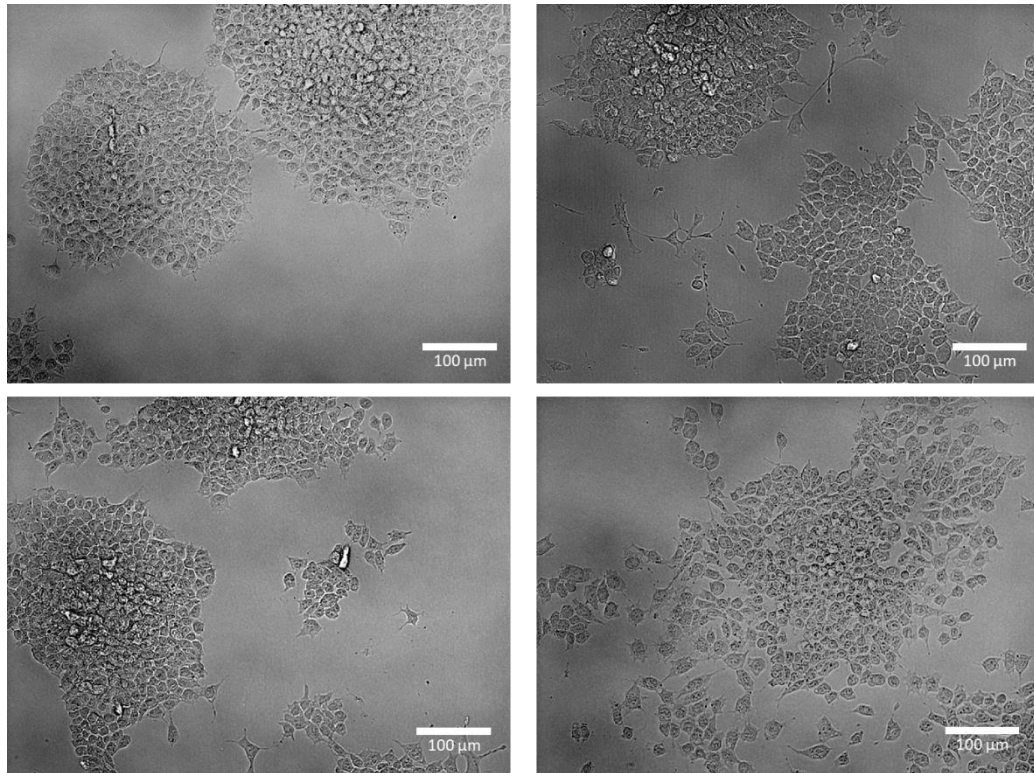


Figure 5.3: E14 cells cultures can be maintained following the addition of Epep, EpepW2R, or DECMA-1 to the culture medium, with Epep and DECMA-1 treated E14 cultures demonstrating a less clustered morphology in comparison to control samples. Brightfield images of E14 cell monolayers in A) regular culture medium, B) culture medium supplemented with 100 μ M Epep peptide, C) culture medium supplemented with 100 μ M EpepW2R peptide, or D) culture medium supplemented with 100 nM DECMA-1 Ab. Each image is a single FOV taken within a sample well and gives a representative indication of the cultures. Arrows indicate example areas where a loss of tight cluster formation is lost in comparison to the control sample, A. Scale bars = 100 μ m.

(FOV) within a sample well, and when analysis was being performed several locations within each sample well were imaged for a more accurate representation. Reviewing Figure 5.3 it can be seen that E14 cells were successfully cultured in each of the treatment conditions, including the Epep and EpepW2R treated samples. The DECMA-1 treated sample seen in Figure 5.3D shows a loss of cell-cell contact, as would be expected following the addition of a functional blocking antibody. A similar, although less prominent, loss of cell-cell contact can also be seen in the Epep treated cultures. These observations agree with those stated in previous publications using the Epep sequence for inhibition of E-cadherin contacts^{12,15,93}.

To perform accurate analysis of the cells, first it was required that individual cells were identified in images to provide a representative cell population, with an example of this process shown in Figure 5.4. Using the detection of DAPI stained cell nuclei, the analysis software attempts to define each cell individually, as shown by the coloured perimeters applied in the left image of Figure 5.4. However, although

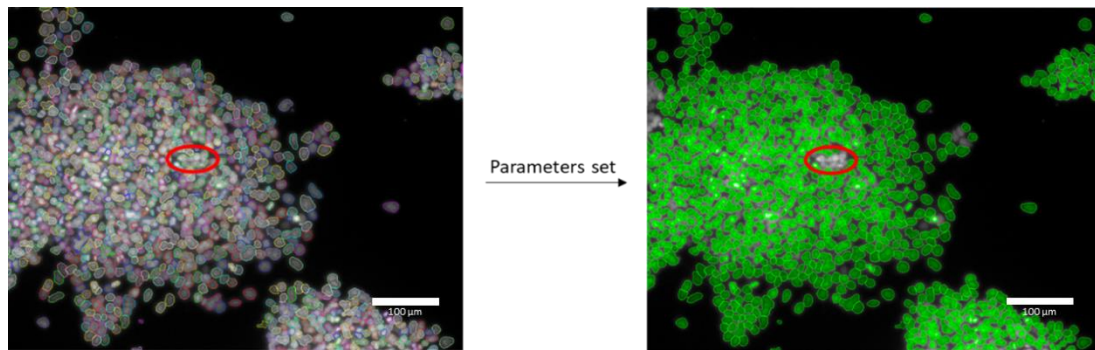


Figure 5.4: Cell nuclei can be isolated effectively using the Operetta analysis software, although some sensitivity is lost when analysing images with very tight clusters with 3-dimensional cell growth which is successfully accounted for by applying parameters within the software. An example of the automated analysis conducted within the instrument software. Cell Nuclei were delineated using DAPI staining of the cultures, as shown by the coloured perimeters in the left image. Parameters were added to the analysis software to remove cells that could not be individually identified, such as those highlighted by the red area. The right image shows the cell population used for analysis, with cell clusters removed. Scale bars = 100 µm.

the process does show a high degree of success in our analysis, there were still some cell clusters that could not be segmented efficiently, as highlighted by the red area in the images. This correlates with the presence of 3D aggregates, as the analysis software reviews the cell samples in a 2D image plane. This leads to overlapping of cell nuclei and subsequent error in the delineation of individual cells. Therefore, further semi-automated parameters were implemented whereby criteria were introduced to remove spurious results, specifically by setting a threshold for the nuclei size and roundness. The threshold values were determined by careful review of the samples, and effectively eliminated cell clusters that could not be segmented. This is shown in the right image of Figure 5.4, as the red area (showing a non-segmented cell cluster) is not included in the cell population for analysis (shown by the green highlighted nuclei). Similar processes were then applied for other relevant cell characteristics such as cytoplasm area or fluorescence intensity.

For the three biological repeats tested (N=3, characterised by the use of cells cultures at different passages), a minimum of 2 sample wells were stained for each antibody target (n=2), with the percentage of positive cells within each population determined to provide insight into marker expression, alongside the subsequent fluorescence intensity. The average number of cells recorded in each treatment condition, the cytoplasm/nucleus ratio, and several other parameters outlined previously in this chapter were quantified, and the values obtained from the treated cultures were compared to the corresponding data for the regular media condition to assess for

significance. Results are displayed in Figure 5.5 and Figure 5.6, and summarised in Table 5.4.

As seen in Figure 5.5 and Table 5.4, treatment of E14 cultures with DECMA-1 Ab containing media resulted in a significant change in the average cell number, as well as a shift in the average cytoplasm/nucleus ratio and intensity of Oct4 fluorescence. Interestingly, a similar change in cell number is also noticed in E14 cells cultured in EpepW2R containing media, with no significant change in any of the recorded parameters between regular media and Epep containing media as seen in Figure 5.5, Figure 5.6, and Table 5.4. It can be seen that the reduction in cell number for EpepW2R and DECMA-1 treated samples was similar for both conditions, perhaps suggesting a similar method of activation for the effect. A reduction in Oct4 intensity was also observed solely in the DECMA-1 samples, which may be related to the concurrent shift in cytoplasm to nucleus ratio due to the localisation of Oct4 within the cell nucleus. Finally, the DECMA-1 treated samples demonstrated an increase in

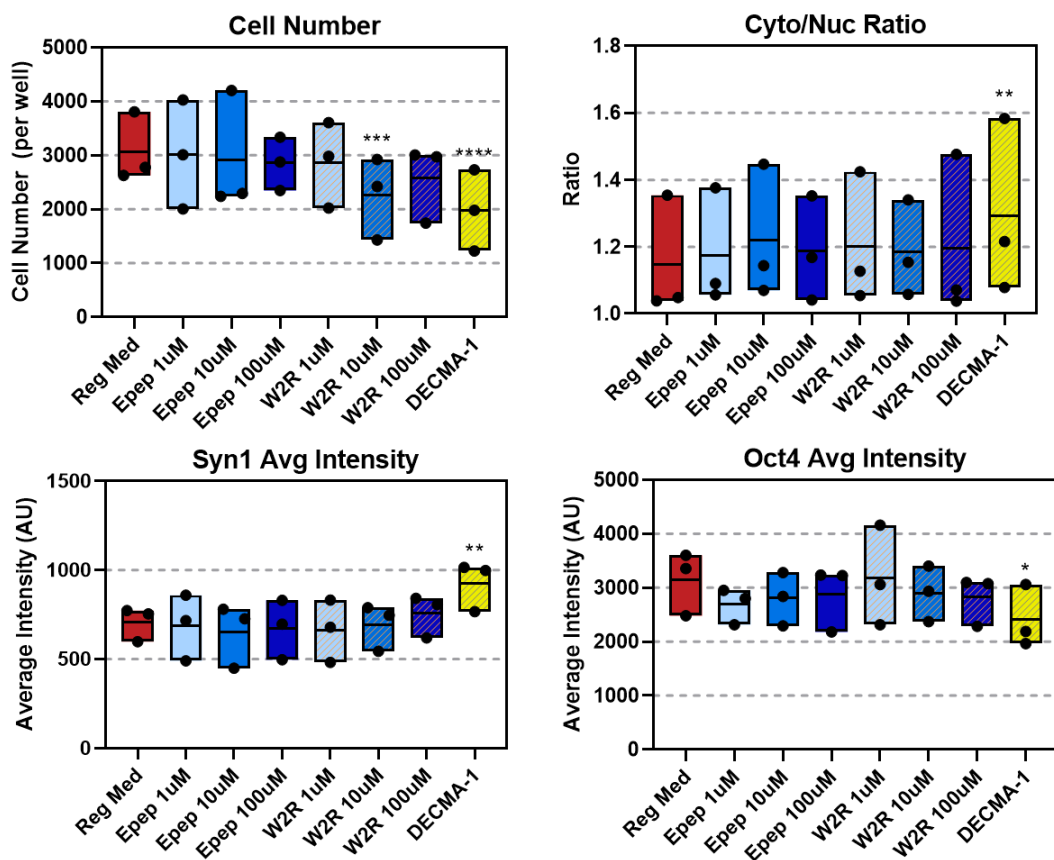


Figure 5.5: Peptide treated E14 cultures demonstrate a change in some of the tested cell characteristics. Bar charts showing the average values for parameters seen in Table 5.4 that displayed a significant change between treatment conditions ($N=3$), with the individual averages from each repeat shown by the black circles ($n=2$).

the cell surface proteoglycan, Syndecan-1, but with no noticeable change in Syndecan-4 expression as seen in Table 5.4.

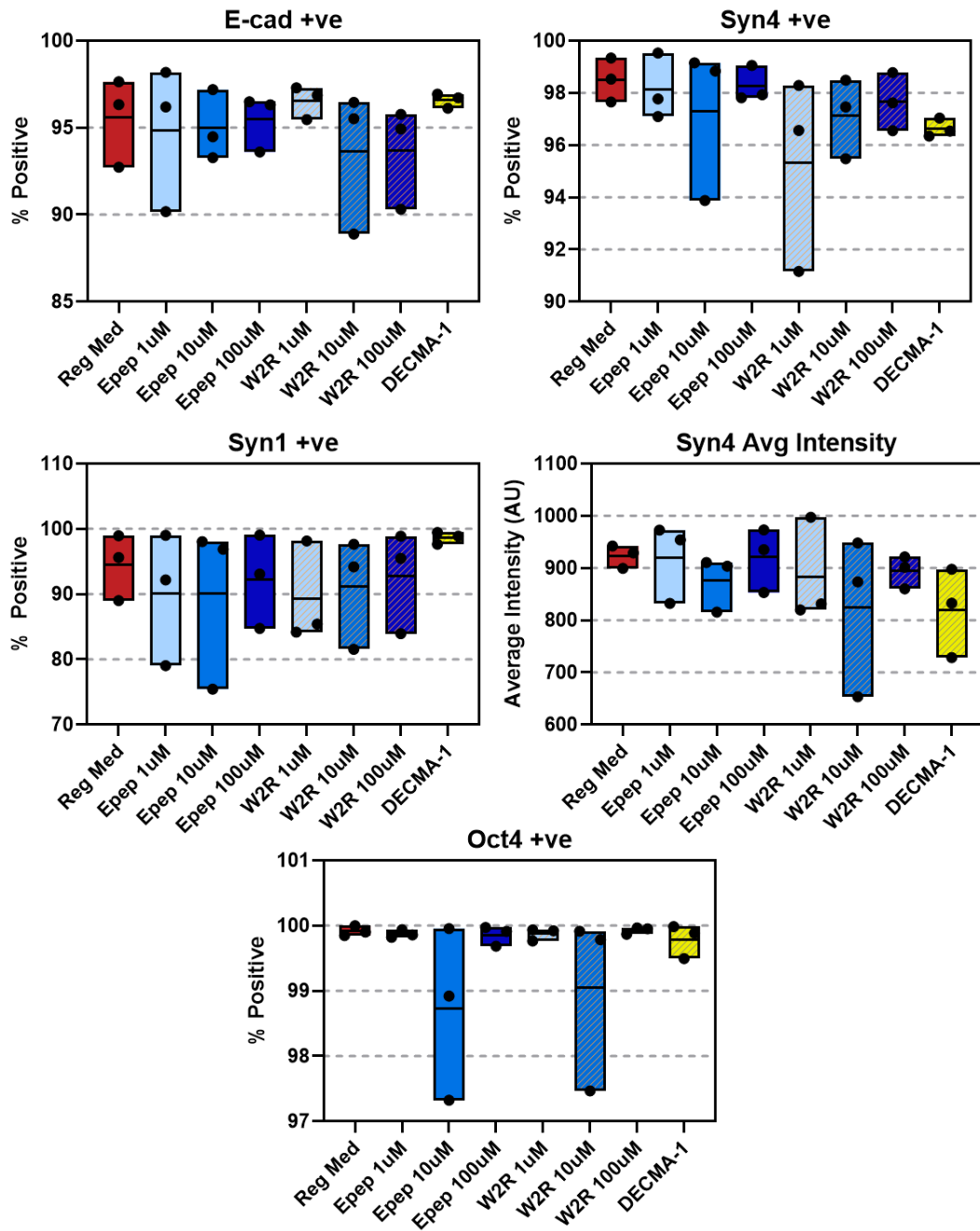


Figure 5.6: Selected cell characteristics observed for peptide treated E14 cultures do not demonstrate any change between conditions. These graphs show the remaining parameters supplementary to Figure 5.5 that are shown to have no statistically significant changes between any treatment conditions tested during analysis ($N=3$, $n=2$).

*Table 5.4: A summary of the data acquired when comparing E14 cell cultures treated with Epep, EpepW2R, or DECMA-1 supplemented media with regular culture media, showing some significant changes in EpepW2R and DECMA-1 treated samples, but not in Epep treated samples. A comparative analysis of E14 cell cultures treated with peptide containing media for 48 h and imaged using the Operetta instrument. All comparisons made are in relation to regular media cultures. Statistical analysis was performed using an average of the tested samples (N=3), and significance is shown as: NS = no significance, * = P < 0.05, ** = P < 0.01, *** = P < 0.001, **** = P < 0.0001.*

	Epep	W2R	DECMA-1
Cell Number	NS	***	****
Cyto/Nuc Ratio	NS	NS	**
E-cad +ve	NS	NS	NS
Syn4 +ve	NS	NS	NS
Syn4 Intensity	NS	NS	NS
Syn1 +ve	NS	NS	NS
Syn1 Intensity	NS	NS	**
Oct4 +ve	NS	NS	NS
Oct4 Intensity	NS	NS	*

For visual confirmation of antibody staining example images showing the different targets can be seen in Figure 5.7. Within this, Figure 5.7A shows that E-cadherin protein was localised to the cell surface, particularly at cell-cell contacts, as would be expected from the well-established analysis throughout literature. Conversely, staining for N-cadherin shows no specific binding, with Figure 5.7B showing similar fluorescence intensity in the sample background and cell clusters. The staining for the surface proteoglycans, Syndecan-1 and Syndecan-4, was performed as multiplexed samples, as seen in Figure 5.7C. Again, the localisation of these proteins appears to be near to the cell surface, with prominent expression of both targets in the cultures tested. Finally, we can conclude that the targeting of Oct4 within the cell nuclei was successful, as Figure 5.7D shows high intensity expression localised internally. These images provide an understanding of the physical expression of the selected targets in the cell samples to compare alongside Table 5.4 and Figure 5.5, with a single fluorescence image shown due to the consistent expression between all samples.

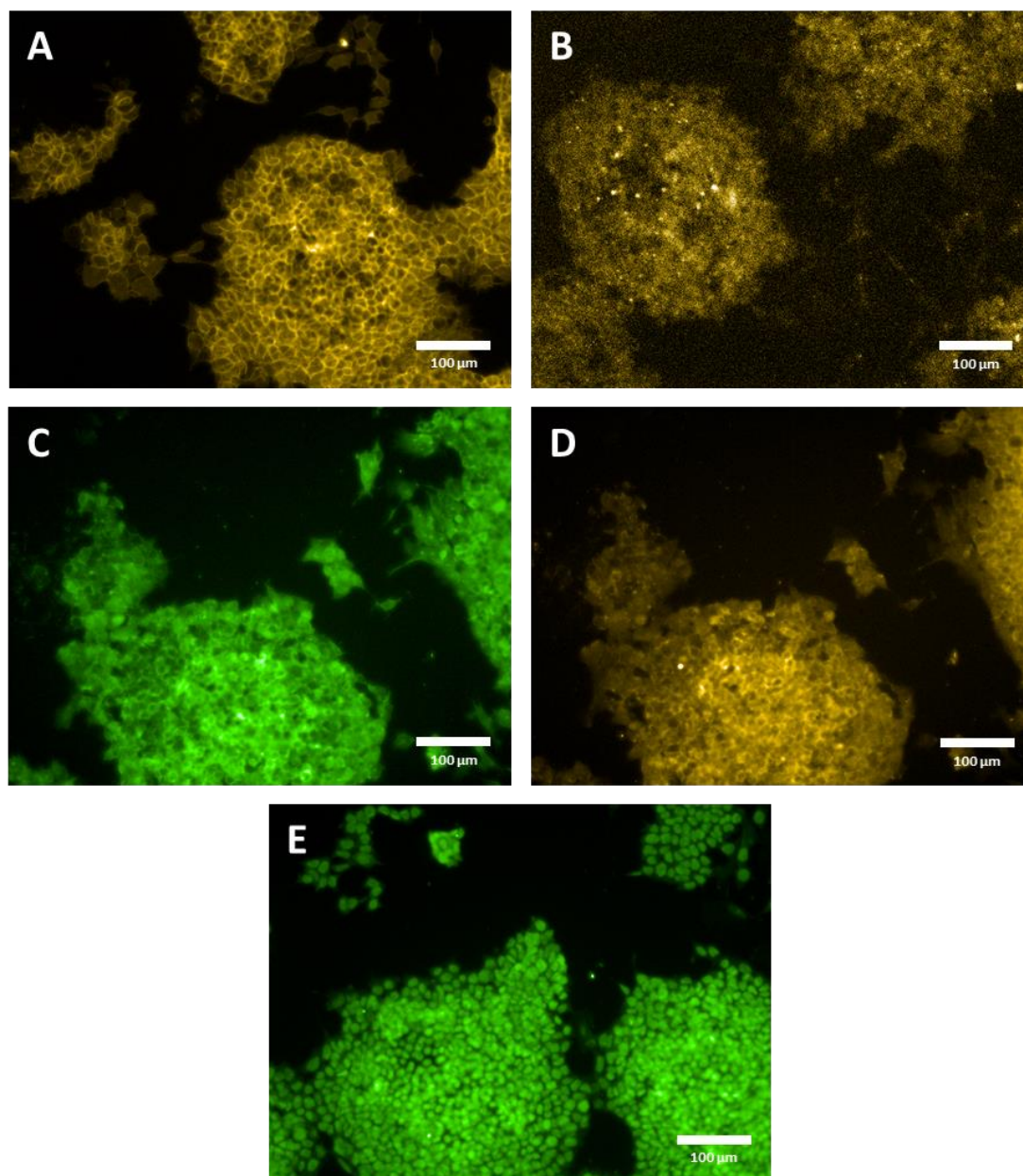


Figure 5.7: **Immunostaining and subsequent fluorescence imaging of E14 cultures using the Operetta instrument.** Fluorescence imaging of E14 cultures for, A) E-cadherin (yellow), B) N-cadherin (yellow), C) Syndecan-4 (green), D) Syndecan-1 (yellow), and E) Oct-4 (green). Scale bars are 100 μm , and image fluorescence is automatically enhanced by the software for viewing. These images represent a single FOV of a sample well, and are shown to provide insight into the sample fluorescence as quantifiable analysis was performed automatically by the software.

5.2.2.3 Unique Response of Ecad^{-/-} Cultures to Peptide and DECMA-1 Treatment

As with the E14 cultures above, to further understand the interaction of Epep and EpepW2R peptides on the selected cell lines, Ecad^{-/-} cell samples were treated with multiple concentrations of each peptide sequence (1, 10, and 100 μM) and fixed after 48 h. Using the Operetta imaging and analysis systems, fluorescence images were acquired on samples stained with DAPI, and subsequently processed to determine cell number by delineation of individual nuclei. Example brightfield images are shown

in Figure 5.8, with the corresponding fluorescence of the DAPI stained samples shown in Figure 5.9.

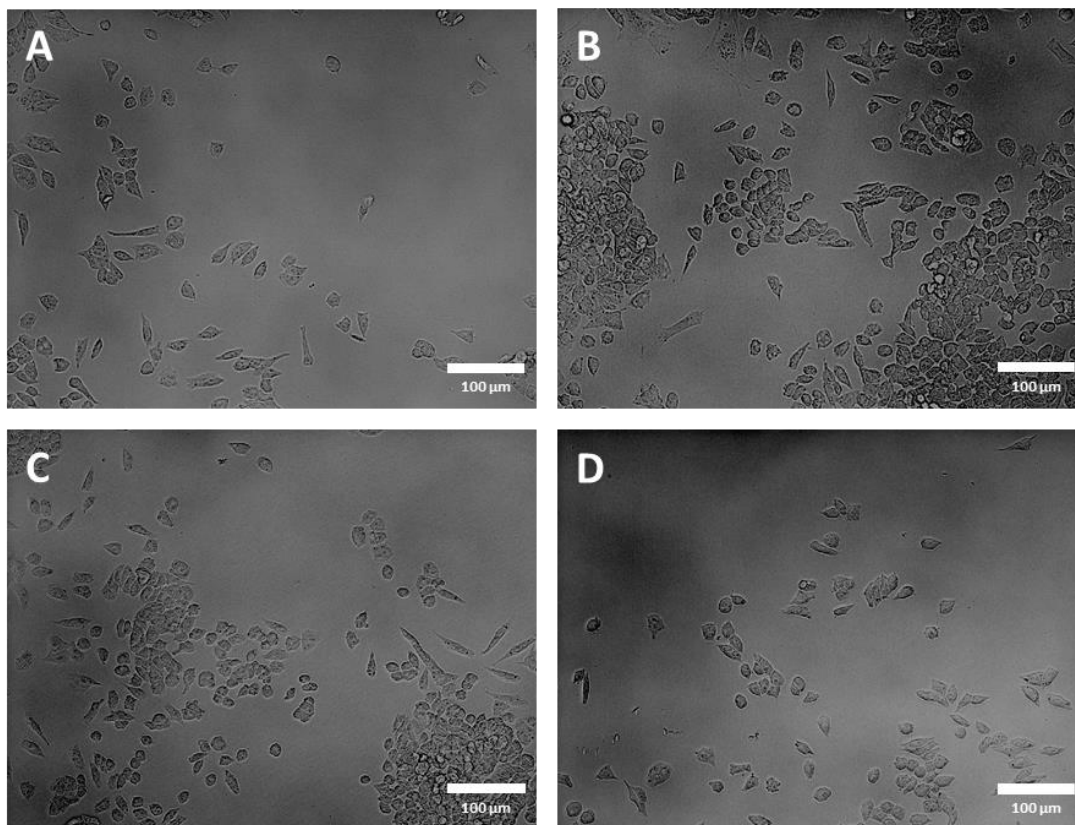


Figure 5.8: Successful culture and phase contrast imaging of Ecad^{-/-} cell cultures in a range of treated media conditions. Brightfield images corresponding to the fluorescence images shown in Figure 5.9, providing a visual representation of the cell cultures in each of the conditions: A) Regular culture medium, B) culture medium supplemented with 100 µM Epep peptide, C) culture medium supplemented with 100 µM EpepW2R peptide, or D) culture medium supplemented with 100 nM DECMA-1 Ab. Scale bars = 100 µm.

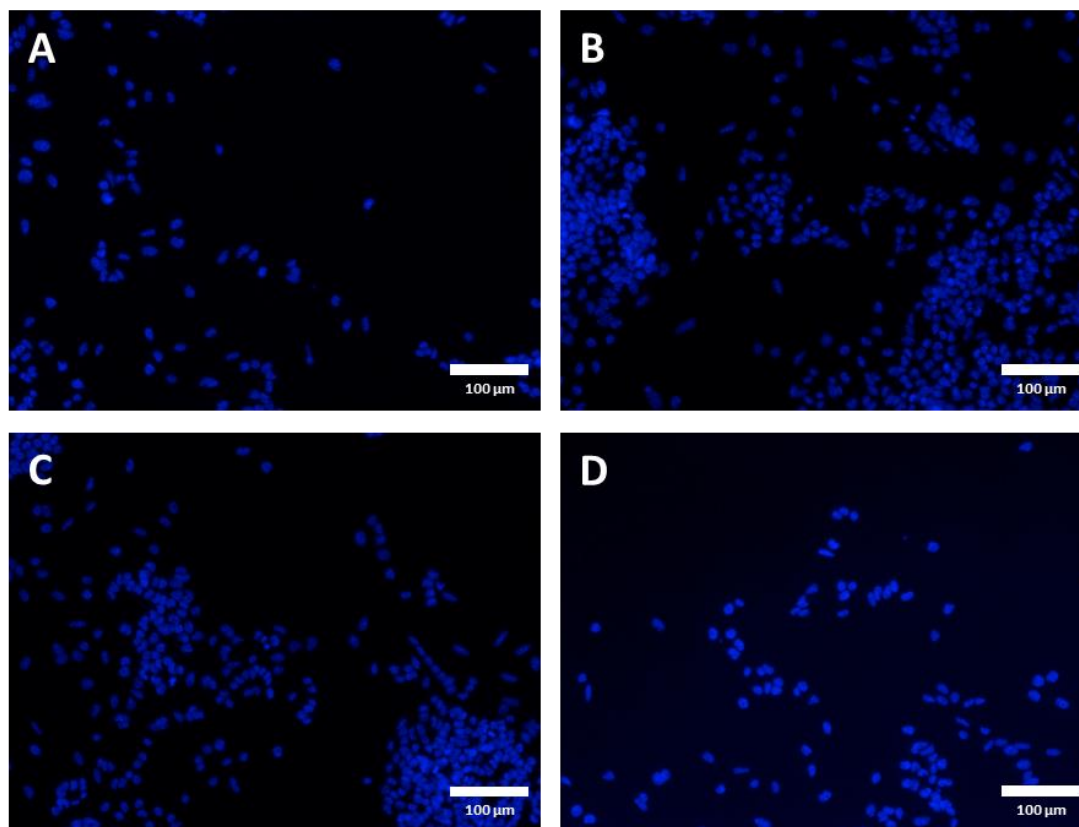


Figure 5.9: **DAPI staining of Ecad^{-/-} cultures via Operetta imaging indicates successful staining and imaging of the cell samples.** Operetta fluorescence images of Ecad^{-/-} cells with DAPI nuclear stain. Each sample well had several different locations imaged to provide a representative analysis of the cell sample, and each image in this figure is selected to show one of these locations for each treatment condition. The samples shown above were cultured for 48 h in, A) regular culture medium, B) culture medium supplemented with 100 μM Epep peptide, C) culture medium supplemented with 100 μM EpepW2R peptide, or D) culture medium supplemented with 100 nM DECMA-1 Ab.

These images show successful culture and adherence of cells to the plate surface, with a more individual growth characteristic when compared to the E14 cultures seen in Figure 5.3. This change in growth morphology is expected due to the absence of E-cadherin expression and subsequent loss of E-cadherin mediated cell-cell contacts, and is well reported in literature and from our initial culture experiments discussed in section 5.2.2.1. The images shown in Figure 5.9 and Figure 5.8 were selected to show a representative single FOV for each treatment condition, and as such it could be suggested that the confluency of the samples differ between treatments.

Figure 5.10 highlights the cell characteristics shown to be influenced by a change in culture media, such as the change in cell number reported for the Epep treated samples. Contrary to the change observed for E14 cell samples no significant change is seen in the number of cells in EpepW2R or DECMA-1 samples, despite the shift in cytoplasm/nucleus ratio shown from the latter in both E14 and Ecad^{-/-} cultures. From

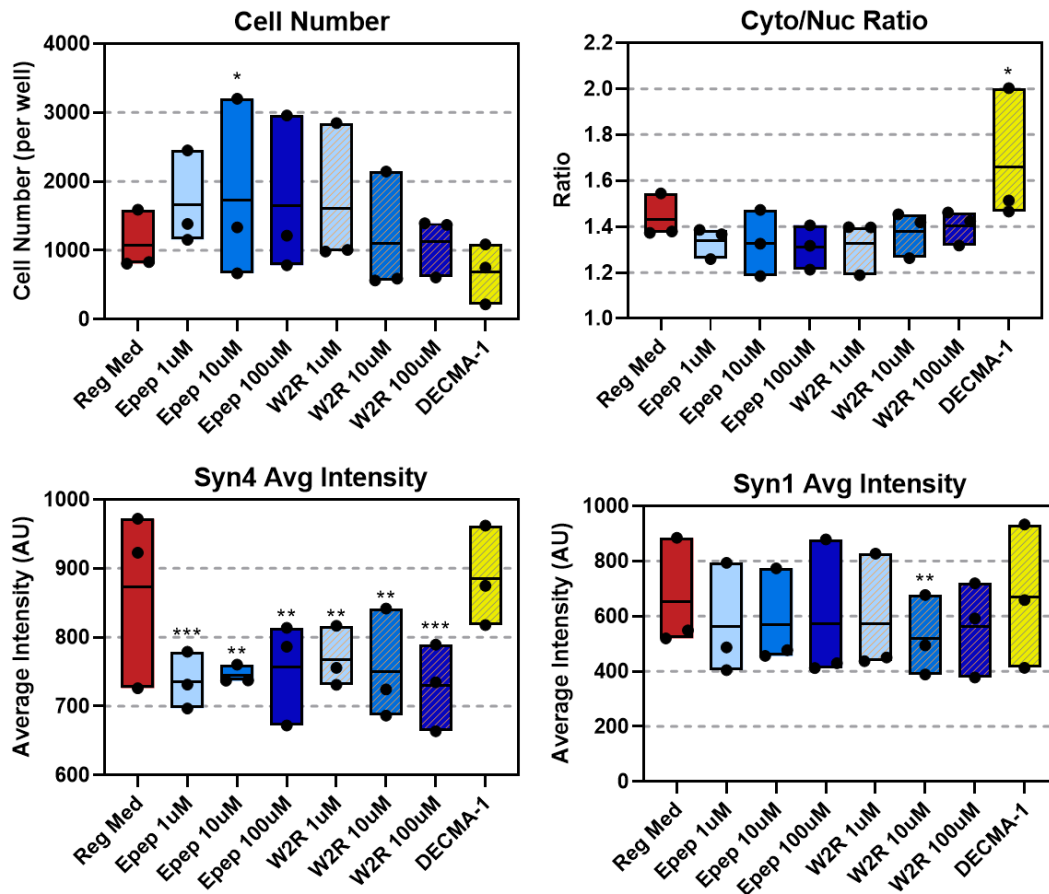


Figure 5.10: Peptide treated Ecad^{-/-} cultures demonstrate a change in some of the tested cell characteristics. Bar charts showing the average values for tested parameters that displayed a significant change between treatment conditions (N=3), with the individual averages from each repeat shown by the black circles (n=2) (summarised in Table 5.5).

Figure 5.10 it can be seen that the 10 μ M Epep environment produced a significantly increased cell number in the samples tested, although no significant response is seen in the other Epep concentrations shown in Figure 5.11. This data is summarised in Table 5.5.

Interestingly, there appears to be a distinct shift in the intensity of Syndecan-4 expression in samples treated with either the Epep or EpepW2R peptide, with a loss of intensity observed when compared to the regular media and DECMA-1 treated conditions. A significant reduction in Syndecan-1 intensity is also seen solely in the 10 μ M EpepW2R treated cells, with these peptide-mediated Syndecan changes not seen in the E14 cell samples, suggesting an alternative interaction process in the absence of E-cadherin.

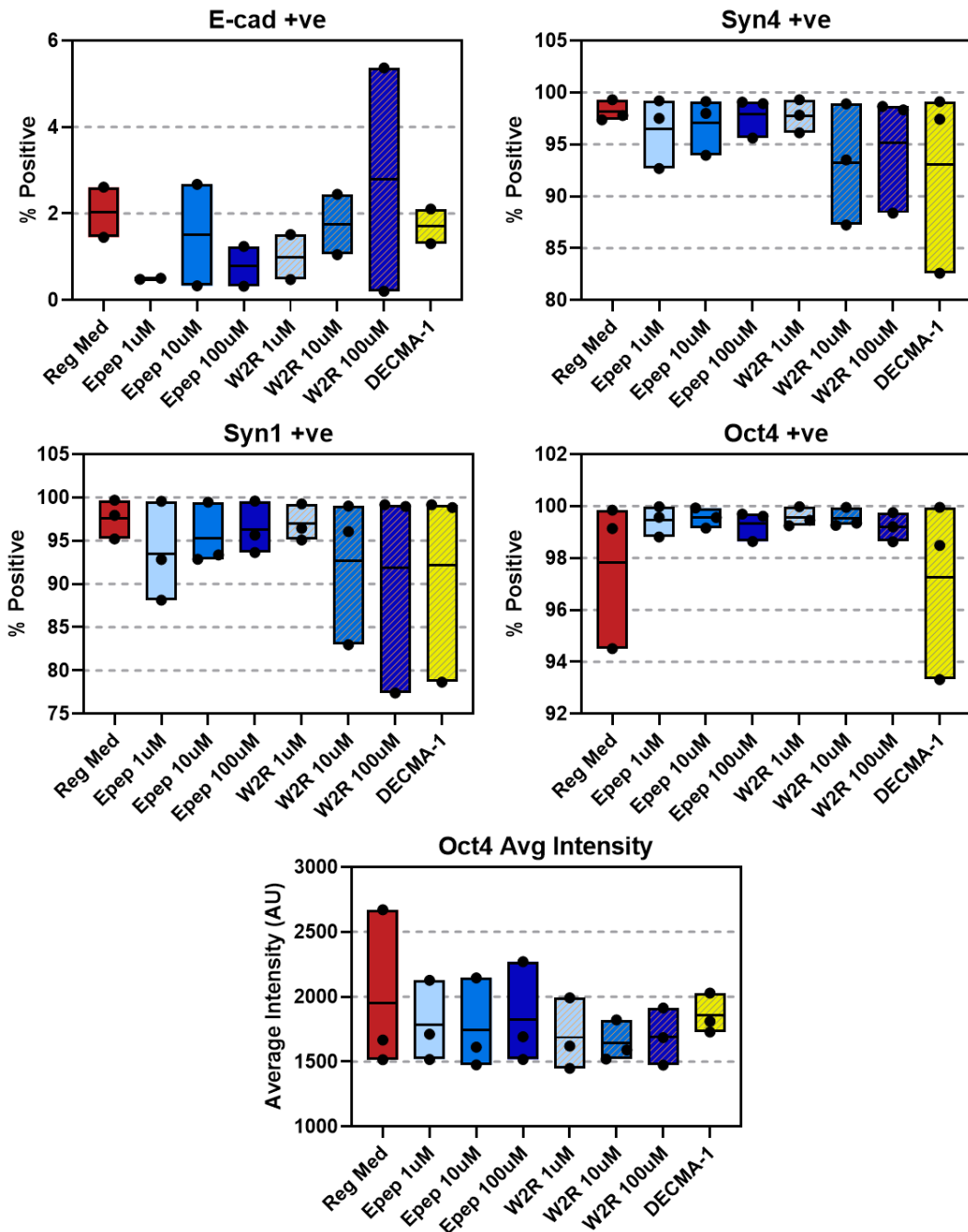


Figure 5.11: Some cell characteristics observed for peptide treated Ecad^{-/-} cultures do not demonstrate any change between conditions. Bar charts showing the average values for tested parameters that did not display a significant change between treatment conditions (N=3), with the individual averages from each repeat shown by the black circles (n=2) (summarised for simplicity in Table 5.5).

Review of Table 5.5 and Figure 5.10 indicate activity of both the Epep and EpepW2R peptides with the Ecad^{-/-} cell cultures, with a response in the intensity of Syndecan expression seen in all peptide concentrations, but not in the DECMA-1 treated samples. To further probe this relationship, representative fluorescence images of the antibody targets for analysis is shown in Figure 5.12. These images provide

*Table 5.5: Peptide treated Ecad^{-/-} cultures experience a unique response to Epep and EpepW2R peptides when compared to E14 cultures. A comparative analysis of Ecad^{-/-} cell cultures treated with peptide or nAb media for 48 h and imaged using the Operetta instrument. All comparisons made are in relation to regular media cultures. Statistical analysis was performed using an average of the tested samples (N=3), and significance is shown as: NS = no significance, * = P < 0.05.*

	Epep	W2R	DECMA-1
No of Objects	*	NS	NS
Cyto/Nuc Ratio	NS	NS	*
E-cad +ve	NS	NS	NS
Syn4 +ve	NS	NS	NS
Syn4 Intensity	***	***	NS
Syn1 +ve	NS	NS	NS
Syn1 Intensity	NS	**	NS
Oct4 +ve	NS	NS	NS
Oct4 Intensity	NS	NS	NS

an example of the fluorescence imaging performed by the Operetta instrument, and as such the localisation and success of the antibody targets used.

From this, we can infer an absence of E-cadherin protein in the samples due to the lack of specific fluorescence and high background intensity seen in Figure 5.12A (contrast with Figure 5.7A). Similarly, the targeting of extracellular N-cadherin via antibody staining (Figure 5.12B) shows a low specific intensity, and relatively high background fluorescence. However, the Syndecan-4 fluorescence is shown to be very well localised to the cell surface, with Syndecan-1 similarly present but with less intensity as seen in Figure 5.12C and Figure 5.12D respectively, with the protein position on the cell surface synonymous with that expected from literature²²⁶. Finally, there is clear evidence for the expression of Oct4 shown in Figure 5.12E, localised to the cell nuclei. This is an important indication of pluripotency in the cultures, and the high intensity fluorescence and well-defined nuclei regions seen in both E14 and Ecad^{-/-} cultures provide reassurance of the successful long-term culture of the cells.

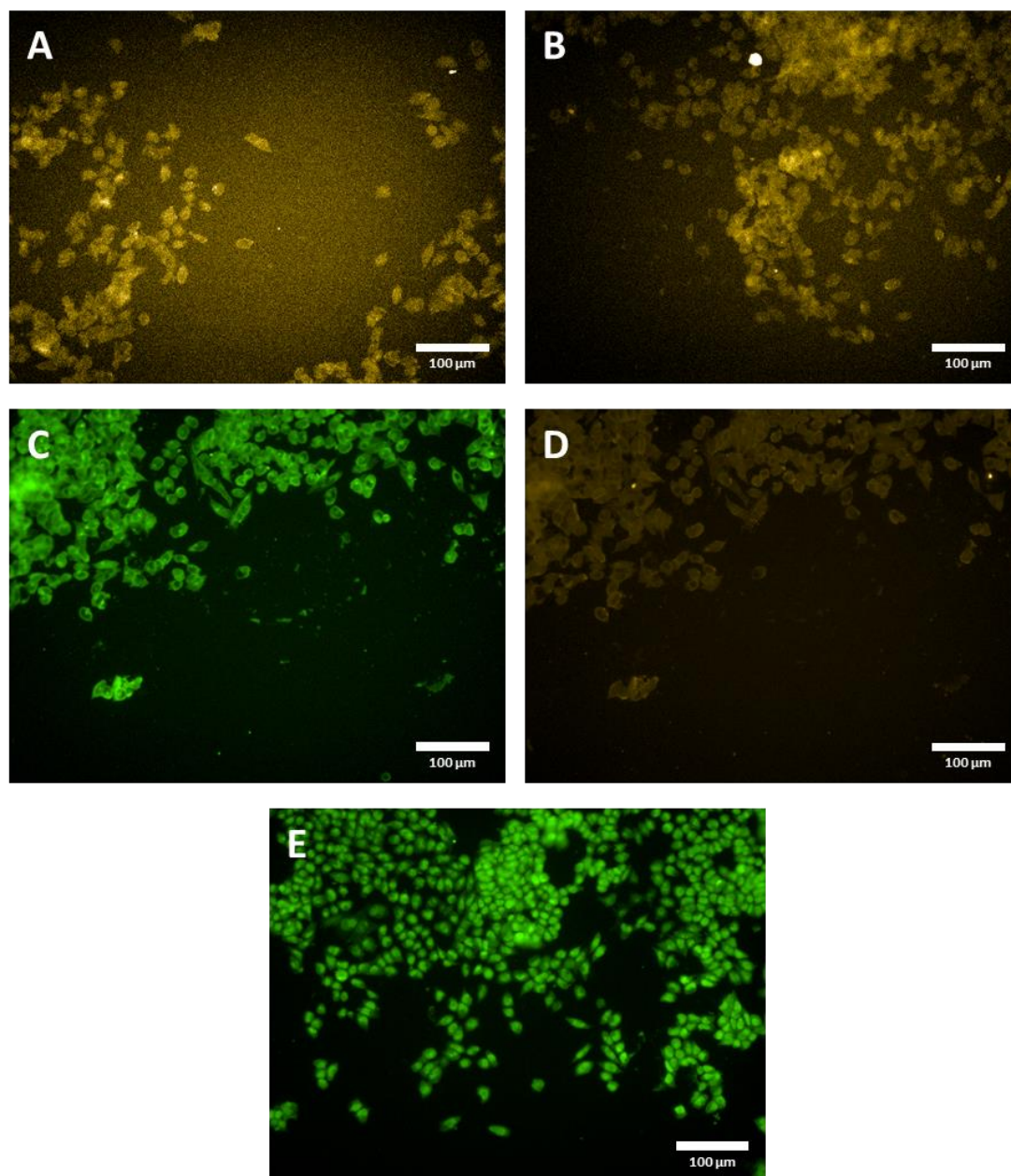


Figure 5.12: Immunostaining and subsequent fluorescence imaging of Ecad^{-/-} cultures using the Operetta instrument was successful in recording the fluorescent probes used, and confirms the continued absence of E-cadherin protein. Fluorescence imaging of Ecad^{-/-} cultures for, A) E-cadherin (yellow), B) N-cadherin (yellow), C) Syndecan-4 (green), D) Syndecan-1 (Yellow), and E) Oct-4 (green). Scale bars are 100 µm, and image fluorescence is automatically enhanced by the software for viewing. These images represent a single FOV of a sample well, and are shown to provide insight into the sample fluorescence as quantifiable analysis was performed automatically by the software.

5.2.3 Discussion

Throughout this chapter we have used E14 and Ecad^{-/-} cell lines to probe the effect of treating the cultures with Epep and EpepW2R peptide, in comparison to regular culture media and DECMA-1 treated media. To effectively complete the objectives of this work we first had to ensure that both cell lines could be maintained throughout continuous culture. Alongside regular observation of cell samples during continuous

culture via phase contrast imaging, we also used fluorescence imaging of stained samples to assess for E-cadherin protein on the cell surface, as shown in section 5.2. It is well accepted that wild type mESCs strongly express E-cadherin protein, localised to the cell surface, to act in the formation and maintenance of cell-cell contact^{36,222}, and as seen in Figure 5.1 the wild type mES cell line used (E14) did show localised E-cadherin expression at the cell surface. Furthermore, the image suggests a more dense distribution of E-cadherin at points of cell-cell contact. Conversely, as expected the Ecad^{-/-} cultures showed no E-cadherin expression, again supporting the specificity of the antibody staining used. This is in line with current literature depicting the E-cadherin expression of different mES cell lines, and underpins the associated cellular targets selected in this work^{28,227,228}.

Following confirmation of key cell characteristics, experiments were extended to also include the use of peptide treated media. As seen in section 5.2.2, the use of fluorescent imaging and subsequent automated quantification via the High Content Operetta system allowed for a robust analysis of cell samples. Firstly, we showed in Figure 5.3 and Figure 5.4 that the brightfield images aligned with the DAPI staining used to delineate cell nuclei, and as such the automated cell segmentation could be used with tailored analysis parameters to ensure consistent analysis between samples. This allowed for many more FOVs and sample wells to be tested within the experiment, and as such improved the accuracy and reliability of the work.

From the literature it is suggested that abrogation of E-cadherin contacts in mESCs may correspond to a change in cell proliferation¹¹, and thus our initial focus was directed at studying the effect of the peptides on the cell number recorded in each sample. Table 5.4 and Figure 5.5 show that the average cell number recorded for each sample well was significantly less in EpepW2R and DECMA-1 treated samples compared to regular media or Epep treatment conditions, with the latter showing the largest change. Eastham *et al.* report that in human ES cells inhibition of E-cadherin mediated cell-cell contacts resulted in a reduction of their proliferative function²²⁹, supported by evidence that ligation of E-cadherin contacts via protein labelled beads also inhibited proliferation²³⁰, a response that was later shown by Kim *et al.* to be dependent on the presence of α -catenin and mediated via the Hippo

signalling pathway³⁴. This eludes to the diverse and complex nature of E-cadherin mediation, and indeed the associated cell functions, with many different signalling pathways incorporated throughout cadherin mechanisms²³¹.

Experimentally, Hawkins *et al.* suggested that the addition of DECMA-1 to mESC samples does not increase cell proliferation, but may improve the percentage of viable cells, although a loss of the tight colony formation did occur²³². However, when cultured in suspension the cell doubling time was reported to reduce for treated cells⁹³. Therefore, the inhibition of cell proliferation following the addition of the neutralising antibody (nAb) DECMA-1 in our own studies, was similar to the response observed in hESCs, and as seen in literature the abrogation of E-cadherin adhesions in mESCs resulted in a more visually mesenchymal type morphology such as that in Figure 5.3D²³³. However, work by Segal and Ward showed the interaction of Epep and EpepW2R with E-cadherin to be unique compared to DECMA-1, with no loss of cell-cell contact in EpepW2R treated cell cultures⁹³. Thus, it could be suggested that the reduction in cell number following EpepW2R treatment in Figure 5.5 may have been due to an unknown interaction of the EpepW2R peptide with E14 cultures, and indeed previous work did show a response in cell signalling following EpepW2R treatment despite a lack of cell-cell contact inhibition⁹³. However, the EpepW2R treatment only showed this change at the 10 μ M concentration, with the 1 μ M and 100 μ M solutions showing a slight but not significant reduction, highlighting the need for continued studies to further investigate the impact of peptide concentration.

This observation can be linked to the diverse range of cellular pathways and processes in which cadherin proteins are implicated, as seen in recent research. For example, phosphorylation is suggested by Surapaneni *et al.* to alter E-cadherin transcription²³⁴, which can be considered alongside factors such as interactions with local biological molecules such as syndecans²³⁵. This provides an abundance of potential targets to be monitored in addition the work shown in this chapter, with the potential to help elucidate the impact mechanisms of proposed non-binding peptides such as EpepW2R. Further, this could account for the unpredicted response of peptides tested in this work, and previous relate publications^{11,12,93}.

No further effects were observed from Operetta analysis following treatment of E14 cells with Epep and EpepW2R, as seen in Table 5.4, although the DECMA-1 treated samples showed an increase and decrease in Syndecan-1 and Oct4 intensity, respectively. First considering the change in Syndecan-1 expression, this could be due to a shift in the morphology of the cells, as suggested by the increased cytoplasm/nucleus ratio, and visual changes observed in Figure 5.3. As Syndecan-1 is often presented at the cell surface, the loss of tight cell-cell contact due to E-cadherin inhibition may interfere with the protein localisation^{78,235}s. As the percentage of cells expressing Syndecan-1 remained unchanged in all conditions it is not possible to draw any definitive conclusions from the change in intensity, particularly due to the different cell morphology observed in the treated cultures. The same is true for the expression intensity of Oct4. Again, a change in the intensity was observed in the DECMA-1 treated samples, but there was no significant change in the percentage of expressing cells. This could be explained by the increased cytoplasm/nucleus ratio as the expression may be more dispersed.

It is important to note that treatment with Epep and EpepW2R peptides did not induce any change in the tested targets for E14 cells, including no loss of pluripotency or significant change in cytoplasm/nucleus ratio. The latter is particularly prevalent due to the ability for Epep to inhibit cell-cell contact, which we can see for DECMA-1 correlates with a change in cell morphology. Thus, the use of peptides may provide an alternative inhibitor to the targeting antibody, while maintaining more consistent cell morphology and characteristics, as cell number and cytoplasm/nucleus ratio remained unchanged in Epep treated samples. However, Segal and Ward reported a reduction in the expression of key mESC pluripotency markers following peptide treatment, including Nanog. The Nanog protein is closely associated with Oct4 as regulators of stem cell pluripotency^{228,236}, and as such the stable expression of Oct4 reported from our work in 5.2.2.2 provides a greater understanding of the maintained pluripotent characteristics of peptide treated cultures. However, it is important to recall that many other key regulatory pathways are not explored in this work, which may provide a complimentary approach to be used in future work. For example, the Hippo pathway mentioned previously, and subsequently the associated

PI3K signalling pathway, is implicated in literature to be related to cadherins in the mediation of cell processes³⁴. Furthermore, snail and slug pathways are also reviewed with regards to their relationship to E-cadherin transcription and processing, with ongoing reference to the crucial EMT process observed in mESCs^{237,238}.

Comparing these responses to those of Ecad^{-/-} cultures, it can be seen that several discrepancies appear. As the Ecad^{-/-} cell line was specifically chosen to highlight to E-cadherin dependence of interactions, and their resulting effects, we can begin to study the processes of Epep and EpepW2R peptide inhibition. Table 5.5 shows that the E-cadherin targeting antibody, DECMA-1, had relatively little effect compared to the treated E14 sample, as would be expected due to the lack of specific target for the antibody. As such, the only observed change for DECMA-1 treated Ecad^{-/-} cells was an increased cytoplasm/nucleus ratio, with no noticeable difference in the cell number or protein expression, as was observed in E14 cultures. Further, Figure 5.10 shows that the increased ratio is only observed in a single experiment out of the three tested, and as such may need further validation to confirm this conclusion via further repeats. It is important to consider that this lack of response to the nAb could be expected due to the known absence of E-cadherin in the cell cultures, and thus the absence of a biological target for the antibody, with this interaction instead providing insight into potential off-target interactions that may occur. However, the ability to target specific antibody-mediated sites, such as DECMA-1 binding of E-cadherin proteins, is utilised in research as a proposed method of probing and perhaps manipulating cell functions. Brouxhon *et al.*²⁰⁰ explore the relationship of DECMA-1 with several cellular pathways including HER and PI3K, which are both strongly linked to carcinogenesis, with similar relationships tested by a range of other groups^{229,239,240}.

The response to peptide treatment also showed differences between the two cell lines tested, with Ecad^{-/-} responding to Epep with an increased cell number and a reduction in Syndecan-4 intensity, and to EpepW2R with a reduced Syndecan-4 and Syndecan-1 intensity. The change in cell number was completely contrasting to that observed in E14 cells, as in the Ecad^{-/-} samples only Epep showed any effect. This may

suggest a secondary interaction with mESCs in the absence of the primary E-cadherin binding target, that perhaps relates to the dual E-/N-cadherin binding affinity proposed by Devemy and Blaschuk during the initial isolation of the Epep sequence¹². This could also be inferred due to the consistent change in Syndecan fluorescence intensity seen in Figure 5.10, particularly for Syndecan-4. This protein is implicated in the formation and function of focal adhesions alongside integrin adhesion proteins, and as such are recognised for their involvement in key cellular functions and response to mechanical cues^{241,242}. Thus, in the absence of E-cadherin the targeting peptides may be interfering with associated systems, such as the Syndecan pathways which are implicated in processes such as cell proliferation and cell-matrix interactions, resulting in a change in cell expression²⁴³.

To help isolate this relationship in future the use of cell lines with genetically knocked-down or knocked-out Syndecan expression, such as those used by Yu *et al.*²⁴⁴, could be tested alongside wild-type mESCs commonly used in literature such as the D3 cell line used by Segal and Ward⁹³. This work would also naturally benefit from development into human ES cells which are receiving ever-growing interest in research and therapeutics. It is also shown by Hawkins(2012) that Ecad^{-/-} mESCs rely on maintenance of pluripotency via the Activin/Nodal pathway, which is recognised as the same pathway used in hESCs, as opposed to the LIF/STAT3 pluripotency pathway observed in the mESCs²², although these complex relationships are still not fully understood. This may still provide an exciting avenue for continued research, as this system could be used to help probe the underlying mechanisms involved in these vital pathways. For this chapter however, it must be noted that this analysis was drawn from an individual experiment, and as such further work is required to confidently determine the mechanism of these relationships, which unfortunately was not possible in this thesis due to the time-limiting constraints imposed by the COVID-19 pandemic, as already discussed.

5.3 Conclusions

The approach adopted within this chapter was developed to provide a biological analysis to support the AFM experiments conducted in chapter 3 and chapter 4, while attempting to further our understanding of cell response to E-cadherin targeting peptides. Throughout this work we have demonstrated the successful culture and fluorescence labelling of key markers in E14 and Ecad^{-/-} mES cell lines, probing characteristics such as proliferation and protein expression to expand our understanding of cell response to Epep and EpepW2R peptides. Operetta analysis of peptide treated E14 and Ecad^{-/-} cultures displayed consistent expression of the key regulatory marker, Oct4, in all treatment conditions. This develops from the panel of pluripotency markers analysed previously by Segal and Ward⁹³, and suggests the addition of Epep or EpepW2R did not induce differentiation in cell monolayers. However, treatment of E14 cultures with EpepW2R, and of Ecad^{-/-} cultures with Epep, resulted in fewer cells present after 48 h culture in comparison to cells cultured in regular media. Furthermore, both Epep and EpepW2R treated Ecad^{-/-} cultures presented a reduction in the intensity of Syndecan expression, which was not seen in regular medium or DECMA-1 treated samples.

These observations could indicate that the peptides exhibit some off-target influence on the cells, as marker expression and cell number show unique changes following peptide treatment, even in the absence of E-cadherin expression. This is further supported by the AFM-based analysis seen in chapter 4, and it was initially planned that these experiments would be continued to further probe peptide mediated effects in mESCs. However, despite starting this work and conducting preliminary experiments using flow cytometry, the unforeseen shutdown of labs due to the COVID-19 pandemic ultimately prevented its continuation within the time constraints of this project.

Chapter 6 - Conclusions and Future Work

Due to their self-renewal and diverse differentiative capacity, stem cells, such as mESCs, provide a key approach for many different applications, from basic research into gene expression and function, to medical applications for studying diseases and developing novel diagnostic approaches. Subsequently, there is an ever-growing need to understand and regulate ES cell function *in vitro*, with novel targeting peptides one area of particular interest to achieve this. Recently developed E-cadherin targeting peptide sequences, have been shown to affect both the physical and biological functions of mESCs. However, the relationship between the physical and biological effects actioned by these peptides requires further research to understand the processes involved. Therefore, our research aimed to use a multidisciplinary approach to bridge this gap, using the Epep sequence isolated by Devemy and Blaschuk¹², and the analogues of this sequence subsequently developed by Segal and Ward⁹³.

Specifically, this thesis aimed to demonstrate the development of an AFM based approach that would be capable of detecting and investigating the interaction of E-cadherin targeting peptides. This approach was complimented by biological assays aimed at studying the behaviour of mESCs in response to peptide treatment, with the hope of developing this scope to consider a variety of additional cellular targets. Epep and EpepW2R peptides were highlighted in previous research and presented as ideal sequences for this work, as both peptides were shown to induce unique biological marker expression, while demonstrating contrasting abilities to inhibit cell-cell contacts in mESCs. It was hoped that the application of AFM would provide new insight into the response of E-cadherin proteins to peptide treatment by monitoring the frequency and force of individual cadherin bonds, and allow evaluation of the potential of the approach for the screening of E-cadherin interacting substances. Throughout the work, we demonstrated the use of advanced analytical techniques to probe both the biological and physical impact of E-cadherin targeting Epep and EpepW2R peptides, with the aim of observing the impact on mESC cell cultures.

In chapter 3, we showed the development of a robust E-cadherin binding system tailored to isolate E-cadherin adhesions between surfaces functionalised with Ecad-Fc molecules, with measurement of single molecule adhesion and high sensitivity force analysis. This involved optimising the surface functionalisation of samples, and the experimental parameters, to successfully record the unbinding of single E-cadherin bonds via the capture and analysis of F-D curves. Data was categorised using key characteristics of the system, determined from literature and our experimental setup, with the frequency of specific adhesion events monitored to assess the likelihood of detecting interactions attributable to the rupture of single molecular bonds. From this we observed consistent modal rupture forces of 30 or 35 pN as seen in Figure 3.6 and Figure 3.8, which corresponded well with values seen in literature for the characteristic S-dimers formed by E-cadherin molecules. Similarly, rupture forces were consistently observed around 60 – 70 pN, which again correspond well with values for X-dimers seen in literature. Frequency analysis of the data also demonstrated a single adhesion frequency below 20% in all buffer conditions, indicating an SMFS system with accuracy >90%, supporting the viability of the AFM system developed in this work.

Importantly, known inhibitors of homotypic E-cadherin interactions, such as EGTA and the DECAM-1 antibody, were used to confirm the specificity of recorded interactions. Measurements recorded in the presence of such agents were compared to measurements recorded in a Ca²⁺ rich environment; a reduction in adhesion frequency, in line with the expected response of E-cadherin mediated adhesion, confirmed the specificity of the probe-sample interactions. Our system was additionally shown to be successful in acquiring and analysing SMFS data in multiple liquid environments, tested sequentially, which provided a crucial platform for the advancement of the approach for the assessment of targeting peptides.

By developing the AFM system validated in chapter 3, the work in chapter 4 introduced the Epep and EpepW2R peptides to the E-cadherin functionalised samples. The impact of the peptides on the frequency and force of specific E-cadherin adhesion events was monitored. This novel analysis indicated a reduction in the adhesion frequency following the addition of both peptides, an observation

not expected for the EpepW2R variant, as in previous biological assays the application of this peptide had not resulted in abrogation of cell-cell contacts. This highlights the potential of using an AFM system capable of recording single molecule interactions with high force sensitivity, and could suggest the presence of preferential off-target binding of the EpepW2R sequence when testing cell monolayers, that is not seen when isolating E-cadherin interactions. Further, the inhibitory effect for both peptides was shown to be reversible following the replacement of the experimental environment with Ca^{2+} buffer. Building on the results of chapter 3, these findings again highlight the advantages of the AFM based analysis for the investigation of cadherin-peptide interactions. The results demonstrate the ability to sequentially apply different test environments, whilst maintaining a robust SMFS system throughout an experiment. Importantly, this was achieved using a single sample and AFM probe, using relatively small test compound (peptide) volumes ($\approx 100\text{-}150\ \mu\text{L}$), providing advantages over ensemble techniques, such as SPR. The initial experiments conducted in this chapter, on E14 mES cell monolayers in the presence of Epep, also indicate the potential of developing this technique to probe, and potentially screen, peptide interactions with more biologically relevant surfaces.

Finally, Chapter 5 details the biologically focussed assays conducted to probe the effect of peptide treated media on E14 and *Ecad*^{-/-} mESC cultures. These experiments were performed to build on the AFM results obtained in chapter 4. Previous work by Segal and Ward suggested a unique response of marker expression in mESCs in response to Epep or EpepW2R treatment, and attempted to isolate the peptide regions responsible for the influences observed on cell cultures. However, there exists a plethora of other key markers that were not considered but may be implicated in peptide interaction, such as off-target bio-mechanically active proteins, for example Syndecans. The experiments seen in chapter 4 highlight the need to analyse the response of proteins associated with E-cadherin function, as the inhibitory activity of EpepW2R seen in the AFM studies is not seen in previous cell-based analysis, and thus indicates the influence of cell components not yet considered in previous experiments. By comparing the response of E14 and *Ecad*^{-/-}

cultures It was hoped that we could further our understanding of the peptide interaction with cell cultures, as any change seen in Ecad^{-/-} cells after exposure to peptide would not be E-cadherin-mediated, and may reveal off-target interactions, for example with associated surface proteins such as Syndecans.

High-content Operetta analysis of peptide treated E14 and Ecad^{-/-} cultures demonstrated success in imaging and quantifying expression of selected cell markers, displaying consistent Oct4 expression in E14 and Ecad^{-/-} cultures in all treatment conditions. Quantifiable analysis of fluorescently labelled cell samples suggested a possible influence of the peptides on cell proliferation, with EpepW2R treated cell samples displaying a lower cell number after 48 h in comparison to regular culture medium. It was also seen that peptide treatment of Ecad^{-/-} cells resulted in a change in the intensity of Syndecan expression, which was not seen in regular medium or DECMA-1 treated samples. This response highlights the impact of the targeting peptides in the absence of E-cadherin, again suggesting off-target interactions, as supported by the AFM-based analysis seen in chapter 4. However, the unforeseen shutdown of labs due to the COVID-19 pandemic prevented the planned development of this analysis to include flow cytometry, which we hoped would further probe the influence of the peptides on a single cell scale. This approach could provide in-depth analysis of the subpopulations that may be present within treated cell cultures, isolating individual cell characteristics within the samples, and providing a basis to develop this work into more complex biological systems. Some preliminary studies using flow cytometry were completed, as discussed later in section 0, with an advanced analysis panel developed for this work as an ideal approach for continuing this work in the future.

Throughout this thesis we have therefore demonstrated work towards the development and validation of an AFM system, capable of detecting and observing the influence of E-cadherin targeting peptides on the interactions between E-cadherin molecules. This novel analysis has revealed inhibitory effects not previously reported when using ensemble-based analytical techniques; namely, the ability for EpepW2R to inhibit E-cadherin adhesion. Subsequent experiments demonstrated the potential to incorporate cell monolayers into the AFM

experimental system, highlighting the potential to analyse impact of peptide treatment on mESC cultures. Biological assays such as high-content Operetta imaging presented a unique response of E14 and Ecad^{-/-} mES cell lines in the expression of key targets, including cadherin proteins and pluripotency markers, following the addition of Epep and EpepW2R. This suggests an exciting avenue for developing this work to further analyse the biophysical impact of novel targeting peptides and highlights the potential for this system to be used in future peptide screening experiments. This research could provide a more robust and informative analysis of peptide interaction for many different cell types, that can be utilised in research fields such as scale up cell culture, differentiation assays, and development of therapeutics.

6.1 Future Work

Throughout this thesis we have demonstrated the multidisciplinary nature of this work, and as such there are many opportunities for further development. The complex relationships and processes mediated by mechanical and biological functions of targets such as E-cadherin highlight the potential to understand, and perhaps manipulate, key cellular characteristics.

The work in this thesis shows the development of a robust E-cadherin binding system using functionalised AFM samples, with isolation of single molecule adhesion and high sensitivity force analysis. Similar systems have been developed previously to test a wide range of biological targets and provide a notable basis to be used throughout future work, as many different cellular targets can be assessed using this technique. However, our system specifically demonstrates the use of the AFM system as a method for investigating the effect of E-cadherin targeting peptides, which was successful in acquiring and analysing SMFS data on functionalised surfaces in multiple liquid environments, including the peptide samples of interest. Ideally, continued work would conduct complimentary DFS experiments, with the aim of further developing our understanding of the influence of the inhibiting peptides on the mechanical origins of the E-cadherin interactions. As the AFM system has already been shown to be successful in the monitoring of adhesion frequency and force, the use of DFS would provide further detail to the interactions observed, such as the force induced energy landscape and bond lifetime, and how these are affected by the targeting peptides^{118,135,138}.

We also conducted preliminary experiments that explored the ability for the AFM system to be adapted to allow for testing of adherent cell samples, while treating with peptide solutions. Therefore, naturally this work can progress to further assess the mESC cultures seen throughout this thesis, with the hope of providing a more detailed and representative understanding of peptide interactions using more biologically relevant samples. This approach could then be further developed to incorporate hESCs monolayers as the sample surface, initially testing the Epep and EpepW2R sequences to compare the influence of the peptides with the responses seen in mESCs. As discussed in chapter 1, human ESCs are receiving greater interest

as culture processes develop, and would provide a necessary development into human cell lines when considering the development of peptides for applications such as therapeutics. Although similarities exist between mouse and human ESCs, each possess distinct cell characteristics that could prove influential in the function of targeting peptides, such as the different maintenance pathway used for pluripotency. Experiments using cell monolayers have been developed previously by a number of research groups including our own^{133,186,245}, although there is a lack of evidence for the use of cell-AFM to probe the interaction and influence of novel peptide sequences. Therefore, the development of our AFM system to probe cell cultures highlights the potential diverse application of this work into future research.

Further development of this work could be achieved by isolating the interactions of potential additional biological targets discussed in chapter 5, such as Syndecan adhesions. This could be conducted in the presence and absence of cadherin proteins, highlighting any changes mediated by the interaction of the different proteins. Similarly, the use of different protein fragments could also be used to help gain further insight into the processes involved in the peptide mediated effects. For example, functionalising the system with only the EC1-2 domain of E-cadherin, which is regarded as the key binding domain for the formation and stability of classical cadherin bonds, would help determine the mode of action for the peptides. This is true for both Epep and EpepW2R peptides, and subsequently other peptide sequences that may target the E-cadherin binding domain. Similarly, the use of cell cultures modified to express specific protein fragments could provide a more advanced and biologically relevant progression to this work, as the isolation of known active sites on the E-cadherin protein could help determine the specific interaction of the molecules, or alternatively indicate off-target interactions of the peptides. The principle of exploiting protein fragments to isolate interactions is common, particularly with regards to cadherin proteins, and therefore provides a robust platform to develop this work²⁴⁶⁻²⁴⁸. Advancements in the use of AFM tips functionalised with single cells could also provide an exciting application for this research in the future.

In chapter 5 we successfully cultured and treated cell samples with various concentrations of Epep and EpepW2R media, and observed unique responses via high content Operetta analysis. This again provides a vast potential for continuation of this work, as well as incorporation of this approach into wider research projects. As outlined previously, this section was initially planned to be developed via complimentary cellular assays, such as flow cytometry, to enhance our understanding of the peptide effect on cell markers not yet observed or explored. However, the impact of the lab shutdown unfortunately prevented the completion of this work. Despite this, initial progress was made towards developing this experiment, with a comprehensive antibody panel selected and prepared, as seen in Appendix 1. This provides an ideal approach for the continuation of this work, as analysis using the selected markers provide a diverse range of intra- and extra-cellular markers that could be influenced by the peptides. The markers were selected due to their association with cadherin mediated processes, such as mechanical adhesions of surface molecules, or maintenance of key cellular pathways. These develop from the work already seen in literature, while targeting new molecules to attempt to further understand the influence and mechanisms of the peptides.

References

1. Weissman, I. L. Stem Cells: Units of Development, Units of Regeneration, and Units in Evolution. *Cell* **100**, 157–168 (2000).
2. Zakrzewski, W., Dobrzyński, M., Szymonowicz, M. & Rybak, Z. Stem cells: past, present, and future. *Stem Cell Res. Ther.* **10**, 1–22 (2019).
3. Biehl, J. K. & Russell, B. Introduction to Stem Cell Therapy. *J. Cardiovasc. Nurs.* **24**, 105 (2009).
4. Takahashi, K. *et al.* Induction of Pluripotent Stem Cells from Adult Human Fibroblasts by Defined Factors. *Cell* **131**, 861–872 (2007).
5. Rony, I. K. *et al.* Inducing pluripotency in vitro: recent advances and highlights in induced pluripotent stem cells generation and pluripotency reprogramming. *Cell Prolif.* **48**, 140–156 (2015).
6. Kolios, G. & Moodley, Y. Introduction to Stem Cells and Regenerative Medicine. *Respiration* **85**, 3–10 (2013).
7. Martin, G. R. Isolation of a pluripotent cell line from early mouse embryos cultured in medium conditioned by teratocarcinoma stem cells. *Proc. Natl. Acad. Sci. U. S. A.* **78**, 7638 (1981).
8. Evans, M. J. & Kaufman, M. H. Establishment in culture of pluripotential cells from mouse embryos. *Nature* **292**, 154–156 (1981).
9. Romito, A. & Cobellis, G. Pluripotent Stem Cells: Current Understanding and Future Directions. *Stem Cells Int.* **2016**, (2015).
10. Ying, Q.-L. *et al.* The ground state of embryonic stem cell self-renewal. *Nature* **453**, 519–523 (2008).
11. Mohamet, L., Lea, M. L. & Ward, C. M. Abrogation of E-cadherin-mediated cellular aggregation allows proliferation of pluripotent mouse embryonic stem cells in shake flask bioreactors. *PLoS One* **5**, e12921 (2010).
12. Devemy, E. & Blaschuk, O. W. Identification of a novel dual E- and N-cadherin

-
- antagonist. *Peptides* **30**, 1539–1547 (2009).
13. Soncin, F. & Ward, C. M. *The function of E-cadherin in stem cell pluripotency and self-renewal*. *Genes* **2**, 229–259 (Multidisciplinary Digital Publishing Institute (MDPI), 2011).
 14. Ghimire, S. *et al.* Comparative analysis of naive, primed and ground state pluripotency in mouse embryonic stem cells originating from the same genetic background. *Sci. Rep.* **8**, 1–11 (2018).
 15. Sharaireh, A. M., Fitzpatrick, L. M., Ward, C. M., McKay, T. R. & Unwin, R. D. Epithelial cadherin regulates transition between the naïve and primed pluripotent states in mouse embryonic stem cells. *Stem Cells Journals* **38**, 1292–1306 (2020).
 16. Chen, G., Guo, Y., Li, C., Li, S. & Wan, X. Small Molecules that Promote Self-Renewal of Stem Cells and Somatic Cell Reprogramming. *Stem Cell Rev. Reports* **16**, 511–523 (2020).
 17. Passanha, F. R., Geuens, T. & LaPointe, V. L. S. Sticking together: Harnessing cadherin biology for tissue engineering. *Acta Biomater.* **134**, 107–115 (2021).
 18. Zhang, Y., Qin, Z., Qu, Z., Ge, M. & Yang, J. Cadherin-based biomaterials: Inducing stem cell fate towards tissue construction and therapeutics. *Prog. Nat. Sci. Mater. Int.* **30**, 597–608 (2020).
 19. Pieters, T. & van Roy, F. Role of cell-cell adhesion complexes in embryonic stem cell biology. *J. Cell Sci.* **127**, 2603–2613 (2014).
 20. Larue, L., Ohsugi, M., Hirchenhain, J. & Kemler, R. E-cadherin null mutant embryos fail to form a trophectoderm epithelium. *Proc. Natl. Acad. Sci. U. S. A.* **91**, 8263–8267 (1994).
 21. Mohamet, L., Hawkins, K. & Ward, C. M. Loss of function of E-cadherin in embryonic stem cells and the relevance to models of tumorigenesis. *J. Oncol.* (2010). doi:10.1155/2011/352616
 22. Hawkins, K. *The role of E-cadherin in mouse embryonic stem cell pluripotency*.

-
- (2012).
23. Mossahebi-Mohammadi, M., Quan, M., Zhang, J.-S. & Li, X. FGF Signaling Pathway: A Key Regulator of Stem Cell Pluripotency. *Front. Cell Dev. Biol.* **8**, (2020).
 24. Zhang, J. *et al.* Dax1 and Nanog act in parallel to stabilize mouse embryonic stem cells and induced pluripotency. *Nat. Commun.* **5**, (2014).
 25. Waghray, A. *et al.* Tbx3 Controls Dppa3 Levels and Exit from Pluripotency toward Mesoderm. *Stem Cell Reports* **5**, 110 (2015).
 26. Sladitschek, H. L. & Neveu, P. A. A gene regulatory network controls the balance between mesendoderm and ectoderm at pluripotency exit. *Mol. Syst. Biol.* **15**, e9043 (2019).
 27. Ye, B. *et al.* Klf4 glutamylation is required for cell reprogramming and early embryonic development in mice. *Nat. Commun.* **9**, 1–16 (2018).
 28. Soncin, F. *et al.* E-Cadherin Acts as a Regulator of Transcripts Associated with a Wide Range of Cellular Processes in Mouse Embryonic Stem Cells. *PLoS One* **6**, e21463 (2011).
 29. Ozaki, C., Obata, S., Yamanaka, H., Tominaga, S. & Suzuki, S. T. The extracellular domains of E- and N-cadherin determine the scattered punctate localization in epithelial cells and the cytoplasmic domains modulate the localization. *J. Biochem.* **147**, 415–425 (2010).
 30. Koirala, R. *et al.* Inside-out regulation of E-cadherin conformation and adhesion. *bioRxiv* 2020.05.02.074187 (2021). doi:10.1101/2020.05.02.074187
 31. Shibata-Seki, T., Nagaoka, M., Goto, M., Kobatake, E. & Akaike, T. Direct visualization of the extracellular binding structure of E-cadherins in liquid. *Sci. Rep.* **10**, 1–10 (2020).
 32. Cailliez, F. & Lavery, R. Cadherin mechanics and complexation: The importance of calcium binding. *Biophys. J.* **89**, 3895–3903 (2005).
 33. Niessen, C. M. Tight Junctions/Adherens Junctions: Basic Structure and

-
- Function. *J. Invest. Dermatol.* **127**, 2525–2532 (2007).
34. Kim, N.-G., Koh, E., Chen, X. & Gumbiner, B. M. E-cadherin mediates contact inhibition of proliferation through Hippo signaling-pathway components. *Proc. Natl. Acad. Sci. U. S. A.* **108**, 11930–5 (2011).
 35. Perez-Moreno, M. & Fuchs, E. Catenins: Keeping Cells from Getting Their Signals Crossed. *Dev. Cell* **11**, 601–612 (2006).
 36. Soncin, F. *et al.* Abrogation of E-cadherin-mediated cell-cell contact in mouse embryonic stem cells results in reversible LIF-independent self-renewal. *Stem Cells* **27**, 2069–2080 (2009).
 37. Couchman, J. R. Syndecan-1 (CD138), Carcinomas and EMT. *Int. J. Mol. Sci.* **22**, 4227 (2021).
 38. Filatova, A., Pagella, P. & Mitsiadis, T. A. Distribution of syndecan-1 protein in developing mouse teeth. *Front. Physiol.* **5**, 518 (2015).
 39. Harjunpää, H., Asens, M. L., Guenther, C. & Fagerholm, S. C. Cell adhesion molecules and their roles and regulation in the immune and tumor microenvironment. *Front. Immunol.* **10**, 1078 (2019).
 40. Yoshida, C. & Takeichi, M. Teratocarcinoma cell adhesion: Identification of a cell-surface protein involved in calcium-dependent cell aggregation. *Cell* **28**, 217–224 (1982).
 41. Pećina-Šlaus, N. Tumor suppressor gene E-cadherin and its role in normal and malignant cells. *Cancer Cell International* **3**, 17 (2003).
 42. Saito, M., Tucker, D. K., Kohlhorst, D., Niessen, C. M. & Kowalczyk, A. P. Classical and desmosomal cadherins at a glance. *J. Cell Sci.* **125**, 2547–2552 (2012).
 43. Gumbiner, B. M. Regulation of cadherin-mediated adhesion in morphogenesis. *Nature Reviews Molecular Cell Biology* **6**, 622–634 (2005).
 44. Stepniak, E., Radice, G. L. & Vasioukhin, V. Adhesive and signaling functions of cadherins and catenins in vertebrate development. *Cold Spring Harbor*

perspectives in biology **1**, a002949 (2009).

45. Harrison, O. J. *et al.* The Extracellular Architecture of Adherens Junctions Revealed by Crystal Structures of Type I Cadherins. *Structure* **19**, 244–256 (2011).
46. Ivanov, D. B., Philippova, M. P. & Tkachuk, V. A. Structure and functions of classical cadherins. *Biochemistry. (Mosc)*. **66**, 1174–86 (2001).
47. Takeichi, M. Morphogenetic roles of classic cadherins. *Curr. Opin. Cell Biol.* **7**, 619–27 (1995).
48. Tepass, U., Truong, K., Godt, D., Ikura, M. & Peifer, M. Cadherins in embryonic and neural morphogenesis. *Nat. Rev. Mol. Cell Biol.* **1**, 91–100 (2000).
49. Maître, J. L. & Heisenberg, C. P. Three functions of cadherins in cell adhesion. *Curr. Biol.* **23**, 626–633 (2013).
50. Livshits, G., Kobiela, A. & Fuchs, E. Governing epidermal homeostasis by coupling cell - Cell adhesion to integrin and growth factor signaling, proliferation, and apoptosis. *Proc. Natl. Acad. Sci. U. S. A.* **109**, 4886–4891 (2012).
51. Harris, T. J. C. & Tepass, U. Adherens junctions: From molecules to morphogenesis. *Nat. Rev. Mol. Cell Biol.* **11**, 502–514 (2010).
52. Lee, J. L. & Streuli, C. H. Integrins and epithelial cell polarity. *J. Cell Sci.* **127**, 3225 (2014).
53. Kaplan, N. A., Liu, X. & Tolwinski, N. S. Epithelial polarity: interactions between junctions and apical-basal machinery. *Genetics* **183**, 897–904 (2009).
54. Anderson, J. M. & Van Itallie, C. M. Physiology and function of the tight junction. *Cold Spring Harb. Perspect. Biol.* **1**, a002584 (2009).
55. Marchiando, A. M., Graham, W. V. & Turner, J. R. Epithelial Barriers in Homeostasis and Disease. *Annu. Rev. Pathol. Mech. Dis.* **5**, 119–144 (2010).
56. Kourtidis, A., Ngok, S. P. & Anastasiadis, P. Z. p120 catenin: an essential

-
- regulator of cadherin stability, adhesion-induced signaling, and cancer progression. *Prog. Mol. Biol. Transl. Sci.* **116**, 409–32 (2013).
57. Ishiyama, N. *et al.* Force-dependent allostery of the α -catenin actin-binding domain controls adherens junction dynamics and functions. *Nat. Commun.* **9**, (2018).
 58. Yamada, S., Pokutta, S., Drees, F., Weis, W. I. & Nelson, W. J. Deconstructing the cadherin-catenin-actin complex. *Cell* **123**, 889–901 (2005).
 59. Drees, F., Pokutta, S., Yamada, S., Nelson, W. J. & Weis, W. I. α -catenin is a molecular switch that binds E-cadherin- β -catenin and regulates actin-filament assembly. *Cell* **123**, 903–915 (2005).
 60. Priest, A. V., Shafraz, O. & Sivasankar, S. Biophysical basis of cadherin mediated cell-cell adhesion. *Exp. Cell Res.* **358**, 10–13 (2017).
 61. Leckband, D. E. E. & De Rooij, J. Cadherin Adhesion and Mechanotransduction. *Annu. Rev. Cell Dev. Biol.* **30**, 291–315 (2014).
 62. Adhikari, S., Moran, J., Weddle, C. & Hinczewski, M. Unraveling the mechanism of the cadherin-catenin-actin catch bond. *PLoS Comput. Biol.* **14**, (2018).
 63. Shapiro, L. & Weis, W. I. Structure and biochemistry of cadherins and catenins. *Cold Spring Harbor perspectives in biology* **1**, (2009).
 64. Manibog, K. *et al.* Molecular determinants of cadherin ideal bond formation: Conformation-dependent unbinding on a multidimensional landscape. *Proc. Natl. Acad. Sci. U. S. A.* **113**, E5711–E5720 (2016).
 65. Shapiro, L. *et al.* Structural basis of cell-cell adhesion by cadherins. *Nature* **374**, 327–337 (1995).
 66. Tamura, K., Shan, W. S., Hendrickson, W. A., Colman, D. R. & Shapiro, L. Structure-function analysis of cell adhesion by neural (N-) cadherin. *Neuron* **20**, 1153–1163 (1998).
 67. Brasch, J., Harrison, O. J., Honig, B. & Shapiro, L. Thinking outside the cell: how cadherins drive adhesion. *Trends Cell Biol.* **22**, 299–310 (2012).

-
68. Rakshit, S., Zhang, Y., Manibog, K., Shafraz, O. & Sivasankar, S. Ideal, catch, and slip bonds in cadherin adhesion. *Proc. Natl. Acad. Sci. U. S. A.* **109**, 18815–18820 (2012).
 69. Evans, E. A. & Calderwood, D. A. Forces and bond dynamics in cell adhesion. *Science (80-.).* **316**, 1148–1153 (2007).
 70. Leckband, D. & Prakasam, A. Mechanism and Dynamics of Cadherin Adhesion Cadherin: calcium-dependent adhesion molecules that mediate cell-cell interactions. (2006). doi:10.1146/
 71. Wu, Y., Vendome, J., Shapiro, L., Ben-Shaul, A. & Honig, B. Transforming binding affinities from three dimensions to two with application to cadherin clustering. *Nature* **475**, 510–513 (2011).
 72. Wu, Y., Kanchanawong, P. & Zaidel-Bar, R. Actin-Delimited Adhesion-Independent Clustering of E-Cadherin Forms the Nanoscale Building Blocks of Adherens Junctions. *Dev. Cell* **32**, 139–154 (2015).
 73. Carvalho, S., Reis, C. A. & Pinho, S. S. Cadherins Glycans in Cancer: Sweet Players in a Bitter Process. (2016). doi:10.1016/j.trecan.2016.08.003
 74. Langer, M. D., Guo, H., Shashikanth, N., Pierce, J. M. & Leckband, D. E. N-glycosylation alters cadherin-mediated intercellular binding kinetics. *J. Cell Sci.* **125**, 2478–2485 (2012).
 75. Chen, J., Newhall, J., Xie, Z. R., Leckband, D. & Wu, Y. A Computational Model for Kinetic Studies of Cadherin Binding and Clustering. *Biophys. J.* **111**, 1507–1518 (2016).
 76. Huber, A. H., Stewart, D. B., Laurents, D. V, Nelson, W. J. & Weis, W. I. The cadherin cytoplasmic domain is unstructured in the absence of beta-catenin. A possible mechanism for regulating cadherin turnover. *J. Biol. Chem.* **276**, 12301–9 (2001).
 77. Cepek, K. L. *et al.* Adhesion between epithelial cells and T lymphocytes mediated by E-cadherin and the $\alpha E \beta 7$ integrin. *Nat.* 1994 3726502 **372**, 190–

-
- 193 (1994).
78. Sun, D., Mcalmon, K. R., Davies, J. A., Bernfield, M. & Hay, E. D. Simultaneous loss of expression of syndecan-1 and E-cadherin in the embryonic palate during epithelial-mesenchymal transformation. *Int. J. Dev. Biol.* **42**, 733–736 (1998).
 79. Kalmouni, M., Al-Hosani, S. & Magzoub, M. Cancer targeting peptides. *Cellular and Molecular Life Sciences* **76**, 2171–2183 (2019).
 80. Gaston, J. *et al.* Intracellular delivery of therapeutic antibodies into specific cells using antibody-peptide fusions. *Sci. Rep.* **9**, 1–12 (2019).
 81. Patel, S. G. *et al.* Cell-penetrating peptide sequence and modification dependent uptake and subcellular distribution of green florescent protein in different cell lines. *Sci. Reports 2019 91* **9**, 1–9 (2019).
 82. Hoffmann, K. *et al.* A platform for discovery of functional cell-penetrating peptides for efficient multi-cargo intracellular delivery. *Sci. Rep.* **8**, 1–16 (2018).
 83. Eagle, H. The minimum vitamin requirements of the L and HeLa cells in tissue culture, the production of specific vitamin deficiencies, and their cure. *J. Exp. Med.* **102**, 595–600 (1955).
 84. Salazar, A., Keusgen, M. & Von Hagen, J. Amino acids in the cultivation of mammalian cells. *Amino Acids* **48**, 1161–1171 (2016).
 85. Eagle, H. The specific amino acid requirements of a mammalian cell (strain L) in tissue culture. *J. Biol. Chem.* **214**, 839–852 (1955).
 86. Yao, T. & Asayama, Y. Animal-cell culture media: History, characteristics, and current issues. *Reprod. Med. Biol.* **16**, 99–117 (2017).
 87. Vestweber, D. Cadherins in tissue architecture and disease. *J. Mol. Med.* **93**, 5–11 (2015).
 88. Yang, J. & Weinberg, R. A. Epithelial-Mesenchymal Transition: At the Crossroads of Development and Tumor Metastasis. *Dev. Cell* **14**, 818–829

-
- (2008).
89. Clark, A. G. & Vignjevic, D. M. Modes of cancer cell invasion and the role of the microenvironment. *Curr. Opin. Cell Biol.* **36**, 13–22 (2015).
 90. Figueiredo, J. *et al.* E-cadherin signal sequence disruption: a novel mechanism underlying hereditary cancer. *Mol. Cancer* **17**, 1–7 (2018).
 91. Battistini, C. *et al.* Rhomboid-Like-2 Intramembrane Protease Mediates Metalloprotease-Independent Regulation of Cadherins. *Int. J. Mol. Sci.* **20**, 5958 (2019).
 92. Song, Y., Ye, M., Zhou, J., Wang, Z. W. & Zhu, X. Q. Targeting e-cadherin expression with small molecules for digestive cancer treatment. *Am. J. Transl. Res.* **11**, 3932–3944 (2019).
 93. Segal, J. M. & Ward, C. M. Novel peptides for deciphering structural and signalling functions of E-cadherin in mouse embryonic stem cells. *Sci. Rep.* **7**, 41827 (2017).
 94. Harrison, O. J. *et al.* Two-step adhesive binding by classical cadherins. *Nat. Struct. Mol. Biol.* **17**, 348–357 (2010).
 95. Li, Y. *et al.* Mechanism of E-cadherin dimerization probed by NMR relaxation dispersion. *Proc. Natl. Acad. Sci. U. S. A.* **110**, 16462–16467 (2013).
 96. Yap, A. S., Niessen, C. M. & Gumbiner, B. M. The juxtamembrane region of the cadherin cytoplasmic tail supports lateral clustering, adhesive strengthening, and interaction with p120ctn. *J. Cell Biol.* **141**, 779–89 (1998).
 97. Nagar, B., Overduin, M., Ikura, M. & Rini, J. M. Structural basis of calcium-induced E-cadherin rigidification and dimerization. *Nature* **380**, 360–364 (1996).
 98. Yap, A. S., Duszyc, K. & Viasnoff, V. Mechanosensing and mechanotransduction at cell–cell junctions. *Cold Spring Harb. Perspect. Biol.* **10**, a028761 (2018).
 99. Orr, A. W., Helmke, B. P., Blackman, B. R. & Schwartz, M. A. Mechanisms of

-
- Mechanotransduction. *Dev. Cell* **10**, 11–20 (2006).
100. Leckband, D. Single-molecule measurements and biomedical engineering. *Current Opinion in Biomedical Engineering* **12**, A1–A3 (2019).
 101. Leckband, D. & Israelachvili, J. Intermolecular forces in biology. *Q. Rev. Biophys.* **34**, 105–267 (2021).
 102. Vahabi, S., Nazemi Salman, B. & Javanmard, A. Atomic force microscopy application in biological research: A review study. *Iran. J. Med. Sci.* **38**, 76–83 (2013).
 103. Ungai-Salánki, R. *et al.* A practical review on the measurement tools for cellular adhesion force. *Adv. Colloid Interface Sci.* **269**, 309–333 (2019).
 104. Leckband, D. Measuring the forces that control protein interactions. *Annu. Rev. Biophys. Biomol. Struct.* **29**, 1–26 (2000).
 105. Šmít, D. *et al.* BFPTool: A software tool for analysis of Biomembrane Force Probe experiments. *BMC Biophys.* **10**, 2 (2017).
 106. Panorchan, P. *et al.* Single-molecule analysis of cadherin-mediated cell-cell adhesion. *J. Cell Sci.* **119**, 66–74 (2006).
 107. Sako, Y., Nagafuchi, A., Tsukita, S., Takeichi, M. & Kusumi, A. Cytoplasmic regulation of the movement of E-cadherin on the free cell surface as studied by optical tweezers and single particle tracking: corralling and tethering by the membrane skeleton. *J. Cell Biol.* **140**, 1227–40 (1998).
 108. Baumgartner, W., Schütz, G. J., Wiegand, J., Golenhofen, N. & Drenckhahn, D. Cadherin function probed by laser tweezer and single molecule fluorescence in vascular endothelial cells. *J. Cell Sci.* **116**, 1001–1011 (2003).
 109. Ounkomol, C., Yamada, S. & Heinrich, V. Single-cell adhesion tests against functionalized microspheres arrayed on AFM cantilevers confirm heterophilic E- and N-cadherin binding. *Biophys. J.* **99**, L100 (2010).
 110. Evans, E., Ritchie, K. & Merkel, R. Sensitive Force Technique to Probe Molecular Adhesion and Structural Linkages at Biological Interfaces. *Biophys.*

-
- J.* **68**, 2580–2587 (1995).
111. Friedrichs, J. *et al.* A practical guide to quantify cell adhesion using single-cell force spectroscopy. *Methods* **60**, 169–178 (2013).
 112. Pokutta, S. & Weis, W. I. Structure and Mechanism of Cadherins and Catenins in Cell-Cell Contacts. *Annu. Rev. Cell Dev. Biol.* **23**, 237–261 (2007).
 113. Binnig, G., Quate, C. F. & Gerber, C. Atomic Force Microscope. *Phys. Rev. Lett.* **56**, 930–933 (1986).
 114. Parot, P. *et al.* Past, present and future of atomic force microscopy in life sciences and medicine. *J. Mol. Recognit.* **20**, 418–431 (2007).
 115. Lee, G. U., Chrisey, L. A. & Colton, R. J. Direct measurement of the forces between complementary strands of DNA. *Science* **266**, 771–3 (1994).
 116. Florin, E. L., Moy, V. T. & Gaub, H. E. Adhesion forces between individual ligand-receptor pairs. *Science* **264**, 415–7 (1994).
 117. Wong, J., Chilkoti, A. & Moy, V. T. Direct force measurements of the streptavidin–biotin interaction. *Biomol. Eng.* **16**, 45–55 (1999).
 118. Merkel, R., Nassoy, P., Leung, A., Ritchie, K. & Evans, E. Energy landscapes of receptor–ligand bonds explored with dynamic force spectroscopy. *Nature* **397**, 50–53 (1999).
 119. Baumgartner, W. *et al.* Cadherin interaction probed by atomic force microscopy. *Proc. Natl. Acad. Sci. U. S. A.* **97**, 4005–4010 (2000).
 120. Dufrêne, Y. F. *et al.* Five challenges to bringing single-molecule force spectroscopy into living cells. *Nat. Methods* **8**, 123–127 (2011).
 121. Lehenkari, P. P. & Horton, M. A. Single integrin molecule adhesion forces in intact cells measured by atomic force microscopy. *Biochem. Biophys. Res. Commun.* **259**, 645–650 (1999).
 122. Yang, B., Liu, Z., Liu, H. & Nash, M. A. Next Generation Methods for Single-Molecule Force Spectroscopy on Polyproteins and Receptor-Ligand

-
- Complexes. *Frontiers in Molecular Biosciences* **7**, (2020).
123. Allen, S. *et al.* In situ observation of streptavidin-biotin binding on an immunoassay well surface using an atomic force microscope. *FEBS Lett.* **390**, 161–164 (1996).
 124. Williams, P. M. *et al.* On the dynamic behaviour of the forced dissociation of ligand-receptor pairs. *J. Chem. Soc. Perkin Trans. 2* 5–8 (2000). doi:10.1039/a907750b
 125. Dufrêne, Y. F. Atomic force microscopy in microbiology: New structural and functional insights into the microbial cell surface. *MBio* **5**, (2014).
 126. Whited, A. M. & Park, P. S. H. Atomic force microscopy: A multifaceted tool to study membrane proteins and their interactions with ligands. *Biochimica et Biophysica Acta - Biomembranes* **1838**, 56–68 (2014).
 127. El Kirat, K., Burton, I., Dupres, V. & Dufrene, Y. F. Sample preparation procedures for biological atomic force microscopy. *J. Microsc.* **218**, 199–207 (2005).
 128. Müller, D. J., Engel, A. & Amrein, M. Preparation techniques for the observation of native biological systems with the atomic force microscope. in *Biosensors and Bioelectronics* **12**, 867–877 (Elsevier Science Ltd, 1997).
 129. Chada, N. *et al.* Glass is a Viable Substrate for Precision Force Microscopy of Membrane Proteins. *Sci. Reports 2015 51* **5**, 1–8 (2015).
 130. King, W. T., Su, M. & Yang, G. Monte Carlo simulation of mechanical unfolding of proteins based on a simple two-state model. *Int. J. Biol. Macromol.* **46**, (2010).
 131. Tych, K. M. *et al.* Optimizing the calculation of energy landscape parameters from single-molecule protein unfolding experiments. *Phys. Rev. E - Stat. Nonlinear, Soft Matter Phys.* **91**, 12710–12719 (2015).
 132. Hinterdorfer, P., Baumgartner, W., Gruber, H. J., Schilcher, K. & Schindler, H. *Detection and localization of individual antibody-antigen recognition events by*

-
- atomic force microscopy (ligand-receptor interaction/human serum albumin/imaging/crosslinker)*. *Biophysics* **93**, (1996).
133. Graumuller, F. Investigating stem cell interactions using Atomic force microscopy. (University of Nottingham, 2019).
 134. Greenleaf, W. J., Woodside, M. T. & Block, S. M. High-resolution, single-molecule measurements of biomolecular motion. *Annual Review of Biophysics and Biomolecular Structure* **36**, 171–190 (2007).
 135. Williams, P. M. Analytical descriptions of dynamic force spectroscopy: behaviour of multiple connections. *Anal. Chim. Acta* **479**, 107–115 (2003).
 136. Chesla, S. E., Selvaraj, P. & Zhu, C. Measuring two-dimensional receptor-ligand binding kinetics by micropipette. *Biophys. J.* **75**, 1553–1572 (1998).
 137. Shafraz, O. *et al.* E-cadherin binds to desmoglein to facilitate desmosome assembly. *Elife* **7**, (2018).
 138. Evans, E. *Introductory Lecture Energy landscapes of biomolecular adhesion and receptor anchoring at interfaces explored with dynamic force spectroscopy*. *Faraday Discussions* **111**, 1–16 (The Royal Society of Chemistry, 1999).
 139. Johnson, K. C. & Thomas, W. E. How Do We Know when Single-Molecule Force Spectroscopy Really Tests Single Bonds? *Biophys. J.* **114**, 2032–2039 (2018).
 140. Ando, T. High-speed atomic force microscopy and its future prospects. *Biophysical Reviews* **10**, 285–292 (2018).
 141. Hughes, M. L. & Dougan, L. The physics of pulling polyproteins: a review of single molecule force spectroscopy using the AFM to study protein unfolding. *Reports Prog. Phys.* **79**, 076601 (2016).
 142. Alonso, J. L. & Goldmann, W. H. Feeling the forces: Atomic force microscopy in cell biology. *Life Sciences* **72**, 2553–2560 (2003).
 143. Neuman, K. K. C. & Nagy, A. Single-molecule force spectroscopy: optical tweezers, magnetic tweezers and atomic force microscopy. *Nat. Methods* **5**, 491–505 (2008).

-
144. Marshall, B. T. *et al.* Direct observation of catch bonds involving cell-adhesion molecules. *Nature* **423**, 190–193 (2003).
145. Hutter, J. L. & Bechhoefer, J. Calibration of atomic-force microscope tips. *Rev. Sci. Instrum.* **64**, 1868–1873 (1993).
146. Lévy, R. & Maaloum, M. Measuring the spring constant of atomic force microscope cantilevers: Thermal fluctuations and other methods. *Nanotechnology* **13**, 33–37 (2002).
147. Asylum Research. *Asylum Research MFP-3D Manual*. (Asylum Research, 2008).
148. Hammond, K., Ryadnov, M. G. & Hoogenboom, B. W. Atomic force microscopy to elucidate how peptides disrupt membranes. *Biochimica et Biophysica Acta - Biomembranes* **1863**, 183447 (2021).
149. Maghsoudy-Louyeh, S., Kropf, M. & Tittmann, B. R. Review of Progress in Atomic Force Microscopy. *Open Neuroimag. J.* **12**, 86–104 (2018).
150. Kramers, H. A. Brownian motion in a field of force and the diffusion model of chemical reactions. *Physica* **7**, 284–304 (1940).
151. Hänggi, P., Talkner, P. & Borkovec, M. Reaction-rate theory: Fifty years after Kramers. *Rev. Mod. Phys.* **62**, 251–341 (1990).
152. Evans, E. & Williams, P. Dynamic Force Spectroscopy. in *Physics of biomolecules and cells. Physique des biomolécules et des cellules* (eds. F. Flyvbjerg, F. Jülicher, P. Ormos & F. David) **75**, 145–204 (Springer, Berlin, Heidelberg, 2002).
153. Green, N. H. *et al.* Single-molecule investigations of RNA dissociation. *Biophys. J.* **86**, 3811–3821 (2004).
154. Brampton, C., Wahab, O., Batchelor, M. R., Allen, S. & Williams, P. M. Biomembrane force probe investigation of RNA dissociation. *Eur. Biophys. J.* **40**, 247–257 (2011).
155. Evans, E. Probing the Relation Between Force—Lifetime—and Chemistry in Single Molecular Bonds. *Annu. Rev. Biophys. Biomol. Struct.* **30**, 105–128

-
- (2001).
156. Borgia, A., Williams, P. M. & Clarke, J. Single-Molecule Studies of Protein Folding. *Annu. Rev. Biochem.* **77**, 101–125 (2008).
 157. Liyanage, M. R., Bakshi, K., Volkin, D. B. & Middaugh, C. R. Ultraviolet absorption spectroscopy of peptides. *Methods Mol. Biol.* **1088**, 225–236 (2014).
 158. Liyanage, M. R., Bakshi, K., Volkin, D. B. & Middaugh, C. R. Fluorescence spectroscopy of peptides. *Methods Mol. Biol.* **1088**, 237–246 (2014).
 159. Prasad, S. *et al.* Near UV-Visible electronic absorption originating from charged amino acids in a monomeric protein. *Chem. Sci.* **8**, 5416–5433 (2017).
 160. Anthis, N. J. & Clore, G. M. Sequence-specific determination of protein and peptide concentrations by absorbance at 205 nm. *Protein Sci.* **22**, 851–858 (2013).
 161. Goldfarb, A. R. & Sidel, L. J. Ultraviolet absorption spectra of proteins. *Science (80-)*. **114**, 156–157 (1951).
 162. Walton, A. G. & Maenpa, F. C. Application of fluorescence spectroscopy to the study of proteins at interfaces. *J. Colloid Interface Sci.* **72**, 265–278 (1979).
 163. Da Silva, J. C., Queiroz, A., Oliveira, A. & Kartnaller, V. Advances in the Application of Spectroscopic Techniques in the Biofuel Area over the Last Few Decades. in *Frontiers in Bioenergy and Biofuels* (InTech, 2017). doi:10.5772/65552
 164. Cox, G. *Optical Imaging Techniques in Cell Biology*. (CRC Press, 2012).
 165. Stender, A. S. *et al.* Single cell optical imaging and spectroscopy. *Chemical Reviews* **113**, 2469–2527 (2013).
 166. Dirks, R. W., Molenaar, C. & Tanke, H. J. Methods for visualizing RNA processing and transport pathways in living cells. *Histochem. Cell Biol.* **115**, 3–11 (2001).

-
167. Fukuyama, R. & Shimizu, N. Detection of Epidermal Growth Factor Receptors and E-Cadherins in the Basolateral Membrane of A431 Cells by Laser Scanning Fluorescence Microscopy. *Japanese J. Cancer Res.* **82**, 8–11 (1991).
168. Duocastella, M., Surdo, S., Zunino, A., Diaspro, A. & Saggau, P. Acousto-optic systems for advanced microscopy. *JPhys Photonics* **3**, 12004 (2021).
169. Gao, W., Zhao, L., Jiang, Z. & Sun, D. Advanced Biological Imaging for Intracellular Micromanipulation: Methods and Applications. *Appl. Sci.* **10**, (2020).
170. Sheppard, C. J. R. Confocal Microscopy – Principles, Practice and Options. in *Fluorescent and Luminescent Probes for Biological Activity* 303–309 (Elsevier, 1999). doi:10.1016/b978-012447836-7/50023-3
171. Trotman, W. E., Taatjes, D. J. & Bovill, E. G. Multifluorescence Confocal Microscopy: Application for a Quantitative Analysis of Hemostatic Proteins in Human Venous Valves. in 85–95 (2012). doi:10.1007/978-1-62703-056-4_4
172. Jonkman, J. & Brown, C. M. Any way you slice it—A comparison of confocal microscopy techniques. *J. Biomol. Tech.* **26**, 54–65 (2015).
173. Stern, M., Taatjes, D. J. & Mossman, B. T. Multifluorescence labeling techniques and confocal laser scanning microscopy on lung tissue. in *Cell Imaging Techniques: Methods and Protocols* (eds. Taatjes, D. J. & Mossman, B. T.) **319**, 67–76 (Humana Press, 2006).
174. Massey, A. J. Multiparametric cell cycle analysis using the operetta high-content imager and harmony software with PhenoLOGIC. *PLoS One* **10**, (2015).
175. PerkinElmer. Operetta[®] High Content Imaging System. (2013). Available at: www.perkinelmer.com/operetta. (Accessed: 21st January 2021)
176. PerkinElmer. Microplates For High Content Analysis and High Content Screening Assays | Application Support Knowledgebase | Lab Products & Services | PerkinElmer. (2021). Available at: <https://www.perkinelmer.com/uk/lab-products-and-services/application->

support-knowledgebase/microplates/high-content-screening-plates.html.

(Accessed: 21st January 2021)

177. Taylor, I. Before FlowJo™ | FlowJo, LLC. (2021). Available at: <https://www.flowjo.com/learn/flowjo-university/flowjo/before-flowjo/58>. (Accessed: 22nd January 2021)
178. McKinnon, K. M. Flow cytometry: An overview. *Curr. Protoc. Immunol.* **120**, 5.1.1-5.1.11 (2018).
179. Vembadi, A., Menachery, A. & Qasaimeh, M. A. Cell Cytometry: Review and Perspective on Biotechnological Advances. *Front. Bioeng. Biotechnol.* **7**, 147 (2019).
180. Puchner, E. M. & Gaub, H. E. Force and function: probing proteins with AFM-based force spectroscopy. *Current Opinion in Structural Biology* **19**, 605–614 (2009).
181. Manosas, M. *et al.* Force Unfolding Kinetics of RNA using Optical Tweezers. II. Modeling Experiments. *Biophys. J.* **92**, 3010–3021 (2007).
182. Zhang, Y., Sivasankar, S., Nelson, W. J. & Chu, S. Resolving cadherin interactions and binding cooperativity at the single-molecule level. *Proc. Natl. Acad. Sci. U. S. A.* **106**, 109–14 (2009).
183. Manibog, K., Li, H., Rakshit, S. & Sivasankar, S. Resolving the molecular mechanism of cadherin catch bond formation. *Nat. Commun.* **5**, 3941 (2014).
184. Blaue, C., Kashef, J. & Franz, C. M. Cadherin-11 promotes neural crest cell spreading by reducing intracellular tension-Mapping adhesion and mechanics in neural crest explants by atomic force microscopy. *Semin. Cell Dev. Biol.* **73**, 95–106 (2018).
185. Fichtner, D. *et al.* Covalent and Density-Controlled Surface Immobilization of E-Cadherin for Adhesion Force Spectroscopy. *PLoS One* **9**, e93123 (2014).
186. Viji Babu, P. K., Mirastschijski, U., Belge, G. & Radmacher, M. Homophilic and heterophilic cadherin bond rupture forces in homo- or hetero-cellular systems

-
- measured by AFM based SCFS. *bioRxiv* 2020.02.11.943597 (2020). doi:10.1101/2020.02.11.943597
187. Sigma-Aldrich. E-Cadherin/Fc Chimera from mouse >90% (SDS-PAGE), recombinant, expressed in NSO cells, lyophilized powder. (2021). Available at: <https://www.sigmaaldrich.com/GB/en/product/sigma/e2153>. (Accessed: 13th July 2021)
 188. Niessen, C. M., Leckband, D. & Yap, A. S. Tissue Organization by Cadherin Adhesion Molecules: Dynamic Molecular and Cellular Mechanisms of Morphogenetic Regulation. *Physiol. Rev.* **91**, 691–731 (2011).
 189. Creasey, R. *et al.* Atomic force microscopy-based antibody recognition imaging of proteins in the pathological deposits in Pseudoexfoliation Syndrome. *Ultramicroscopy* **111**, 1055–1061 (2011).
 190. Ebner, A., Hinterdorfer, P. & Gruber, H. J. Comparison of different aminofunctionalization strategies for attachment of single antibodies to AFM cantilevers. *Ultramicroscopy* **107**, 922–927 (2007).
 191. Moldovan, A. *et al.* Simple cleaning and conditioning of silicon surfaces with UV/ozone Sources. in *Energy Procedia* **55**, 834–844 (Elsevier Ltd, 2014).
 192. Michl, J., Park, K. C. & Swietach, P. Evidence-based guidelines for controlling pH in mammalian live-cell culture systems. *Commun. Biol.* **2**, 1–12 (2019).
 193. Kim, S. A., Tai, C. Y. C.-Y., Mok, L. P. L.-P. L. P., Mosser, E. A. & Schuman, E. M. Calcium-dependent dynamics of cadherin interactions at cell-cell junctions. *Proc. Natl. Acad. Sci. U. S. A.* **108**, 9857–9862 (2011).
 194. Rothen-Rutishauser, B., Riesen, F. K., Braun, A., Günthert, M. & Wunderli-Allenspach, H. Dynamics of tight and adherens junctions under EGTA treatment. *J. Membr. Biol.* **188**, 151–162 (2002).
 195. Willemsen, O. H. *et al.* A physical approach to reduce nonspecific adhesion in molecular recognition atomic force microscopy. *Biophys. J.* **76**, 716–724 (1999).

-
196. Perez, T. D. & Nelson, W. J. Cadherin Adhesion: Mechanisms and Molecular Interactions. in *Handbook of experimental pharmacology* 3–21 (NIH Public Access, 2010). doi:10.1007/978-3-540-68170-0_1
197. Shen, Y., Wu, T., Zhang, Y. & Li, J. Comparison of two-typed (3-mercaptopropyl)trimethoxysilane-based networks on Au substrates. *Talanta* **65**, 481–488 (2005).
198. Yang, Y., Bittner, A. M., Baldelli, S. & Kern, K. Study of self-assembled triethoxysilane thin films made by casting neat reagents in ambient atmosphere. *Thin Solid Films* **516**, 3948–3956 (2008).
199. Zhu, M., Lerum, M. Z. & Chen, W. How to prepare reproducible, homogeneous, and hydrolytically stable aminosilane-derived layers on silica. *Langmuir* **28**, 416–423 (2012).
200. Brouxhon, S. M. *et al.* Monoclonal antibody against the ectodomain of E-cadherin (DECMA-1) suppresses breast carcinogenesis: Involvement of the HER/PI3K/Akt/mTOR and IAP pathways. *Clin. Cancer Res.* **19**, 3234–3246 (2013).
201. Muhamed, I. *et al.* E-cadherin-mediated force transduction signals regulate global cell mechanics. *J. Cell Sci.* **129**, 1843–1854 (2016).
202. Ozawa, M., Hoschützky, H., Herrenknecht, K. & Kemler, R. A possible new adhesive site in the cell-adhesion molecule uvomorulin. *Mech. Dev.* **33**, 49–56 (1990).
203. Crampton, N., Bonass, W. A., Kirkham, J. & Thomson, N. H. Formation of Aminosilane-Functionalized Mica for Atomic Force Microscopy Imaging of DNA. doi:10.1021/la050972q
204. Brochier Salon, M. C., Bayle, P. A., Abdelmouleh, M., Boufi, S. & Belgacem, M. N. Kinetics of hydrolysis and self condensation reactions of silanes by NMR spectroscopy. *Colloids Surfaces A Physicochem. Eng. Asp.* **312**, 83–91 (2008).
205. Rotsch, C. & Radmacher, M. Mapping local electrostatic forces with the atomic

-
- force microscope. *Langmuir* **13**, 2825–2832 (1997).
206. Lyubchenko, Y. L. *et al.* Atomic force microscopy imaging of double stranded dna and rna. *J. Biomol. Struct. Dyn.* **10**, 589–606 (1992).
207. Qian, X., Karpova, T., Sheppard, A. M., McNally, J. & Lowy, D. R. E-cadherin-mediated adhesion inhibits ligand-dependent activation of diverse receptor tyrosine kinases. *EMBO J.* **23**, 1739–1784 (2004).
208. Thermo Fisher Scientific. CD324 (E-Cadherin) Monoclonal Antibody (DECMA-1), Functional Grade, eBioscience™ from Thermo Fisher Scientific, catalog # 16-3249-82, RRID AB_10734213. Available at: <https://www.thermofisher.com/antibody/product/CD324-E-Cadherin-Antibody-clone-DECMA-1-Monoclonal/16-3249-82>. (Accessed: 17th November 2020)
209. Lowe, A., Harris, R., Bhansali, P., Cvekl, A. & Liu, W. Intercellular Adhesion-Dependent Cell Survival and ROCK-Regulated Actomyosin-Driven Forces Mediate Self-Formation of a Retinal Organoid. *Stem Cell Reports* **6**, 743–756 (2016).
210. Ruggeri, F. S., Šneideris, T., Vendruscolo, M. & Knowles, T. P. J. Atomic force microscopy for single molecule characterisation of protein aggregation. *Arch. Biochem. Biophys.* **664**, 134–148 (2019).
211. Evans, E., Leung, A., Heinrich, V. & Zhu, C. Mechanical switching and coupling between two dissociation pathways in a P-selectin adhesion bond. *Proc. Natl. Acad. Sci. U. S. A.* **101**, 11281–11286 (2004).
212. O. du Roure, †, ‡, A. Buguin, †, H. Feracci, §, || and & P. Silberzan*, †. Homophilic Interactions between Cadherin Fragments at the Single Molecule Level: An AFM Study. (2006). doi:10.1021/LA0531852
213. Nishiguchi, S., Yagi, A., Sakai, N. & Oda, H. Divergence of structural strategies for homophilic E-cadherin binding among bilaterians. *J. Cell Sci.* **129**, 3309–3319 (2016).

-
214. Shi, Q., Chien, Y. H. & Leckband, D. Biophysical properties of cadherin bonds do not predict cell sorting. *J. Biol. Chem.* **283**, 28454–28463 (2008).
215. Spencer, H. L. *et al.* E-Cadherin Inhibits Cell Surface Localization of the Pro-Migratory 5T4 Oncofetal Antigen in Mouse Embryonic Stem Cells. *Mol. Biol. Cell* **18**, 2838–2851 (2007).
216. Overton, K. *et al.* Qualitative and Quantitative Changes to *Escherichia coli* during Treatment with Magainin 2 Observed in Native Conditions by Atomic Force Microscopy. *Langmuir* **36**, 659 (2020).
217. Pérez-Peinado, C. *et al.* Mechanisms of bacterial membrane permeabilization by crotalicidin (Ctn) and its fragment Ctn(15–34), antimicrobial peptides from rattlesnake venom. *J. Biol. Chem.* **293**, 1549 (2018).
218. Andäng, M., Moliner, A., Doege, C. A., Ibañez, C. F. & Ernfors, P. Optimized mouse ES cell culture system by suspension growth in a fully defined medium. *Nat. Protoc.* **3**, 1013–1017 (2008).
219. Trier, N., Hansen, P. & Houen, G. Peptides, antibodies, peptide antibodies and more. *Int. J. Mol. Sci.* **20**, 6289 (2019).
220. Dang, S. M., Gerecht-Nir, S., Chen, J., Itskovitz-Eldor, J. & Zandstra, P. W. Controlled, Scalable Embryonic Stem Cell Differentiation Culture. *Stem Cells* **22**, 275–282 (2004).
221. Hooper, M., Hardy, K., Handyside, A., Hunter, S. & Monk, M. HPRT-deficient (Lesch–Nyhan) mouse embryos derived from germline colonization by cultured cells. *Nature* **326**, 292–295 (1987).
222. Larue, L. *et al.* A role for cadherins in tissue formation. *Development* **122**, 3185–94 (1996).
223. Hirai, H., Karian, P. & Kikyo, N. Regulation of embryonic stem cell self-renewal and pluripotency by leukaemia inhibitory factor. *Biochemical Journal* **438**, 11–23 (2011).
224. Ohtsuka, S., Nakai-Futatsugi, Y. & Niwa, H. LIF signal in mouse embryonic stem

-
- cells. *JAK-STAT* **4**, 1–19 (2015).
225. Murray, P. *et al.* The self-renewal of mouse embryonic stem cells is regulated by cell–substratum adhesion and cell spreading. *Int. J. Biochem. Cell Biol.* **45**, 2705 (2013).
226. Szatmári, T. *et al.* Molecular targets and signaling pathways regulated by nuclear translocation of syndecan-1. *BMC Cell Biol.* **18**, 1–20 (2017).
227. Ramirez Moreno, M., Stempor, P. A. & Bulgakova, N. A. Interactions and Feedbacks in E-Cadherin Transcriptional Regulation. *Front. Cell Dev. Biol.* **9**, 1685 (2021).
228. Redmer, T. *et al.* E-cadherin is crucial for embryonic stem cell pluripotency and can replace OCT4 during somatic cell reprogramming. *EMBO Rep.* **12**, 720–726 (2011).
229. Eastham, A. M. *et al.* Epithelial-mesenchymal transition events during human embryonic stem cell differentiation. *Cancer Res.* **67**, 11254–11262 (2007).
230. Perrais, M., Chen, X., Perez-Moreno, M. & Gumbiner, B. M. E-cadherin homophilic ligation inhibits cell growth and epidermal growth factor receptor signaling independently of other cell interactions. *Mol. Biol. Cell* **18**, 2013–2025 (2007).
231. Ratheesh, A. & Yap, A. S. A bigger picture: classical cadherins and the dynamic actin cytoskeleton. *Nat. Rev. Mol. Cell Biol.* **13**, 673–679 (2012).
232. Hawkins, K. *et al.* Novel Cell Lines Isolated From Mouse Embryonic Stem Cells Exhibiting De Novo Methylation of the E-Cadherin Promoter. *Stem Cells* **32**, 2869–2879 (2014).
233. Leggett, S. E. *et al.* Morphological single cell profiling of the epithelial-mesenchymal transition †. *Integr. Biol* **8**, 1144 (2016).
234. Kumar Surapaneni, S., Rafiq Bhat, Z., Tikoo, K., Nagar, S. & Ajit Singh Nagar, S. MicroRNA-941 regulates the proliferation of breast cancer cells by altering histone H3 Ser 10 phosphorylation. *Sci. Reports 2020 101* **10**, 1–17 (2020).

-
235. Huang, M.-F. *et al.* Syndecan-1 and E-cadherin expression in differentiated type of early gastric cancer. *World J. Gastroenterol.* **11**, 2975–80 (2005).
236. Bhatt, T., Rizvi, A., Batta, S. P. R., Kataria, S. & Jamora, C. Signaling and Mechanical Roles of E-cadherin. *Cell Commun. Adhes.* **20**, 189–199 (2013).
237. Russell, H. & Pranjol, M. Z. I. Transcription factors controlling E-cadherin down-regulation in ovarian cancer. *Biosci. Horizons Int. J. Student Res.* **11**, (2018).
238. Yang, J. *et al.* Guidelines and definitions for research on epithelial–mesenchymal transition. *Nat. Rev. Mol. Cell Biol.* 2020 216 **21**, 341–352 (2020).
239. Scott, A. M. *et al.* A phase I clinical trial with monoclonal antibody ch806 targeting transitional state and mutant epidermal growth factor receptors. *Proc. Natl. Acad. Sci.* **104**, 4071–4076 (2007).
240. Yu, W., Yang, L., Li, T. & Zhang, Y. Cadherin Signaling in Cancer: Its Functions and Role as a Therapeutic Target. *Front. Oncol.* **9**, (2019).
241. Ravikumar, M., Smith, R. A. A., Nurcombe, V. & Cool, S. M. Heparan Sulfate Proteoglycans: Key Mediators of Stem Cell Function. *Front. Cell Dev. Biol.* **8**, 581213 (2020).
242. Chronopoulos, A. *et al.* Syndecan-4 tunes cell mechanics by activating the kindlin-integrin-RhoA pathway. *Nat. Mater.* **19**, 669–678 (2020).
243. Kraushaar, D. C. *et al.* Heparan Sulfate Facilitates FGF and BMP Signaling to Drive Mesoderm Differentiation of Mouse Embryonic Stem Cells. *J. Biol. Chem.* **287**, 22700 (2012).
244. Yu, C. *et al.* Syndecan-1 facilitates the human mesenchymal stem cell osteo-adipogenic balance. *Int. J. Mol. Sci.* **21**, 1–21 (2020).
245. Harjumäki, R. *et al.* AFM Force Spectroscopy Reveals the Role of Integrins and Their Activation in Cell-Biomaterial Interactions. *ACS Appl. Bio Mater.* **3**, 1406–1417 (2020).
246. Prakasam, A. K., Maruthamuthu, V. & Leckband, D. E. Similarities between heterophilic and homophilic cadherin adhesion. *Proc. Natl. Acad. Sci.* **103**,

15434–15439 (2006).

247. Sivasankar, S., Gumbiner, B. & Leckband, D. Direct measurements of multiple adhesive alignments and unbinding trajectories between cadherin extracellular domains. *Biophys. J.* **80**, 1758–1768 (2001).
248. Qin, E. C. *et al.* Comparative effects of N-cadherin protein and peptide fragments on mesenchymal stem cell mechanotransduction and paracrine function. *Biomaterials* **239**, 119846 (2020).

Appendix 1

1.1 - Preliminary Analysis of E14 and Ecad^{-/-} Cells Using Flow Cytometry

As outlined previously, the work shown in chapter 5 would naturally be supported by further analysis of peptide treated E14 and Ecad^{-/-} cell cultures, with flow cytometry presenting a suitable technique to assess the effect of Epep and EpepW2R peptide sequences. This method allows for detailed single cell analysis of fluorescently labelled markers, while providing a basic interpretation of cell characteristics via forward and side scatter measurements. Preliminary development of this experiment was performed within this work, and highlights the potential for development going forward. However, the optimisation and progression of this technique was unfortunately not possible due to the unforeseen shutdown of labs during the COVID-19 pandemic. Therefore, this section details the initial flow cytometry work completed as a continuation of the data reviewed in chapter 5, providing the basis for the continuation of future work.

1.1 - Materials and Methods

1.1.1 - Sample preparation

To prepare samples for flow cytometry, the cell cultures were first passaged using gentle cell dissociation reagent (GCDR) (STEMCELL Technologies, Canada) for at least 3 passages prior to experimentation. This reagent is an enzyme-free chemically defined dissociation buffer, providing a gentler passaging process compared to the commonly used trypsin seen in general cell culture: section 5.1.1.1. Cultures were treated with GCDR at 37°C until cells naturally began detachment from the culture surface, up to a maximum of 15 minutes. Following detachment, the buffer was transferred to a sample tube capable of centrifuging, and a gentle PBS wash of the culture surface was performed, adding this solution to the centrifuge tube. The cell suspension was then centrifuged at 300g for 3 minutes and the supernatant was removed. The cell pellet was then resuspended in the appropriate culture medium and reseeded into culture flasks. For experiment samples, peptide or antibody medium was used as required, and the cell cultures were seeded into larger gelatin coated T75 or T175 flasks until ≈70% confluent or after 48 h incubation. Once

confluent the cultures were detached from the culture flask using GCDR as previously detailed and resuspended in 0.22 µm filtered 10% (v/v) goat serum in DPBS (staining buffer), before being divided into individual samples containing 1×10^6 cells, as required for antibody staining and testing using flow cytometry.

1.2.1 - Immunostaining

For intracellular staining samples were first fixed using 100 µL of 4% (v/v) PFA in DPBS with 15 minutes incubation at room temperature. The cell suspension was then centrifuged at 300g for 3 minutes and the PFA solution was removed. Multiple PBS washes were then performed, before adding 100 µL of 0.4% (v/v) TritonX-100 in DPBS (permeabilisation buffer) and incubating for 20 minutes at room temperature. The samples were then centrifuged to remove the remaining permeabilisation buffer, and multiple PBS washes performed.

For all samples, blocking using staining buffer or permeabilisation buffer was performed for 0.5 h, for extra-cellular and intra-cellular targeting, respectively. Meanwhile, antibodies were diluted in staining buffer or permeabilisation buffer and incubated on the samples for 1 h in the dark at room temperature following blocking. The following antibodies/controls were used: E-cadherin (Cell Signalling Technologies, 3199s, AF488) / rabbit DA1E (Cell Signalling Technologies, 2975s, AF488), N-cadherin (Miltenyi Biotech, 130-116-171, APC) / mouse MOPC-21 (BioLegend, 400120, APC), Syndecan-1 (BioLegend, 142514, PE/Cy7) / rat RTK2758 (BioLegend, 400522, PE/Cy7), Syndecan-4 (BD Biosciences, 550352, PE) / rat R35-95 (BD Bioscience, 553930, PE), Nanog (BD Biosciences, 560278, AF488) / Mouse MOPC-21 (BioLegend, 400134, AF488), Oct-4 (BioLegend, 653704, PE) / mouse MPC-11 (BioLegend, 400312, PE), Sox-2 (BioLegend, 656112, PB) / mouse MOPC-21 (BioLegend, 400151, PB), SSEA-1 (BioLegend, 125618, APC) / mouse MM-30 (BioLegend, 401616, APC), SSEA-4 (BioLegend, 330420, PE/Cy7). Samples were again centrifuged following incubation, several PBS washes performed to remove any unbound antibody. Finally, each sample was resuspended in 500 µL of PBS and covered to protect it from light, and tested immediately.

1.3.1 - Instrument and Data Acquisition

Samples were analysed using a Beckman Coulter Astrios EQ cell sorter, with UV (335 nm), Violet (405 nm), Blue (488 nm), Yellow/Green (561 nm) and Red (633 nm) lasers to allow for multi-colour imaging experiments. Events recorded by the instrument were between 50,000 and 100,000 for each sample, with control samples used to correct for background emission and perform fluorescence compensation during testing. Samples were monitored continuously to check for any blockages or bubbles in the system, and data was interpreted using Kaluza analysis software v1.1 (Beckman Coulter).

1.2 - Preliminary Flow Cytometry Analysis of Epep and EpepW2R Treated mESCs

Analysis via flow cytometry records properties of single cells as they flow through the analysis chamber, using various excitation lasers to measure the fluorescence response of the sample. This response does not provide any information regarding location on the cell, as is seen for example in Operetta analysis, but gives detailed insight into subpopulations of cells and sample uniformity. Furthermore, a large cell population can be tested in a single flow cytometry experiment, with a plethora of fluorescent tags available due to the prevalence of the technique. Therefore, the first process required when reviewing this data is to select the appropriate cell population from the events recorded. As seen in Figure A1., this is achieved by using the forward scatter (FS) and side scatter (SS) properties of the cells within the sample, which correspond to the cell size and granularity, respectively. The ratio of these values provides insight into the physical characteristics of the sample population, and it is therefore possible to omit the uncharacteristic values from the analysis. In Figure A1.A the highlighted region depicts the suspected single cell population, omitting debris as seen via the annotations, classified due to the low FS and SS values. This is further refined in Figure A1.B, whereby suspected cell doublets are also omitted, giving the refined sample population that is used for analysis.

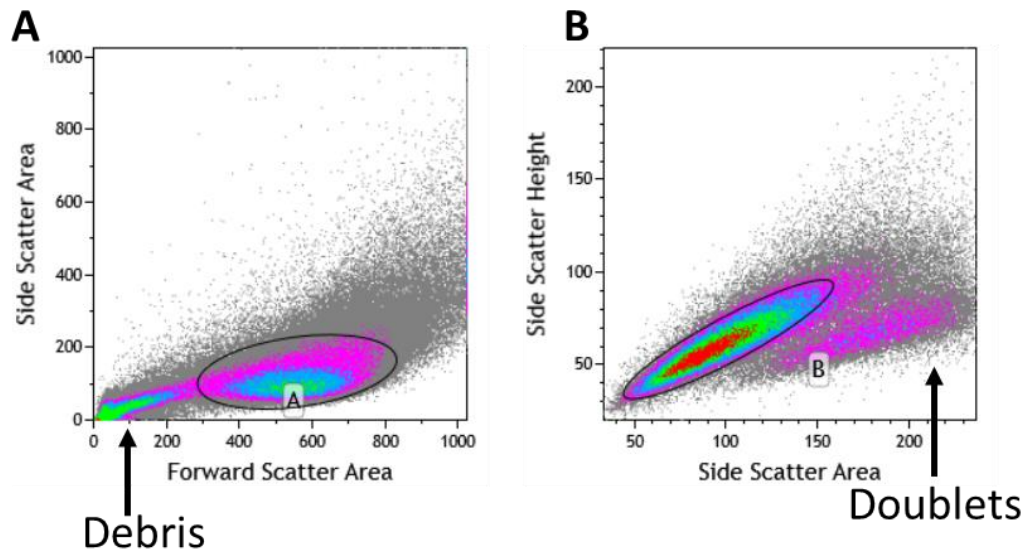


Figure A1.1: *Graphs showing the isolation of the single cell population from an E14 cell sample using common FC analysis processes. The regions within the outlines represent the selected population, showing the omission of A) debris within the sample, and B) cell doublets.*

After selection of the cell population for each sample, the expression of labelled markers can be viewed. Each antibody stain was used alongside a negative control, allowing comparison of the sample data to the control to determine a positive or negative expression, as outlined in section 2.2.1.3. Subsequently, histograms showing the fluorescence intensity of each labelled target were created, and gated to determine the percentage of cells within the sample that exhibited positive expression for the target (data not shown). The results were then collated into Table A1.0.1 for easier comparison.

Table A1.0.1: Table showing data from FC analysis of E14 cell cultures treated with Epep and EPepW2R peptide media. Collated analysis of E14 cell samples showing the percentage of cells expressing the corresponding targeting fluorophore. Samples were cultured in different treatment media as outlined in the table.

E14	Reg Med	Epep 100uM	W2R 100uM	DECMA-1
E-cadherin	2.20	2.76	5.00	2.27
N-cadherin	1.06	1.13	3.06	0.68
Syndecan-1	89.51	84.89	85.35	93.08
Syndecan-4	28.92	25.09	32.11	34.02
Nanog	95.49	94.39	94.41	95.89
Oct4	98.08	97.51	98.17	99.05
Sox2	97.56	96.30	96.36	97.28
SSEA-1	99.52	99.47	98.90	99.67
SSEA-4	56.28	61.18	69.03	53.12

Preliminary experiments were also conducted on Ecad^{-/-} cell cultures treated with peptide media, following the same analysis process. Again, the histograms used to determine the percentage of the cell population exhibiting positive expression are not shown, with the data from this analysis shown instead in Table A1.0.2.

Review of Table A1.0.1 and Table A1.0.2 indicates the negative expression of E-cadherin in all cell conditions, suggesting the labelling process for this protein was

Table A1.0.2: Table showing data from FC analysis of Ecad^{-/-} cell cultures treated with Epep and EPepW2R peptide media. Collated analysis of Ecad^{-/-} samples from FC experiments, following the same fluorescent panel as seen for E14 cells previously. The values show the percentage of each cell sample that exhibit positive expression of each marker.

Ecad ^{-/-}	Reg Med	Epep 100uM	W2R 100uM	DECMA-1
E-cadherin	1.39	1.54	1.55	1.07
N-cadherin	1.36	1.53	1.72	1.61
Syndecan-1	96.95	97.68	96.49	96.85
Syndecan-4	67.30	73.04	65.26	60.99
Nanog	25.09	27.38	24.83	22.93
Oct4	92.99	78.11	57.63	58.51
Sox2	23.80	20.04	20.04	15.89
SSEA-1	92.35	91.45	91.63	91.68
SSEA-4	94.19	91.13	90.46	88.64

unsuccessful, as the studies in this thesis and in the literature demonstrate a characteristic expression of E-cadherin in E14 cultures. Despite this, the analysis seen in Table A1.0.2 indicates that other selected targets may be more closely optimised within this initial experiment. This is evidenced by the varied expression of cell markers seen in E1 and *Ecad*^{-/-} treated samples. This experiment therefore succeeds in providing an ideal foundation for the progression of future work, despite the limitations preventing the optimisation of this experiment within this thesis. Continuing this approach, some key comparisons may be possible between selected markers, providing a more complete understanding of Epep and EpepW2R peptide induced effects on mESCs. Indeed, the experimental process outlined in this chapter highlights the potential progression of this work in the future, focussing on the optimisation of the antibody panel shown to provide a more complete understanding of marker expression, and using the findings from these studies to further refine and develop our understanding of peptide interactions.

Appendix 2

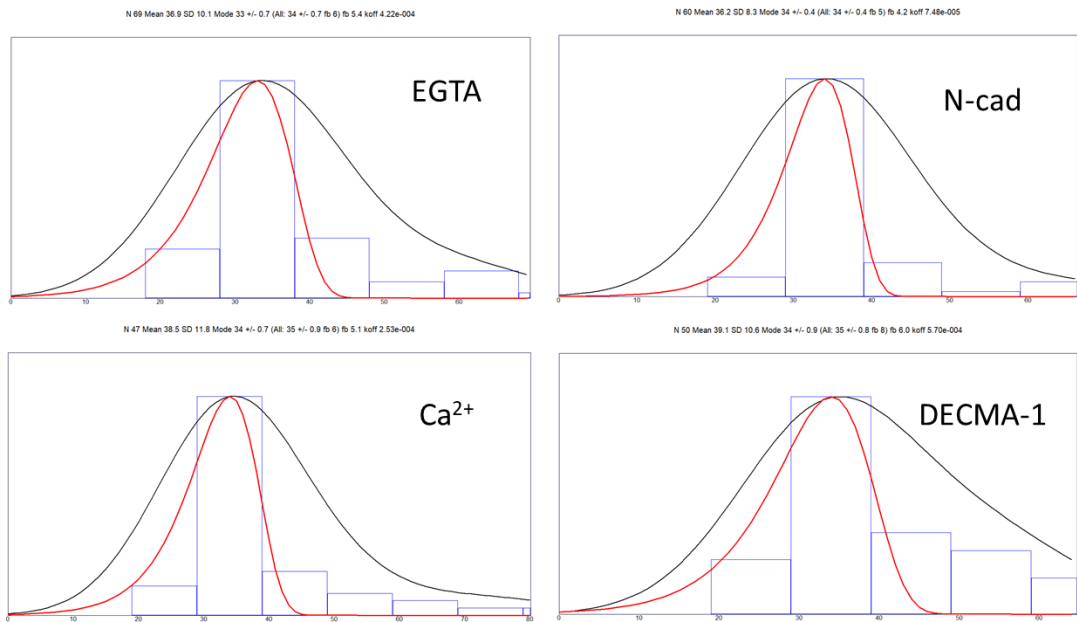


Figure A2.1: *Fdist* analysis of the data shown in Figure 3.8, providing the modal force for specific adhesions as outlined in chapter 3.

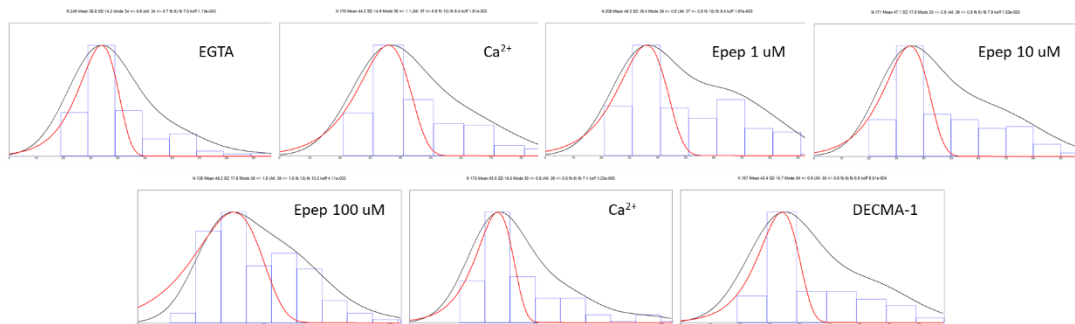


Figure A2.2: *Fdist* analysis of the data shown in Figure 4.6, providing the modal force for specific adhesions as outlined in chapter 3.

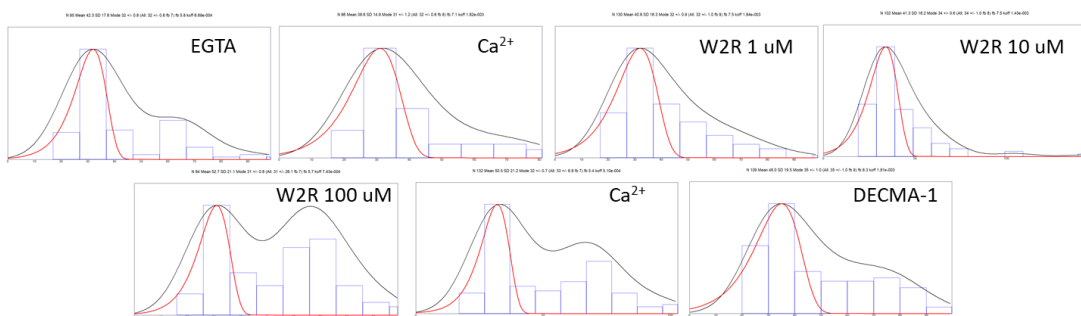


Figure A2.3: *Fdist* analysis of the data shown in Figure 4.9, providing the modal force for specific adhesions as outlined in chapter 3.

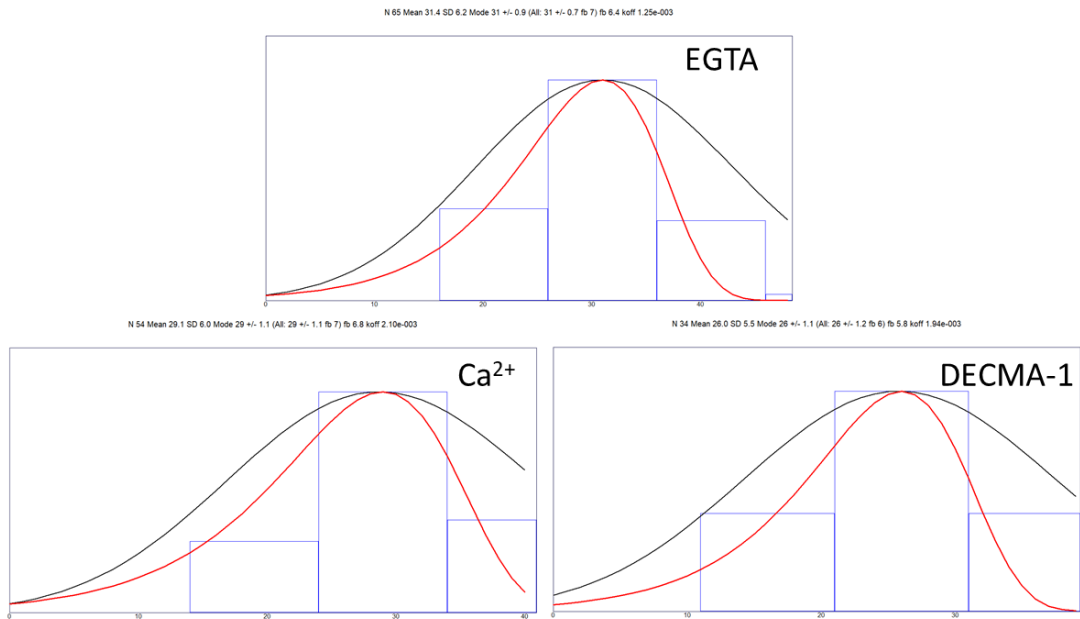


Figure A2.4: Fdist analysis of the data shown in Figure 4.12, providing the modal force for specific adhesions as outlined in chapter 3.